



If you have discovered material in AURA which is unlawful e.g. breaches copyright, (either yours or that of a third party) or any other law, including but not limited to those relating to patent, trademark, confidentiality, data protection, obscenity, defamation, libel, then please read our [Takedown Policy](#) and [contact the service immediately](#)

Reactive Processing Methods for Functionalisation  
of Polymers and *In-situ* Compatibilisation of  
Poly(ethylene terephthalate)-based Blends

WEI KONG

Doctor of Philosophy

ASTON UNIVERSITY

January 2001

This copy of the thesis has been supplied on condition that anyone who consults it is understood to recognise that its copyright rest with its author and that no quotation from the thesis and no information derived from it may be published without proper acknowledgement.

# ASTON UNIVERSITY

## Reactive Processing Methods for Functionalisation of Polymers and *In-situ* Compatibilisation of Poly(ethylene terephthalate)-based Blends

WEI KONG

Doctor of Philosophy

### SUMMARY

One of the main objectives of this study was to functionalise various rubbers (i.e. ethylene propylene copolymer (EP), ethylene propylene diene terpolymer (EPDM), and natural rubber (NR)) using functional monomers, maleic anhydride (MA) and glycidyl methacrylate (GMA), via reactive processing routes. The functionalisation of the rubber was carried out via different reactive processing methods in an internal mixer. GMA was free-radically grafted onto EP and EPDM in the melt state in the absence and presence of a comonomer, trimethylolpropane triacrylate (TRIS). To optimise the grafting conditions and the compositions, the effects of various parameters on the grafting yields and the extent of side reactions were investigated. Precipitation method and Soxhlet extraction method was established to purify the GMA modified rubbers and the grafting degree was determined by FTIR and titration. It was found that without TRIS the grafting degree of GMA increased with increasing peroxide concentration. However, grafting was low and the homopolymerisation of GMA and crosslinking of the polymers were identified as the main side reactions competing with the desired grafting reaction for EP and EPDM, respectively. The use of the tri-functional comonomer, TRIS, was shown to greatly enhance the GMA grafting and reduce the side reactions in terms of the higher GMA grafting degree, less alteration of the rheological properties of the polymer substrates and very little formation of polyGMA. The grafting mechanisms were investigated. MA was grafted onto NR using both thermal initiation and peroxide initiation. The results showed clearly that the reaction of MA with NR could be thermally initiated above 140°C in the absence of peroxide. At a preferable temperature of 200°C, the grafting degree was increased with increasing MA concentration. The grafting reaction could also be initiated with peroxide. It was found that 2,5-dimethyl-2,5-bis(ter-butylproxy) hexane (T101) was a suitable peroxide to initiate the reaction efficiently above 150°C.

The second objective of the work was to utilize the functionalised rubbers in a second step to achieve an *in-situ* compatibilisation of blends based on poly(ethylene terephthalate) (PET), in particular, with GMA-grafted-EP and -EPDM and the reactive blending was carried out in an internal mixer. The effects of GMA grafting degree, viscosities of GMA-grafted-EP and -EPDM and the presence of polyGMA in the rubber samples on the compatibilisation of PET blends in terms of morphology, dynamical mechanical properties and tensile properties were investigated. It was found that the GMA modified rubbers were very efficient in compatibilising the PET blends and this was supported by the much finer morphology and the better tensile properties. The evidence obtained from the analysis of the PET blends strongly supports the existence of the copolymers through the interfacial reactions between the grafted epoxy group in the GMA modified rubber and the terminal groups of PET in the blends.

Keywords: Ethylene propylene copolymer, Ethylene propylene diene terpolymer, Polyethylene terephthalate, Glycidyl methacrylate, Maleic anhydride, Reactive processing, Compatibilisation, Comonomer-assisted grafting, Functionalisation of polymers.

## **ACKNOWLEDGEMENT**

*I wish to acknowledge with gratitude the guidance, advice and encouragement given by my supervisor Dr. S Al-Malaika in carrying out the present work.*

*My thanks are also to Dr. H. H. Sheena, especially for his technical advice and discussion, and to other researchers of Polymer Processing and Performance Group for useful discussions during the research work and friendship.*

*I also thank our research partners, Prof. J. Karger-Kocsis and Mr. N. Papke from University of Kaiserslautern, Germany, Prof. B. Pukanszky from Technical University of Budapest, Hungary, and Dr. M. Szulman-Binet from Leather Plastic and Shoe Development Co. Ltd., Hungary, for their useful discussions during the research work.*

*I would like to thank the European Community for a financial support through COPERNICUS (grant number: ERBIC15 CT 96-0706) and an ORS Award through the Overseas Research Students Awards Scheme.*

*Last but by no means least, I gratefully remember my parents, my wife and my son for their love, support and encouragement in these years.*



<b>LIST OF CONTENTS</b>	<b>Page</b>
THESIS TITLE PAGE	1
SUMMARY	2
ACKNOWLEDGEMENT	3
LIST OF CONTENTS	4
LIST OF SCHEMES	9
LIST OF TABLES	10
LIST OF FIGURES	12
LIST OF ABBREVIATIONS	20
<u>CHAPTER 1 INTRODUCTION</u>	
1.1 INTRODUCTION	23
1.2 POLYMER BLENDS	24
1.2.1 Factors Affecting Performance of Polymer Blends	24
1.2.2 Compatibility of Polymer Blends	25
1.2.2.1 Definitions of Compatibility	25
1.2.2.2 Thermodynamics Consideration	25
1.3 COMPATIBILISATION OF POLYMER BLENDS	26
1.4 COMATIBILISATION OF POLY(ETHYLENE TEREPHTHLATE), PET, BLENDS	32
1.4.1 PET Property Profile	32
1.4.2 PET Blends	33
1.4.2.1 Impact Modification	34
1.4.2.2 Compatibilisation of PET/PE Blends	37
1.4.2.3 Compatibilisation of PET/PP Blends	39
1.4.2.4 Compatibilisation of PET Blends with EPR or PS	42
1.5 FREE RADICAL GRAFTING REACTIONS FOR POLYMER FUNCTIONALISATION	43
1.6 FUNCTIONALISATION OF POLYMERS VIA REACTIVE PROCESSING	45
1.6.1 Grafting Maleic Anhydride (MA) onto Polymers	46

1.6.2	Grafting Glycidyl Methacrylate (GMA) onto Polymers	50
1.6.3	Functionalisation of Polymers with Other Reactive Monomers	51
1.7	ENHANCING GRAFTING BY USING CO-MONOMER	54
1.8	CHALLENGES OF MELT FREE RADICAL GRAFTING	57
1.9	PROCESS CONSIDERATION	58
1.9.1	Reactive Extrusion	58
1.9.2	Batch Mixers	59
1.10	AIM AND OBJECTIVES OF THIS STUDY	60

## CHAPTER 2 EXPERIMENTAL AND ANALYTICAL TECHNIQUES

2.1	MATERIALS	62
2.1.1	Polymers	62
2.1.2	Reagents and Additives	62
2.1.3	Solvents	63
2.2	PROCESSING	66
2.2.1	Preparation of GMA Functionalised Polyolefins	66
2.2.2	Preparation of MA Functionalised Natural Rubber	67
2.2.3	Polymer Blending	67
2.3	PREPARATION OF POLYMER FILMS, PLAQUES AND SHEETS	68
2.3.1	Preparation of Polymer Films for FTIR Analysis	68
2.3.2	Preparation of polymer Plaques and Sheets	69
2.4	PURIFICATION OF REACTION PRODUCTS FROM REACTIVELY PROCESSED POLYMERS	69
2.4.1	Precipitation	69
2.4.2	Soxhlet extraction	70
2.5	DETERMINATION OF THE GRAFTING DEGREE	70
2.5.1	Determination of the Grafting Degree of GMA by Titration	70
2.5.2	Determination of the Grafting Degree of GMA by FTIR Method	71
2.5.3	Determination of the Grafting Degree of MA by FTIR Method	72
2.6	DETERMINATION OF INSOLUBLE GELS	73
2.7	MEASUREMENT OF MELT FLOW INDEX	74
2.8	FOURIER TRANSFORM INFRARED (FTIR) SPECTROSCOPY	74
2.9	SCANNING ELECTRON MICROSCOPY (SEM)	75

2.10	MEASUREMENT OF DYNAMIC MECHANICAL PROPERTIES	75
2.11	TENSILE PROPERTY MEASUREMENT	76
2.12	DIFFERENTIAL SOLVENT FRACTIONATION OF GMA GRAFTED EPDM/PP MIXTURE	76
2.13	FTIR ANALYSIS OF PET BLEND	77
2.14	POLYMERISATION OF POLYGMA POLYTRIS AND GMA-CO-TRIS	77
2.14.1	Homopolymerisation of GMA in Chloroform	78
2.14.2	Homopolymerisation of TRIS in Benzene	78
2.14.3	Copolymerisation of TRIS and GMA in Toluene	78

### CHAPTER 3 FUNCTIONALISATION OF POLYOLEFINS WITH GLYCIDYL METHACRYLATE

3.1	OBJECTIVE AND METHODOLOGY	94
3.2	RESULTS	96
3.2.1	Characterisation of PolyGMA, PolyTRIS and GMA-co-TRIS	96
3.2.1.1	Characterisation of PolyGMA	96
3.2.1.2	Characterisation of PolyTRIS	97
3.2.1.3	Characterisation of GMA -co-TRIS	98
3.2.2	Separation of Reaction Products and Characterisation of GMA Functionalised EP	99
3.2.3	Determination of Grafted GMA and PolyGMA in the GMA grafted EP	100
3.2.4	Grafting GMA onto EP in the Absence of TRIS	102
3.2.5	Grafting GMA onto EP in the Presence of TRIS	106
3.2.5.1	Processing EP in the Presence of TRIS	107
3.2.5.2	Optimisation of the Addition Sequence	109
3.2.5.3	Effect of T101 Concentration on Grafting Degree	111
3.2.5.4	Effect of TRIS Concentration on the Grafting Degree	112
3.2.5.5	The Kinetics of Grafting Reaction in the Presence of TRIS	112
3.2.5.6	Effect of Processing Temperature on Grafting Degree	113
3.2.6	Grafting GMA onto EPDM	114
3.2.7	Grafting GMA onto a Mixture of EPDM and PP	119
3.3	DISCUSSION	124

3.3.1	Grafting GMA onto EP in the Absence of Comonomer	124
3.3.1.1	Grafting reaction vs Side Reactions	124
3.3.1.2	The GMA-Grafting Mechanisms in the Absence of Comonomer	126
3.3.2	Effect of the Presence of Comonomer , TRIS, on GMA Grafting onto EP	127
3.3.3	The Mechanisms of GMA-Grafting on EP in the Presence of Comonomer, TRIS	130
3.3.4	Features of Grafting GMA onto EPDM	132
3.3.5	Effect of PP on GMA Grafting onto EPDM	134

#### CHAPTER 4 FUNCTIONALISATION OF NATURAL RUBBER WITH MALEIC ANHYDRIDE

4.1	Objective and Methodology	175
4.2	Results	177
4.2.1	Characterisation of Maleic Anhydride Grafted Natural Rubber	177
4.2.2	Grafting MA onto NR by Thermal Initiation	181
4.2.3	Grafting MA onto NR by Free Radical Initiation	184
4.2.4	Optimal Conditions	187
4.2.5	Analysis of the Reaction Products	187
4.3	Discussion	188

#### CHAPTER 5 REACTIVE COMPATIBILISATION OF POLY(ETHYLENE TEREPHTHALATE) BASED BLENDS USING GLYCIDYL METHACRYLATE FUNCTIONALISED POLYOLEFINS

5.1	OBJECTIVE AND METHODOLOGY	213
5.2	RESULTS	215
5.2.1	Compatibilisation of PET with GMA Grafted EP	215
5.2.1.1	Processing Characteristics	215
5.2.1.2	Morphology Observation	218
5.2.1.3	Dynamic Mechanical Properties	222
5.2.1.4	Interphase Reaction between PET and EP-g-GMA during the reactive blending	226

5.2.1.4.1 Solubility Test	226
5.2.1.4.2 FTIR Analysis of PET Blends	227
5.2.2 Compatibilisation of PET with GMA Grafted EPDM	228
5.2.2.1 Processing Characteristics of PET/EPDM-g-GMA Blends	228
5.2.2.2 Morphology of PET/EPDM or PET/EPDM-g-GMA Blends	229
5.2.2.3 Tensile Properties	232
5.2.2.4 Dynamic Mechanical Properties	234
5.2.2.5 Characterisation of Interphase Reactions by FTIR Analysis	235
5.3 DISCUSSION	236
5.3.1 Compatibilisation of EP-g-GMA with PET	236
5.3.2 Compatibilisation of EPDM-g-GMA with PET	239
5.3.3 Interfacial Reactions between PET and GMA grafted EP or EPDM	240

## CHAPTER 6 CONCLUSIONS AND RECOMMENDATIONS FOR FUTURE WORKS

6.1 CONCLUSIONS	274
6.2 SUGGESTIONS FOR FUTURE WORK	281
REFERENCES	284

## LIST OF SCHEMES

Scheme 1-1	Possible reactions between epoxide units with PBT hydroxyl and carboxyl end groups	36
Scheme 1-2	Possible reactions between LDPE-g-HI and PET hydroxyl and carboxyl end groups during reactive blending	39
Scheme 3-1a	Methodology for grafting GMA onto EP in the absence of TRIS	136
Scheme 3-1b	Methodology for grafting GMA onto EP in the presence of TRIS	137
Scheme 3-2	Flow chart for analysis of EP-g-GMA by titration and FTIR	138
Scheme 3-3	Methodology for grafting GMA onto EPDM	139
Scheme 3-4	Methodology for differential solvent extraction	140
Scheme 3-5	Methodology for grafting GMA onto EPDM/PP	141
Scheme 3-6	Grafting and homopolymerisation of GMA onto EP in the Absence of TRIS	142
Scheme 3-7	Grafting of GMA onto EP in the presence of TRIS	143
Scheme 4-1	Flow chart for grafting maleic anhydride (MA) onto natural rubber	192
Scheme 4-2	Flow chart for analysing MA grafted natural rubber by mixing on a cold two-roll mill	193
Scheme 4-3	Flow chart for analysing MA grafted natural rubber	194
Scheme 4-4	The mechanisms of grafting MA onto natural rubber (a) thermal initiation, (b) peroxide initiation	195
Scheme 5-1	Methodology for compatibilisation of PET/rubbers blends	243
Scheme 5-2	Possible interfacial reactions of GMA grafted rubbers with end groups of PET	244

## LIST OF TABLES

Table 1-1	Examples of common compatibilising reactions between functionalised blend constituents	28
Table 1-2	Compatibilisation through the reaction of functionalised blend Components	29
Table 1-3	Compatibility through non-reactive copolymer	30
Table 1-4	Compatibilisation through reactive copolymers or functionalised polymer added separately	31
Table 1-5	Functionalisation of Polymers with MA	49
Table 1-6	Functionalisation of Polymers with GMA	52
Table 2-1	Chemical structure of polymers	63
Table 2-2	Chemicals used in the experiments	64
Table 2-3	Compounding for Making Cured NR Films	68
Table 3-1	The Experimental Composition and Results GMA grafting onto EP system (a) EP+GMA+T101 system (in the absence of TRIS)	144
	(b) EP+GMA+TRIS+T101 system (in the presence of TRIS)	145
	(c) EP+GMA+T29B90 system (in the absence of TRIS)	147
Table 3-2	The Experimental Composition and Results GMA grafting onto EPDM system (in the absence and presence of TRIS)	148
Table 3-3	The Experimental Composition and Results GMA grafting onto EPDM/PP system (in the absence and presence of TRIS)	149
Table 4-1	The Experimental Conditions and Results (a) Thermal Initiation in the absence of peroxide ( Raw SMR-L without purification used) (b) Thermal Initiation in the absence of peroxide (Purified SMR-L used)	196
Table 4-2	The Experimental Conditions and Results (a) peroxide initiation using BPO, (b) peroxide initiation using T101	197

Table 4-3	Major absorption bands and probable functional assignments in the FTIR spectra of NR, MA, SA, SAN, MA-g-NR	199
Table 4-4	Determination of the amount of insoluble fraction in toluene	200
Table 5-1	Compositions and conditions for preparation of PET/EP-g-GMA blends	
	(a) Composition and condition for EP-g-GMA samples preparation	245
	(b) PET/EP-g-GMA blend compositions and conditions	246
Table 5-2	Peaks of $\tan\delta$ curves corresponding to the glass transition of individual component for different types of PET/EP (or EP-g-GMA) blends	247
Table 5-3	Compositions and conditions for preparation of PET/EPDM-g-GMA blends	248
Table 5-4	The tensile properties of different PET blends	249
Table 5-5	Glass transition temperatures ( $T_g$ ) of different blends measured by DMTA	249



## LIST OF FIGURES

Figure 1-1	The chemical structure of poly(ethylene terephthalate)	32
Figure 1-2	Overall scheme of free-radical grafting onto a polymer backbone	45
Figure 1-3	Chemical structure of MA	46
Figure 1-4	Chemical structure of GMA	50
Figure 1-5	Chemical structure of OXA	53
Figure 1-6	Chemical structure of 2-isopropenyl-2-oxazoline	53
Figure 1-7	Formation of a charge transfer complex (CTC)	55
Figure 1-8	The mechanism of the melt free radical grafting GMA onto PP with and without styrene (a) GMA alone (b) GMA and styrene	56
Figure 1-9	Chemical structure of TRIS	56
Figure 2-1	FTIR spectrum of EP (Tafmer P0480) from pressed film	80
Figure 2-2	FTIR spectrum of EPDM (Buna 447) from filmed	80
Figure 2-3	FTIR spectrum of PP (HF-26) from pressed filmed	81
Figure 2-4	FTIR spectrum of SMR-L film casted from benzene	81
Figure 2-5	FTIR spectrum of PET from pressed film	82
Figure 2-6	FTIR spectrum of neat GMA film between KBr cells	82
Figure 2-7	FTIR spectrum of maleic anhydride using pressed KBr disc	83
Figure 2-8	FTIR Spectrum of neat TRIS film between KBr cells	83
Figure 2-9	FTIR spectrum of BPO using pressed KBr disc	84
Figure 2-10	FTIR spectrum of neat T101 between KBr cells	84
Figure 2-11	FTIR spectrum of neat T29B90 between KBr cells	85
Figure 2-12	FTIR spectrum of AIBN using KBr disc	85
Figure 2-13	FTIR spectrum of maleic acid in NUJOL	86
Figure 2-14	FTIR spectrum of succinic acid in NUJOL	86
Figure 2-15	FTIR spectrum of succinic anhydride in NUJOL	87
Figure 2-16	FTIR spectrum of pressed film of GMA functionalised EP	87
Figure 2-17	Area boundaries for absorption peak area calculation of GMA functionalised EP	88
Figure 2-18	Calibration curve obtained from correlation between grafting degree measured by titration and area ratio ( $A_{909\text{ cm}^{-1}}/A_{720\text{ cm}^{-1}}$ ) from FTIR	89

Figure 2-19	Area boundaries for absorption peak area calculation of MA functionalised NR	90
Figure 2-20	FTIR spectrum of an example of SMR-L/maleic acid film casted from solution (diethyl ether) on a KBr cell for calibration	90
Figure 2-21	Calibration curve from maleic acid / SMR-L films	91
Figure 2-22	Dimensions of dumb-bell shape tensile test specimen	91
Figure 2-23	Idealised tensile stress-strain curve for a typical plastics material	91
Figure 2-24	FTIR spectrum of polyGMA using KBr disc	92
Figure 2-25	FTIR spectrum of polyTRIS using KBr disc	92
Figure 2-26	FTIR spectrum of copolymer GMA-co-TRIS using KBr disc	93
Figure 3-1	Comparison of FTIR spectra of polyGMA using KBr disc (red line) with GMA (black line)	150
Figure 3-2	Comparison of FTIR spectra of polyTRIS using KBr disc (red line) with TRIS (black line)	150
Figure 3-3	FTIR spectrum of copolymer GMA-co-TRIS using KBr disc	151
Figure 3-4	Comparison of spectra of polyGMA (red line), polyTRIS (green line), and PolyGMA-co-TRIS (blue line)	151
Figure 3-5	Spectra of EP-g-GMA (without TRIS) pressed films with different purification Methods	152
Figure 3-6	Variation of GMA concentration in polymer with different purification methods Without TRIS	152
Figure 3-7	Spectrum of EP-g-GMA (with TRIS) pressed films (purified in acetone)	153
Figure 3-8	Structures of GMA grafted EP before and after the ring open reaction with trichloroacetic acid	153
Figure 3-9	Comparison of spectra before and after the reaction of EP-g-GMA with trichloroacetic acid	154
Figure 3-10	Effect of T101 concentration on grafting degree on EP with different amounts of GMA	155
Figure 3-11	Effect of peroxide concentration on alteration of rheological properties	155
Figure 3-12	Effect of GMA concentration on grafting degree with different level of T101	156

Figure 3-13	Effect of T101 concentration on amounts of grafted GMA and polyGMA formed in the melt grafting	156
Figure 3-14	Effect of GMA concentration on amounts of grafted GMA and polyGMA formed in the melt grafting	156
Figure 3-15	Effect of processing time on grafting degree	157
Figure 3-16	The effect of processing temperature on the grafting degree in GMA+T101 system	157
Figure 3-17	The effect of GMA concentration on the grafting degree in GMA+ T29B90 system at low temperature	158
Figure 3-18	Variation of torque with processing time for shear-initiated reaction of TRIS in EP (with different level of TRIS) and curves of GMA alone (6phr) processed with EP and that of EP alone as control	158
Figure 3-19	Variation of torque with processing time for peroxide-initiated reaction of TRIS in EP (T101/TRIS mole ratio=0.01 with TRIS=1phr) and curves of GMA (6phr) (T101/GMA mole ratio=0.04) processed with EP and that of EP alone as control	159
Figure 3-20	Comparison of FTIR spectra of white particle collected from the modified polymer (red line) , GMA-co- TRIS (blue line) and EP (green line)	159
Figure 3-21	Effect of T101 concentration on the grafting degree	160
Figure 3-22	Effect of T101 concentration on the grafting degree	160
Figure 3-23	Effect of TRIS concentration on grafting degree and TRIS grafting	161
Figure 3-24	Effect of processing time on grafting degree	162
Figure 3-25	The effect of processing temperature on the grafting degree in the presence of TRIS	163
Figure 3-26	The effect of T101 concentration on the grafting degree in the presence of TRIS	163
Figure 3-27	The effect of T101 concentration on MFI	164
Figure 3-28	FTIR spectra of purified EPDM-g-GMA sample and unmodified EPDM	164
Figure 3-29	Effect of peroxide concentration on grafting degree and gel of GMA grafted EPDM in the absence of TRIS	165

Figure 3-30	Effect of peroxide concentration on grafting degree and gel of GMA grafted EPDM in the presence of TRIS	165
Figure 3-31	Effect of peroxide concentration on grafting degree and gel of GMA grafted EPDM in the presence of TRIS	166
Figure 3-32	Comparison of weight percentage of separated fractions of two samples of EPDM-g-GMA which were prepared either in the presence of TRIS or in the absence of TRIS by differential solvent extraction	166
Figure 3-33	Comparison of FTIR spectra recorded from the hexane soluble fraction and hexane insoluble fraction of EPDM-g-GMA <sub>TRIS</sub> sample DM-3	167
Figure 3-34	Comparison of FTIR spectra recorded from the hexane soluble fraction and hexane insoluble fraction of EPDM-g-GMA <sub>TRIS</sub> sample DM-9	167
Figure 3-35	FTIR of the blend of EPDM/PP (weight ratio=75/25)	168
Figure 3-36	FTIR of EPDM/PP-g-GMA	168
Figure 3-37	Effect of peroxide concentration on grafting degree and gel of GMA grafted EPDM/PP in the absence of TRIS	169
Figure 3-38	Effect of peroxide concentration on grafting degree and gel of GMA grafted EPDM/PP in the presence of TRIS	169
Figure 3-39	Effect of peroxide concentration on grafting degree and gel of GMA grafted EPDM/PP in the presence of TRIS	170
Figure 3-40	Weight percentage of separated fractions of the blend of EPDM/PP which were prepared under conditions of temperature, 180°C; speed, 65 rpm; time, 10minutes by differential solvent extraction (hexane, toluene, and xylene )	170
Figure 3-41	Comparison of FTIR spectra of virgin PP (top one) and virgin EPDM (bottom one)	171
Figure 3-42	FTIR spectra of EPDM/PP blend (PM-0) (top one) and its hexane soluble fraction (middle one) and xylene soluble fraction (bottom one)	171
Figure 3-43	Weight percentage of separated fractions of EPDM/PP-g-GMA <sub>TRIS</sub> (sample PM-2 in Table 3-3 ) by differential	172

	solvent extraction (hexane, toluene, and xylene)	
Figure 3-44	FTIR spectra of EPDM/PP g-GMA <sub>T101</sub> (PM-2) and its soluble fractions (a) before extraction, (b) hexane soluble fraction, (c) toluene soluble fraction, and (d) xylene soluble fraction	172
Figure 3-45	Weight percentage of separated fractions of EPDM/PP-g-GMA <sub>TRIS</sub> (sample PM-8 in Table 3-3) by differential solvent extraction (hexane, toluene, and xylene)	173
Figure 3-46	FTIR spectra of EPDM/PP g-GMA <sub>TRIS</sub> (PM-8) and its soluble fractions (a) before extraction, (b) hexane soluble fraction, (c) toluene soluble fraction, and (d) xylene soluble fraction	173
Figure 3-47	FTIR spectrum of the hexane soluble fraction of EPDM/PP-g-GMA <sub>TRIS</sub> (PM-8)	174
Figure 4-1	FTIR spectrum of extracted SMR-L (Extracted for 24 hours with acetone, pressed film: 150°C × 15 seconds)	201
Figure 4-2	Comparison of spectra obtained from cured film both before extraction (film A) and after extraction (film B) with acetone for 24 hours	201
Figure 4-3	Comparison of FTIR spectra obtained from cured films both before extraction (film A) and after extraction in acetone (film B) for 24 hours	202
Figure 4-4	FTIR spectrum of MA modified natural rubber prepared by mixing MA and natural rubber on a two-roll mill	202
Figure 4-5	FTIR spectrum of MA grafted natural rubber (Thermal initiated —sample A3-9: SMR-L 100 phr; MA 6 phr; Temp. 200 °C; time 15 min)	203
Figure 4-6	FTIR spectrum of MA grafted natural rubber (Peroxide initiated —sample D3-51: SMR-L 100 phr; MA 6 phr; T101 0.04phr, Temp. 150 °C; time 15 min)	203
Figure 4-7	Comparison of FTIR spectra of MA grafted rubber with maleic anhydride, succinic anhydride and succinic acid)	204
Figure 4-8	Effect of processing temperature on MA grafting degree	204
Figure 4-9	Torque-time curves— (a) samples A3-5 ~ A3-10	205

	(b) low processing temperature (samples A3-5 ~ A3-7),	
	(c) high processing temperature (samples A3-8 ~ A3-10)	
Figure 4-10	Effect of processing temperature on peak time and peak torque value of raw and purified NR processed with MA (6 phr) and no peroxide for 15 min effect of processing temperature on peak time, (b) effect of processing temperature on peak torque value	206
Figure 4-11	Torque-time curves—Purified SMR-L(100phr), MA(6 phr), no peroxide, 15 min.	207
Figure 4-12	Effect of MA concentration on MA grafting degree	207
Figure 4-13	Effect of processing time on MA grafting degree	208
Figure 4-14	Effect of BPO concentration on MA grafting degree	208
Figure 4-15	Effect of T101 concentration and processing temperatures on MA grafting degree	208
Figure 4-16	Effect of MA concentration on MA grafting degree	209
Figure 4-17	Torque-time curves—Raw SMR-L:100phr, T101: 0.04 phr, temp.: 150°C, time: 15 min.	209
Figure 4-18	Effect of processing time on MA grafting degree	210
Figure 4-19	Comparison of effect of processing temperature on MA grafting degree by different initiation techniques	210
Figure 4-20	FTIR spectrum of soluble fraction in toluene of reaction product casted from solution using KBr disc	211
Figure 4-21	FTIR spectrum of soluble fraction in toluene of reaction products cast from solution using KBr disc(Sample A3-9)	211
Figure 5-1	The torque-time curves of blending of PET/EP with three weight ratios : 80/20, 60/40, 50/50	249
Figure 5-2	The torque-time curves of blending of PET/EP-g-GMA	249
Figure 5-3	The torque-time curves of blending PET with EP-g-GMA <sub>T101</sub> (unpurified containing grafted GMA and polyGMA, sample GP-11, and purified containing only grafted GMA) at a weight ratio of 80/20, and PET with and without polyGMA	249
Figure 5-4	The torque-time curves of blending PET with EP-g-GMA <sub>TRIS</sub> — effect of grafting degree of EP-g-GMA <sub>TRIS</sub> on the torque value	250

	at a weight ratio of 80/20	
Figure 5-5	The torque-time curves of blending PET with different types of EP-g-GMA at a weight ratio of 80/20	250
Figure 5-6	SEM of 80/20 PET/EP or EP-g-GMA <sub>TRIS</sub> blends: the effect of grafting degree of EP-g-GMA on the morphology	252
Figure 5-7	SEM of 80/20 PET/ EP-g-GMA <sub>TRIS</sub> blends: the effect of viscosity of EP-g-GMA on the morphology of the blends	253
Figure 5-8	SEM of 80/20 PET/EP-g-GMA <sub>T101</sub> blends: the effect of polyGMA of EP-g-GMA on the morphology of the blends	254
Figure 5-9	SEM of 60/40 PET/EP or EP-g-GMA: the effect of different types of EP-g-GMA on the morphology of the blends	255
Figure 5-10	DMTA curves for EP (virgin) as a function of E' and Tan $\delta$	256
Figure 5-11	DMTA curves for PET (virgin) as a function of E' and Tan $\delta$	256
Figure 5-12	DMTA curves for PET/EP (80/20, 60/40, and 50/50) blends as a function of Tan $\delta$	257
Figure 5-13	Comparison of DMTA curves between PET/EP blend and PET/EP-g-GMA (80/20) blends as a function of Tan $\delta$	257
Figure 5-14	DMTA curves for PET/EP (EP-g-GMA) 80/20 blends as a function of E'	258
Figure 5-15	DMTA curves for PET/EP (EP-g-GMA) 60/40 blends as a function of Tan $\delta$	258
Figure 5-16	DMTA curves for PET/EP (EP-g-GMA) 60/40 blends as a function of E'	259
Figure 5-17	DMTA curves for PET/EP (EP-g-GMA) 50/50 blends as a function of tan $\delta$	259
Figure 5-18	DMTA curves for PET/EP (EP-g-GMA) 50/50 blends as a function of E'	260
Figure 5-19	Comparison of FTIR spectra of virgin polymers (PET and EP) and separated PET fraction from PET/EP blend and PET/EP-g-GMA blend (80/20w/w)	261
Figure 5-20	Comparison of torque-time curves of blends of PET with different EPDM-g-GMA samples	262
Figure 5-21	Comparison of torque-time curves of ternary blends of PET/	262

	EPDM/EPDM-g-GMA with different weight ratios	
Figure 5-22	Comparison of torque-time curves of blends of PET with different types of EPDM-g-GMA (EPDM-g-GMA <sub>T101</sub> : sample DM-4 and EPDM-g-GMA <sub>TRIS</sub> : sample DM-10) or EPDM	263
Figure 5-23	SEM of physical blend of PET/EPDM 80/20 and compatibilised blends PET/EPDM-g-GMA	265
Figure 5-23a	SEM of physical blend of PET/EPDM 80/20 and compatibilised blends PET/EPDM-g-GMA	267
Figure 5-24	SEM of binary blend of PET/EPDM-g-GMA (80/20) and ternary blends of PET/EPDM/EPDM-g-GMA with different ratios	268
Figure 5-25	SEM of binary blend of PET/EPDM-g-GMA <sub>TRIS</sub> (80/20) and ternary blends of PET/EPDM/EPDM-g-GMA <sub>TRIS</sub> with different ratios	269
Figure 5-26	Tensile properties of virgin PET and EPDM	270
Figure 5-27	Stress-strain curves of tensile test of PET/EPDM (80/20) physical blend and PET/EPDM-g-GMA (80/20)	271
Figure 5-28	Tensile properties of PET/EPDM or PET/EPDM-g-GMA with different rubber samples	271
Figure 5-29	DMTA curves for PET/EPDM (80/20) blend and PET/EPDM-g-GMA (80/20) blends as a function of Tan $\delta$	272
Figure 5-30	Comparison of FTIR spectra of virgin polymers (PET and EPDM) and separated PET fractions from PET/EPDM blend and PET/EPDM-g-GMA blends (80/20w/w)	273



## ABBREVIATION AND SYMBOLS

ABS	Acrylonitrile-butadiene-styrene terpolymer
ABS-g-MA	Maleic anhydride grafted ABS
AIBN	$\alpha,\alpha'$ -Azoisobutyronitrile
AM	Acrylamide
BPO	Benzoyl peroxide
BR	Polybutadiene rubber
CTC	Charge transfer complex
DCP	Dicumyl peroxide
DHBP	2,5-Di(t-butyl-peroxy)-2,5-dimethylhexane
DTBPIB	1,3-Bis(tert-butylperoxy-isopropyl)benzene
EAA	Poly(ethylene-co-acrylic acid)
E-GMA	Ethylene glycidyl methacrylate copolymer
E-EA-GMA	Ethylene ethylacrylate glycidyl methacrylate terpolymer
E-EeA-g-GMA	Maleic anhydride modified ethylene methacrylate copolymer
ENR	Epoxidized natural rubber
EP	Ethylene propylene copolymer
EP-g-GMA	Glycidyl methacrylate grafted ethylene propylene copolymer
EPM or EPR	Poly(ethylene-co-propylene) elastomer
EPM-g-MA	Maleic anhydride grafted EPM
EPDM	Ethylene propylene diene terpolymer
EPDM-g-GMA	Glycidyl methacrylate grafted ethylene propylene diene terpolymer
EPDM-g-MA	Maleic anhydride grafted EPDM
EPDM-g-MMA	Methyl methacrylate grafted EPDM
EVA	Poly(ethylene-co-vinyl acetate)
FTIR	Fourier Transform Infrared
GMA	Glycidyl methacrylate
KOH	Potassium hydroxide
HDPE	High density polyethylene
LDPE	Low density polyethylene

MA	Maleic anhydride
NR	Natural rubber
OPS	Oxazoline modified PS
PA-6	Polyamide 6
PA-6,6	Polyamide 6,6
PAR	Polyarylate
PBT	Polybutylene terephthalate
PC	Polycarbonate
PCL	Polycaprolactone
PE	Polyethylene
PET	Polyethylene terephthalate
PF	Phenol-formaldehyde resin
PF-g-MMA	Methyl methacrylate grafted phenol-formaldehyde resin
PF-g-S	Styrene grafted phenol-formaldehyde resin
phr	Part per hundred
PMMA	Poly(methyl methacrylate)
PP	Polypropylene
PP-g-AA	Acrylic acid grafted PP
PP-g-MA	Maleic anhydride grafted PP
PPE	Poly(2,6-dimethyl-1,4-phenylene ether)
PPE-g-MA	Maleic anhydride grafted PPE
PS	Polystyrene
PS-g-MA	Maleic anhydride grafted PS
PVC	Polyvinyl chloride
PVDF	Polyvinylidene fluoride
R*	Macroradical
SA	Succinic anhydride
SAN	Poly(styrene-co-acrylonitrile)
SB	Styrene-butadiene diblock copolymer
SBR	Poly(styrene-co-butadiene)
SBS	Styrene-butadiene-styrene triblock copolymer
SEBS	Styrene-ethylene/butadiene-styrene triblock copolymer
SEBS-g-MA	Maleic anhydride grafted SEBS
SEP	Styrene-ethylene/propylene diblock copolymer

SIS	Styrene-isoprene-styrene triblock copolymer
S-I-HDB	Styrene-isoprene-hydrogenated butadiene triblock copolymer
SMA	Styrene-maleic anhydride copolymer
St	Styrene
TSE	Twin screw extruder
T101	(2,5-dimethyl-2,5-bis-tertiarybutyl peroxy)hexane
TRIS	Trimethylolpropane trimethacrylate
MW	Molecular weight
M	Molarity

# CHAPTER 1 INTRODUCTION

## 1.1 INTRODUCTION

Mixing two or more polymers together to produce blends or alloys is a well-established strategy for achieving a specified portfolio of physical properties, without the need to synthesise specialised polymer systems [1]. Although synthesis of new polymers from new monomers to develop new engineering materials is possible, blending of existing polymers with complementary properties has become a more attractive approach. Polymer blends have become versatile and economically viable solution to the needs of industry in terms of improving the performance of engineering and speciality plastics. Consequently, the field of polymer blends has been developing rapidly, in terms of both scientific understanding and commercial utility.

However, most polymer pairs are immiscible due to high interfacial tension and lack of interfacial adhesion in the solid state leading to gross phase separation hence poor mechanical properties. Compatibilisation techniques are therefore key to achieving good performance in polymer blends. Generally, compatibility can be achieved either by adding a third component (compatibiliser) capable of specific interfacial and/or chemical reactions with the blend constituents or by blending suitable functionalised polymer(s) capable of enhanced specific interaction and /or chemical reactions [2].

Poly (ethylene terephthalate) (PET) is a very important engineering polyester because of its excellent mechanical properties, heat resistance and chemical resistance. Furthermore, its negligible permeability to CO<sub>2</sub>, mechanical strength, transparency, non-toxic nature, and lack of influence of flavour, have made PET an ideal candidate for use in beverage bottles applications which are increasingly replacing glass bottles. The rapid increase in PET consumption is forecast to continue for a decade [3]. Blends of PET with other polymers, especially polyolefins, for the purpose of property modification, new materials or recycling have received considerable interest [4-8]. Physical blending of these polymers leads to poor mechanical properties due to their incompatibility. Thus, many researchers have directed their efforts to studies of their compatibilisation [4-8]. Reactive blending is one of the widely used approaches. Functional end groups in one polymer or functionalised polymers would react with the appropriate corresponding reactive groups in the second

polymer to form in-situ copolymers during the reactive blending process. The copolymers are located at the interfaces and the interfacial tension can be greatly reduced giving rise to good adhesion which results in enhanced compatibility of the polymer blends.

## **1.2 POLYMER BLENDS**

### **1.2.1 Factors Affecting Performance of Polymer Blends**

Polymer blends are mixtures at least of two macromolecular species, polymers and/or copolymers. Depending on the nature of the blending components, polymer blends can either be miscible, characterised by single phase morphology and exhibiting only one glass transition temperature, or be immiscible. Though quite few polymer pairs have been identified as miscible, most physical blends of different high molecular weight polymers are immiscible [9]. That is when mixed together, the blend components are likely to separate into phases containing predominantly their own kind. Phase separated immiscible blends, exhibiting glass transition temperatures of each blend component, is due to the low entropy of mixing of long polymer chains [10-13]. This characteristics of the immiscible polymer blends however provide the advantage of maintaining some of the individual properties of the blend's components. Their overall performance depends significantly upon the morphology of the blends and the interfacial properties between the blend component phases [11].

Taylor first studied the deformation and disintegration of a single Newtonian drop under the simple shear field [14]. He pointed out that the drop size depended on the interfacial tension between two components, the shear rate, the matrix viscosity, and the viscosity ratio of drop component to matrix component. In the polymer blend system, it is now well established that in addition to composition of the polymer blends, rheological properties and type or extent of interactions between the blend components play a very important role on the morphology of the blends and their interfacial properties [2]. The morphology of polymer blends is also influenced by processing parameters such as temperature and shear rate. For most immiscible polymer blends, the high interfacial tension and the effect of coalescence lead to coarse morphology and sharp interfaces, thus poor adhesion at the interfaces. As a result, physical blending of immiscible polymers often gives rise to poor mechanical properties. It is obvious that satisfactory overall physical and mechanical properties of an immiscible blend should be related to low interfacial tension and strong adhesion between phases. Various compatibilisation techniques have been reported and all

aim to utilize specific interactions between the blend components to achieve a finely dispersed phase and good resistance to gross phase segregation.

## 1.2.2 Compatibility of Polymer Blends

### 1.2.2.1 Definitions of Compatibility

There are a number of definitions for compatibility of polymer blends: (i) miscibility on a molecular scale [10]. Although this is a straight forward clear definition, it has the disadvantage of being confined to compatibility that encompasses only blends showing true thermodynamic miscibility, and thereby excluding a very large number of blends, which may otherwise be considered compatible. (ii) polymer mixtures which are characterised by the presence of a finely dispersed phase and which are resistant to gross phase segregation [2]. Here the satisfactory physical and mechanical properties of an immiscible blend are related to low interfacial tension and strong adhesion between the phases. (iii) blends being considered as compatible when they possess a desirable set of properties (preferably commercially) [11]. In this work, the second definition is adopted throughout.

### 1.2.2.2 Thermodynamics Consideration

Briefly, it is recognised that miscibility between polymers is determined by a balance of enthalpic and entropic contributions to the free energy of mixing according to equation 1 [10-13].

$$\Delta G_{\text{mix}} = \Delta H_{\text{mix}} - T\Delta S_{\text{mix}} \quad (\text{eq. 1})$$

$$\Delta H_{\text{mix}} = V_{\text{ZW}}\Phi_1\Phi_2/V_s \quad (\text{eq. 2})$$

$$\Delta S_{\text{mix}} = -\kappa [N_1 \ln \Phi_1 + N_2 \ln \Phi_2] \quad (\text{eq. 3})$$

where  $\Delta G_{\text{mix}}$  -Gibbs free energy of mixing;

$\Delta H_{\text{mix}}$  - enthalpy of mixing;

$\Delta S_{\text{mix}}$  - entropy of mixing;

T - temperature;

$\kappa$  - the universal gas constant;

$N_i$  - moles of component i;

$\Phi_i$  – volume fraction of component i;

$V_s$  – interacting segment volume;  
 $V$  – the total volume;  
 $w$  – interaction energy;  
 $z$  – coordination number.

For a system to be fully miscible, showing homogeneity by intimacy on a molecular level, the mixing free energy  $\Delta G_{\text{mix}}$  must be negative ( $\Delta G_{\text{mix}} < 0$ ). According to the classical Flory-Huggins theory [12, 13], entropy change on mixing (eq.3) is an inverse function of the molecular weight of each component due to the intrinsic order in a system from limited possible arrangements of linked segment. This will make a negligible contribution to the free energy of mixing. Enthalpy of mixing (eq. 2) is independent of molecular size and is a measure of the energy change associated with the net intermolecular attractions [13]. As a consequence,  $\Delta G_{\text{mix}} \cong \Delta H_{\text{mix}}$ , and miscibility depends entirely on the energetics of intermolecular interaction between the blend components (e.g. H-bonding, ionic, dispersion).

In practice, only few polymers form truly miscible blends characterised by a single  $T_g$  and homogeneity at a 5-10nm scale. Examples include the binary blends of poly(phenylene ether) (PPE)/polystyrene (PS), and poly(vinyl chloride) (PVC)/polymeric plasticisers [15]. The majority of blends are immiscible, i.e. possess a phase separated morphology [2, 16]. Phase separated immiscible blends exhibit glass transition temperature and/or melting temperature of each constituent. However, blends of this type are often preferred over the miscible ones, since they combine some of the important characteristics of both blend constituents. Their overall performance depends not only upon the properties of the individual constituents but depends also significantly upon the morphology of the blends and the interfacial properties between the phases.

### **1.3 COMPATIBILISATION OF POLYMER BLENDS**

In accordance with the previous discussion on miscibility, most polymers do not mix during processing and as a result a sharp interface may occur between the two polymer phases. Their overall performance is related to the size and morphology of the dispersed phase and its stability to coalescence or gross segregation [17]. However, high interfacial tension and lack of interfacial adhesion in immiscible blends lead to coarse and unstable morphology and poor overall physical and mechanical performance. The goal of

compatibilisation is to obtain a stable and reproducible dispersion which would lead to the desired morphology and properties [18].

Compatibilisation of immiscible blends is achieved by: 1) reducing the interfacial tension in the melt, causing an emulsifying effect and leading to an extremely fine dispersion of one phase in another; 2) increasing the adhesion at phase boundaries, giving improved stress transfer; 3) stabilising the dispersed phase against growth during annealing, again by modifying the phase boundaries interface [11].

There are two general routes for improving compatibility [2]:

- (a) By adding a third component (compatibilizer) capable of specific interactions and/or chemical reactions with the blend constituents. Block and graft copolymers and a variety of low molecular weight (MW) reactive chemicals fall under this category. The choice of a block or graft copolymer as compatibiliser is based on the miscibility or reactivity of its segments.
- (b) By blending suitable functionalized polymers capable of enhanced specific interactions and/or chemical reactions. Functionalization can be carried out in solution or in a compounding extruder and may involve the formation of block or graft copolymers, halogenation, sulfonation, hydroperoxide formation, end capping, etc.

Generally, compatibilisation can be achieved by the following approaches [1,2,16]:

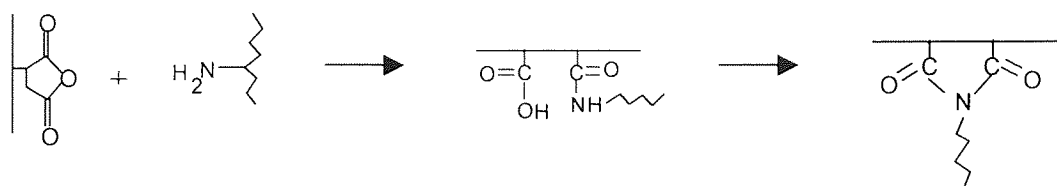
### ***1. Reactive blending***

A comparatively new method of producing compatible thermoplastic blends is via reactive blending, which relies on in situ formation of copolymers or interaction between polymers. This differs from other compatibilisation routes in that the blend components themselves are either chosen or modified so that a reaction occurs during melt blending, with no need for addition of a separate compatibiliser. Table 1-1 shows examples of reactions between various functionalised polymers in the absence of any other catalytically acting compounds. Compatibilising reactions in continuous processing equipment usually involve highly reactive functional groups that are stable under processing conditions. The reaction should be fast and irreversible. Functional groups, such as anhydride, epoxy, oxazoline, are highly reactive and polymers containing those groups are often chosen for reactive blending. Some important

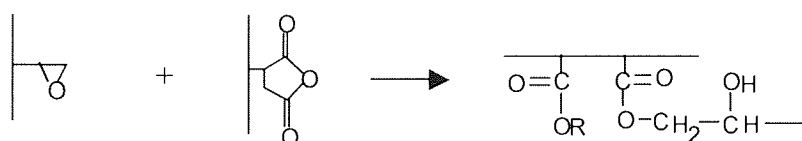


Table 1-1 Examples of common compatibilising reactions between functionalised blend constituents [16]

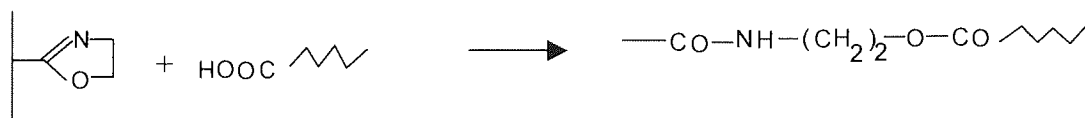
1. Anhydride and amine



2. Epoxy and anhydride



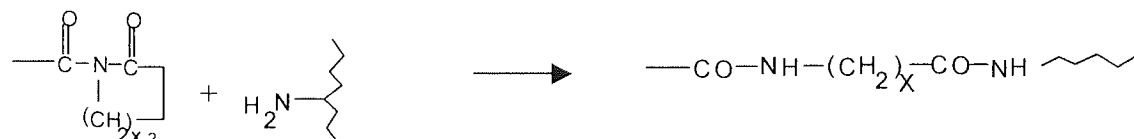
3. Oxazoline and carboxylic acid



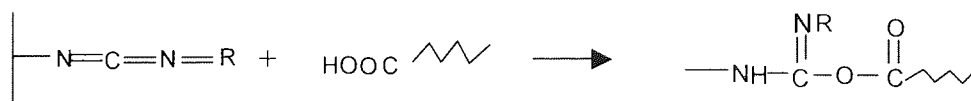
4. Isocyanate and carboxylic acid



5. Acyllactam and amine



6. Carbodiimide and carboxylic acid



7. Zinc salt and zinc salt



8. Radical and radical



Table 1-2 Compatibilisation through the reaction of functionalised blend components [16]

Compatibilising reaction	Polymer blend
Anhydride or carboxyl /Amine	PP-g-MA/PA-6 PP-g-AA/PA-6 EAA/PA-6 EPM-g-MA/PA-6 EPDM-g-MA/PA-6 SMA or PS-g-MA/PA-6 ABS-g-MA/PA-6 SEBS-g-MA/PA-6 PPE-g-MA/PA-6,6 Photooxidized LDPE/PA-6 PA-6/Ethylene-acrylic ester-MA terpolymer
Epoxy/Anhydride or carboxyl	(PPE +SMA)/EVA-co-GMA PBT/Ethylene- acrylic ester-GMA terpolymer
Oxazoline/ Carboxyl	OPS/EAA
Isocyanate/Hydroxyl or Carboxyl	PBT/PCL (isocyanate terminated )
Acyllactam/Amine	EPM-g-acyllactam/PA-6
Carbodiimide/Carboxyl	PBT/PPE ( carbodiimide functionalised )
Transesterification	PC/PBT PC/PAR PC/Phenoxy

compatibilising reactions that can take place easily across polymer phase boundaries are described in Table 1-2.

The reactions between the pendant anhydride group of ‘maleated’ polymers and the terminal amino groups and/or the backbone amide groups of polyamide have been well investigated [19,20]. In recent years, the reactions between functionalised polymers

containing highly reactive groups, such as epoxy and oxazoline, with polymers having carboxyl and hydroxyl groups have received much attention [21-26].

## 2. *Addition of block and graft copolymers (non-reactive copolymers)*

Interfacially active graft or block copolymers of type A-B or A-C may compatibilise the immiscible polymers A and B provided that C is also miscible (at least partly) with B. Block copolymers have been more frequently investigated than graft copolymers, and in particular block copolymers containing blocks chemically identical to the blend component polymers. Copolymer structure and molecular weight have important influences on their effectiveness as compatibilisers and the copolymer should locate preferentially at the blend interfaces. Table 1-3 lists various compatibilised systems that have been studied recently.

Table 1-3 Compatibility through non-reactive copolymer [2]

Major component	Minor component	Compatibiliser
PE or PS	PS or PE	SB, SEP, SIS, S-I-HBD, SEBS, SBS, PS/PE graft copolymer
PP	PS or PMMA	SEBS
PE or PP	PP or PE	EPM, EPDM
EPDM	PMMA	EPDM-g-MMA
PS	PA-6 or EPDM or PPE	PS/PA-6 block copolymers or SEBS
PET	HDPE	SEBS
PF	PMMA or PS	PF-g-MMA or PF-g-S
PVDF	PS/PPE	PS/PMMA block copolymers
PVC	PS or PE or PP	PCL/PS block copolymer or CPE
SAN	SBR	BR/PMMA block copolymer

Table 1-4 Compatibilisation through reactive copolymers or functionalised polymer added separately [2]

Compatibilising reaction	Polymer blend	Compatibiliser
Anhydride or carboxyl / Amine	PP or PE or EPM/ PA-6 or PA-6,6 ABS/PA-6  ABS/(PA-6-co-PA-6,6 PA-6/Acrylate rubber (hydroxyl modified) PPE/PA-6,6 or PA-6 PPE/PA-6,6  PBT/PA-6	PP-g-MA, PP-g-AA,EAA, EPM-g-MA, ionomers PMMA-g-(carboxyl modified acrylic) SAN-co-MA SMA  SEBS-g-MA EPM-g-MA + epoxidized EVA PS-co-MA-co-GMA
Oxazoline/ Carboxyl	PPE/EAA	OPS
Epoxy/Carboxyl or hydroxyl or anhydride or amine	PPE/PBT NR/PE PBT/PA-6	PS-g-(epoxy modified PS) PE-g-MA/ENR PCL-co-S-co-GMA
Interchain salt formation	(PS+PPE)/Sulfonated EPDM zinc salt (PS+PPE)/EPM-g-diethyl vinyl phosphonate	Sulfonated PS zinc salt  Sulfonated PS zinc salt & zinc stearate

### 3. Addition of functional polymers (reactive polymers)

The addition of functional polymers as compatibilisers has been studied by many workers. Usually, a polymer chemically identical to one of the blend components is modified to contain functional (or reactive) units, which have some affinity for the second component; this affinity is usually the ability to chemically react with the second blend component, but other types of interactions (e.g. ionic) are possible. Table 1-4 shows examples of recently studied systems that are compatibilised through reactive polymers. The reactions in these ternary polymer systems are the same as

those presented in Table 1-1. Reactive blending (polymers containing highly reactive groups such as epoxy, anhydride and oxazoline) is a widely used route to compatibilise engineering plastics blends [27-50].

#### 4. *Addition of low molecular weight (MW) compatibilising compounds*

The addition of low MW compounds in a polymer blend may promote compatibility through the formation of copolymers (random; block, graft) or through the combined effects of copolymer formation and crosslinking. Low MW compounds are usually added at relatively low concentrations (typically 0.1 to 3 wt%) [2,16].

### 1.4 COMATIBILISATION OF POLY(ETHYLENE TEREPHTHALATE), PET, BLENDS

#### 1.4.1 PET Property Profile

Poly(ethylene terephthalate) (PET) is a polycondensation polymer that is most commonly produced from a reaction of ethylene glycol with either purified terephthalic acid or dimethyl terephthalate, using a continuous melt-phase polymerisation [51]. It has a regular linear structure with the connecting ester carbon bonds attached directly to the aromatic ring in the backbone of the molecular chain. It has the repeat unit as shown in Figure 1-1.

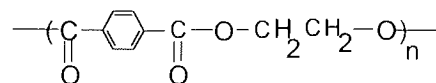


Figure 1-1 The chemical structure of poly(ethylene terephthalate)

PET is a crystallisable polymer whose morphology can vary widely depending on the fabrication process. The polymer can be obtained as a “glassy” or “amorphous” transparent solid by rapidly quenching the melt below the glass transition temperature,  $T_g$  [52]. The glass transition temperature,  $T_g$ , depends on the degree of crystallinity and the technique of measurement and is reported in the range of 70~120°C [53]. Its melting temperature is about 255°C. PET is widely used in synthetic fibres, films, blow-moulded containers and injection-moulded engineering components. The merits of PET fibres are their relatively high melting and glass transition temperature, insensitivity to moisture and common solvents, and the wide range of mechanical properties attainable by variations of molecular weight, orientation, and crystallinity, giving characteristics suitable at one extreme for uses

in apparel, curtains, upholstery, and fiberfill, and at the other, for industrial applications such as sewing threads, tyre cords, and filter fabrics [53]. Besides its wide use in fibres, the consumption of PET in films, packaging, electrical insulation and beverage bottles has increased rapidly [3].

#### **1.4.2 PET Blends**

Blends of PET with other polymers, especially polyolefins, for the purpose of property modification, new materials or recycling have received considerable interest [4-8]. The incompatibility of polymers has resulted in studies of different compatibilisation techniques: physical compatibilisation utilizing a pre-made copolymer as the compatibiliser and chemical compatibilisation with an in situ reactive compatibiliser [2,16]. In the case of physical compatibilisation, a block or a graft copolymer is used and this typically contains blocks or grafts identical to, or miscible with, the base polymers of the blends. Such a copolymer is preferably located at the interfaces, in order to reduce the interfacial tension, help the dispersion of the minor phase in the matrix, enhance the interfacial adhesion and stabilise the morphology. A major drawback of this 'ex-situ' compatibilisation method is that each polymer blend requires a specific copolymer, whose preparation is often tedious and costly. Also, for dynamic and thermodynamic reasons, there are always some copolymer chains which can not get to the interfaces where they are most needed. Dispersion of the copolymer in a polymer matrix is not easy and its diffusion to the interfaces is often slow. The copolymer may also form micelles useless for compatibilisation [46]. It has been found that the molecular weight (MW) of a copolymer, the copolymer's structure and composition, and the interfacial concentration of the copolymer are the key parameters influencing on the interfacial properties, and thus the blend morphology [34].

In order to avoid these shortcomings, reactive blending techniques has been widely used in compatibilisation of different polymer blending systems [27-50]. In this compatibilisation method, desired copolymers are produced through interfacial reactions between reactive polymers directly during blending. The morphology of incompatible polymer blends with an in-situ compatibiliser becomes very fine, since copolymers formed by the reaction between functional groups existing in constituent components in the blend can reduce the interfacial tension between the dispersed phase and the matrix. This finer morphology can

persist even at higher shear stresses [33,34]. In-situ, or reactive, compatibilisation is more attractive and cost-effective because it allows the formation of compatibilisers in-situ at the interfaces without separate preparation step. When two polymers are to be compatibilised and only one contains functional groups and the other one is chemically inert with respect to it, the latter will have to be functionalised. Otherwise, a functional copolymer, which is compatible with the latter one and bears reactive groups capable of chemical reaction with the former polymer must be added to the blend.

The ester groups in the main chain of PET have a high potential for specific interreactions. For example, polyester may interact via hydrogen bonding with hydroxyl groups. Polyester may give rise to interchange reactions in blends with other polycondensation polymers during mixing or processing in the molten state. A widely commercially available blend system which relies on this transesterification reaction to improve the compatibility is based on a polyester/polycarbonate polymers, e.g. PET/polycarbonate and PBT (poly(butylenes terephthalate) )/polycarbonate [18]. Another important characteristics of the chemical structure of polyester polymers like PET and PBT is that they contain two types of terminal groups: carboxylic and hydroxyl. These functional groups are very useful for reactive compatibilisation since they can readily react with a number of reactive functions, such as anhydride, epoxy, oxazoline, isocyanate and carbodiimide which become attached onto the polymer backbones leading to graft copolymers during melt blending [16]. This approach has gained great success for the in situ compatibilisation of PET or PBT blends with polyethylene [7,10,32,36,49,54-56], polypropylene [26, 29-31, 40,41,45-48,57-62], polystyrene [33-35,50], EPDM [22,23,63]. It was reported that polyester related reactive compatibilised blends were currently the second largest group after the polyamide related blends [64].

#### **1.4.2.1 Impact Modification**

Although polar engineering thermoplastics such as polyamides, polyesters and polycarbonate are tough in an unnotched state, they tend to be notch-sensitive and stress concentration can cause the fracture mode to change from ductile to brittle [4]. Impact-modified version of these thermoplastics have been developed by rubber-toughening without seriously compromising other properties. A number of commercial alloys and blends have been developed, based on this class of polymers [65]. Tanrattanakul et al. [4,5] studied the toughening of PET by blending with a functionalised SEBS block copolymer.

SEBS was a triblock copolymer with styrene end blocks and a functionalised ethylene/butylene mid block. The mid block was grafted with 0—4.5 wt% MA. It was found that particle size was strongly dependent on the elastomer functionality: the higher the functionality, the smaller the particle size and the narrower the particle size distribution. It was proposed that a graft copolymer by reaction of PET hydroxyl end groups with maleic anhydride was formed in situ and the graft copolymer acted as an emulsifier to decrease the interfacial tension and reduce the tendency of the dispersed particles to coalesce, hence promoting adhesion between phases in the blend. Evidence for the presence of a graft copolymer was obtained by IR analysis of blend extracts. A detailed study on impact modification of PBT by using acrylonitrile-butadiene-styrene (ABS) and methyl methacrylate-glycidyl methacrylate-ethyl acrylate terpolymers has been conducted by Hage et al [37-39, 66]. They found that PBT could be impact modified by blending with appropriate ABS materials within a limited range of processing conditions. However, the morphology of these uncompatibilised blends was unstable and the dispersed phase became coarser when the melt was subjected to low shear conditions, e.g. during certain moulding conditions, which had a deleterious effect on the final blend properties. Methyl methacrylate, glycidyl methacrylate, and ethyl acrylate terpolymers (MGE) have been used as compatibiliser for blends of PBT with ABS or styrene-acrylonitrile copolymers (SAN) resulting in improvement in the dispersion of SAN or ABS and morphological stability [38]. It was demonstrated that at least 5% GMA in the terpolymer (0.25% GMA total in blend) was required to achieve significant reduction in particle size, however, the particle size was not reduced much further as the GMA content was increased beyond this level. Compatibilised PBT/ABS blends showed greatly improved low temperature toughness with a small loss in room temperature impact strength. Model compounds were also used to investigate the potential reactions of the hydroxyl and carboxyl end groups of PBT with epoxides that may create graft copolymers at the interface during melt processing conditions [38]. Such graft copolymers strengthen the interface between domains, but perhaps more importantly reduce interfacial tension and provide steric stabilisation to reduce rate of coalescence, all of which shift the balance between drop break up and coalescence to giving a finer dispersion and more stable morphology. Additionally, the grafting reactions increase the blend viscosity which can aid in the dispersion of ABS dispersion but may compromise some melt processing features of such blends. Possible reactions between epoxide units with PBT hydroxyl and carboxyl end groups are shown in Scheme 1-1. Evidence from blending ethylene-glycidyl methacrylate





### 1.4.2.2 Compatibilisation of PET/PE Blends

The steady growth in plastic materials used for packaging applications has caused increased environmental concern and the problems of solid waste disposal [32]. Post-consumer recycling of plastics has therefore become not only necessary but also increasingly mandatory. Blends with polyesters, especially blends of PET with polyolefins (e.g. PE, PP) are of particular interest because large amounts of these polymers are available through recycling technology, and because PET is widely used as a thermoplastic for packaging, electronics, beverage bottles, and other applications [67]. Thus, a large volume amount of post-consumer PET materials is available for recycling. In the area of polymer blends, the challenge is to recycle mixed plastics, but at the same time to maintain an acceptable level of properties and cost. In general, high performance properties such as high impact strength, and ductility, solvent and heat resistance are highly desirable in polymer blends and result in enhancing their value and application potential. However, in order to develop such high performance blends from recycled polymers, it is essential to have not only acceptable quality of the feedstocks but also have effective methods for the compatibilisation and toughening of the blends.

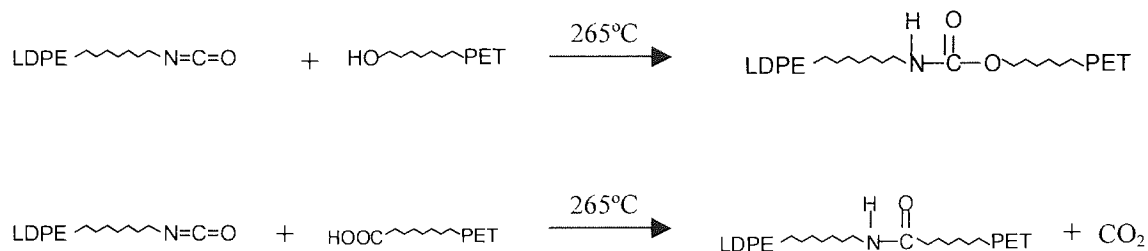
Much research has been conducted on the compatibilisation techniques of PET/PE blends [7,9,32,49,54-56] and considerable success has been achieved. Kalfoglou et al. [63] carried out comparison of effectiveness of compatibilisers for PET/HDPE blends using ethylene-GMA copolymer (E-GMA), ethylene ethylacrylate-GMA terpolymer (E-EA-GMA), hydrogenated styrene-butadiene-styrene copolymer-grafted with MA (SEBS-g-MA) and MA-modified ethylene-methylacrylate copolymer (E-MeA-g-MA). On the basis of morphological evidence and tensile testing, the compatibilising effectiveness was found to decrease in the sequence: E-GMA > E-EA-GMA > SEBS-g-MA > E-MeA-g-MA. The reactivity of GMA was shown to be higher than that of MA contained in these compatibilisers. Spectroscopic investigation of the blends was carried out to establish the reaction of glycidyl epoxy groups of the compatibiliser (E-EA-GMA, E-GMA) with the PET end groups (-COOH, -OH). The study of PET/E-GMA binary blends by using FTIR showed that the oxirane absorption at  $912\text{ cm}^{-1}$ , (corresponding to GMA epoxy groups from E-GMA), disappeared and the peak ratio  $874\text{ cm}^{-1}/846\text{ cm}^{-1}$  of pure PET was altered in the blends, indicating the formation of a new chemical species. The effectiveness of E-GMA in the compatibilisation of PET/PE blends has also been demonstrated by Akkapeddi et al. [32] and Pietrasanta et al. [36]. The E-GMA copolymer itself was found to form

fairly miscible blends with polyolefins (HDPE, LDPE, EPR) without any detectable phase separation. However, owing to the presence of high GMA content (8%) in the copolymer, a high level of coupling reaction took place between PET and E-GMA, resulting in a substantial increase in the melt viscosity and some entrapment of E-GMA as dispersed micelles inside PET. In a typical PET/LDPE blend (50/40), addition of 10% E-GMA caused a reasonable level of compatibilisation between PET and LDPE, but the increased viscosity of PET resulted in a phase inversion. Accordingly, the morphology of such blends indicated fine dispersion of PET in the LDPE matrix. It was believed that the extent of reaction and phase inversion could be reduced by using an E-GMA copolymer of low GMA comonomer content [32]. The elongation at break and the notched Izod impact strength of PET/PE blends were improved upon the addition of 10-15% E-GMA as a reactive compatibiliser, compared with the uncompatibilised blends [32].

Chen et al. used EPR and SEBS (styrene-ethylene-butylene-styrene block copolymers) functionalised with minor amount of acid groups to toughen PET/HDPE blends from recycled beverage bottles [56]. It was concluded that a small amount of suitable elastomer made the PET/HDPE blend a super tough plastic. Functionalised SEBS had much better compatibilisation effect on this blend. PET/PE blends were toughened using SEBS, maleic anhydride functionalised SEBS (MA-g-SEBS) and maleic anhydride functionalised PE (MA-g-PE). It was found that SEBS did not improve the toughness of the blends but MA-g-SEBS had the highest toughening effect giving rise to a considerable improvement in elongation at break. The addition of MA-g-PE to the blends had also improved the toughness but it was not as effective as MA-g-SEBS. It was suggested that although in the case of both compatibilizers (MA-g-PE and MA-g-SEBS) reactions of PET end groups with grafted anhydride groups took place, it was the higher viscosity of the MA-g-PE which was responsible for the difficult mixing of the two phases.

Another route to compatibilise PET/LDPE blends is to utilise reaction between an isocyanate ( $-N=C=O$ ) functionalised LDPE with PET during melt blending [49]. LDPE was grafted with 2-hydroxyethyl methacrylate-isophorone diisocyanate (LDPE-g-HI) in solution and then blended with PET. The chemical reaction took place in the melt blending of PET/LDPE-g-HI blends and was confirmed by its IR spectra. The morphology and mechanical properties of PET/LDPE-g-HI were much better than for uncompatibilised

PET/LDPE blends with. The following reactions were proposed to take place (see Scheme 1-2).



Scheme 1-2 Possible reactions between LDPE-g-HI and PET hydroxyl and carboxyl end groups during reactive blending [49]

### 1.4.2.3 Compatibilisation of PET/PP Blends

Blending of PP with engineering thermoplastics has been an effective way to improve the properties of PP. For example, PP/polyamide blends are intensively investigated in the literature [42,43,68,69]. Considerable work has also been focused on blending polyester with PP and reactive compatibilisation techniques have been adopted to compatibilise PET/PP and PBT/PP blends.

Maleic anhydride functionalised SEBS block copolymers were also used as compatibilisers in PET/PP blends [6]. The effects of the compatibilisers could be evaluated by studies on their morphology and mechanical, thermal and rheological properties. The addition of 5 wt% of unfunctionalised SEBS copolymer was found to stabilise the blend morphology and improve impact strength. The effect was, however, far more pronounced with SEBS functionalised with MA (SEBS-g-MA) and GMA (SEBS-g-GMA). SEBS-g-GMA was found to be a more effective compatibiliser than SEBS-g-MA. This was observed in particular for PET-rich blends, which showed significant improvement in toughness combined with relatively high values of strength and modulus. Lepers et al. studied how the relative role of coalescence suppression and interfacial tension reduction influenced the particle size at various level of in situ compatibilisation of PET/PP blends in the presence of maleic anhydride functionalised SEBS [45,60].

A series of studies carried out by Hu et al. showed a great success for the in situ compatibilisation of PBT/PP blends by using free radical grafted PP with glycidyl methacrylate (GMA) (PP-g-GMA) and oxazoline (PP-g-OXA) as reactive compatibilisers [29-31,46,61,62]. PP-g-GMA and PP-g-OXA were prepared by free radical grafting of GMA and oxazoline on to PP in a screw extruder or an internal mixer. The epoxy and oxazoline groups attached to the polymer backbone can readily react with the terminal carboxyl group of the PBT giving rise to graft copolymers thus resulting in the compatibilisation of PBT/PP blends [46]. For example, the addition of PP-g-OXA compatibilises PBT/PP blends and results in significant improvement in morphology, impact strength and tensile properties. The particle size of the dispersed phase (PBT) in PBT/PP (30/70 w/w) blends was reduced from 2-5 to 0.5-1  $\mu\text{m}$  when PP-g-OXA was added, and the notched impact strength and the elongation at break exhibited an approximate three fold and eightfold increase respectively with the addition of PP-g-OXA.

Dynamic mechanical properties of the blends were examined to identify changes in glass transition behaviour of the blend components. It was suggested that if specific interchain interaction existed, then a clear shift in temperature corresponding to the peaks of loss modulus, reflecting the glass transition ( $T_g$ ) of blend components, and/or change in the intensity of the peaks of the loss modulus vs temperature curve might be noted. The results showed that an increase in the amount of PP-g-OXA in the blends resulted in decrease in  $T_g$  of the PBT phase [62]. For example, in PP/PBT blend containing 20 wt% of PP-g-OXA a  $T_g$  of 42.2°C for PBT phase was observed, while in the uncompatibilised blend, the  $T_g$  of the PBT phase was 48.5°C. It was also shown that the functionalisation of PP with GMA or oxazoline and the compatibilisation of PBT/PP blends could be performed by one-step reactive extrusion [30,61]. A model kinetic study showed that the reaction between oxazoline and carboxylic functionalities is very fast [29,62]. Cartier et al. investigated the effects of the molecular structure of GMA functionalised PP on the compatibilisation of PBT/PP blends in a co-rotating twin screw extruder [46]. In this study, two series of PP-g-GMA were used: the first was based on PP-g-GMA having the same molecular weight but different GMA contents, while the second series of PP-g-GMA had the same GMA content but different molecular weight. The compatibilising efficiency of the two series of PP-g-GMA had been examined in terms of morphology and mechanical properties of the blends. It was found that for the first series, the higher the GMA content (in the PP-g-GMA), the smaller the PBT particle size and the higher

elongation at break and impact strength. For the second series containing the same amount of GMA, the higher the molecular weight, the higher the compatibilising efficiency. Although the correlation between the mechanical properties of an in situ compatibilised PP/PBT blend, its morphology and the interfacial adhesion is not always obvious, a reduction in particle size of the PBT phase was shown to be always accompanied by an increase in elongation at break and impact strength [46].

Pang et al. used three maleic anhydride-grafted-polypropylene derivatives [N,N-dihydroxyethyl monomaleic amide, octodecyl monomaleate, and 2-(N,N-dihydroxyethylamino) ethyl monomaleate] to compatibilise PP/PET blends [60]. They found that the compatibilising effects of three PP grafts were very different and strongly dependent on the functional groups present. 2-(N,N-dihydroxyethylamino) ethyl monomaleate grafted PP produced the finest dispersed phase morphology, whereas octodecyl monomaleate grafted PP had little compatibilising effect. The reasons for this was the difference in the structure of the grafted functional groups. It was explained that the best compatibilising effect of 2-(N,N-dihydroxyethylamino) ethyl monomaleate grafted PP resulted from the fact that it contained an extra tertiary amine functional group. This group was beneficial for increasing the interactions between PP and PET phases because it increased the polarity of the compatibiliser, thus may form a salt with carboxyl end groups of PET. A maleic anhydride grafted PP was also blended with PET and improvement of the phase morphology in PET/PP-g-MA than PET/PP blend was observed [60].

It was mentioned earlier that ethylene-co-glycidyl methacrylate (E-GMA) is a very effective reactive compatibiliser in PET/PE blends. Similarly, E-GMA was also used to compatibilise PBT/PP blends [41]. Higher GMA content in the E-GMA copolymer or a higher quantity of E-GMA in the PBT/PP blends resulted in a better compatibilised blends in terms of finer phase domains, higher viscosity, and better mechanical properties. The presence of only 50 ppm catalyst (ethyltriphenyl phosphonium bromide) in the E-GMA compatibilised blend further improved the blend compatibility substantially. The copolymer of polypropylen-co-acrylic acid [57, 58] and a terpolymer [40], ethylene-ethyl acrylate/glycidyl methacrylate, were found to be effective in compatibilising PET/PP blends and PBT/PP blends respectively.

#### 1.4.2.4 Compatibilisation of PET Blends with EPR or PS

Toughening of PBT was achieved by addition of maleic anhydride functionalised ethylene-propylene rubber (EPR) [63]. The in situ formation of a graft acting as an interfacial agent had been indirectly demonstrated by DSC analysis of the insoluble fraction recovered from PBT/EPR-g-MA blend using selective extraction to dissolve both EPR and PBT phases. A small peak corresponding to pure PBT melting point was observed (by DSC) in the insoluble fraction. Compatibilised and dynamically vulcanised thermoplastic elastomer blends of PBT and EPDM could be prepared by using a GMA functionalised EPDM [23]. During melt mixing the epoxy groups react with PBT end groups to form graft copolymer. The compatibilised blends can be dynamically vulcanised by conventional vulcanisation agents for EPDM such as a peroxide, e.g. 2,5-dimethyl-2,5-bis(t-butyl peroxy)hexane, or by vulcanisation agents that react with residual epoxy groups on the EPDM such as diamines, e.g. 6-amino hexyl carbamic acid. Compatibilisation with EPDM-g-GMA improved significantly the tensile properties of the blend compared to unfuctionalised EPDM. As a new class of thermoplastics, dynamically vulcanised plastics/rubber blends have gained importance in recent years due to the ability to be melt processed as thermoplastics and the behaviour at ambient temperatures to be like an elastomer [70].

In the compatibilisation of PBT/polystyrene (PS) blends, poly(styrene-ran-GMA) (PS-GMA) was used as a compatibiliser and the blends were prepared by both melt and solution blending methods [33,34,35]. The concentration of in situ formed graft copolymers (PS-g-PBT) via the reaction of epoxy group in the PS chains with the end groups of PBT was quantitatively determined by solvent extraction followed by Fourier transform infrared spectroscopy (FTIR) analysis [35]. On the basis of FTIR and high-temperature gel permeation chromatography (GPC), it was concluded that the PS-g-PBT graft copolymer in the blends had 1.3-2 PBT chains grafted onto every PS-GMA chain. It was also proposed that only small amount of in situ formed graft copolymers (~2%) was enough to stabilise the blend morphology [35]. Even if a large amount of PS-PBT graft copolymer was obtained in melt blended samples, it was not guaranteed to be located at the interface. Some parts of in situ formed graft copolymers existed in the matrix as micelles with sizes of 20-50 nm.

In summary, PET and PBT blends with polyolefins and other polymers can be successfully compatibilised via reactive blending to achieve the desired phase morphology and mechanical properties. The compatibilisation methods may be classified into two groups: (1) the use of functionalised blend components that produce in situ compatibilising interchain copolymers. These include different functionalised polymers with different functional monomers such as maleic anhydride, glycidyl methacrylate, oxazoline. mainly using free radical grafting. (2) the use of specially synthesised copolymers such as E-GMA, E-EA-GMA, MGA. which contain functional groups capable of specific reaction with the end groups of polyester polymers. All those reactive compatibilisation systems utilise the specific reaction between the terminal groups of PET or PBT (carboxyl ( $-\text{COOH}$ ) and hydroxyl ( $-\text{OH}$ )) and functional groups from the blending components or addition of compatibilisers as listed in Table 1-1, Scheme 1-1 and Scheme 1-2. These reactions lead to in situ formation of graft copolymers during the melt blending. Such copolymers can reduce the interfacial tension, help the dispersion of the minor phase in the matrix, enhance the interfacial adhesion and stabilise the morphology hence achieve the desired mechanical properties. Among these functional groups, epoxy groups from GMA exhibit the best reactivity and best compatibilisation effect in different blending systems. It can be concluded that either GMA-functionalised polymers or GMA-containing copolymers are the best candidates for the reactive compatibilisation of PET or PBT blends.

### **1.5 FREE RADICAL GRAFTING REACTIONS FOR POLYMER FUNCTIONALISATION**

Chemical modification of existing polymers is important since it provides an inexpensive and rapid way to obtain new polymers without having to search for new monomers and this is widely achieved through free-radical grafting. This typically involves reaction of a polymer with a vinyl-containing monomer or a mixture of monomers capable of forming grafts onto the polymer backbone. If the grafts are long, the modified polymer becomes a true graft copolymer, of which the properties will be very different from those of the original polymer substrate. When the grafts are short with less than, say, five moieties, most of the physical and /or mechanical properties of the original polymer substrate will be retained. However, the chemical properties of the modified polymer may become quite different, this often being the ultimate objective. For example, the GMA or oxazoline



functionalised PP has been used successfully as a reactive compatibiliser in blends of PBT/PP [29-31,46,61,62 ].

A free-radical grafting system usually contains three types of reactants: polymer, unsaturated molecule, such as vinyl monomer, and free radical initiator. Irrespective of their nature, a typical free-radical grafting scheme can be represented by Fig.1-2 [73]. Primary free radicals ( $R^*$ ) are generated by some mechanism of initiator decomposition ( $k_a$ ) in the presence of monomer (M) and polymer. A primary free radical thus formed may follow two completely different reaction pathways, with one leading to undesired homopolymerisation ( $k_{pi}$ ) and the other one desired grafting ( $k_H$ ). When it reacts with a monomer molecule ( $k_{pi}$ ), the undesired homopolymerisation is initiated forming a monomer radical ( $RM^*$ ). If this monomer radical continues to react with more monomer molecules ( $k_p$ ) an oligomer or polymer will be formed. The grafting of this oligomer or polymer onto the desired polymer backbone rarely occurs because a propagating monomer radical usually has a limited hydrogen abstracting capacity unless it is very reactive, such as the vinyl acetate radical. On the other hand, when the primary free radical undergoes transfer with the polymer upon abstracting a hydrogen from the polymer backbone ( $k_H$ ) a macroradical is then formed. This macroradical may lead to one of the following three reactions, the probability of which depends on its structure: chain scission ( $k_s$ ), crosslinking ( $k_c$ ) and grafting ( $k_{gi}$ ). When the macroradical reacts with a monomer molecule, this monomer is then grafted (or fixed) onto the polymer backbone forming a branched macroradical ( $k_{gp}$ ). This branched macroradical may continue to react with more monomer molecules forming longer grafts ( $k_{gp}$ ). It may also undergo transfer with a hydrogen atom of the same or another polymer backbone forming a new macroradical ( $k_{Hi}$ ). The macroradical transfer can be important step for grafting as the newly formed macroradical is expected to repeat the grafting cycle desired above, yielding more grafts. Of course, various termination reactions may occur.

The use of batch mixers or screw extruders as chemical reactors means that the free-radical grafting reaction would takes place without a solvent. There are three particular features related to melt free-radical grafting: elevated temperature, high viscosity and heterogeneity. Owing to the absence of a solvent, melt free-radical grafting should be carried out at temperatures 50—150°C higher than those frequently employed for solution free-radical grafting. Grafting temperatures usually exceed 150°C and can be as high as

300°C. On the other hand, due to the high viscosity, it would be difficult to disperse small fractions of low-viscosity monomers and peroxides into high viscous polymer melt. These features give rise to tremendous challenges to melt free-radical grafting in terms of reactivity, selectivity and process control.

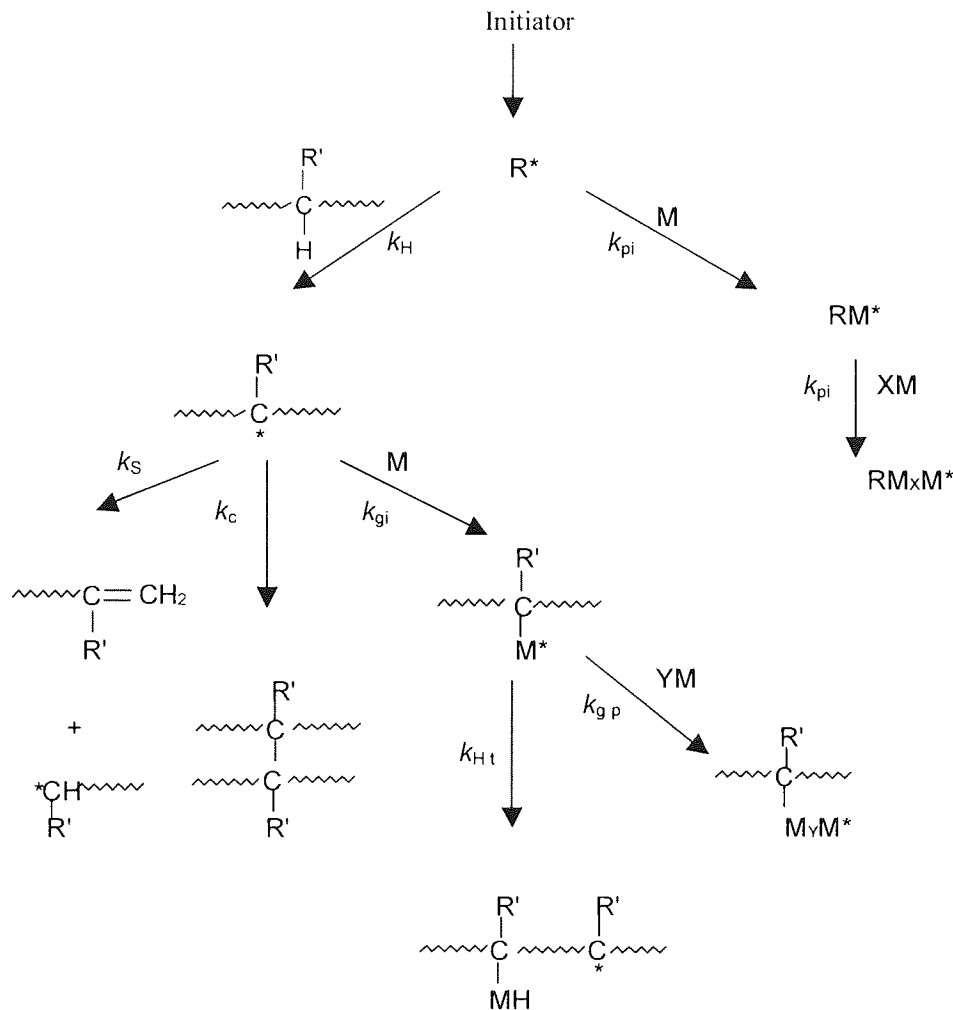


Figure 1-2 Overall scheme of free-radical grafting onto a polymer backbone

## 1.6 FUNCTIONALISATION OF POLYMERS VIA REACTIVE PROCESSING

A wide range of vinyl monomers have been successfully grafted onto a number of polymer substrates by free radical chemistry. The most widely used monomers are maleic anhydride (MA), glycidyl methacrylate (GMA), oxazoline, and diethyl maleate (DMA) due to the high reactivity of their functional groups. The grafting of these monomers onto various types of polymers, mainly polyolefins, can greatly promote the functional and/or mechanical properties of the polymers. Polyolefins such as polypropylene (PP) and

polyethylene (PE) have been preferred as polymer substrates for these functionalisation because of their ready availability, low cost versatile properties and growing commercial applications but lack of chemical functionality. Introduction of these functional groups onto the chains of these polymers can significantly improve their compatibility with other polymers, their paintability, adhesion to metal or glass [73].

### 1.6.1 Grafting Maleic Anhydride (MA) onto Polymers

Maleation is one of the most widely used methods for the functionalisation of polymers, especially for reactive processing. Maleations take advantage of the dual-functionality of MA (see Fig 1-3)—the ‘ene’ or radically active double bond and the nucleophilically reactive anhydride or ester group [76]. MA can be grafted onto either saturated or unsaturated polymers under a variety of conditions [77]. Table 1-5 lists some studies of functionalisation of polymers with MA.

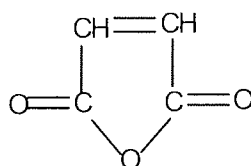


Figure 1-3 Chemical structure of MA

MA is known to add readily to natural rubber (NR) or polyisoprene at elevated temperatures or in the presence of free radical initiators in solution [78-82]. This reaction can be carried out in the solid state by thermal initiation and mastication [78,82-85]. Farmer et al. [80] studied the reaction of MA with the rubber by heating a solution of MA with natural rubber in the presence of benzoyl peroxide and a series of addition products were obtained. These varied from rubbery to fibrous products containing increasing concentration of MA. Bras [83,84] studied the same reaction by passing a mixture of MA and natural rubber between the tight rolls of a cold mill. Pinazzi [86,87] studied the reaction of natural rubber and MA and other ethylene monomers, such as imide N-methylmaleic, maleic acid, fumaric acid with different radical initiators in solution. It was found that the reaction could also be carried out at high temperature (180–240°C), along with a considerable excess of MA. The products obtained by thermal and free-radical initiation were shown not to be the same [87]. Infrared spectra of the products obtained by thermal initiation showed up particular bands to indicate that a portion of the double

bonds have been isomerised (formation of vinylidene double bonds outside the main chain).

Considerable efforts have been made to graft MA onto saturated polymers, particularly onto polyolefins, such as PE, PP, EPR, EPDM and ABS. This is due to the lack of reactive groups in these polymers that limits many of their end-uses, particularly those in which adhesion, dyeability, paintability or reactivity with other polymers is needed. Most of the studies were conducted by melt free-radical grafting in mixers or extruders [88-106].

A comprehensive review on the free-radical grafting of monomers onto polymers has been written recently by Hu et. al. [73]. These workers have pointed out that one of the most important challenges facing melt free-radical grafting was to obtain a sufficient amount of grafted MA onto the polymer backbone while retaining the mechanical properties and thus the molecular weight of the virgin polymer. These studies revealed that a major problem for melt free-radical grafting of MA onto PP is the serious competition between the desired grafting reaction and the undesired degradation of the polymer by  $\beta$ -scission. For higher MA grafting yield, a higher peroxide concentration is needed giving rise to more severe PP chain degradation.

Hogt [88] carried out melt free-radical grafting of MA onto PP in a Berstorff 25 mm co-rotating twin screw extruder using 1,3-bis(t-butyl peroxyisopropyl) benzene (DTBPIB). It was found that although an increase in the peroxide concentration increased the MA grafting yield (the magnitude of increase reduced with increasing peroxide concentration) it also caused further PP degradation. When 2 phr MA and 1phr DTBPIB were added, only 0.4 phr (i.e. 20 %) of the total MA was grafted, and the PP thus modified was highly degraded with an MFI greater than 1600 g per 10 min (230°C and 2.16 kg). Roover et al. [89] and Bettini et al. [90] studied the grafting of maleic anhydride onto PP in a batch mixer in the presence of an organic peroxide. Both of them concluded that grafting of maleic anhydride is always associated with molecular weight decrease. The maleic anhydride and peroxide concentrations were those that affected most the level of grafting and the extent of degradation in PP. The increase in peroxide concentration resulted in an increase in grafting yield and in MFI. The increase of initial maleic anhydride concentration led to an increase of grafting yield, passing through a maximum value, with posterior decline.

In the case of PE, EPR, or EPDM polymers, most studies revealed the difficulty of reaching a high monomer grafting yield along with an acceptable degree of cross-linking. Liu et al. have successfully grafted maleic anhydride onto low density polyethylene in dichlorobenzene at a temperature of 160°C in the presence of a peroxide [94]. The grafting yield of maleic anhydride increased with increasing concentration of maleic anhydride and peroxide. Meanwhile, the MFI of grafted PE dramatically decreased, indicating the crosslinking of PE during the grafting reaction. Wu et. al. studied the grafting of MA onto EPR using an internal mixer [103]. The gel content increased up to 50 wt% with increase in MA and Dicumyl peroxide (DCP) concentrations. Gaylord investigated degradation and cross-linking of EPR and LDPE on reaction with MA [105]. Three different peroxides were used. The analysis results showed that considerable crosslinking had occurred.

Oostenbrink et. al. [29] studied the melt grafting of MA onto EPDM in a co-rotating twin screw extruder using DTBPIB as the free radical initiator. It was observed that the grafted MA content increased strongly with increasing initiator concentration, and with increasing added MA amounts, the grafted MA content increased to a maximum (4% initially added MA) and then decreased with further increase of MA initially added.

Coutinho [34] investigated the optimisation of reaction conditions for grafting MA onto EPDM using a Brabender-like rheometer Rheomix 600 of Haak system 40. It was found that for a fixed initiator concentration the main process control variables were shear rate, mixing temperature, and MA concentration. High amount of gel was also formed during the reaction.

In an attempt to minimise the oxidative degradation of PP or crosslinking reaction of PE without compromising the level of grafting different approaches were used including 'electron-donating' organic additives such as dimethylformamide (DMF) and dimethylacetamide (DMAC) [107-112]. It was found that although the extent of PP degradation and PE cross-linking was reduced, the grafting yield of MA was also reduced. Recently, Lambla et al. [73] reported that addition of styrene as a comonomer not only allowed an increase in the grafting yield of MA but also led to a reduction of PP degradation. Maleic anhydride has also been successfully grafted onto other polymer including ethylene vinyl acetate (EVA) [95], high impact polystyrene (HIPS) [96], and

Table 1-5 Functionalisation of Polymers with MA

Polymer to be modified	Mixer or extruder type used, or solution	MA initially added	Peroxide type	Peroxide concentration	MA grafted	Gel (%)	Ref.
NR	Cyclohexanone solution (80°C)	25-100 mol%	BPO				79
	P-xylene solution (115°C)	25-100 mol%	BPO				
NR	Toluene solution (100°C)		BPO				80, 82
NR	Cold mill	5-10 phr	No peroxide			90%	83, 84
NR	Xylene or chloronaphthalene solution		No peroxide (180-240°C)				86
			AIBN (130°C)				
PP	Berstorff 25mm TSE	2phr	DTBPIB	1 phr	0.4 %		88
PP	Haake Rheocord mixer/ Werner & Pfleiderer ZSK-30 TSE	MA alone 5phr	DTBPIB	0.5phr	0.6phr		73
		MA +St 10phr	DTBPIB	0.5phr	2.7phr		
PP	Haake torque rheometer	1.5-6.5phr	DTBPH	0.05-0.1 phr	0.7%		90
PE	Brabender single extruder	1%	BP	0-1%			93
EPDM	Berstorff 25mm TSE	2%	DTBPIB	0.5%	1.05%		102
EPR	Haake-Buchler Rheomix 600 Mixer	2 phr	DCP	1 phr		<5%	103
EPR	Brabender Plasticorder mixer	5%	DCP(180° C)	0.25%		65%	105
			BPO(160° C)	1%		29%	
EPDM	Rheomix 600 of Haake System 40 mixer	5 phr	DCP	2.0phr	3.1%	94%	106

styrene-*b*-(ethylene-co-1-butene)-*b*-styrene triblock copolymer (SEBS) [98]. Derivatives of maleic anhydride such as diethyl maleate have been grafted onto PE [92,99,100].

### 1.6.2 Grafting Glycidyl Methacrylate (GMA) onto Polymers

In recent years GMA has been utilised as the grafting monomer in polyolefins and these functionalised polymers have been used as in situ compatibilisers of polymer blends. GMA bears a double bond (free-radical reactivity) and an epoxy group (functional reactivity) (See Fig 1-4). This epoxy group possesses reactivity towards various functional groups such as  $-\text{COOH}$ ,  $-\text{OH}$ ,  $-\text{SH}$  and  $-\text{NH}_2$ . GMA can play an important role in chemical modification of existing polymers as well as in reactive processing. GMA has been free-radically grafted onto EPR, EPDM [23, 113-118], PP [119-125] and PE [113,126] in the molten state and various polymer blends have been compatibilised with GMA containing copolymers. Table 1-6 lists the studies of functionalisation of polymers with GMA.

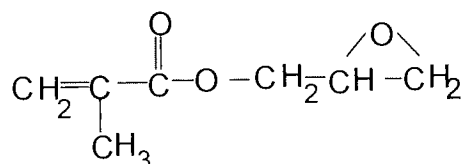


Figure 1-4 Chemical structure of GMA

Similar to grafting reactions of MA onto polymers described earlier, the melt free radical grafting reactivity of GMA in polymers is low. Unless a large excess of a peroxide is employed, the conversion of GMA monomer to grafted GMA onto PP has been reported not to exceed 10% [113,119-121,125]. Sun et al. [120,121] studied the reaction of grafting GMA onto PP using both a batch mixer and a co-rotating twin screw extruder. 1,3-bis(tert-butylperoxy-isopropyl)benzene (Perk-14) and 2,5-dimethyl-2,5-di(tert-butylperoxy)hexane (DHBP) were used as radical initiators. When GMA alone was grafted onto PP in the mixer, the grafting yield was reported to be a mere 0.68 phr with respect to 5.8 phr GMA introduced in the presence of 0.24 phr DTBPH at 200°C [120]. When the DTBPH concentration was raised to 0.44 phr, there was not much increase in the GMA grafting yield. When a comonomer, styrene, was added to the GMA/PP system, the GMA grafting yield was increased by a factor of more than 3 and the PP molecular weight was not reduced significantly. These workers [119-121] found that with styrene in GMA/PP system, the GMA grafting yields reached a plateau within 2 or 3 minutes. The grafting

reaction was also studied using a twin screw extruder. The presence of styrene led to a significant increase in GMA grafting yield.

Hu et al. [30,61] carried out in situ compatibilising of PP/PBT blends by one-step reaction extrusion. In this work, the functionalisation of GMA onto PP and blending PP/PBT in the same extrusion process was executed. The functionalisation was carried out in the first part of the extruder, followed by subsequent interfacial reaction between the functional and functionalised polymers. The processing parameters were investigated.

Chen [123] also studied the melt grafting of GMA onto PP with styrene in a batch mixer and found that styrene could increase the GMA grafting yield and reduced the extent of  $\beta$ -scission. Wong [124] carried out the melt grafting of GMA onto PP with styrene and studied the melt rheological properties of graft modified PP.

Huang [122] reported that a novel method was developed to obtain a high grafting degree with little degradation of PP using acrylamide (AM) as the initiating agent. It was shown that the grafting degree increased rapidly with increasing AM concentration and reach a high level of 4.7% at an AM concentration of 0.5 wt% with 5 wt% GMA added initially. It was assumed that the grafting reaction could take place during, or even before, the melting of PP, i.e. solid state grafting, as a result of the early decomposition of AM.

### **1.6.3 Functionalisation of Polymers with Other Reactive Monomers**

Oxazoline has been grafted onto PP and PE owing to the reactivity of oxazoline towards a carboxylic group to form an esteramide [29,62]. This reactivity is useful for the compatibilization of blends of which one polymer component contains a carboxylic group. The oxazoline group can also react with other functional groups such as amine, phenol, and mercatan [29].

Vainio et al. [29,62] have investigated grafting of ricinoloxazoline maleinate (OXA) onto PP by melt free radical grafting in a mixer and a co-rotating twin-screw extruder. Ricinoloxazoline maleinate is in a liquid form and exhibits very low volatility (bp>25°C at 0.1mbar) [62]. Its structure is presented in Figure 1-5. 1,3-bis(tert-butylperoxy-isopropyl)benzene was chosen as the initiator. The reaction was very fast and the co-monomer styrene was reported not to enhance the grafting yield of OXA because the two



monomers do not copolymerize easily. Recently, Anttila et al. have attempted grafting reaction of ricinoloxazoline maleinate on polyethylene (PE), ethylene propylene copolymer (EP) and styrene ethylene/butylenes styrene (SEBS) in a twin-screw extruder [127]. The maximum conversions of the ricinoloxazoline maleinate were about 30% for EP and SEBS

Table 1-6 Functionalisation of Polymers with GMA

Polymer To be modified	Mixer extruder or type used	GMA initially added	Peroxide type	Peroxide concentration	GMA grafted	Ref.
PE	Haake mixer	10% 5%	DCP	0.6%	2.38% 1.62%	113
EPR	Haake mixer	10%	DCP	1.1%	2.08%	
EP	Brabender-like mixer	6%	DCP	0.2%	0.77mol%	114
EPR	Rheocord Haake mixer	6phr with St	DCP	0.3phr	3.5phr	118
PP	Rheocord Haake mixer	6phr with St	DHBP	0.2phr	1.42%	119, 120
		6phr without St	DHBP	0.2phr	0.42%	
PP	Werner & Pfleiderer ZSK-30 TSE	3phr with St	DTBPIB	0.3phr	0.9phr	121
		3phr without St	DTBPIB	0.3phr	0.3phr	
PP	Haake Rheocord 90 mixer	5%	AM	0.5%	4.7%	122
PP	Haake Rheomix 600 Mixer	18 % with St	DHBP	1.1phr	3.8%	123, 124
		11% with St			2.8	
EPDM	TSE				6%	23
PE	Rheocord Haake mixer	10 phr with St	DHBP	0.4phr	5.2phr	126

and about 23% for PE. Increasing concentrations of peroxide and ricinoloxazoline maleinate increased grafting, but MFI decreased, especially for PE even with a low initial monomer and peroxide concentrations, as an indication of crosslinking. With a suitable choice of peroxide concentration grafted polymers could be produced with good yield and without gel formation.

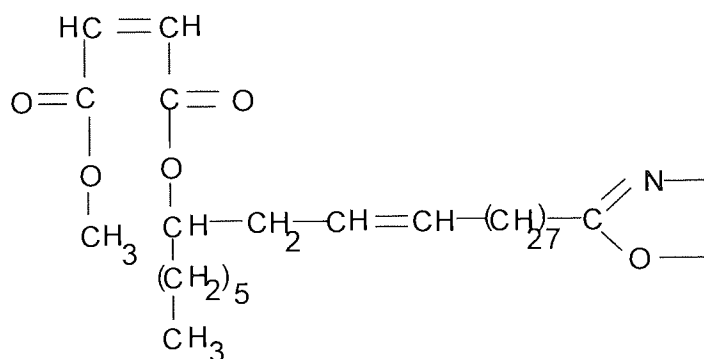


Figure 1-5 Chemical structure of OXA

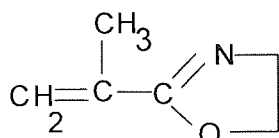


Figure 1-6 Chemical structure of 2-isopropenyl-2-oxazoline

2-iso-propenyl-2-oxazoline (see Figure 1-6) and vinyl oxazoline were reported to graft onto PP and PS and were used for reactive blending with polymers which contain carboxylic acid groups, such as acrylonitrile-butadiene rubber [21,128-131].

It was reported that the nitrile groups of an acrylonitrile/butadiene/styrene (ABS) copolymer [132] and a hydrogenated nitrile rubber [133] could be modified into oxazoline in the molten state in the presence of aminoethanol as modifier agent and zinc acetate as a catalyst. The scheme of reaction is shown in Figure 1-8 (conversion of nitrile groups into oxazoline functionality). The reaction was carried out in a batch mixer and in a corotating twin screw extruder [132]. The conversion of the nitrile groups into oxazoline functionality was verified by IR and NMR analysis. The results indicated that the kinetic of grafting was fast and the conversion yield was relatively high. The modified nitrile rubber had been

used as impact modifier for polyamide-6 and impact strength of modified polyamide-6 by addition of the modified rubber was highly improved [133].

Other functional groups have been grafted onto polyolefins and rubbers to obtain good toughening effects or compatibilizing effects. Methyl methacrylate grafted EPR and EPDM have been achieved using EPR or EPDM swollen by a minimum amount of cyclohexane in the presence of benzoyl peroxide or azoisobutyronitrile and of the monomer (methyl methacrylate) at 80°C [134]. The modified rubbers were used to obtain blends with PMMA and with polycarbonate. The preparation of a polymer containing secondary amino groups by grafting of t-BAEMA (t-butylaminoethyl methacrylate) or DMAEMA (2-(dimethylamino) ethyl methacrylate) onto linear low density polyethylene in the melt was investigated by Z.Song et al. [135,136].

### **1.7 ENHANCING GRAFTING BY USING A CO-MONOMER**

As it was described in the above section, side-reactions such as chain scission or crosslinking of polymer substrates, homopolymerisation of monomers always accompany the desired grafting reactions. In order to minimise the side reactions, it is important that the polymer radicals are trapped as rapidly as possible and some monomers are more effective than others at trapping such radicals [75]. This may arise because of the relative solubility of the monomers in the polymer melt or it may be due to the inherent reactivity of the monomers. One strategy involves choosing a monomer combination such that the comonomer is both effective in trapping the polymer radicals formed and that the propagating radicals are highly reactive towards the desired monomer. As an electron-rich comonomer, styrene has been shown to be effective for improving grafting yields and reducing side reactions [73,118-120,137]. For the case of the styrene-MA system, it was proposed that addition of an electron-donating monomer such as styrene can form a charge transfer complex (CTC) with MA (see Figure 1-7).

Because of the instability of PP tertiary macroradicals associated with their tertiary character, the degradation process is extremely fast and important at elevated temperature. The weak free-radical reactivity of MA lead to low MA grafting yields together with severe PP degradation. The formation of CTC can 'activate' the double bond of MA and promote the free-radical reactivity of the double bond of MA [73].

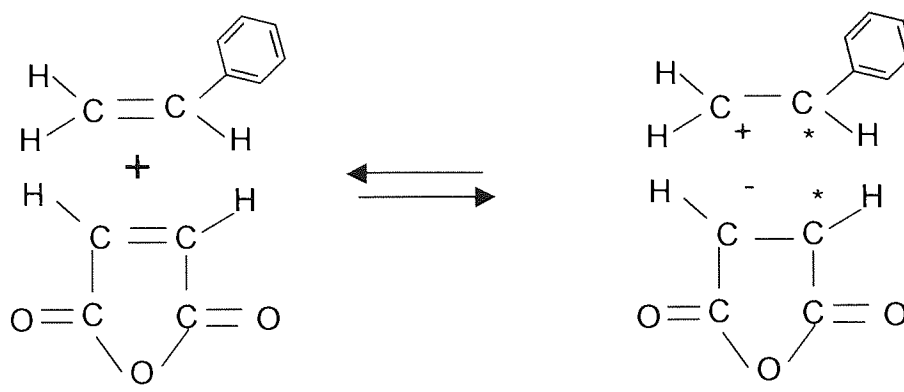
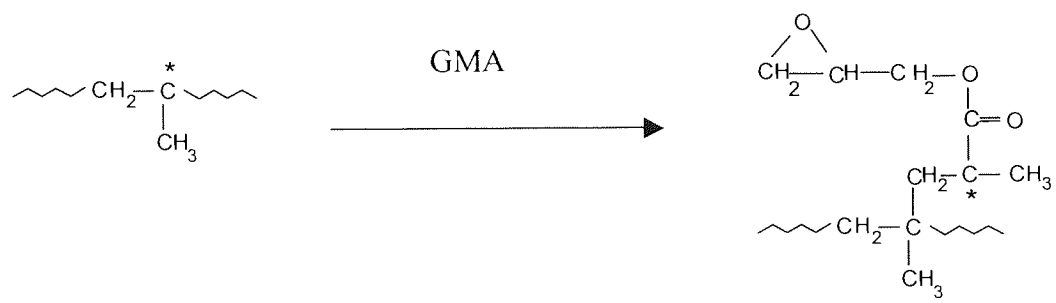
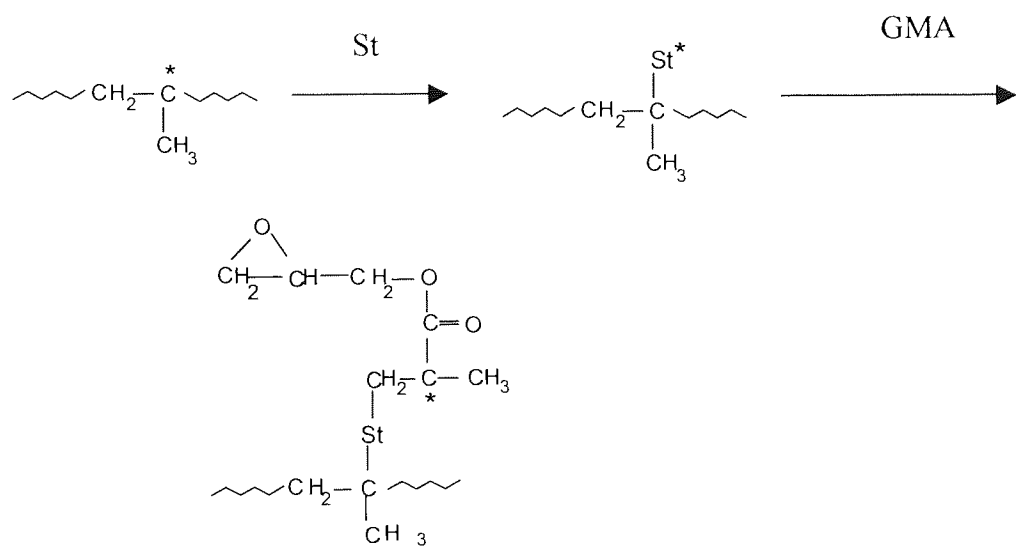


Figure 1-7 Formation of a charge transfer complex (CTC) [73]



(a) GMA alone



(b) GMA + styrene (St)

Figure 1-8 The mechanism of the melt free radical grafting GMA onto PP with and Without styrene (a) GMA alone (b) GMA and styrene [119]

Cartier et. al. [119] have recently investigated the reaction mechanism of GMA grafting onto PP with assistance of styrene. The effect of styrene on the increasing GMA grafting yield and reducing PP degradation was studied in details. A reaction mechanism in the presence of styrene was proposed (see Fig.1-8 b) [119]. When styrene was added, styrene reacts first with PP macroradicals and the resulting free radicals then copolymerise with GMA. The higher reactivity of styrene towards PP macroradical compared to that of GMA might be due to the resonance effect between the double bond and the benzene ring of the former. The higher grafting yields obtained with styrene may be associated with longer chain grafts and more grafting sites [75]. Rates of copolymerisation of electron donor-electron acceptor pairs are substantially greater than that for homopolymerisation (of MA or GMA). However, styrene is ineffective at improving the grafting yield of maleate esters to PP [29,62]. This can be understood in terms of the low reactivity of the styryl propagating species towards the maleate esters.

Al-Malaika et al. have adopted the use of polyfunctional monomers, in particular trimethylolpropane triacrylate (TRIS), as a comonomer for improving the grafting yields of various monomers onto PP [138-141]. The structure of TRIS is presented in Figure 1-9.

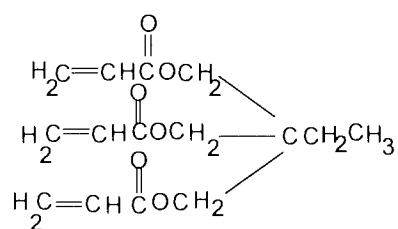


Figure 1-9 Chemical structure of TRIS

It was shown that the use of TRIS as a comonomer with different reactive modifiers, such as antioxidant [138] and maleic anhydride [140, 141], gave rise to a dramatic increase in the level of grafting of these monomers on PP. During the grafting, TRIS acts as a reactive linker between the monomer and the polymer. The mechanism of grafting an antioxidant, 3,5-di-tert-butyl-4-hydroxy benzyl acrylate (DBBA), onto PP in the presence of TRIS. It was proposed comprising three main steps [138]. During the early stages of processing a graft antioxidant copolymer was formed. The antioxidant, DBBA, became fully attached to a crosslinked structure based on the TRIS moiety, which was in turn attached to the polymer (e.g. through (DBBA-TRIS)<sub>COP</sub> units grafted on PP). Further processing of the melt at high temperature made the onset of a preferential scission of the graft copolymer

chains, which led to the restructuring of crosslinks and further antioxidant grafting. The success of the use of TRIS as a comonomer to enhance the grafting relies on achieving a delicate balance between the molar ratios of the reagents (monomer, comonomer, peroxide) and the process conditions.

Besides styrene and TRIS, various solvents, transfer agents and inhibitors have also been used to enhance grafting yields or limit side reactions during polymer modification [75].

### **1.8 CHALLENGES OF MELT FREE RADICAL GRAFTING**

The chemistry of melt free radical grafting is complicated by the high temperature, high viscosity and heterogeneity of the reacting medium. First of all, the desired grafting reaction is always accompanied by undesirable polymer degradation reaction and homopolymerisation of monomers which can alter significantly their valuable mechanical properties and processing characteristics. PP undergoes mainly chain scission and higher grafting levels are generally achieved at higher peroxide concentrations which result in severe degradation of PP [73]. In the case of PE, EPR, or EPDM, crosslinking is the main problem and the challenge is to obtain sufficient amount of grafting while retaining the mechanical properties of the virgin polymer substrates. Good understanding of the effects of processing parameters, the grafting mechanisms and the microstructure of grafts help achieving successful grafting reactions [73]. Though the overall free radical grafting mechanism can be more or less depicted by Figure 1-1, little quantitative information is available about each individual step. Also, experimental evidence for the microstructure of grafts (grafting sites, graft length, graft sequence distribution) is not sufficient. Thus the mechanisms of free-radical grafting or microstructures of the resulting grafts have to be speculated. For example, the grafting of GMA onto PP could be enhanced by addition of styrene as a comonomer, resulting in high grafting yields [119-121]. However, it was found that the GMA grafted PP in the presence of styrene was less effective in compatibilising the PP/NBR blends than GMA grafted on PP without using styrene [27]. This means that the microstructure of the GMA grafts with or without styrene are different, which determines the efficiency of the grafted GMA groups towards other functional groups during reactive blending, and this difference may result from the different grafting mechanisms. However, little information is available on the microstructure of GMA grafts. With more studies made on the grafting mechanism and microstructure of grafts by

using model compounds and  $^{13}\text{C}$  or  $^1\text{H}$  NMR, the fundamental understanding of melt free radical grafting will become more clear.

## **1.9 PROCESS CONSIDERATION**

Both reactive blending and functionalisation of polymers can be carried out in a batch mixer or extruder (reactive processing). A mixer or extruder acts as a reactor where the specific chemical reaction takes place. A particular advantage of reactive processing is the absence of solvent as the reaction medium so no solvent stripping or recovery process is required, and product contamination by solvent or solvent impurities is avoided [74]. The fundamental basis behind the successful use of these types of machines in melt free radical grafting or reactive blending is primarily related to their ability to handle and mix highly viscous polymer fluids [73].

### **1.9.1 Reactive Extrusion**

Reactive extrusion refers to the performance of chemical reactions during extrusion processing of polymers [74]. Reactive extrusion is carried out in single- and twin-screw extruders, capable of transporting and mixing highly viscous fluids in an environment where temperature and pressure are controlled. An advantage of an extrusion device as a reactor is the combination of several process operations into one piece of equipment with accompanying high space-time yields of product. An extruder reactor is ideally suited for continuous production of material after equilibrium is established in the extruder barrel for the desired chemical processes.

Because of their versatility, most extruder reactors are twin-screw extruders, which possess a segmented barrel, each segment of which can be individually cooled or heated externally. Extruder screws often have specialised sections or configurations. Twin-screw extruder screws may be equipped with interchangeable screw elements that provide different degrees of mixing and surface area exposure by varying the depth between screw flights, the individual flight thickness, and direction and degree of flight pitch. By providing individual barrel segments with external openings it is possible to introduce solid, liquid, or gaseous reactants at specified points in the chemical process. Their residence time in the reactor is controlled by the distance between the injection point and the die. The choice of chemical system is restricted, however, by the residence time in the equipment (usually of

the order of minutes) by the operating temperature range of the extruder (usually below 300°C) and by the tolerance of the equipment to corrosion. On the other hand, small commercial continuous extruders require a minimum 100-1000 g of material for a typical experiment. Such extruder reactions may not be convenient for running a large matrix of screening experiments to optimise processing conditions, especially when limited amount of valuable starting materials are involved [74]. The types of reactions that have been performed by reactive extrusion include bulk polymerisation, grafting reaction, interchain copolymer formation, coupling or branching reaction, controlled molecular weight degradation, and functionalisation of polymers. Melt free radical grafting of monomers onto polymers and compatibilisation of polymer blends through reactions during compounding have become one of the most important application of reactive extrusion technology.

### 1.9.2 Batch Mixers

Haake Rheocord or Brabender type of batch mixers is also used as reactors for reactive processing. Generally, a batch mixer consists of two rotors which turn in opposite directions in a mixing chamber. The temperature of the mixing chamber is generally controlled by an oil heater. Due to its particular structure, the mixing chamber of the mixer is not perfectly sealed. This may bring about complications when adding liquid monomers and/or other types of additives whose boiling points are low compared to the temperature in the mixing chamber. In such a case, loss of liquid and/or easy-to-sublime reactants can become important. Its mixing capacity can not match that of a twin screw extruder. Despite its limitations, a batch mixer is often preferred over a screw extruder as a chemical reactor for achieving a fundamental understanding of melt free radical grafting or reactive blending. Unlike reactive extrusion, mixing time or reaction time can be changed with ease. A batch mixer also bears other useful features [73]:

- Its ability to mix highly viscous polymers;
- The relatively small capacity of the mixing chamber (e.g. 50 cm<sup>3</sup>), which permits trials with expensive or exotic chemicals and facilitates temperature control;
- The possibility of varying the following processing parameters which resemble more or less those encountered in a screw extruder: temperature, mixing time, mixing intensity, via the rotating speed of rotors, and the mode with which reactants are charged to the mixing chamber.



In fact, so far a batch mixer is considered a unique device that best suits the need to understand the chemistry of reactive processing for subsequent continuous processing in a screw extruder.

### **1.10 AIM AND OBJECTIVES OF THIS STUDY**

The primary overall aim of this project (involving various European partners) was to convert post-consumer PET bottles into a value-added thermoplastic elastomeric product with outstanding performance, especially at high temperature, in order to compete in markets dominated by the more expensive speciality polymers.

It is clear that high performance properties such as high impact strength, ductility, solvent and heat resistance are highly desired in polymer blends to enhance their value and application potential. However, in order to develop such high performance blends from recycled polymers both the quality of the feedstocks and technology for compatibilisation have to be considered. PET is not compatible with other polymers, leading to poor mechanical performance due to phase separation and poor phase adhesion. Thus compatibilisation via reactive blending approach was adopted.

For the Aston's contribution to achieving the overall aim of this project, two major objectives had been identified for this study:

#### *(1) Functionalisation of various rubbers with reactive monomers via reactive processing*

One of the major objectives was to examine the functionalisation process of various rubbers, e.g. NR, EPR, EPDM, for the purpose of subsequent compatibilisation of PET blends. This involved the in situ melt free radical grafting of functional monomers, e.g. MA and GMA, onto the rubbers using an internal mixer (torque rheometer) as a chemical reactor. However, due to the low reactivity of GMA and MA towards the rubbers, which would result in low grafting yields, a novel approach (developed at Aston University PPP research group) was used where a co-reactive monomer (or enhancing agent) was used in combination with the functional modifiers (i.e. GMA and MA). Appropriate methodology was established and the chemical compositions and reactive processing parameters were examined and optimised. The functionalised rubbers were characterised using various techniques and accurate

methods were developed to evaluate the grafting levels of the functional monomers (i.e. MA and GMA). The reaction mechanisms were also investigated.

*(2) Compatibilisation of PET/rubber blends using functionalised rubbers produced via reactive processing (from the objective one)*

Compatibilising PET blends with GMA or MA functionalised rubbers via reactive blending constituted the second major objective for this study. It is important to point out here that in this study only virgin PET polymer used throughout for the blending work and no postconsumer PET bottle-based material was used. The compatibilisation strategy used here involved the in situ formation of copolymers through reactions between the PET end groups (carboxyl and hydroxyl) and the functional groups grafted onto the rubbers, (e.g. grafted GMA or MA), during melt blending. PET was blended with the functionalised rubbers in an internal mixer. The compatibility of the resulted blends was determined in terms of morphology, dynamic mechanical properties and mechanical properties, hence the optimal functionalised rubbers were screened. The reactions between PET end groups and grafted functional groups (GMA or MA) onto the rubbers were investigated and the copolymer formed during melt blending was isolated and characterised.

## CHAPTER 2 EXPERIMENTAL AND ANALYTICAL TECHNIQUES

### 2.1 MATERIALS

#### 2.1.1 Polymers

Five different polymers were used in this work. Their chemical structures are listed in Table 2-1.

- (i) Ethylene-propylene copolymer (EP): Commercial grade ethylene/alpha-olefin copolymer (Tafmar P0480), pellets, supplied by Mitsui Chemical. It has an ethylene:propylene ratio of 80:20 mole/mole and a melt flow index (MFI) of 1.7 g/10min (ASTM-1238 - 2.16Kg load, 230°C)
- (ii) Ethylene propylene diene terpolymer (EPDM): Commercial grade EPDM (Buna AP 447), bale, supplied by Bayer. It has 74% ethylene and 5% 5-ethylidene-2-norbornene.
- (iii) Polypropylene (PP): Commercial grade unstabilised PP (Propathene ICI, HF-26), white powder, supplied by ICI Plastics Division Ltd. It has a melt flow index (MFI) of 1.7 g/10min (ASTM-1238 - 2.16Kg load, 230°C)
- (iv) Natural rubber (NR): Commercial grade NR (SMR-L), bale, supplied by MRPRA.
- (v) Poly(ethylene terephthalate (PET): Film grade of PET (Eastapak<sup>TM</sup> PET 9921W), Pellets, supplied by Eastman Chemical Limited.

#### 2.1.2 Reagents and Additives

High purity maleic anhydride (MA) (99% purity), glycidyl methacrylate (GMA) (97% purity), and trimethylolpropane triacrylate (TRIS) were all purchased from Aldrich Chemical Co. Ltd. and used as received. Four different peroxides, e.g. benzoyl peroxide (BPO), 2,5-dimethyl-2,5-bis(tert-butylproxy) hexane (T101), 1,1-di(tert-butylperoxy)-3,3,5-trimethylcyclohexane (90% solution in butyl phthalate) (T29B90), and azoisobutyronitrile (AIBN), were used without further purification. Trichloroacetic acid (TCA) and 0.50 N potassium hydroxide solution in methanol were of analytical grade and were supplied by Aldrich Chemical Co. Ltd. All other chemical were of reagent grade and were used without further purification. Table 2-2 gives the main chemicals used in the work reported here.

### 2.1.3 Solvents

Solvents employed for normal purpose (hexane, toluene, xylene, acetone, methanol, ethyl acetate, chloroform) were laboratory reagent grades, used as supplied from Fisons. All solvents used in titration were HPLC grade from Fisons.

Table 2-1 Chemical structure of polymers

No.	Name	Grade	Structure (repeat unit)	Form	Supplier	FTIR
I	Ethylene-propylene copolymer (EP)	Tarfmer P0480	$\text{---}(\text{CH}_2\text{---CH}_2\text{---})_m\text{---}(\text{CH}_2\text{---}\overset{\text{CH}_3}{\underset{ }{\text{CH}}}\text{---})_n\text{---}$	Pellets	Mitsui Chemical	Fig. 2-1
II	Ethylene propylene diene terpolymer (EPDM)	Buna AP 447	$\text{---}(\text{CH}_2\text{CH}_2)_m\text{---}(\text{CH}(\text{CH}_3)\text{CH}_2)_n\text{---}(\text{CH}(\text{CH}_2\text{CH}(\text{CH}=\text{CHCH}_3))\text{CH}_2)_k\text{---}$	Crumb bale	Bayer	Fig. 2-2
III	Polypropylene (PP)	HF-26	$\text{---}(\overset{\text{CH}_3}{\underset{ }{\text{CH}}}\text{CH}_2)_n\text{---}$	White powder	ICI	Fig. 2-3
IV	Natural rubber (NR)	SMR-L	$\text{---}(\text{CH}_2\text{---}\overset{\text{CH}_3}{\underset{ }{\text{C}}}\text{=CH---CH}_2)_n\text{---}$	Bale	MRPRA	Fig. 2-4
V	Polyethylene terephthalate (PET)	Eastapak <sup>TM</sup> PET 9921W (film grade)	$\text{---}(\text{C}(=\text{O})\text{---}\text{C}_6\text{H}_4\text{---}\text{C}(=\text{O})\text{---}\text{O---CH}_2\text{CH}_2\text{---}\text{O})_n\text{---}$	Pellets	Eastman Chemical (UK) Limited	Fig. 2-5

Table 2-2 Chemicals used in the experiments

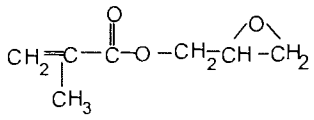
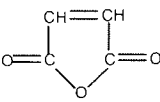
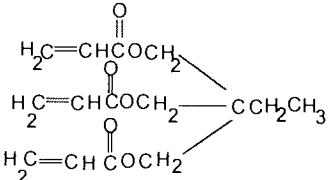
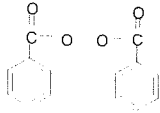
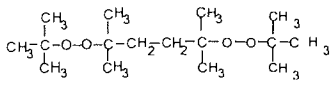
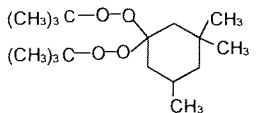
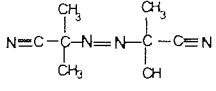
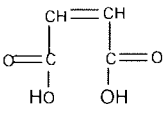
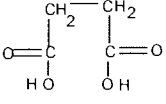
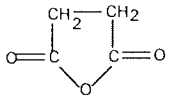
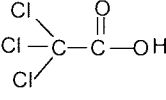
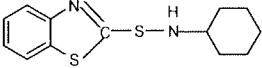
Name	Formula (M.w.)	Manufacturer	Purity (%)	Colour & form	FTIR
Glycidyl methacrylate (GMA)	 <p>(142)</p>	Aldrich Chemical Co. Ltd	97	Transparent liquid	Fig.2-6
Maleic anhydride (MA)	 <p>(98)</p>	Aldrich Chemical Co. Ltd	99	White pellets	Fig.2-7
Trimethylolpropane triacrylate (TRIS)	 <p>(296)</p>	Aldrich Chemical Co. Ltd		Viscous liquid	Fig.2-8
Benzoyl peroxide (BPO)	 <p>(242)</p>	Fluka Chemika	97	White powder	Fig.2-9
2,5-dimethyl-2,5-bis(t, butyl peroxy)hexane (T101)	 <p>(290)</p>	AKZO Chemie bv		Transparent liquid	Fig.2-10
1,1-di(tert-butylperoxy)-3,3,5-trimethylcyclohexane (T29B90)	 <p>(320)</p>	AKZO Chemie bv	90 (in butyl phthalate)	Transparent liquid	Fig.2-11
$\alpha, \alpha'$ -Azobisisobutyronitrile (AIBN)	 <p>(164)</p>	ACROS Chimica n.v.	98	White powder	Fig.2-12

Table 2-2 Chemicals used in the experiments  
(continued)

Name	Formula (M.w.)	Manufacturer	Purity (%)	Colour & form	FTIR
Maleic Acid	 (116)	BDH Chemicals Ltd.	99.9	White powder	Fig.2-13
Succinic acid	 (118)	Fisons Scientific Apparatus Ltd.	99.5	White powder	Fig.2-14
Succinic anhydride	 (100)	Aldrich Chemical Co. Ltd	99	White pellets	Fig.2-15
Trichloroacetic acid (TCA)	 (163)	Aldrich Chemical Co. Ltd	99.5	White powder	
N-Cyclohexyl-2-benzotiazole sulphamide (CBS)	 (264)	Robinson Brother Ltd.	75	Green pellets	
Zinc oxide	ZnO (81)	BDH Chemicals Ltd.	99.7	White powder	
Stearic acid	CH <sub>3</sub> (CH <sub>2</sub> ) <sub>16</sub> COOH (284)	BDH Chemicals Ltd.	99	White pellets	
Sulfur	S <sub>8</sub> (256)	Robinson Brother Ltd.	80	Yellow powder	

## 2.2 PROCESSING

An internal mixer, Hampden-RAPRA Torque Rheometer (TR), consisting of a pair of counter rotating rotors in a mixing chamber heated by oil and run with a Brabender motor drive, having a digital torque displaying unit, was used to carry out functionalisation of rubbers with MA and GMA and blending of polymers. The TR ram can be pressed down to maintain a closed system and exert pressure on the polymer during mixing depending on the volume of polymer used per batch. The temperature of the mixing chamber was controlled by a Churchill heater with temperature up to 300°C. The rotor speed is also adjustable (0—250 rpm). EPDM and natural rubber supplied as a large rubbery slab were cut into wafers, then stripes and finally cut into small cubes before processing.

### 2.2.1 Preparation of GMA Functionalised Polyolefins

Melt free radical grafting of GMA onto EP, EPDM, or a mixture of EPDM and PP (weight ratio: EPDM/PP=75/25) was carried out in the torque rheometer in the absence or presence of comonomer, TRIS. Unless otherwise stated, compounds for reactive processing were prepared by pre-weighing exact amount of polymer, GMA, TRIS and peroxide (total weight 33g). In the absence of TRIS, the polymer sample was charged into a preheated mixing chamber which was flushed with oxygen-free nitrogen for more than 15 seconds, followed by injection of a mixture of GMA and T101 into the chamber using a long needle syringe to avoid losses. The ram was lowered down quickly to keep a closed system during mixing to minimise the loss of GMA due to its high vapour pressure and volatility. The reaction product was removed from the chamber and cooled down to room temperature under nitrogen atmosphere. The processed polymer samples were kept in air tight polyethylene bags before storing in a dry and cool place. During mixing, the torque readings were recorded. When TRIS was included in the formulation, polymer and TRIS were tumble mixed and then introduced into the mixing chamber. After mixing for 1 minute, the mixture of GMA and peroxide was injected into the chamber. The ram was raised up and lowered down quickly for this action. The processing of all samples was carried out at a constant rotor speed of 65 rpm. The processing temperature and time were varied.

The addition level of monomer and comonomer was expressed by phr (parts per hundred resin of polymer). For example, addition of 10 phr GMA and 1 phr T101 to EP means that 10 g GMA and 1 g T101 are added to 100g EP. The actual weight of each ingredient for each batch of sample preparation could be accordingly calculated. The amount of peroxide was also expressed as a molar ratio (m.r.) of the peroxide to the total moles of the monomer and comonomer.

### **2.2.2 Preparation of MA Functionalised Natural Rubber**

The required amount of SMR-L (unextracted and unprocessed or extracted) was cut into small pieces and charged in the preheated chamber of torque rheometer which was flushed with oxygen-free nitrogen for more than 15 seconds. The ram was pressed down to keep a closed system during mixing. The ram was lifted up for the purpose of adding chemicals to the chamber and this was done quickly before lowering the ram down to maintain an inert atmosphere. Two minutes pre-mixing was performed followed by the addition of the required amount of MA was introduced into the mixing chamber. After the mixing processes were performed at a given temperature, the reaction product was discharged from the torque rheometer and placed into a cup with nitrogen atmosphere maintained until it was cooled down to below 90°C to avoid further oxidation. During the mixing, torque changes were recorded. When an initiator was used, the peroxide was added to the chamber after mixing of MA with SMR-L for two minutes to allow a rough dispersion of MA into the rubber (see Scheme 4-1 in Chapter 4).

### **2.2.3 Polymer Blending**

Blending PET with EP, EPDM and GMA functionalised EP and EPDM was also carried out in the torque rheometer. The PET was dried at 135°C and the rubber samples (which was granulated into pellets) were dried at 85°C for more than 20 hours in vacuum oven before blending. Due to the difference in density between PET and the rubbers, the weight to fill the mixing chamber depends on the blending weight ratio of PET to rubber. It was found that at ratios of 50/50, 60/40 and 80/20 PET/EP or EPDM, the actual weights of blending components were 20g/20g, 24.9g/16.6g and 37g/9.25g PET/rubber, respectively. Pre-weighed PET and rubbers or functionalised rubbers were tumble mixed in a paper cup. The mixture was introduced into the preheated mixing chamber after flushing with



nitrogen and then the ram was lowered down quickly to keep a closed mixing system. The mixing temperature, rotor speed and mixing time were fixed at 275°C, 65rpm and 10 minutes. The melt polymer blend was then removed from the chamber after mixing and placed between two PTFE fabric sheets to press into plaques about 5-6mm thick. After the blend had cooled down to about 50°C, the PTFE sheets were removed and the blend was placed into an air-tight plastics bag.

## 2.3 PREPARATION OF POLYMER FILMS, PLAQUES AND SHEETS

### 2.3.1 Preparation of Polymer Films for FTIR Analysis

Thin films (0.1-0.2 mm thick) for FTIR analysis were compression moulded using a press equipped with electrically heated platens which could be cooled down with circulating cooling water. For GMA functionalised polymer samples, about 0.15g purified sample was placed between two PTFE coated fabric sheets placed between polished stainless plates, and pressed into thin films for 0.5 minute in an electrically heated press under a pressure of about 40 kg/cm<sup>2</sup>, after 2 min preheating at 150°C-180°C. The mould plates were taken out and the film samples were removed after cooling down to ambient temperature.

For MA functionalised natural rubber, it was difficult to prepare thin films directly because the rubber is tacky thus thin cured films were used for FTIR measurements. The rubber ingredients, zinc oxide, stearic acid, accelerator CBS, and sulfur (see Table 2-3) were compounded with MA functionalised natural rubber on a two-roll mill before or after extraction with acetone to eliminate the unreacted MA. About 0.2g compounded sample was placed between a folded sheet of Cellophane and placed between polished stainless plates. This was placed directly between the electrically heated platens of the press, set at 150°C. A pressure of 80 kg/cm<sup>2</sup> was gradually applied and maintained for 20 minutes. The mould plates were taken out and the film samples removed.

Table 2-3 Compounding for Making Cured NR Films

Ingredients	Composition (phr)	Curing conditions
NR-MA Reaction product	100	150°C for 20 min
Zinc oxide	3	
Stearic acid	2.5	
Accelerator CBS	0.7	
Sulfur	3	

### **2.3.2 Preparation of polymer Plaques and Sheets**

3 mm thick plaques were prepared by compression moulding for dynamic mechanical thermal analysis (DMTA) and scanning electron microscopy (SEM) analysis. The blends were dried in a vacuum oven at 85°C for 24 hours before moulding. About 7-9g polymer sample was placed in the centre of a spacer which was laminated across both surfaces with a folded sheet of aluminium foil and then covered with two polished stainless steel plates. This was placed directly between the electrically heated platens of the press, set at 275°C, and held for 6 minutes under minimum load. The lower platen was raised up slowly and a pressure of 100 kg/cm<sup>2</sup> applied for 1 minute, heating was isolated and cold water circulated through the platens, whilst maintaining pressure. Mould plates were taken out once it was cooled below 100°C in the press.

1 mm thick sheets were also prepared for tensile properties measurement using similar procedure as above. To get smooth surface, PTFE fabric sheets were used for mould release. Instead of cooling in the press, mould plates were taken out and placed into cool water to cool down below 50°C.

## **2.4 PURIFICATION OF REACTION PRODUCTS FROM REACTIVELY PROCESSED POLYMERS**

In order to ensure accurate evaluation of the grafting degree, the reaction products were purified to eliminate any unreacted monomer, homopolymer and copolymer of the monomer and the co-agent which might be formed during reactive processing. Two methods were used.

### **2.4.1 Precipitation**

Precipitation was used to purify the GMA functionalised polyolefins. A 3g sample was dissolved in 120 ml hot toluene or xylene (in the absence of the comonomer) or Soxhlet extracted (24h) with toluene (in the presence of the comonomer). When the comonomer (TRIS) was used, the homopolymer of TRIS (polyTRIS), the copolymer of TRIS and GMA (TRIS-co-GMA) and crosslinked polymer, were separated out as toluene or xylene-insolubles. The toluene or xylene-soluble fraction was precipitated in 7 times excess volume of acetone to give a soluble fraction containing the modifier monomers (GMA, and

TRIS when used) and GMA-homopolymer (poly-GMA) and an insoluble fraction containing the GMA-grafted polymer. The precipitated polymer was then dried overnight in a vacuum oven at 80-85°C. This method was used throughout for determining the yield of graft GMA.

#### **2.4.2 Soxhlet extraction**

Soxhlet extraction was used to purify the MA functionalised natural rubber samples. Thin sheets of the reaction products or thin cured films for FTIR measurements were exhaustively Soxhlet extracted to remove any free MA and other low molecular mass materials by using acetone. Acetone was found to be the most suitable solvent not only due to the high solubility of MA in acetone [78] but also due to the good extraction ability for natural rubber. 24 hours extraction was sufficient to remove free MA. The extracted samples were dried overnight in a vacuum oven at room temperature. Raw natural rubber was also Soxhlet extracted to remove natural substances other than polyisoprene and low molecular fraction of polyisoprene using the same procedure above.

### **2.5 DETERMINATION OF THE GRAFTING DEGREE**

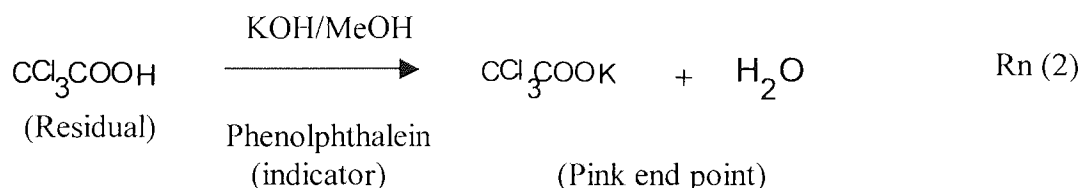
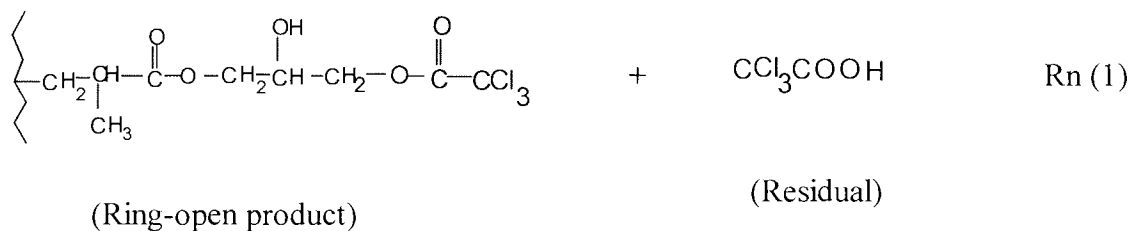
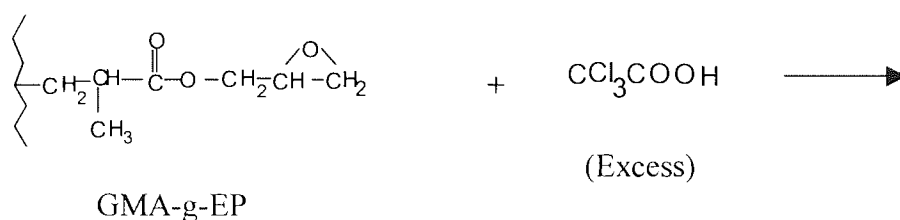
(a) Grafting Degree: The grafting degree of a functional monomer is defined as the weight percentage of grafted monomer in the polymer. For example, if 1 g modified rubber contains 0.1 g grafted GMA the grafting degree of GMA is 10%.

(b) Grafting Efficiency: The grafting efficiency of a functional monomer is defined as the conversion percentage of total functional monomer initially added to the amount of grafted monomer onto polymer after reaction. For example, if 10g GMA is added initially to 100g polymer and 1g is actually grafted after processing, the grafting efficiency is 10%.

#### **2.5.1 Determination of the Grafting Degree of GMA by Titration**

A non-aqueous back-titration method was established to determine the grafting degree of GMA [113,122]. 1.0g of the purified GMA modified polymer was completely dissolved in 75 ml hot toluene or xylene, followed by addition of 3.5 ml 0.3M trichloroacetic acid solution in toluene. The mixture was thoroughly mixed and was kept at 100—110°C for more than 90 min in order to achieve complete ring open reaction of epoxy group with the

acid (see Rn 1). The solution was then precipitated into 100 ml ethyl acetate with continuous stirring, filtered, and washed. The filtrate (residual trichloroacetic acid) was titrated with 0.1 M KOH solution in methanol (see Rn 2). 0.1% phenolphthalein in methanol was used as an indicator. KOH solution was added to the filtrate until the first pink point as the end point. 1.0 g of unmodified polymer was titrated using the above procedure and correction was made based on these results. The percent error of the grafting degree determined by titration was found to be around  $\pm 6\%$ .



### 2.5.2 Determination of the Grafting Degree of GMA by FTIR Method

FTIR was used to characterise the reaction products and evaluate the grafting degree of GMA onto EP. About 0.15 g of purified samples was pressed to a thin film and FTIR

spectra of all films were recorded. It was shown that the characteristic peaks of grafted GMA appeared at  $1730\text{ cm}^{-1}$  corresponding to carbonyl absorption and  $909\text{ cm}^{-1}$ ,  $850\text{ cm}^{-1}$  corresponding to epoxy ring absorption (see Fig.2-16). The peak at  $909\text{ cm}^{-1}$  can be used to evaluate the grafting degree and the peak at  $720\text{ cm}^{-1}$  corresponding to  $-(\text{CH}_2)_n$  ( $n>4$ ) rocking absorption of EP was used as the EP reference peak. The epoxy group absorption peak area boundaries were defined from  $893\text{ cm}^{-1}$  to  $925\text{ cm}^{-1}$  for peak maximum at  $909\text{ cm}^{-1}$  and the reference absorption peak boundaries from  $670\text{ cm}^{-1}$  to  $785\text{ cm}^{-1}$  (see Fig 2-17), and the amount of grafted GMA was calculated from absorption area ratio  $909\text{ cm}^{-1}$  to  $720\text{ cm}^{-1}$  ( $A_{909\text{ cm}^{-1}}/A_{720\text{ cm}^{-1}}$ ). The level of grafted GMA was determined by comparison of the absorption ratio to a calibration curve established by correlation of FTIR to the amount of grafted GMA measured by titration method. The percent error of the grafting degree determined by FTIR was found to be around  $\pm 5\%$ .

A calibration curve was established based on the correlation of the grafting degree measured by titration and absorption area ratio ( $A_{909\text{ cm}^{-1}}/A_{720\text{ cm}^{-1}}$ ) for the same purified sample. A set of data was plotted with a linear line for the samples (see Fig.2-18) and a calibration curve equation was derived from the calibration curve as follows:

$$Y=43.5X \qquad \text{Eqn. (1)}$$

Where Y is the grafting degree of GMA and X is absorption area ratio ( $A_{909\text{ cm}^{-1}}/A_{720\text{ cm}^{-1}}$ ).

### 2.5.3 Determination of the Grafting Degree of MA by FTIR Method

A typical FTIR spectrum of the MA functionalised rubber shows that the grafted MA in cured film is present mostly in an acid form as indicated by absorption peak at  $1710\text{ cm}^{-1}$  and the grafted MA in the form of anhydride was so small that only a weak should at  $1780\text{ cm}^{-1}$  corresponding to the anhydride absorption peak was observed (see Fig.2-19). Compared with the amount of acid, the anhydride can not be taken into consideration for calculation of the grafting degree of MA.

For quantitative measurements from FTIR spectra of polymer films, a known reference peak corresponding to the polymer backbone absorption is used in order to eliminate

experimental error due to thickness variation of the films. The absorption peak of natural rubber at  $2725\text{ cm}^{-1}$  ( $>\text{CH}_2$  vibration) was chosen as the reference peak. The grafting degree of MA was examined by measuring absorption peak area ratio of the acid group at  $1710\text{ cm}^{-1}$  to the reference peak at  $2725\text{ cm}^{-1}$  ( $A_{1710\text{ cm}^{-1}}/A_{2725\text{ cm}^{-1}}$ ). With reference to Figure 2-20, the reference area boundaries were defined from  $2705\text{ cm}^{-1}$  to  $2748\text{ cm}^{-1}$  for peak maximum at  $2725\text{ cm}^{-1}$  and the acid area boundaries from  $1684\text{ cm}^{-1}$  to  $1751\text{ cm}^{-1}$  for peak maximum at  $1710\text{ cm}^{-1}$  and area calculation was then carried out by the spectrometer software. The actual grafting degree was determined by comparison of the area ratio to a calibration curve. The percent error of the grafting degree determined by FTIR was found to be around  $\pm 5\%$ .

The FTIR calibration was established by measuring standard natural rubber films containing known amount of acid in the natural rubber casted from SMR-L/maleic acid solutions. Different amounts of maleic acid were dissolved in about 25 ml diethyl ether. 1.0g SMR-L which was already Soxhlet extracted with acetone was dissolved in the above solution (maleic acid concentration to rubber: 0—4 wt%). The solutions were dropped on KBr discs directly to cast thin films on the discs. After the solvent had evaporated, the FTIR spectra were recorded. A typical FTIR spectrum (see Fig. 2-20) shows an absorption peak at  $1705\text{ cm}^{-1}$  corresponding to the acid group of maleic acid and rubber  $>\text{CH}_2$  vibration absorption peak at  $2725\text{ cm}^{-1}$  used as reference peak. A series of area ratio of acid peak to rubber reference peak were calculated with same peak area boundaries above to establish a calibration curve (see Fig. 2-21). The calibration curve equation to calculate maleic acid concentration in MA functionalised rubber from FTIR was derived from the calibration curve as follows:

$$y = 1.12 X + 0.1 \quad \text{Eqn (2)}$$

Where Y is the area ratio ( $A_{1708\text{ cm}^{-1}}/A_{2725\text{ cm}^{-1}}$ ) and X is concentration of acid respectively.

## 2.6 DETERMINATION OF INSOLUBLE GELS

The insoluble gel is a measure of the insoluble fraction caused by crosslinking of a modified polymer after being exhaustively extracted with a solvent that dissolves the

virgin polymer. A known weight of finely cut processed polymer sample was placed in a known weight paper thimble and was Soxhlet extracted using toluene as a solvent for 8 to 30 hours. Nitrogen was introduced into the system to avoid oxidation during the extraction. After that the thimble was dried in vacuum at room temperature for more than 24 hours and reweighed. The net weight of the residue was obtained and gel content was calculated as shown in equation 3.

$$\text{Gel content \%} = (w_1/w_2) \times 100 \quad \text{Eqn. (3)}$$

Where  $w_1$  is the residual weight of the extracted polymer (insoluble in the thimble) and  $w_2$  is the original weight of the polymer before extraction.

## 2.7 MEASUREMENT OF MELT FLOW INDEX

The melt flow index (MFI) is a measure of melt viscosity and is related to the molecular weight of the polymer. It is defined as the mass (g) of the molten polymer extruded under a given weight through a standard die in a given time. To determine the alteration of melt viscosity of EP resulting from the processing, the MFI of GMA functionalised EP samples was measured by using a Devonport Melt Flow Indexer at constant extrusion temperature of 230°C and 2.16 kg load in accordance with ASTM D 1238. A standard die of 1mm diameter was used for all samples. After the samples were granulated, 3g of each sample was charged into the barrel within one minute. The sample was preheated for 4 min before placing the load to drive the molten polymer through the die. The time interval for the cut-offs was 1-4 minutes depending on the flow rate of each sample.

## 2.8 FOURIER TRANSFORM INFRARED (FTIR) SPECTROSCOPY

FTIR measurements were performed on a Nicolet spectrophotometer 5DXC over a range of 4000-400  $\text{cm}^{-1}$  at a 4  $\text{cm}^{-1}$  resolution and spectral collection over 64 scans. A dedicated computer was used to control the spectrophotometer with an OMINC software. Polymer film specimens were clamped by a magnetic ring onto a metal plate having a 25×14 mm aperture and presented the sample to the beam in the usual position. Obtained spectra were saved on the computer for subsequent analysis and manipulation. The FTIR spectra of

liquid samples were recorded as thin film of the chemical used held in the infrared beam between two KBr discs. For solid samples, FTIR spectra were obtained using pressed potassium bromide disc.

## **2.9 SCANNING ELECTRON MICROSCOPY (SEM)**

Morphology of the blends was characterised from a cross-section of cryogenically fractured surfaces of the compression moulded plaques by using a Cambridge Instruments Stereoscan 90 Scanning Electron Microscope. Stripes cut from the compression moulded plaques were immersed in liquid nitrogen for more than 15 minutes to cool down and then were taken out to fracture immediately. The middle of the cooled sample stripes was clamped by an adjustable spanner and the free part of the stripes were bended with a quick force by hand to fracture the samples. For better observation, the fractured surfaces were subjected to etching with boiling toluene or xylene for 3-4 hours so that the rubber phase in the fractured surfaces was extracted and then samples were dried overnight in a vacuum oven. The ends with fractured surfaces were sliced with a sharp razor blade and attached to a metal stub using a double sided sticky carbon pad with the fractured surface facing up. The samples were sputter coated with gold using an Emscope SM300 Coater prior to SEM examination. The viewed SEM micrographs at appropriate magnification were saved as individual files for subsequent analysis.

## **2.10 MEASUREMENT OF DYNAMIC MECHANICAL PROPERTIES**

The measurement of dynamic mechanical properties of the PET blends was carried out in a Polymer Laboratories dynamic mechanical thermal analyser (DMTA). The dynamic mechanical properties include storage modulus  $E'$ , loss modulus  $E''$  and the internal friction  $\tan\delta$  ( $\tan\delta = E''/E'$ ). Dynamic mechanical thermal analysis (DMTA) is a good technique for the study of the compatibilisation of polymer blends and the effect of compatibilisation on the dynamic mechanical properties of various polymer blends have been reported [142-146]. Generally, for an incompatible blend, the  $\tan\delta$  vs temperature curve shows the presence of two  $\tan\delta$  or damping peaks corresponding to the glass transition temperatures of the individual polymers [146]. For a highly compatible blend the curve shows only a single peak in between the transition temperatures of the component polymers, whereas there are two separate peaks corresponding to the individual polymer in



the case of partially compatible polymer blends, but the position of the peaks shifts to higher or lower temperature as a function of compositions [144]. DMTA analysis of PET blends or blending components was performed at a fixed frequency of 10 Hz in a bending mode over the temperature range of -80°C to 180°C at a 3°C/min temperature rise, using liquid nitrogen as a cryogenic medium. The dimensions of the test specimens which was cut from the compression moulded plaques were 50×10 ×3mm. The data was processed by a dedicated computer and the storage modulus and  $\tan\delta$  were plotted against temperature.

## **2.11 TENSILE PROPERTY MEASUREMENT**

Tensile test was carried out on an Instron machine (Model 4302), which was equipped with a dedicated computer to collect the data and report a statistical analysis of the selected tensile parameters from five replicates per samples. The test specimens were cut from 1 mm thick compression moulded sheet with a dumb-bell shape cutter (width of 4mm and parallel length of 30 mm) and the dimensions are indicated in Figure 2-22. A pair of pneumatic grips were used to grasp the both ends of dumb-bell specimens and an extensometer was used to measure the elongation. All tensile tests were conducted at a crosshead speed of 100 mm/min in accordance with ISO 527 using gauge length of 20mm to measure the strain. The tensile strength, stress at yielding and elongation at break were measured using 5 dumb-bell shaped specimens each sample and the mean values were reported. The tensile strength is the stress (tensile load per unit cross-sectional area) sustained by the sample during the test and the elongation at break is the gain in length caused by a tensile load expressed as a percentage of original length to break point. The yield stress detected as the peak stress at the point at which an increase in strain first occurred without an increase in stress (position B) (see Figure 2-23).

## **2.12 DIFFERENTIAL SOLVENT FRACTIONATION OF GMA GRAFTED EPDM/PP MIXTURE**

Solvent fractionation of GMA grafted EPDM/PP mixture (EPDM/PP-g-GMA) was carried out with three refluxing solvents of increasing solubility parameters and boiling points. This provides several fractions with different ratios of PP/EPDM. Each fraction can be analysed to examine the difference of GMA grafting.

The virgin polymers, EPDM and PP, are soluble in refluxing hexane and xylene, respectively. Three solvents, hexane, toluene and xylene, were chosen for sequential Soxhlet extraction. A 2-3g of EPDM/PP-g-GMA sample pressed into several thin films was placed into a known weight of paper thimble. After 12 hours extraction with hexane, the thimble was dried in vacuum oven for 24 hours and the weight of the insoluble fraction remaining in the thimble was determined. The thimble was sequentially subjected to Soxhlet extraction with toluene and then xylene and the toluene and xylene insoluble fractions were then determined. The soluble fractions in the three solvents were precipitated in acetone and dried in vacuum oven. These fractions were analysed separately by FTIR.

### **2.13 FTIR ANALYSIS OF PET BLENDS**

To characterise the PET/EPDM-g-GMA or EP-g-GMA blends and determine the formation of graft copolymer of PET-co-EPDM or EP via the reaction of epoxy groups grafted onto the EPDM chains with the end groups of PET (-COOH, -OH) during the reactive blending, a solvent extraction method was used to separate the individual components of the blend (PET and EPDM-g-GMA). The samples were pressed into thin films and dissolved into a mixed solvent of phenol/chlorobenzene/xylene (40/40/20 w/w) at 80°C. Phenol is a good solvent for PET whereas chlorobenzene/xylene mixture is a good solvent for the rubber phase. After the solution was filtered off to remove any impurity, the solution was added to warm toluene to precipitate PET. The PET fraction was filtered off and washed with toluene. The precipitated PET was dried in a vacuum oven at 80°C for more than 20 hours. About 0.1 g of the separated PET was pressed into thin film using a press at a temperature of 275°C. FTIR spectra of all films were recorded on a Nicolet FTIR Spectrometer from 4000 to 400  $\text{cm}^{-1}$  with a 4  $\text{cm}^{-1}$  resolution for 64 scans.

### **2.14 POLYMERISATION OF POLYGMA, POLYTRIS AND GMA-CO-TRIS**

Homopolymerisation of GMA and TRIS and copolymerisation of GMA and TRIS (GMA-co-TRIS) could take place during the melt grafting of GMA onto EP. To analyse the reaction products polyGMA, polyTRIS and GMA-co-TRIS were synthesised on the bench.

### **2.14.1 Homopolymerisation of GMA in Chloroform**

Homopolymerisation of GMA was carried out on the bench using AIBN as an initiator in chloroform. 100 ml chloroform and 8.52g GMA was mixed with 0.1 molar ratio (AIBN/GMA) of initiator AIBN in a 250ml three-neck round bottom flask. After assembling with thermometer, condensor and purging with Argon gas, the solution was refluxed for 4 hours. After cooling the solution down to room temperature, it solution was precipitated into 400 ml methanol, filtered and washed thoroughly with methanol. After drying in vacuum for 24 hours, white particles were obtained. Characterisation by FTIR is given later in Chapter 3 and IR spectrum of the white particles (polyGMA) is shown in Figure 2-24.

### **2.14.2 Homopolymerisation of TRIS in Benzene**

Homopolymerisation of TRIS was carried out on the bench using AIBN as an initiator in benzene. 100 ml benzene and 8.52g TRIS were mixed with 0.3 molar ratio (AIBN/TRIS) of initiator AIBN in a 250ml three necked round bottomed flask. After assembling with thermometer, condensor and purging with Argon gas, the solution was maintained at a temperature of 70°C for 5 hours. After cooling the solution down to room temperature, benzene completely evaporated in air, and then the reaction product was washed thoroughly with dichloromethane. After drying in vacuum for 24 hours, white particles were obtained. Characterisation by FTIR is given later in Chapter 3 and IR spectrum of the white particles (polyTRIS) is shown in Figure 2-25.

### **2.14.3 Copolymerisation of TRIS and GMA in Toluene**

Copolymerisation of TRIS and GMA was carried out on the bench using AIBN as an initiator in toluene. 100 ml toluene, 5.68g GMA and 2.43g TRIS (GMA/TRIS: 7/3 W/W) were mixed with 0.1 molar ratio (AIBN/TRIS+GMA) of initiator AIBN in a 250ml three necked round bottomed flask. After assembling with thermometer, condensor and purging with Argon gas, the solution was maintained at a constant temperature of 70°C for 5 hours. After the solution was cooled down to room temperature, the toluene was evaporated in air. The reaction product was washed thoroughly with acetone to remove any free GMA and

TRIS and polyGMA. After drying in vacuum for 24 hours, white particles were obtained. Characterisation by FTIR is given later in Chapter 3 and IR spectrum of the white particles (GMA-co-TRIS) is shown in Figure 2-26.

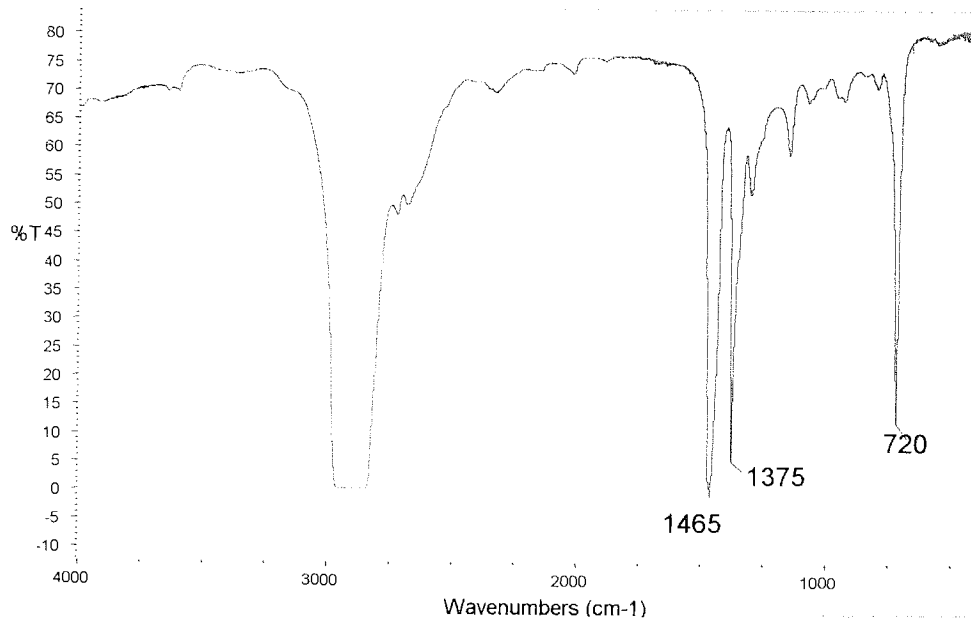


Figure 2-1 FTIR spectrum of EP (Tafmer P0480) from pressed film (thickness: ~0.1mm)  
 ( $\text{CH}_2, \text{CH}_3$  deformation ( $1465 \text{ cm}^{-1}, 1375 \text{ cm}^{-1}$ );  $(-\text{CH}_2-)_n$  rocking ( $720 \text{ cm}^{-1}$ ))

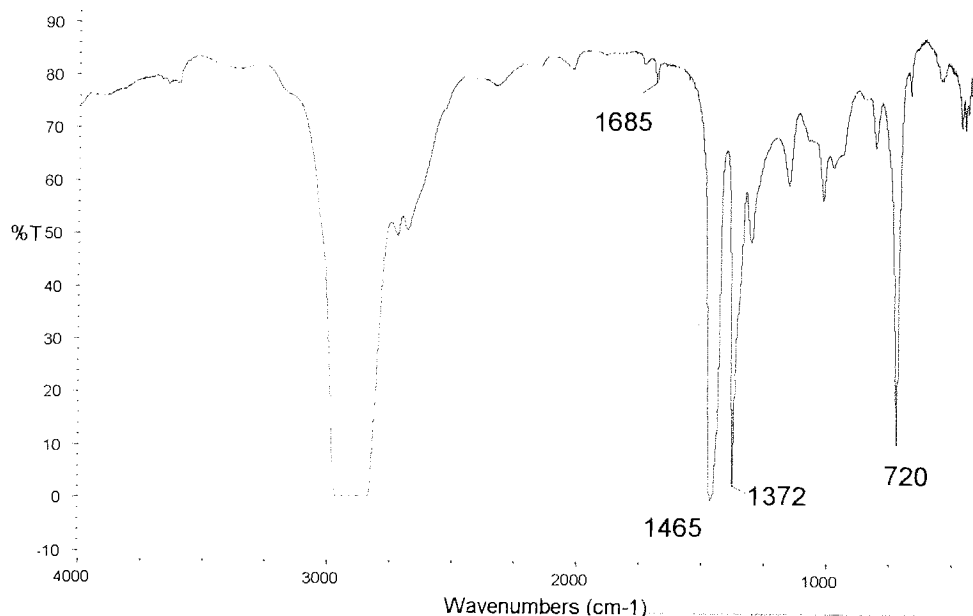


Figure 2-2 FTIR spectrum of EPDM (Buna 447) from filmed (thickness: ~0.1mm)  
 ( $\text{C}=\text{C}$  stretching ( $1685 \text{ cm}^{-1}$ );  $\text{CH}_2, \text{CH}_3$  deformation ( $1465 \text{ cm}^{-1}, 1375 \text{ cm}^{-1}$ );  
 $(-\text{CH}_2-)_n$  rocking ( $720 \text{ cm}^{-1}$ ))

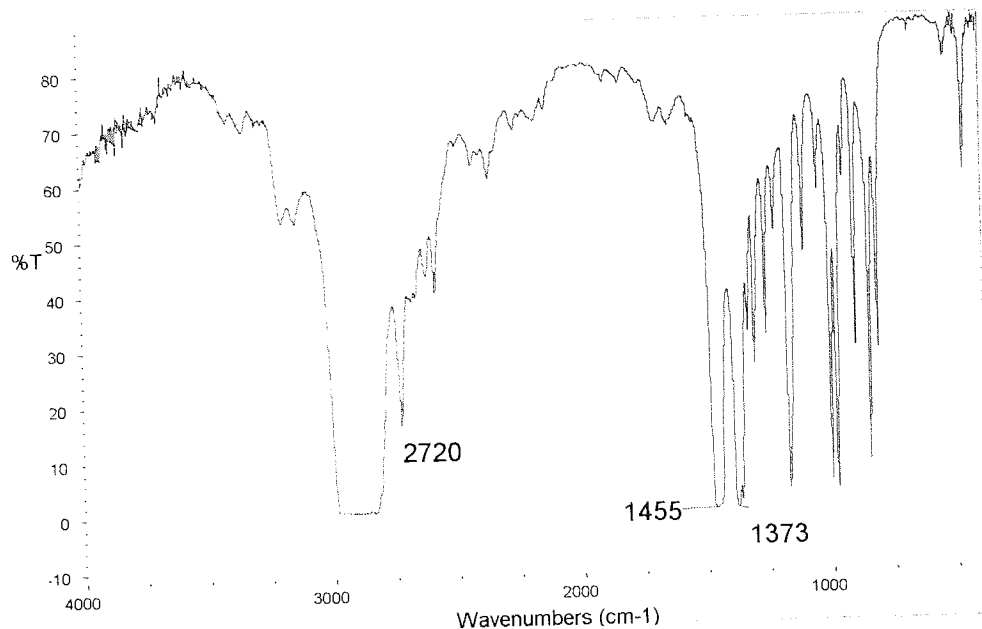


Figure 2-3 FTIR spectrum of PP (HF-26) from pressed film (thickness: ~0.1 mm)  
 (CH<sub>2</sub> stretching (2720 cm<sup>-1</sup>); CH<sub>2</sub>, CH<sub>3</sub> deformation (1465 cm<sup>-1</sup>, 1373 cm<sup>-1</sup>))

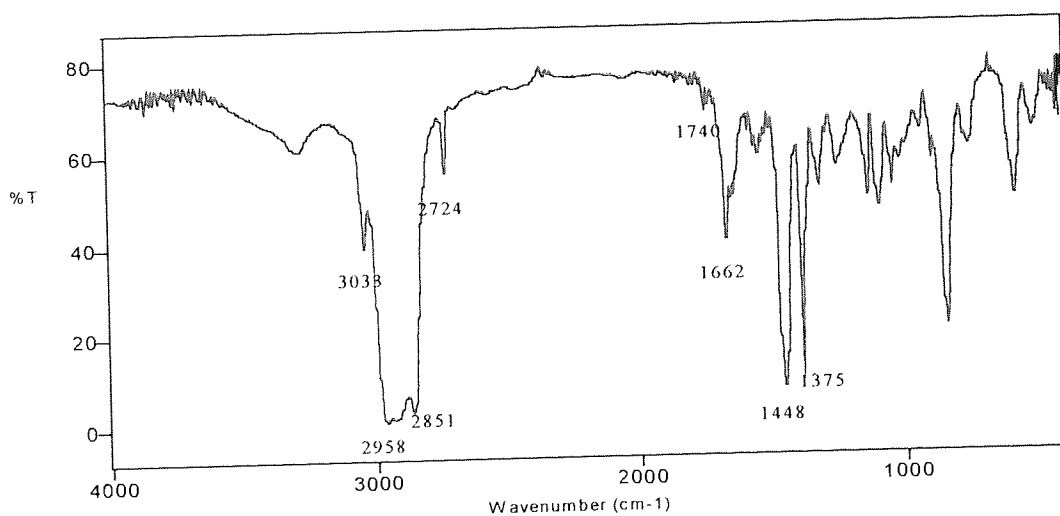


Figure 2-4 FTIR spectrum of SMR-L film casted from benzene (=CH stretching (3033 cm<sup>-1</sup>); CH<sub>2</sub>, CH<sub>3</sub> stretching (2958 cm<sup>-1</sup>, 2851 cm<sup>-1</sup>); CH<sub>2</sub> stretching (2720 cm<sup>-1</sup>); C=C stretching (1662 cm<sup>-1</sup>); CH<sub>2</sub>, CH<sub>3</sub> deformation (1448 cm<sup>-1</sup>, 1375 cm<sup>-1</sup>))

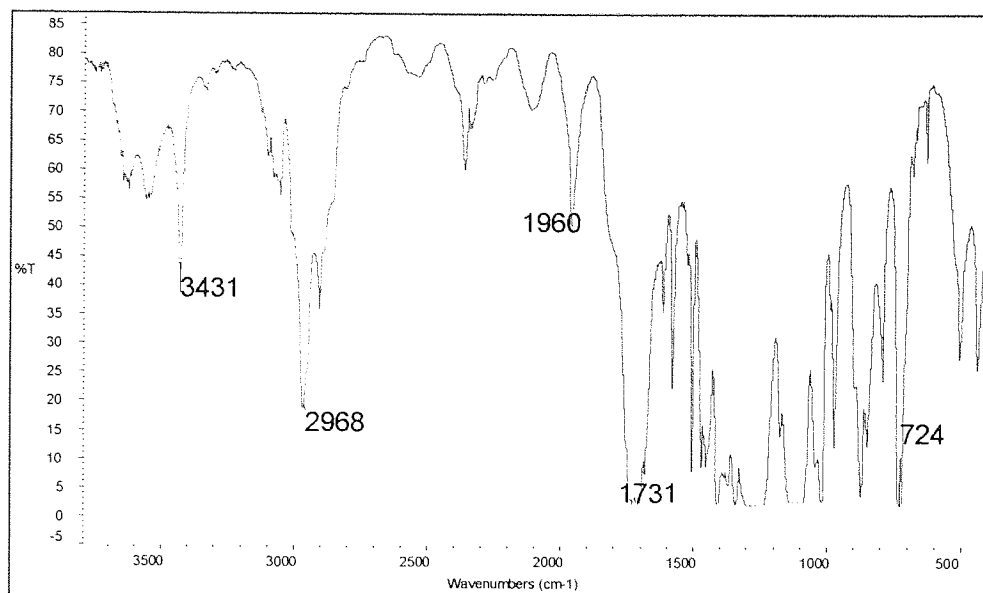


Figure 2-5 FTIR spectrum of PET from pressed film (thickness:  $\sim 0.1$ mm)  
 (-OH stretching ( $3431\text{ cm}^{-1}$ ); CH stretching ( $2968\text{ cm}^{-1}$ );  $>\text{C}=\text{O}$  stretching  
 ( $1731\text{ cm}^{-1}$ );  $(-\text{CH}_2-)_n$  rocking ( $720\text{ cm}^{-1}$ ))

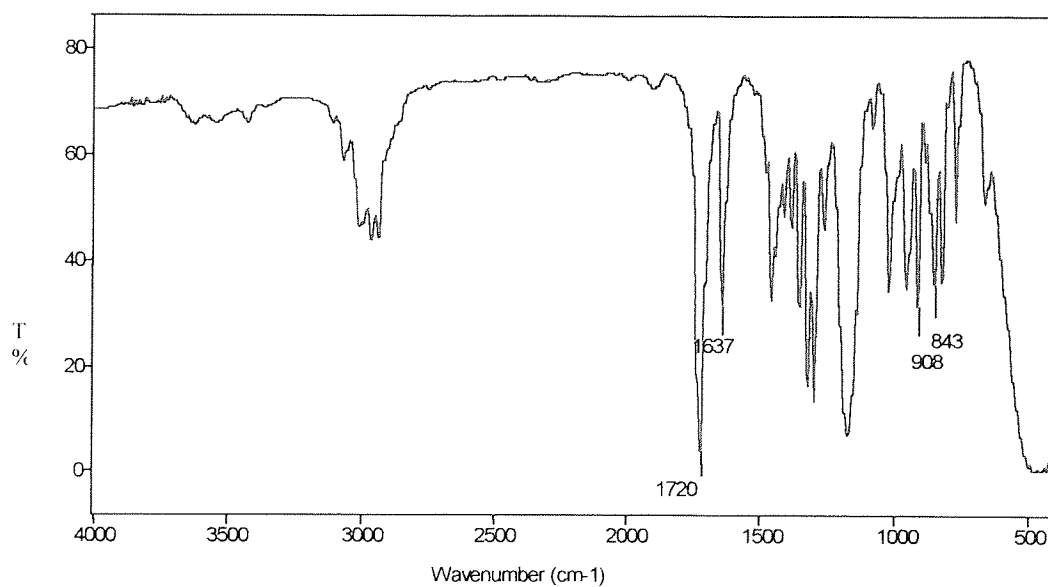


Figure 2-6 FTIR spectrum of neat GMA film between KBr cells ( $>\text{C}=\text{O}$  stretching  
 ( $1720\text{ cm}^{-1}$ );  $\text{C}=\text{C}$  stretching ( $1637\text{ cm}^{-1}$ );  $-\text{C}-\text{O}-\text{C}-$  deformation from  
 epoxy ring ( $908\text{ cm}^{-1}$ ,  $843\text{ cm}^{-1}$ ))

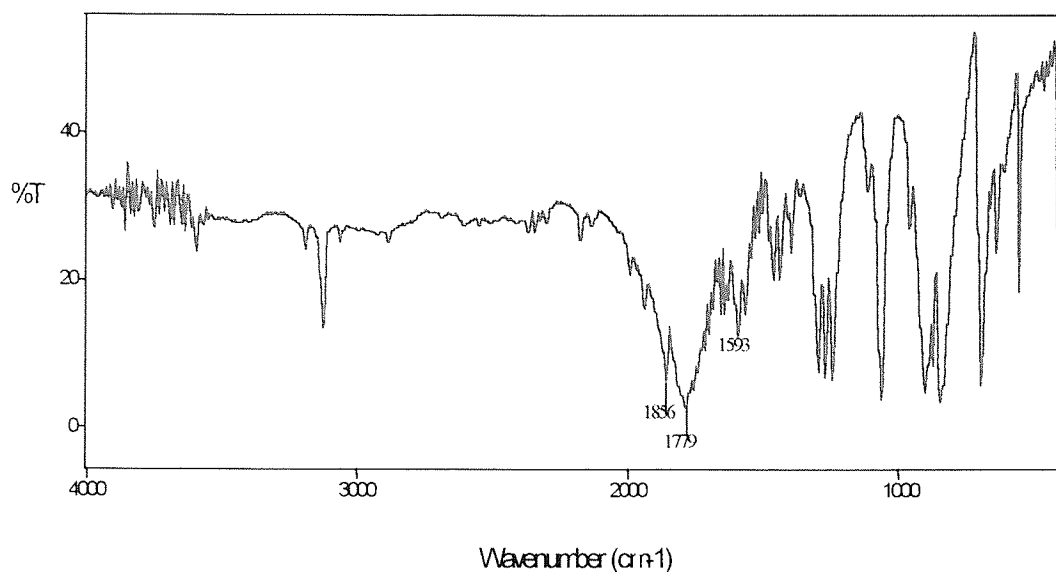


Figure 2-7 FTIR spectrum of maleic anhydride using pressed KBr disc (5-ring cyclic anhydride asymmetric stretching ( $1856\text{ cm}^{-1}$ ); 5-ring cyclic anhydride symmetric stretching ( $1779\text{ cm}^{-1}$ );

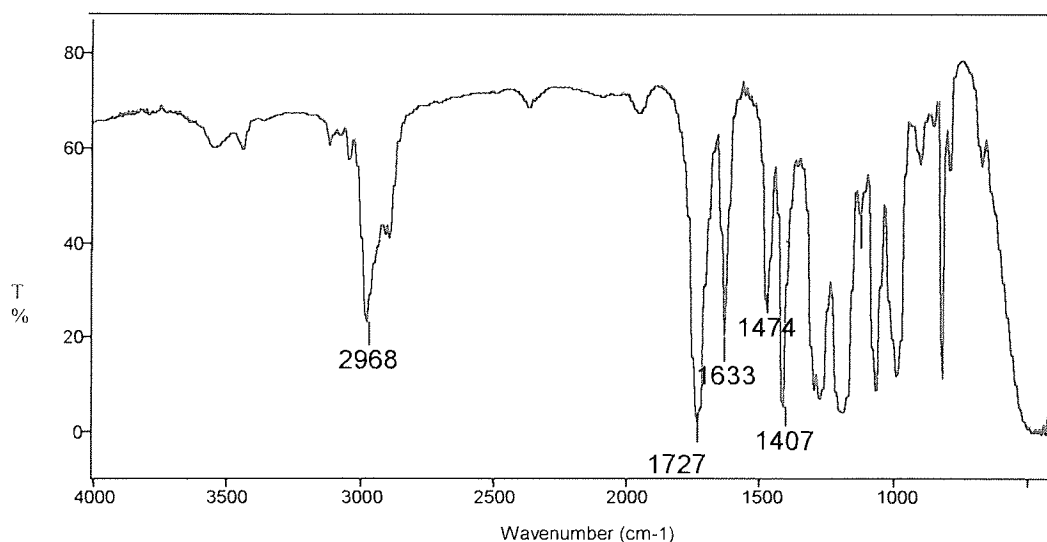


Figure 2-8 FTIR Spectrum of neat TRIS film between KBr cells ( $>\text{C}=\text{O}$  stretching ( $1727\text{ cm}^{-1}$ );  $\text{C}=\text{C}$  stretching ( $1633\text{ cm}^{-1}$ );  $\text{CH}_2, \text{CH}_3$  deformation ( $1474\text{ cm}^{-1}$ ,  $1407\text{ cm}^{-1}$ ))



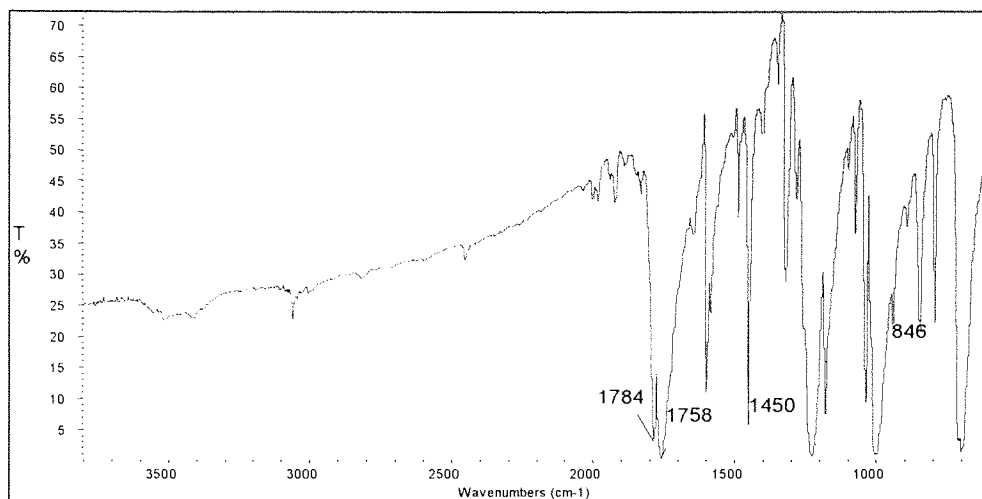


Figure 2-9 FTIR spectrum of BPO using pressed KBr disc  
 (  $>C=O$  stretching ( $1758\text{ cm}^{-1}$ ))

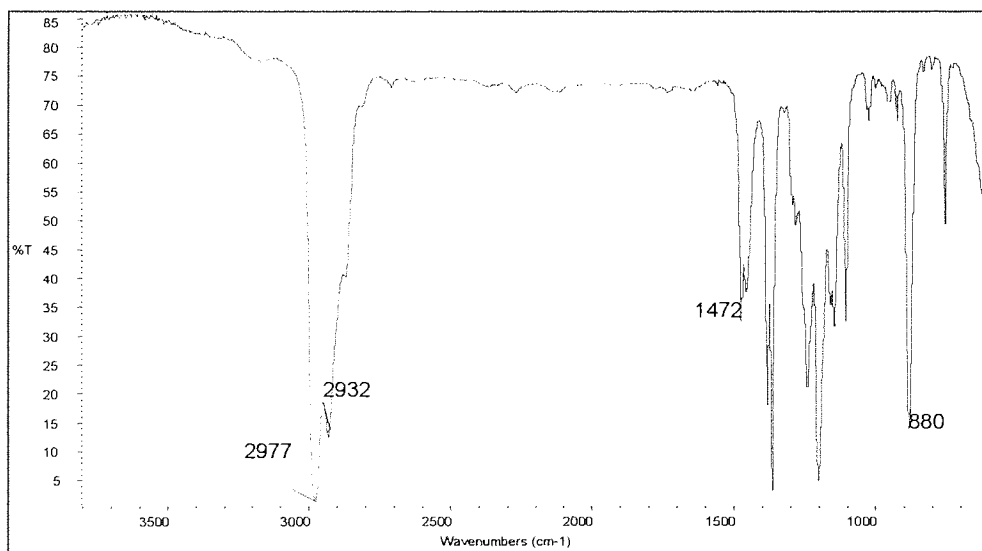


Figure 2-10 FTIR spectrum of neat T101 between KBr cells (CH stretching ( $2977\text{ cm}^{-1}$ ,  $2932\text{ cm}^{-1}$ );  $CH_2$ ,  $CH_3$  deformation ( $1472\text{ cm}^{-1}$ ))

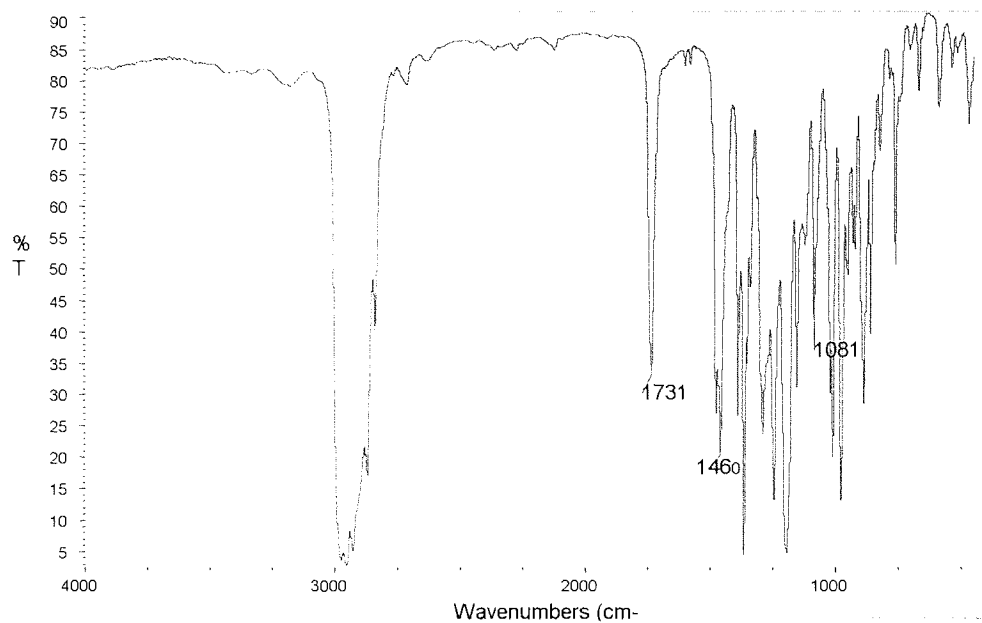


Figure 2-11 FTIR spectrum of neat T29B90 between KBr cells

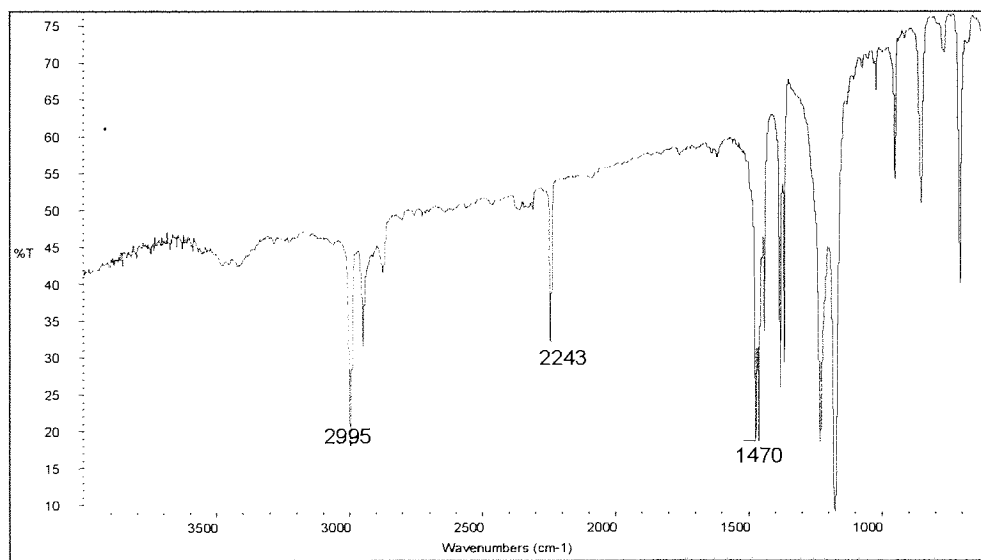


Figure 2-12 FTIR spectrum of AIBN using KBr disc (CH stretching ( $2995\text{ cm}^{-1}$ ); CN stretching ( $2244\text{ cm}^{-1}$ ); CH deformation ( $1470\text{ cm}^{-1}$ ))

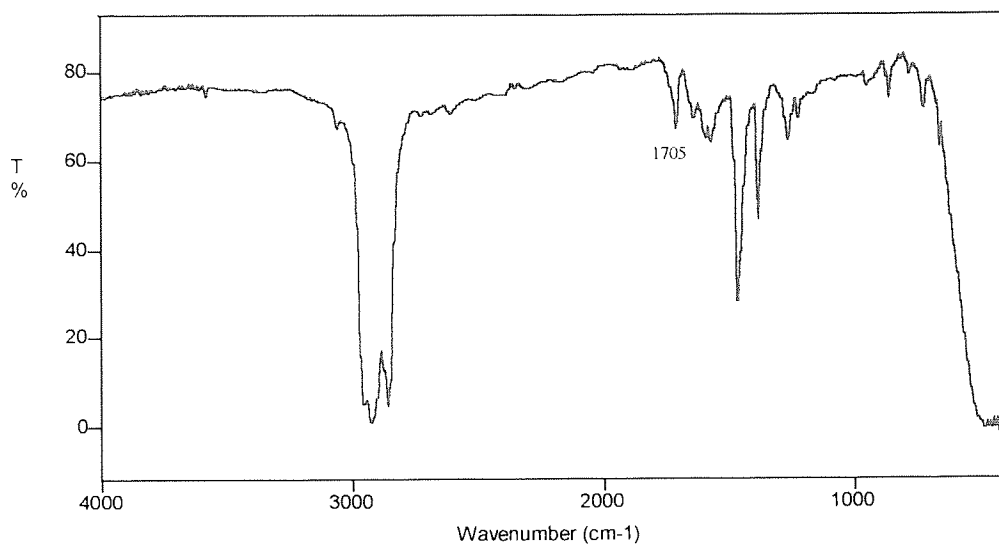


Figure 2-13 FTIR spectrum of maleic acid in NUJOL ( $>C=O$  stretching ( $1705\text{ cm}^{-1}$ ))

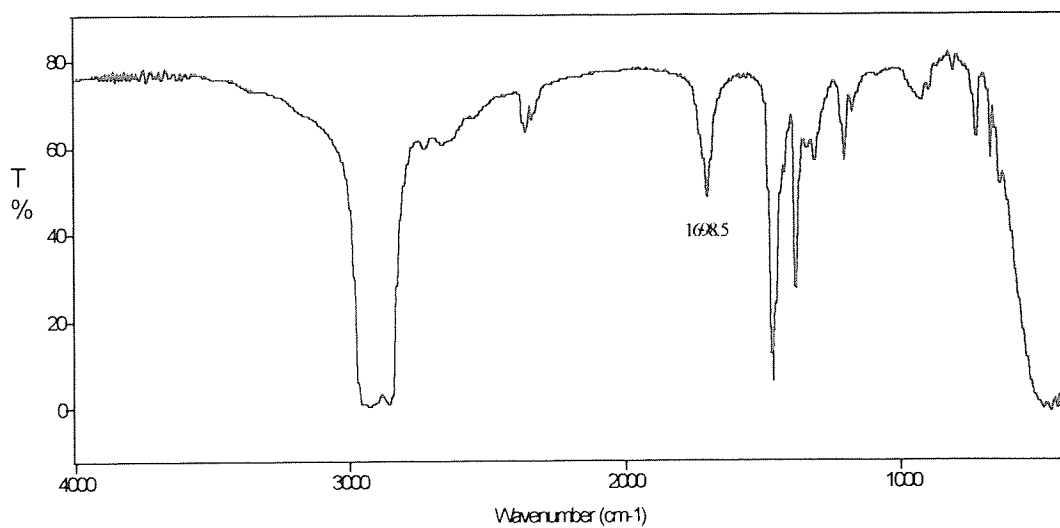


Figure 2-14 FTIR spectrum of succinic acid in NUJOL ( $>C=O$  stretching ( $1699\text{ cm}^{-1}$ ))

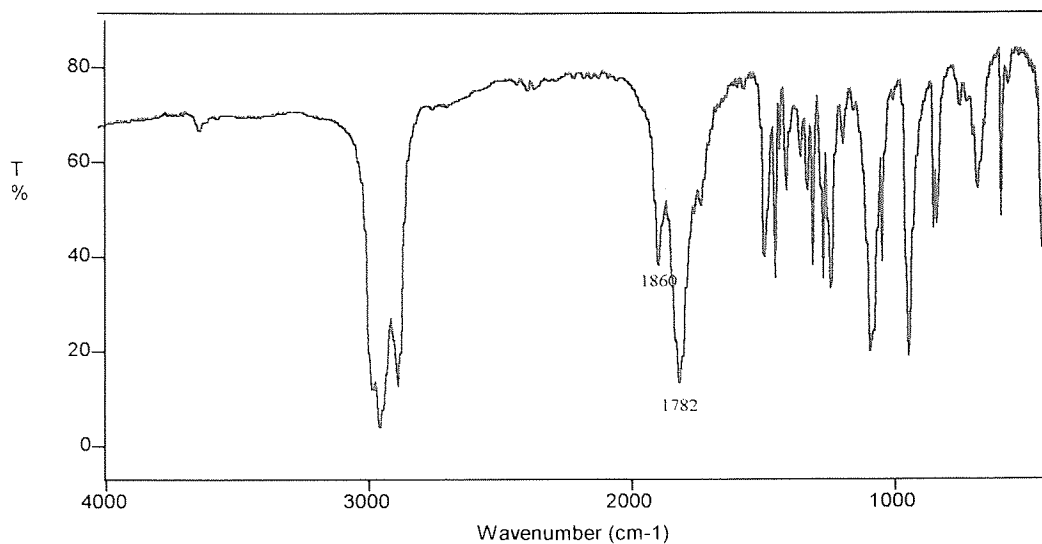


Figure 2-15 FTIR spectrum of succinic anhydride in NUJOL (5-ring cyclic anhydride asymmetric stretching ( $1860\text{ cm}^{-1}$ ); 5-ring cyclic anhydride symmetric stretching ( $1782\text{ cm}^{-1}$ );

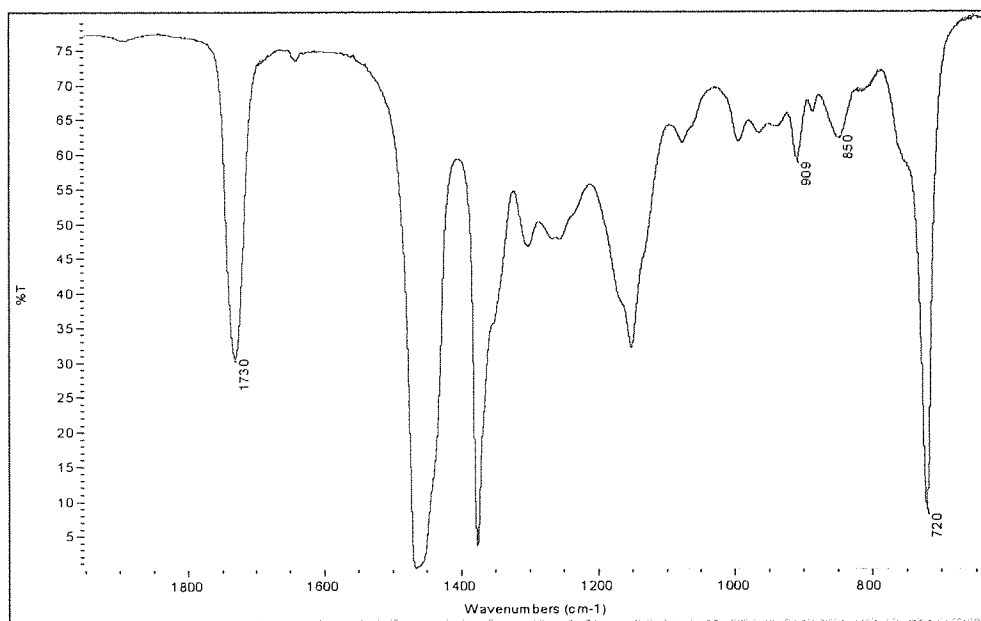
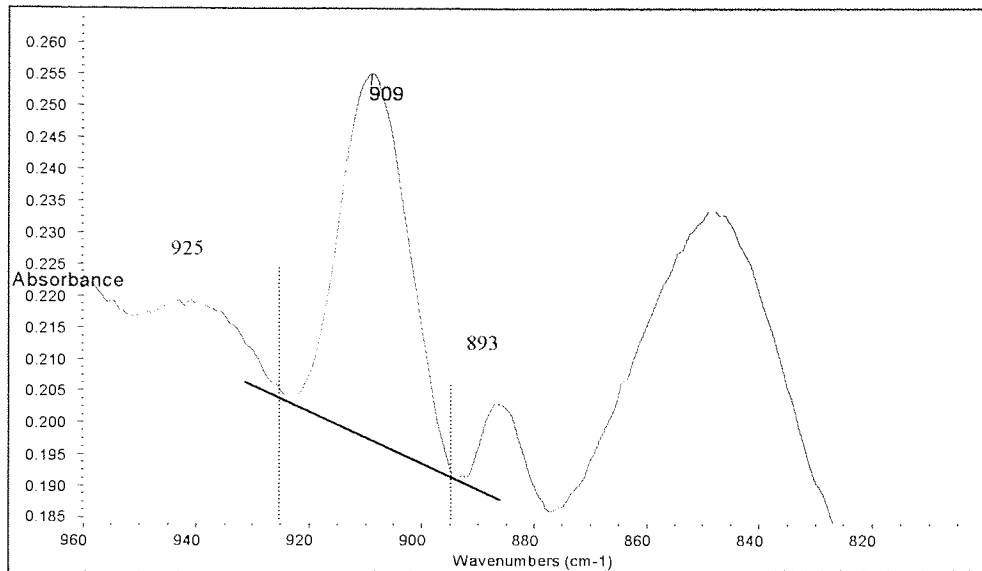
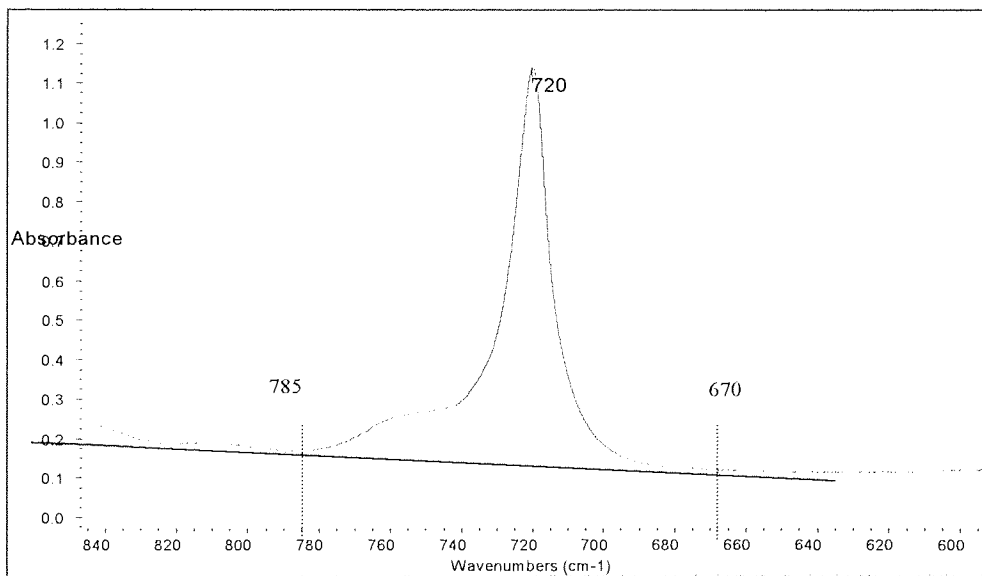


Figure 2-16 FTIR spectrum of pressed film of GMA functionalised EP (thickness:  $\sim 0.1$  mm)



(a) Epoxy group peak at  $909\text{cm}^{-1}$



(b) Reference peak at  $720\text{cm}^{-1}$

Figure 2-17 Area boundaries for absorption peak area calculation of GMA functionalised EP (a) Epoxy group peak at  $909\text{cm}^{-1}$  (b) Reference peak at  $720\text{cm}^{-1}$

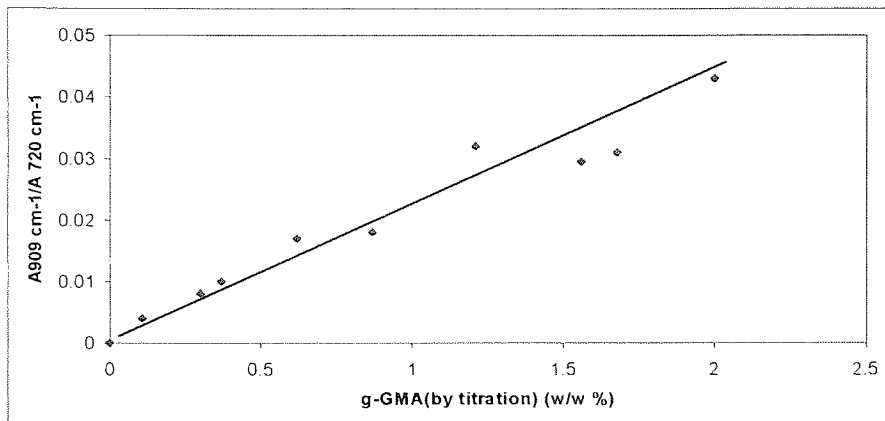
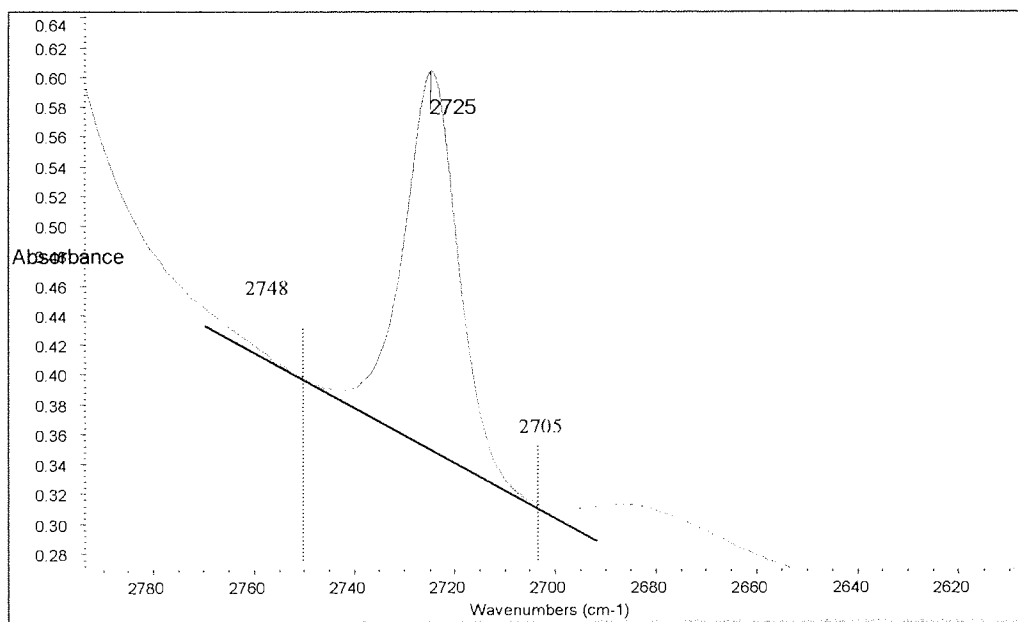
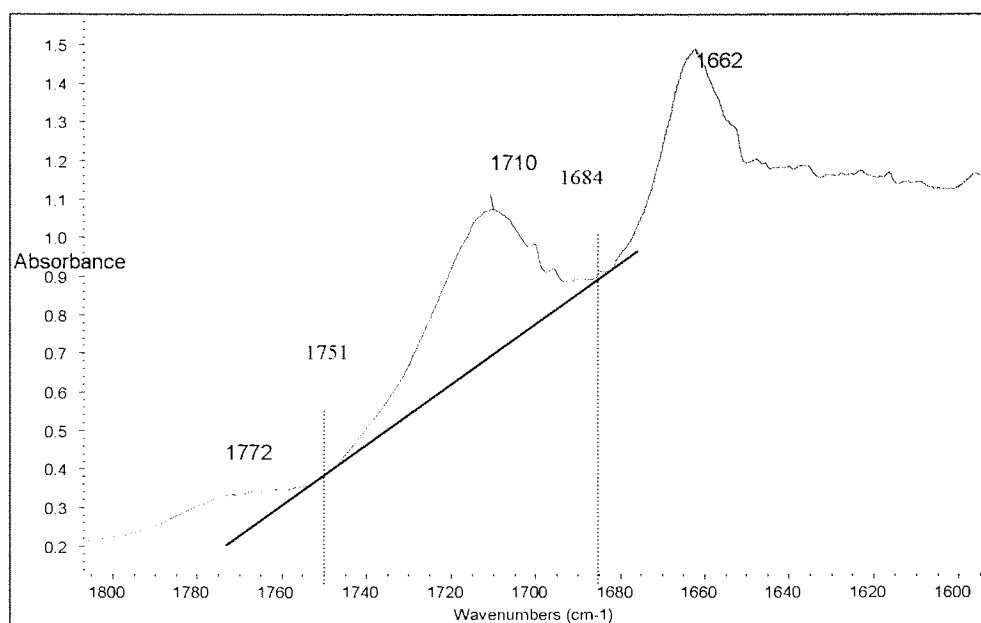


Figure 2-18 Calibration curve obtained from correlation between grafting degree measured by titration and area ratio ( $A_{909\text{ cm}^{-1}}/A_{720\text{ cm}^{-1}}$ ) from FTIR



(a) Reference peak at  $2725\text{cm}^{-1}$



(b) Acid peak at 1710cm<sup>-1</sup>

Figure 2-19 Area boundaries for absorption peak area calculation of MA functionalised NR (a) Reference peak at 2725cm<sup>-1</sup> (b) Acid peak at 1710cm<sup>-1</sup>

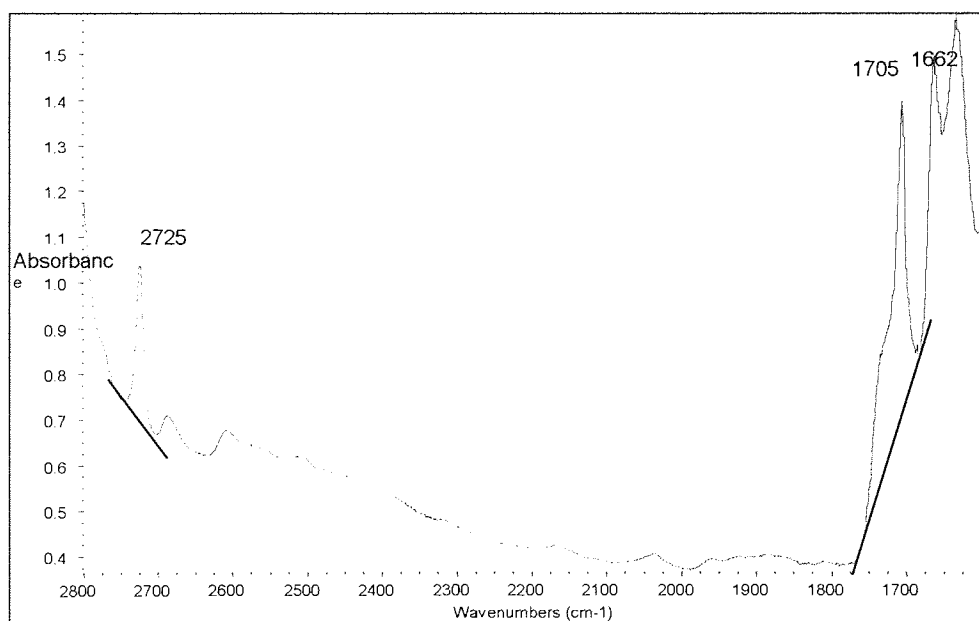


Figure 2-20 FTIR spectrum of an example of SMR-L/maleic acid film casted from solution (diethyl ether) on a KBr cell for calibration

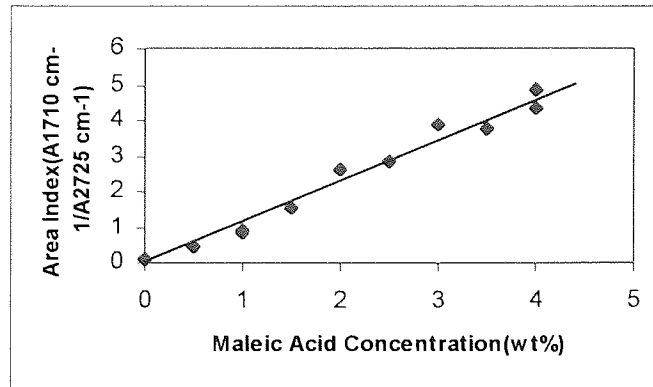


Figure 2-21 Calibration curve from maleic acid / SMR-L films

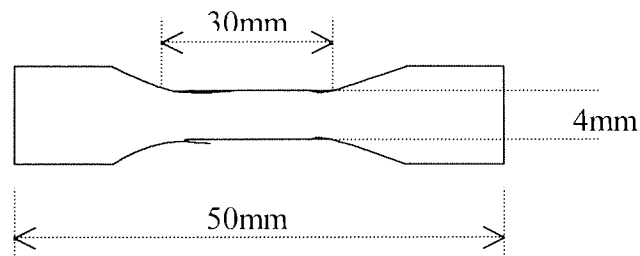


Figure 2-22 Dimensions of dumb-bell shape tensile test specimen

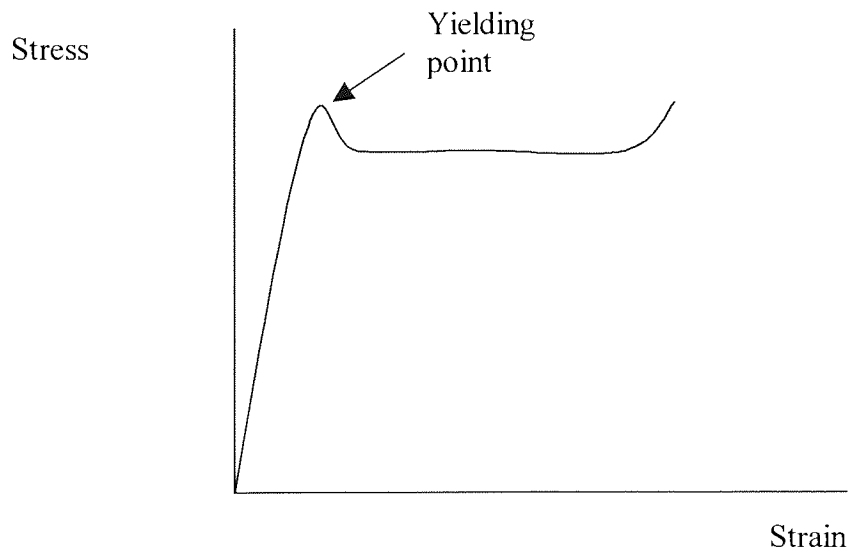


Figure 2-23 Idealised tensile stress-strain curve for a typical plastics material



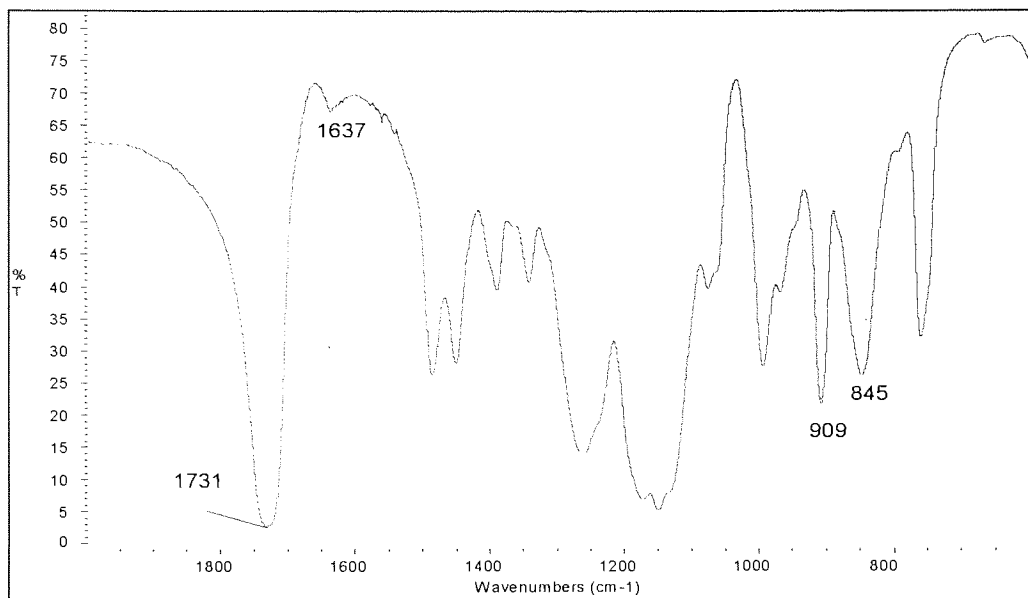


Figure 2-24 FTIR spectrum of polyGMA using KBr disc

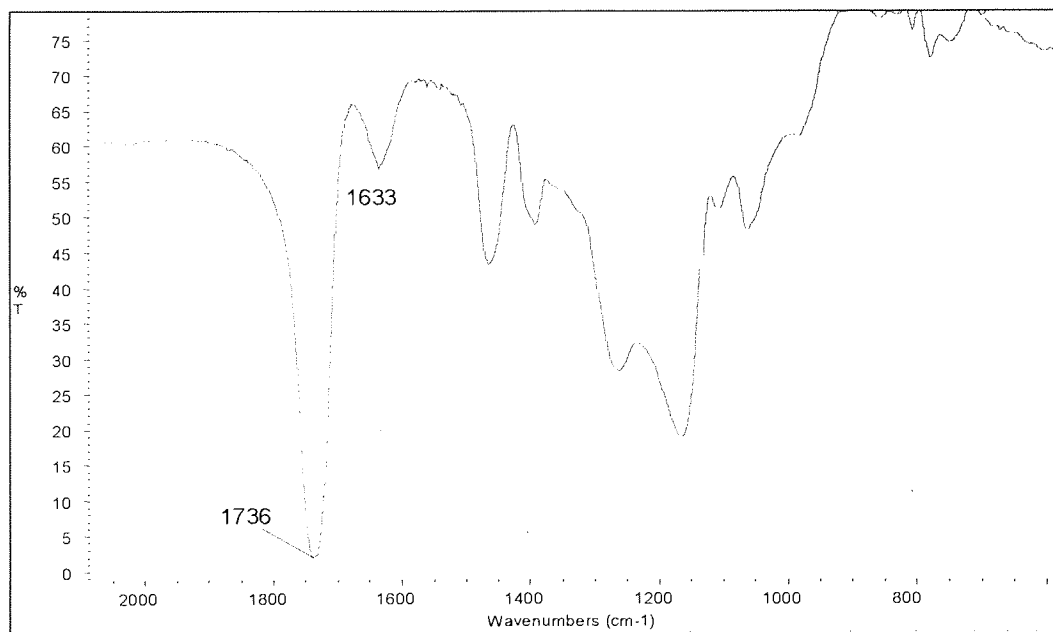


Figure 2-25 FTIR spectrum of polyTRIS using KBr disc

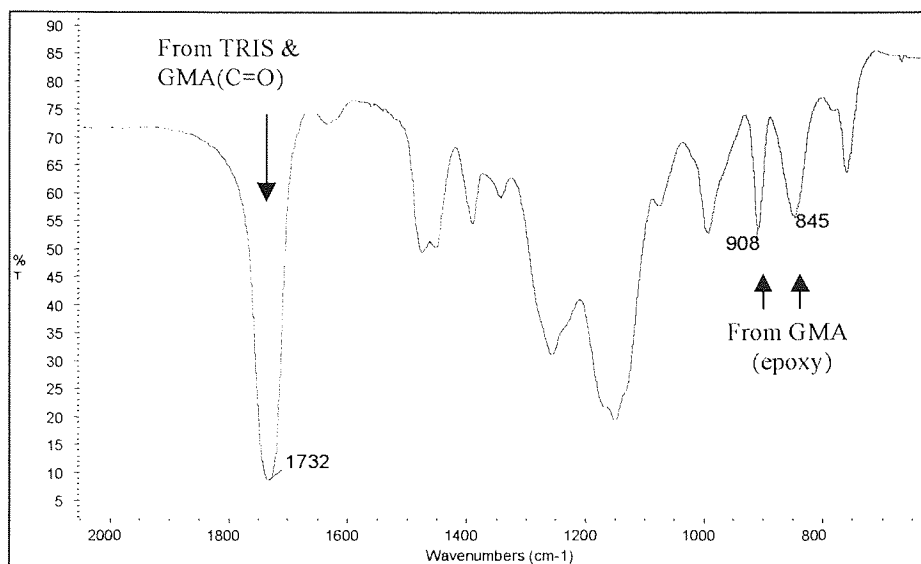


Figure 2-26 FTIR spectrum of copolymer GMA-co-TRIS using KBr disc

## CHAPTER 3 FUNCTIONALISATION OF POLYOLEFINS WITH GLYCIDYL METHACRYLATE

### 3.1 OBJECTIVE AND METHODOLOGY

In recent years glycidyl methacrylate (GMA) has been used extensively as a grafting monomer in polyolefins and in turn these functionalised polymers have been used as in situ compatibilisers of polymer blends. GMA (I) bears a double bond (free-radical reactivity) and an epoxy group (functional reactivity). The epoxy group possesses reactivity towards various functional groups such as  $-\text{COOH}$ ,  $-\text{OH}$ ,  $-\text{SH}$  and  $-\text{NH}_2$ . GMA can play an important role in the chemical modification of commercial polymers which can be achieved by reactive processing methods. GMA has been free-radically grafted onto EPR, EPDM [23,113-118], PP [119-125] and PE [113,126] in the molten state and various polymer blends have been compatibilised with GMA-containing copolymers. However, the melt free radical grafting reactivity of GMA in polymers is low. Unless a large excess of peroxide is employed, the conversion of GMA monomer to grafted GMA onto PP has been reported not to exceed 10% [113,119-121,125]. As it was described in the section 1.6.2, side-reactions such as chain scission or crosslinking of polymer substrates, homopolymerisation of monomers, will always accompany the desired grafting reaction. Some researches have made the attempts to reduce these side-reactions and enhance the grafting reaction by adding a second monomer during melt grafting. For example, styrene has been used as a comonomer during the grafting of MA and GMA onto polyolefins to improve grafting yields and reduce side reactions [118-120].

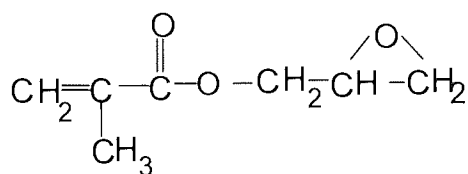
The objective in this part of the study was to functionalise EP, EPDM and a mixture of EPDM/PP with GMA via a melt grafting process in an internal mixer. A novel approach which has been developed at Aston University [138-141] is explored here with the aim of enhancing the grafting efficiency and reducing the side reactions during the melt grating. This involves the use of a multi-functional monomer, TRIS (II), as a comonomer during the reactive processing. It has been shown that the use of TRIS as a comonomer with different reactive modifiers, such as antioxidant [138] and maleic anhydride [140, 141], gave rise to a dramatic increase in the level of grafting of these monomers on PP. A detailed study of GMA grafting onto EP in the absence and presence of TRIS using T101

as a free radical initiator was first conducted to establish the proper methodology and to investigate the grafting mechanism (See Scheme 3-1). A similar methodology was adopted in the grafting of GMA onto EPDM and a mixture of EPDM/PP.

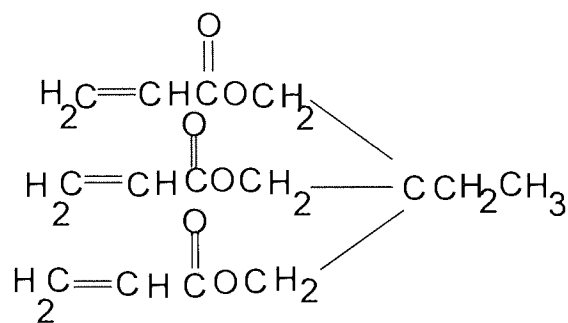
The grafting of GMA onto EP was carried out in a closed system of an internal mixer (torque rheometer). Two free radical initiators, T101 (III) and T29B90 (IV), were used to initiate the grafting reaction of EP with GMA (I) in the presence or absence of the comonomer TRIS (II). The methodology and optimum conditions were established by examining below parameters:

- a) Processing temperature (115°C—190°C);
- b) Processing time (2—15 min);
- c) Concentration of GMA (0—18 phr);
- d) Concentration of TRIS (0—5 phr);
- e) Type of peroxide (T101, T29B90) and their concentrations;
- f) Molar ratio of peroxide to GMA and TRIS;
- g) The addition sequence.

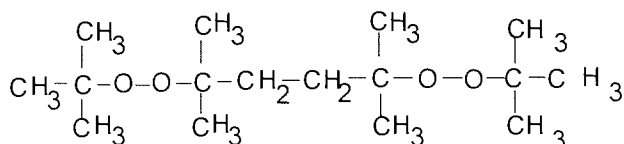
The reaction products were purified by means of Soxhlet extraction and precipitation and then characterised by FTIR. The grafting degree of GMA was evaluated by FTIR method and titration. Tables 3-1, 3-2 and 3-3 list the experimental composition and results for the grafting of GMA onto EP, EPDM and EPDM/PP respectively.



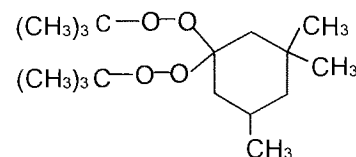
I, GMA



II, TRIS



III, T101



IV, T29B90

To get better understanding of GMA grafting onto polyolefins and analysis of the grafting products, polyGMA, polyTRIS and GMA-co-TRIS were polymerised on the bench and characterised.

## 3.2 RESULTS

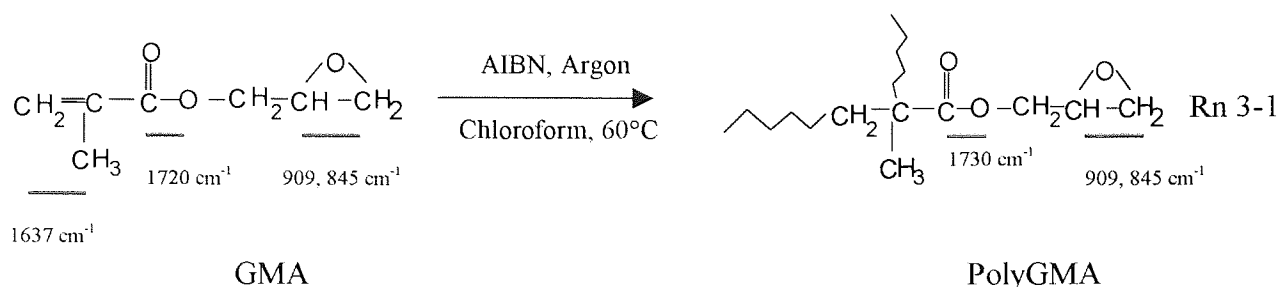
### 3.2.1 Characterisation of PolyGMA, PolyTRIS and GMA-co-TRIS

Homopolymerisation of GMA and TRIS and copolymerisation of GMA and TRIS (GMA-co-TRIS) could take place during the melt grafting of GMA onto EP. To analyse the reaction products, polyGMA, polyTRIS and GMA-co-TRIS were polymerised on the bench using the free radical initiator AIBN (see Section 2.14, p77) and characterised by FTIR.

#### 3.2.1.1 Characterisation of PolyGMA

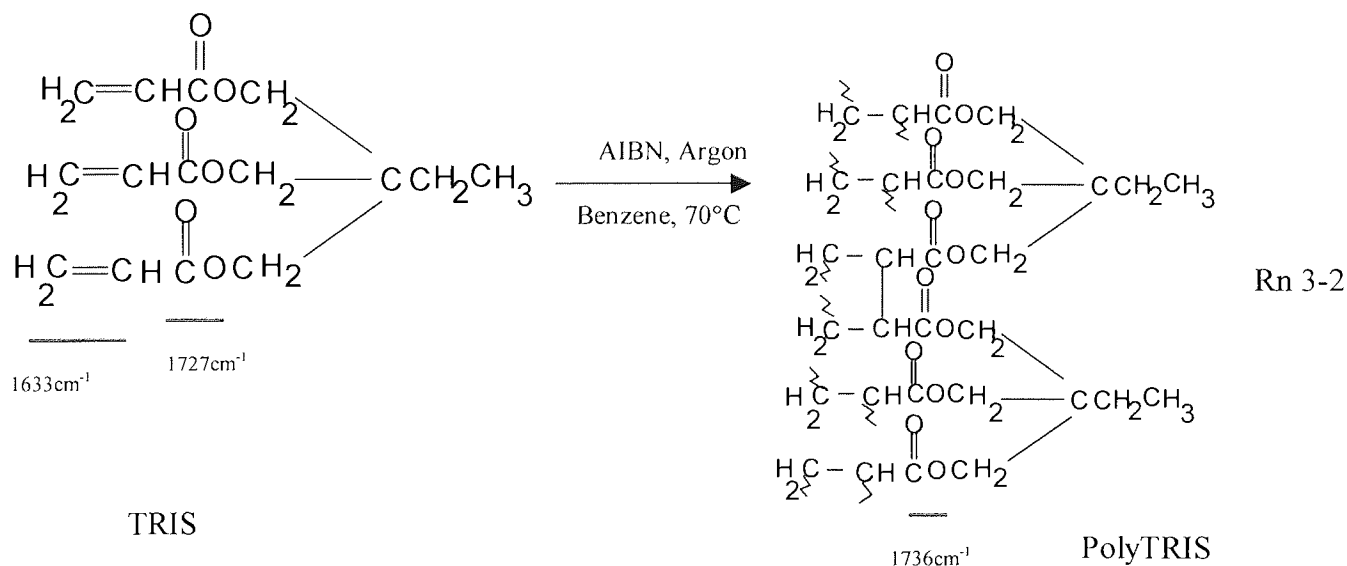
The synthesised polyGMA (see Section 2.14.1, p78) was characterised by comparing its FTIR spectrum with that of fresh GMA. The FTIR spectrum of fresh GMA thin film between two KBr cells (see Fig.2-6) shows that the interesting absorption peaks are at  $1720\text{ cm}^{-1}$  (C=O unsaturated ester group),  $1637\text{ cm}^{-1}$  ( $>\text{C}=\text{CH}_2$  for acrylic double bond) and  $909\text{ cm}^{-1}$  and  $845\text{ cm}^{-1}$  (for epoxy group absorption). After polymerisation, polyGMA was precipitated in methanol to remove free GMA. After filtering, washing and drying, polyGMA white particles were examined by FTIR using KBr disk. The main changes in absorptions were in the saturated carbonyl of the polymer which shifts upto  $1730\text{ cm}^{-1}$  due to saturation (compared to  $1720\text{ cm}^{-1}$  in GMA) and most of the absorption of the acrylic double bond at  $1637\text{ cm}^{-1}$  has disappeared. The absorptions of epoxy group of polyGMA

were still at  $909\text{ cm}^{-1}$  and  $845\text{ cm}^{-1}$  (see Fig.3-1 and Rn 3-1). It was found that polyGMA was soluble in acetone and chloroform and insoluble in methanol.



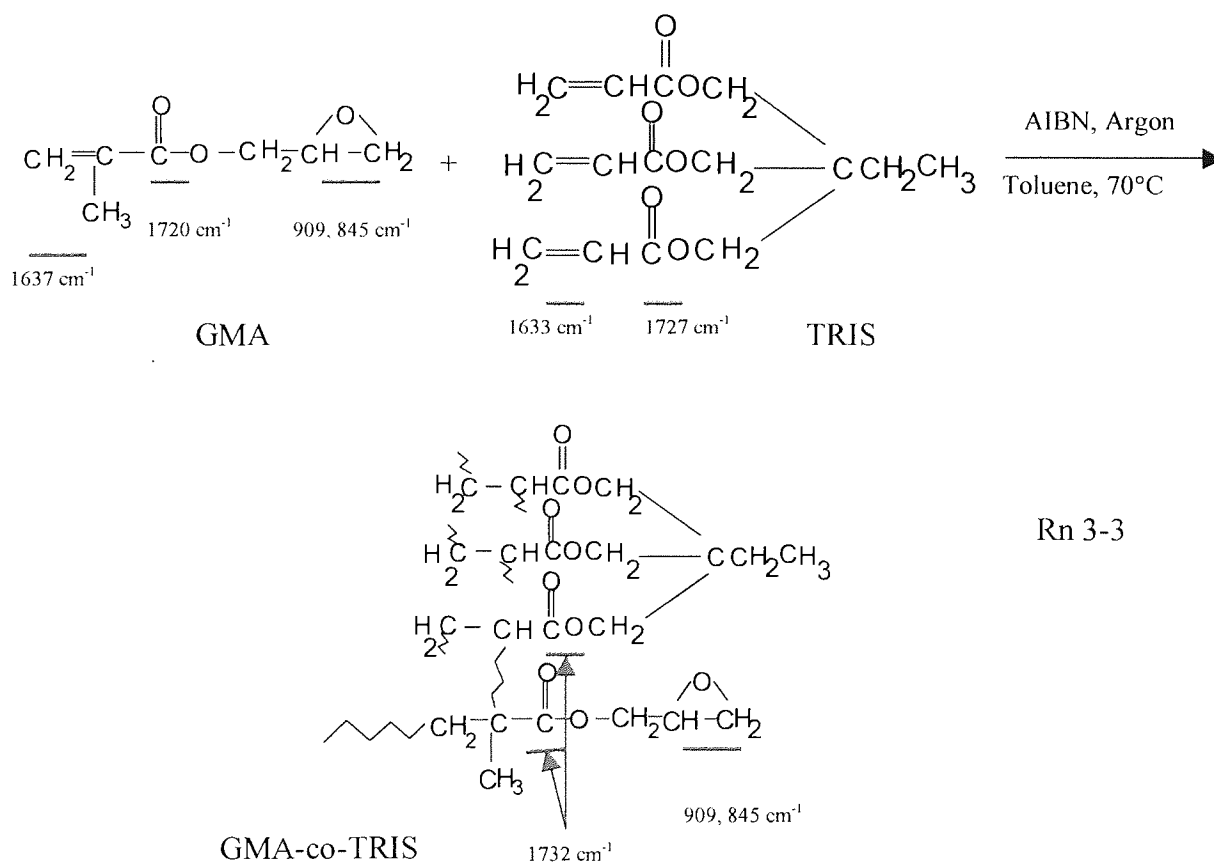
### 3.2.1.2 Characterisation of PolyTRIS

The synthesised polyTRIS (see Section 2.14.2, p78) was characterised by comparing its FTIR spectrum with that of fresh TRIS. The FTIR spectrum of fresh TRIS thin liquid film formed between two KBr cells (see Fig.2-8) shows that the interesting absorption peaks are at  $1727\text{ cm}^{-1}$  ( $\text{C}=\text{O}$  unsaturated ester group),  $1633\text{ cm}^{-1}$  ( $>\text{C}=\text{CH}_2$  for acrylic double bond). After polymerisation, the benzene was exhaustively removed and white particles were obtained. The white particles were washed thoroughly with dichloromethane to remove free TRIS and possible soluble fraction and then dried in the vacuum oven. FTIR spectrum of polymerised TRIS was recorded using KBr disk. The saturated carbonyl of the polymer is now shifted upto  $1736\text{ cm}^{-1}$  (compared to unsaturated ester  $\text{C}=\text{O}$  at  $1727\text{ cm}^{-1}$ ) and most of the absorption of the acrylic double bond at  $1633\text{ cm}^{-1}$  has disappeared (see Fig.3-2 and Rn 3-2). PolyTRIS is almost insoluble in all (normal) organic solvents.



### 3.2.1.3 Characterisation of GMA-co-TRIS

The synthesised copolymer of TRIS and GMA (GMA-co-TRIS) (see Section 2.14.3, p78) was characterised by comparing its FTIR spectrum with those of polyTRIS and polyGMA. After the copolymerisation, the toluene was exhaustively dried to obtain the white particles. These were washed thoroughly with acetone to remove any free GMA and TRIS and polyGMA and dried in vacuum for 24 hours. FTIR spectrum of these white particles was recorded using KBr disc (see Fig. 3-3 and Rn 3-3). These white particles were identified as copolymer of TRIS and GMA by comparing to the FTIR spectra of polyTRIS and polyGMA (see Fig. 3-4). Though its spectrum shows carbonyl absorption at  $1730\text{ cm}^{-1}$  and epoxy group absorption peaks at  $909\text{ cm}^{-1}$  and  $845\text{ cm}^{-1}$  similar to that of polyGMA, its area ratio of carbonyl absorption peak at  $1730\text{ cm}^{-1}$  to epoxy group absorption peak at  $909\text{ cm}^{-1}$  ( $A_{1730\text{cm}^{-1}}/A_{909\text{cm}^{-1}} = 18.8$  for GMA-co-TRIS) is much larger than that of polyGMA ( $A_{1730\text{cm}^{-1}}/A_{909\text{cm}^{-1}} = 11.2$  for polyGMA) which is certainly due to the contribution of the ester group from TRIS to the copolymer. Furthermore, these white particles were found not to be soluble in acetone and chloroform like polyGMA hence they were identified as the copolymer of TRIS and GMA.



### 3.2.1 Separation of Reaction Products and Characterisation of GMA Functionalised EP

To ensure the correct analysis of the reaction products and determination of their grafting degree (of GMA onto EP), any ungrafted GMA must be eliminated. Two different methods were used to purify the reaction products. In EP/GMA/T101 system (referred as GMA+T101 system), the reaction products may contain unreacted GMA and polyGMA which might be formed during the free radical grafting, hence precipitation methods were adopted to eliminate polyGMA (see Scheme 3-1 a (route A)). The procedure was established based on the difference of the solubility of polyGMA in different solvents. The solubility of polyGMA in methanol and acetone was checked by using the synthesised polyGMA. It was found to be soluble in acetone and insoluble in methanol. When the reaction product was dissolved in hot toluene and precipitated by adding the solution into excess amount of acetone, EP precipitated in acetone but the polyGMA and free GMA were soluble in acetone [119,120]. After filtration, and washing with acetone thoroughly, polyGMA and free GMA were eliminated hence the precipitated polymer is expected to contain only grafted GMA onto EP. In order to analyse the extent of the competition between GMA grafting reaction and GMA homopolymerisation, a second precipitation procedure was used. The reaction product was dissolved in hot toluene and precipitated by adding the solution into excess amount of methanol (see Scheme 3-1 a (route B)). In this case, both EP and polyGMA would be precipitated in methanol, but free GMA was soluble in methanol [119,120]. After filtration and washing with methanol, the resulting polymer would be expected to contain both grafted GMA and polyGMA.

In EP/GMA/TRIS/T101 system (Referred as GMA+TRIS+T101 system), the grafting reaction became more complicated. The reaction product is expected to contain free GMA, polyGMA, polyTRIS and GMA-co-TRIS which might be formed during the melt grafting. PolyTRIS and GMA-co-TRIS were in the form of solid particles and not soluble in normal solvents so a Soxhlet extraction procedure was adopted (see Scheme 3-1 b). The reaction product was placed in a paper thimble and was subject to 24 hours extraction with toluene. Virgin EP and GMA-modified EP were soluble in hot toluene. After extraction polyTRIS, GMA-co-TRIS and gel (crosslinked EP) remained in the thimble, but EP, polyGMA and free GMA were in the toluene solution. The solution was then precipitated either in acetone or in methanol.



FTIR was used to characterise the modified EP with GMA via reactive processing. Figure 2-6 shows that the characteristic absorption peaks at  $1720\text{ cm}^{-1}$  corresponding to the ester group of GMA, at  $909\text{ cm}^{-1}$  and  $845\text{ cm}^{-1}$  corresponding to the epoxy group of GMA, and at  $1637\text{ cm}^{-1}$  corresponding to double bond (C=C) in GMA. The FTIR spectra obtained from different purified samples (using the above different purification procedures) show the new characteristic absorption peaks at  $1730\text{ cm}^{-1}$  corresponding to the ester group of the grafted GMA and polyGMA, and at  $909\text{ cm}^{-1}$  and  $850\text{ cm}^{-1}$  corresponding to the epoxy group of the grafted GMA and polyGMA (see Fig. 3-5). The concentration of GMA in the polymers (which was calculated from the peak area index ( $A_{909\text{cm}^{-1}}/A_{720\text{cm}^{-1}}$ ) by FTIR using Eqn (1) in Section 2.5.2, p71, varied greatly, especially at a high concentration of peroxide T101 (see Fig. 3-6). Films from samples purified in acetone have much less GMA (containing only grafted GMA) than that purified in methanol (containing both grafted GMA and polyGMA). This confirms that polyGMA is indeed present in the modified polymer and the polyGMA can be removed using precipitation in acetone. PolyGMA is very likely to be formed during the grafting, especially when high concentrations of T101 are used in GMA+T101 system.

When the comonomer TRIS was added to the system, the FTIR of the purified samples (processed in the presence of TRIS) show the same characteristic absorption peaks at  $1730\text{ cm}^{-1}$ ,  $909\text{ cm}^{-1}$  and  $850\text{ cm}^{-1}$  (see Fig. 3-7). However, the intensity of peak absorption at  $1730\text{ cm}^{-1}$  was much stronger due to the contribution of carbonyl absorption from grafted TRIS and overlapping of the characteristic peak of TRIS at  $1730\text{ cm}^{-1}$  with GMA. The amount of grafted TRIS can only be estimated by the peak absorption ratio of peak  $909\text{ cm}^{-1}$  to  $1730\text{ cm}^{-1}$ .

The FTIR spectra obtained from different samples do not show any  $\text{-OH}$  broad band at around  $3500\text{ cm}^{-1}$ . This indicates that the epoxy rings remained intact after the grafting process and purification, and are available to react with acid groups of PET for the subsequent reactive blending of PET/EP-g-GMA.

### **3.2.2 Determination of Grafted GMA and PolyGMA in the GMA grafted EP**

As shown above, GMA was free-radically grafted onto EP chains in the presence of free radical initiator T101. The grafting degree was determined by FTIR method. Due to the

high volatility of GMA, it is very difficult to establish a calibration curve by preparing a series of EP films which contain known amounts of GMA accurately. A non-aqueous back titration procedure was adopted to determine the grafting degree as described in Section 2.5.2, p70. This method was based on the reaction of epoxy group of GMA with acid (see Rn 1 in Section 2.5.1, p71). To confirm this reaction, neat GMA was used to react with trichloroacetic acid. About 0.1g GMA was mixed with 50ml toluene and 3ml 0.3M trichloroacetic acid solution in toluene in a normal flask. After maintaining a temperature of 100-110°C for 90 min, the solution was titrated with 0.1 M KOH solution in methanol. 0.1% phenolphthalein in methanol was used as an indicator and the first pink point was used as the end point. It was found that only 40% GMA initially added was reacted with the acid due to the high volatility of GMA and the flask was not properly sealed. A 20ml long necked flask with a screwed cap which can be tightly sealed to avoid GMA loss was used instead and the test was repeated. The same procedure, as above, was followed and the results calculated from the titration showed that 93% of GMA initially added had reacted with the acid. A small amount of GMA might have been lost during the operation so less than 100% GMA was reacted. The results confirm the ring-open reaction.

In order to confirm the ring-open reaction of grafted GMA with trichloroacetic acid, the polymer was precipitated in ethyl acetate after the solution of the purified GMA grafted EP sample and trichloroacetic acid in toluene was maintained for more 90 minutes at a temperature of 100-110°C to achieve the epoxy ring open reaction with acid (see Scheme 3-2). The precipitated polymer (ring-open product) (see Fig. 3-8 (b)) was filtered and washed thoroughly with ethyl acetate. After being dried in a vacuum oven at a temperature of 80-85°C for more than 24 hours, the ring-open product was pressed into a thin film, referred as Film Y (see Scheme 3-2). FTIR spectrum of Film Y shows that the characteristic absorption bands at 909  $\text{cm}^{-1}$  and 850  $\text{cm}^{-1}$ , corresponding to epoxy group, from grafted GMA have completely disappeared, and a new band at about 3500  $\text{cm}^{-1}$ , corresponding to -OH group (formed during the ring open reaction) was observed as well as new 1769  $\text{cm}^{-1}$  band due to trichloro ester group (see Fig.3-9). Figure 3-8 (b) shows the structure of ring open product. This confirms the reaction of the epoxy group with trichloroacetic acid hence the grafting degree can be assessed accurately by this method. However, the titration is complicated and is time consuming. Hence a calibration curve was established based on a correlation of the grafting degree measured by titration and the absorption area ratio ( $A_{909\text{cm}^{-1}}/A_{720\text{cm}^{-1}}$ ) by FTIR from a set of purified samples.

The grafting degree of GMA was determined by using FTIR method as described in Section 2.5.2, p71. Purified GMA grafted EP samples which were acetone precipitated were pressed into thin films and FTIR spectra of sample films were recorded. The amount of grafted GMA was calculated from absorption area ratio  $909\text{ cm}^{-1}$  to  $720\text{ cm}^{-1}$  ( $A_{909\text{cm}^{-1}}/A_{720\text{cm}^{-1}}$ ). The level of grafted GMA was determined by comparison of the absorption ratio to a calibration curve established by correlation of FTIR to the amount of grafted GMA measured by titration method. Three films for each sample were used and an average value was reported.

The amount of polyGMA formed in the GMA grafted EP sample during the melt grafting was determined by using methanol precipitated sample. As discussed, methanol precipitated sample was expected containing both polyGMA and grafted GMA so the total amount of polyGMA and grafted GMA could be determined by using FTIR and the Eqn 1 in Section 2.5.2 (same as the determination of grafting degree) was used to calculate the total amount of GMA, including grafted GMA and polyGMA in the sample. Processed sample was dissolved in toluene and half of the solution was precipitated in excess acetone and the other half was precipitated in excess methanol. Both purified samples were pressed into thin films and their FTIR spectra were recorded. The absorption area ratios  $909\text{ cm}^{-1}$  to  $720\text{ cm}^{-1}$  ( $A_{909\text{cm}^{-1}}/A_{720\text{cm}^{-1}}$ ) were calculated and the same equation (Eqn (1) in Section 2.5.2, p71) was used. The amount of polyGMA could be obtained by calculating the difference between these two samples.

### **3.2.4 Grafting GMA onto EP in the Absence of TRIS**

The grafting of GMA onto EP in the absence of TRIS was carried out in a closed system of an internal mixer. Unless stated otherwise, the processing was performed under a standard condition, i.e. temperature:  $190^{\circ}\text{C}$ , rotor speed: 65 rpm and processing time: 15 minutes. Pre-weighed EP was charged into the mixing chamber after the preheated mixing chamber was flushed with oxygen-free nitrogen for more than 15 seconds, followed by immediately injecting the mixture of GMA and T101 into the chamber with a long needle syringe. The ram was lowered down quickly to keep a closed system during mixing to minimise the loss of GMA due to its high vapour pressure and volatility. The reaction product was removed from the chamber and cooled down to room temperature for further analysis. Table 3-1

(a) lists the experimental compositions, processing conditions and GMA grafting degree and grafting efficiency.

#### *(i) Effect of T101 Concentration on GMA Grafting Degree*

When GMA alone was reacted with EP in the presence of T101, the grafting degree increased with the increasing concentration of T101, but the overall grafting yield was low (see Fig. 3-10). For example, when 12 phr GMA and 0.5 phr T101 was added to EP, the grafting degree was 0.4%, i.e. only 3.3% of the total GMA was grafted. When T101 was increased to 1.0 phr, the grafting degree reached to 1.4% (11.6% of total GMA added) and the grafting degree levelled off with further increase of T101 up to 1.5 phr. Even when GMA was fixed at 18 phr, the highest grafting degree was 1.8 % with 1.5 phr T101, i.e. only 9.9% of total GMA was grafted. The same order of magnitude of grafting degree was also reported by Liu [28] and Sun [120].

However, though an increase in peroxide concentration in the grafting system leads to the generation of more macroradical sites resulting in higher GMA grafting, high initiator concentrations would induce higher degree of polymer degradation and, in the case of the EP used here, these experimental results showed that crosslinking/branching predominate the overall degradation process. Figure 3-11 (a) shows the torque curve of the reactive processing. When EP alone was processed, the torque decreased sharply in the first 1-2 min with the melting of the polymer and then maintained a very steady value until the end of the processing. When GMA and T101 were added to the system, the torque increased quickly from a low value to the maximum value in 2-3 minutes due to the dispersion of GMA into the polymer. With proceeding of mixing, the torque decreased slowly. The more T101 was added, the higher the maximum value and an obvious peak was observed. The higher torque value can reflect that some cross-linking occurs during the grafting.

The gel content was determined by Soxhlet extraction with toluene. It was found that only high amount of T101 and high weight ratio of T101 to GMA led to some degree of gel. For example, when EP was processed with 6 phr GMA and 1.5 phr T101 (very high torque values were recorded) about 10% gel was determined in toluene. The EP used in this study is not very liable to form crosslinking and insoluble gel during the melt grafting, but the obvious branching resulted in significant alteration of melt rheological properties. The

extent of alteration was dependent on the concentration of peroxide. Melt flow index (MFI) for these GMA modified EP samples was measured and the results present in Table 3-1 (a). Figure 3-11 (b) shows the variation of MFI with different T101 concentration at a constant concentration of 18 phr GMA. The MFI of virgin EP was measured to be 1.7. With addition of 0.5 phr T101, the MFI dropped to 0.79. Further increase of T101 to 1 phr and 1.5 phr led to further decrease of MFI to 0.44 and 0.05. MFI is a measure of melt viscosity and is related to the molecular weight of the polymer. Lower MFI indicates higher viscosity and higher molecular weight. The increase of peroxide concentration significantly reduces the MFI value of GMA grafted EP. Grafting of GMA was therefore accompanied by increase of melt viscosity.

### ***(ii) Effect of GMA Concentration on GMA Grafting Degree***

With the increase of GMA concentration, the grafting degree changed with different levels of T101. Increasing the concentration of GMA initially added has led to higher grafting. When 1 phr T101 was used, the grafting degree increased sharply from 0.5% to a value of 1.4% with an increase of GMA from 6 phr to 10-12 phr, and then slightly increased to 1.6% with further increase of GMA to 18 phr (see Fig. 3-12). When 1.5 phr T101 was used, the grafting degree levelled up at about 1.3% with increasing GMA concentration from 6 phr to 12 phr, and then increased gradually to 2% with further increase of GMA up to 18 phr (see Fig. 3-12).

### ***(iii) Formation of PolyGMA during the Melt Grafting***

It could be clearly seen that undesired homopolymerisation of GMA strongly competes with the desired grafting reaction. Figure 3-13 shows that both GMA grafting degree and the amount of polyGMA increases with increasing concentrations of T101 (from 0.5 phr to 1 phr) at a fixed concentration of GMA (12 phr) and the actual polyGMA amount already exceeds the grafted GMA. Further increase in T101 concentration (to 1.5 phr) has slightly decreased both the grafted GMA and polyGMA. With a constant concentration of 1 phr T101, the formation of polyGMA is proportional to the increase of GMA initially added but the grafting of GMA initially increases and then levels off when GMA concentration is over 12 phr. The amount of polyGMA is much higher than the grafted GMA when 18 phr

GMA was added (see Figure 3-14). It is clear that increasing GMA concentration leads to great increase in the chance of homopolymerisation of GMA.

#### ***(iv) Effect of Processing Time on GMA Grafting Degree***

Figure 3-15 shows the kinetics of the GMA grafting and homopolymerisation in the GMA system. At a fixed composition (EP: 100phr, GMA: 10phr; T101: 1phr), a set of samples were prepared using different processing time (2-15 minutes) at a rotor speed of 65 rpm and a temperature of 190°C. When the samples were removed from the mixer, they were cut into small pieces and cooled down quickly by flushing with a strong stream of nitrogen to stop further reaction. Both grafting degree and polyGMA were measured and are shown in Figure 3-15. It is clear that both GMA grafting and polymerisation take place at the same time. For the desired grafting, the grafting degree increased rapidly in the first 5 minutes and then levelled off with the continuing processing. However, the polymerisation of GMA proceeded slowly in the first 2 minutes and then took place more rapidly until reaching a peak value at 10 minutes, where it has exceeded the amount of grafted GMA. Comparing the grafting and polymerisation, it is clear that there is a competition between the grafting and GMA polymerisation reactions in the first 5 minutes of processing. After that the polymerisation dominates the overall reaction.

#### ***(v) Effect of Processing Temperature on Grafting Degree***

To optimise the grafting conditions, the effect of processing temperature on the grafting degree in the presence or absence of TRIS was examined. Figure 3-16 shows the temperature effect on both GMA grafting degree and the amount of polyGMA in GMA system (GMA + T101) with a fixed composition of 10 phr GMA and 1.0 phr T101. When the temperature was below 160°C, very small amount of GMA was grafted. When the temperature was raised up to 180°C, the grafting degree increased significantly and reached a peak value at 180°C. With further increase in temperature, the grafting degree dropped sharply. On the other hand, the amount of polyGMA increased gradually with the rise of temperature. This temperature effect may be due to the rate of free radical formation by decomposing the peroxide T101. At a low temperature, T101 decomposes slowly so both grafting reaction and homopolymerisation of GMA were slow. With the increase of

temperature, more free radicals were formed and the grafting degree increased sharply. When the temperature was over 180°C, the grafting degree dropped down while the formation of polyGMA increased sharply. It is obvious that higher temperature (above 180°C) makes the homopolymerisation of GMA more favourable and competes effectively with the grafting reaction. As a result, more GMA monomer was consumed by homopolymerisation and less GMA was grafted onto the rubber chains.

#### *(vi) Effect of Peroxide T29B90 on Grafting Degree*

It was reported that peroxide T29B90 was a very effective initiator for the grafting of GMA onto EP at extremely low temperature [147]. To verify this, three samples were prepared and the composition and processing conditions are listed in Table 3-1 (c). After the required amount of EP was charged into the preheated mixing chamber, set at 115°C, which was flushed with nitrogen, the mixture of GMA and T29B90 was injected into the chamber. After 2 minutes slow mixing at a speed of 20 rpm, the rotor speed was raised to 65 rpm and further 12 minutes mixing was performed.

A similar purification procedure was adopted and the grafting degree was determined by FTIR method. It was interestingly to notice that the grafting of GMA depended on the concentration of the initial GMA added at such a low processing temperature. Almost no GMA was grafted onto the EP when 6 phr GMA was added initially, whereas the grafting degree increased sharply to 6% when 15 phr GMA was added (see Figure 3-17). It seems that a critical value of the initial GMA concentration is needed for the grafting reaction. The amount of polyGMA also increased with increasing the initial GMA concentration, but was overall relatively low. At such a low temperature, the grafting mechanism and the structure of the grafted GMA may be different from that obtained at a high temperature due to the polymer high viscosity. At this temperature, EP is just softened and not completely melted.

### **3.2.5 Grafting GMA onto EP in the Presence of TRIS**

It was demonstrated that GMA could be melt grafted onto EP in the presence of peroxide (GMA+T101 system). However, the overall grafting of GMA was low. Though an increase of concentrations of peroxide led to higher GMA graft, high amount of

homopolymerisation of GMA was formed during the melt grafting as well as crosslinking/branching of EP indicated by high torque during the melt grafting and presence of insoluble gel at high concentration of peroxide. In this system, therefore there is a strong competition from the undesired side reactions with the desired grafting reaction. Similar observations were reported for grafting of GMA onto polypropylene, PP, [120, 121], polyethylene, PE, [113] where high GMA grafting levels were achieved in the polymer at high initiator concentrations giving rise to severe crosslinking in PE or degradation in PP concomitant with a molar mass reduction. To enhance the free radical grafting efficiency of GMA on polymers and reduce the side reactions, the grafting process has been carried out in the presence of comonomers, such as styrene, [118-121] and special initiating agents such as acrylamide [122]. A broad and versatile approach to improving the grafting efficiency of functional modifiers (agents) on polymers by in-situ co-grafting of a small amount of a more reactive (compared to the modifier) di or poly-functional comonomer has been developed by PPP Group, Aston University [138-141]. The success of this method, in which the comonomer acts as a reactive linker between the modifier and the polymer, relies on achieving a delicate balance between the molar ratios of the reagents (monomer, comonomer, initiator) and the process variables (e.g. temperature, residence time) [148]. It was shown, for example, that the use of the trifunctional coagent, trimethylol propane triacrylate, TRIS, with different reactive modifiers, such as and maleic anhydride [140, 141] and antioxidants [138], gave rise to a dramatic increase in the level of grafting of these modifiers on polymers. It was also demonstrated that, for example, in the case of reactive antioxidants, the antioxidant grafts on the polymer are indeed copolymers of the antioxidant and the comonomer which are grafted on the polymer via one, or more, of the reactive sites of the comonomer [138]. Generally, the grafting efficiency of mono-functional antioxidants, for example, can be improved from as low as 10-40% to in excess of 80-90% [138,139].

### **3.2.5.1 Processing EP in the Presence of TRIS**

The effect of the trifunctional TRIS, as a highly reactive comonomer, on the grafting efficiency of the much less reactive modifier GMA in EP copolymer was examined in this work. Due to their high free radical reactivity, monomers containing more than one polymerisable group have been used previously as crosslinking agents for polymers [149]. The novelty of this approach arises from the fact that co-grafting of the same



polyfunctional agents, e.g. TRIS, with modifiers containing mono-vinyl moiety in mixers or extruders can be achieved at much lower peroxide concentrations (as compared to concentration needed in the absence of the comonomer) to yield higher grafting level of the modifiers with minimal polymer degradation [138,139]. Figure 3-18 shows the variation of torque in an internal mixer as a function of processing time for shear-initiated (i.e. in the absence of peroxide initiator) reactions of TRIS, at different concentrations, and that of EP-containing GMA (no TRIS). In the case of GMA (no TRIS) the torque levels-off after an initial decrease, in a similar pattern to that observed for a control sample of the unmodified EP alone. In the presence of TRIS, however, the torque values go to a maximum after an initial decrease. Obviously, the presence of TRIS led to significant increase of the torque value. These torque change during the processing indicates that crosslinking reactions are initiated by shear force. The effect of TRIS concentration appears to cause a displacement of the onset of the torque maximum to shorter times (e.g. 4 min. at 0.5 phr and 2.5 min. at 2.5 phr TRIS) while at the same time showing higher maximum torque values, suggesting an increase in reaction rate with higher reaction yield, arising from the reaction of higher TRIS levels with shear-induced polymer macroradicals.

Figure 3-19 shows the torque behaviour of the free radical-initiated reaction of TRIS, and that of radical-initiated GMA (i.e. with no TRIS), in the polymer melt. The use of a very small concentration of a free radical initiator (T101) in the TRIS-system causes an even more noticeable shift of the onset of the torque peak to shorter times, as well as a further increase in the maximum torque (peak) value; with further processing the torque level drops. This behaviour suggests that the radical-initiated reaction of TRIS with the polymer macroradicals occurs at an even faster rate than the shear-initiated reaction. For example, for the same TRIS concentration of 1 phr in the absence of peroxide the onset of the torque peak occurred at 3.5 minutes and the peak maximum was at 6 minutes, compared to 1.5 and 2 minutes, respectively, in the presence of 0.01 molar ratio, MR, of peroxide. Under similar conditions of free-radical initiation, the changes in the GMA-system (e.g. in a grafting system containing 12 phr GMA and 1 phr T101 (T101/GMA mole ratio = 0.04) is very different: a torque peak is not observed and the overall changes in the torque observed during processing are similar to that of the unmodified polymer. It is evident from this drastic difference in the torque behaviour (when EP is processed in the presence of GMA compared to an EP processed with the trifunctional TRIS, Fig. 3-18 and 3-19), that the free radical reactivity of TRIS towards the polymer macroradicals is much higher than that of

GMA-macroradicals under both shear-initiated and free radical-initiated melt grafting processes.

In the presence of the comonomer TRIS (in the radical-initiated reactions), the large increase in the torque values leading to a peak maximum indicates the occurrence of both grafting/branching and crosslinking reactions which predominate at the earlier stages of processing. However, the subsequent reduction in torque on further processing, suggests that some chain scission occurs at the later stages giving rise to a reduction in the polymer viscosity and lowering of the extent of crosslinking and/or branching. The presence of such a reactive multifunctional co-monomer in the GMA grafting system would be expected, therefore, to result in a more complicated grafting system. Thus, in addition to the formation of poly-GMA a number of other side reactions involving the TRIS are expected to compete with the target GMA-grafting reaction and these may have an even more important contribution to controlling the overall grafting yield of the modifier. These reactions include the formation of ungrafted copolymer between TRIS and GMA (TRIS-co-GMA) as well as a homopolymer of the TRIS (poly-TRIS), together with possible polymer crosslinking that may occur via reaction of the reactive functions of the TRIS with the polymer macroradicals.

### **3.2.5.2 Optimisation of the Addition Sequence**

In the initial study, it was found that when EP and the mixture of GMA, TRIS and T101 were introduced into the mixing chamber and processed for 15 minutes, white particles were formed in the reaction products. Those particles were separated using Soxhlet extraction with paper thimble in toluene. After washing with acetone (to remove polyGMA) and drying, it was found that the white particles were not soluble in normal solvents and were identified as GMA-co-TRIS (by comparing its FTIR spectrum with that of the synthesised GMA-co-TRIS), see Fig. 3-20. This indicates that GMA and TRIS are likely to form copolymer during the processing and should be eliminated or minimised. To get better understanding of the enhance effect of TRIS on GMA grafting, four different addition sequences were investigated (listed in the following table). After processing, the reaction products were all Soxhlet extracted using paper thimbles with toluene. The soluble fraction was precipitated in excess amount of acetone and the GMA grafting degree was determined by FTIR. The insoluble fraction was analysed by using FTIR.

Number	Procedures	Grafting degree (%)	GMA-co-TRIS and/or polyTRIS formed?	Insoluble after extrc. (%)
Method 1	After charging EP in the mixing chamber, inject the mixture of GMA, TRIS and T101 and then processed for 15 minutes	1.1	yes	1.1*
Method 2	1) charge the mixture of EP and TRIS and then mix for 1 min. 2) Inject the mixture of GMA and T101 and then mix for 14 min.	2.0	no	0.5
Method 3	1) Charge EP and the mixture of GMA and T101 and mix for 1 min. 2) Charge TRIS	1.9	yes	8.2 **
Method 4	1) Charge the mixture of EP and TRIS and mix for 1 min. 2) Charge GMA and mix for another 1 min. Charge T101 and mix for 14 min.	1.0	no	0.5

Note: The composition: EPR: 100phr; GMA: 10 phr; TRIS: 1.11 phr; T101: 0.43 phr.

Processing condition: rotor speed: 65 rpm; temp.: 190°C.

\* Toluene insoluble fraction was white particles.

\*\* Toluene insoluble fraction consisted mainly of polymer containing a small amount of white particles

It was shown that the addition sequence has significant effect on grafting degree and the extent of formation of GMA-co-TRIS. First of all, TRIS is a high reactive reagent and can be used as a curing agent for EP [75]. As a result, TRIS can copolymerise with GMA at a high temperature. When the mixture of TRIS, GMA and T101 was processed with EP (method 1), the highest amount of GMA-co-TRIS was formed during the melt grafting. This may be due to the quick formation of GMA-co-TRIS. Primary radicals formed from the decomposition of T101 might initiate the copolymerisation during the dispersion of GMA, TRIS and T101 into the polymer melt and reduce the grafting efficiency. When method 2 was adopted, TRIS could be dispersed in the polymer before the addition of GMA and T101 and the chance of copolymerisation was minimised so no GMA-co-TRIS

was observed in the reaction product and much higher grafting degree was achieved than that with method 1. In the case of method 3, TRIS was added after the premixing of GMA and T101 with EP. White particles were found and were identified as GMA-co-TRIS. During the dispersion of TRIS in the polymer melt, copolymerisation and polyTRIS might be initiated by the free radicals which had already existed in the polymer melt. Though similar grafting degree to that with method 2 was obtained, the gel was much higher. For method 4, GMA, TRIS and T101 were added separately. No GMA-co-TRIS was formed, but it gave the lowest grafting degree among those four methods. This may be attributed to the fact that a very small amount of T101 was difficult to disperse evenly in the polymer melt within a short period of time. With the dispersion of T101, the decomposition took place at the same time so the initial efficiency was reduced.

It was demonstrated that the addition sequence of TRIS, GMA and T101 could greatly affect the grafting yield and formation of TRIS-co-GMA due to the high reactivity of TRIS towards GMA. If the copolymerisation was minimised or even eliminated, TRIS could enhance the grafting of GMA onto the EP chains. Method 2 was found to be the best one. In the following investigation of the effect of TRIS on the grafting degree, method 2 was adopted for all samples.

### **3.2.5.3 Effect of T101 Concentration on Grafting Degree**

Figures 3-21 and 3-22 show the effect of T101 on the grafting degree in the presence of TRIS. When GMA to TRIS ratio (w/w) was fixed at 9/1 with 10 phr GMA, the grafting degree increased gradually with increasing T101 concentration and reached to a maximum value with 0.5 phr T101. With further increase of T101 concentration, the grafting degree levelled off. When GMA to TRIS ratio was raised to 8/2 with 10 phr GMA initially added, much less T101 was needed. The grafting degree increased sharply from 1.0% to 2.2% with the increase of T101 from 0.12 phr to 0.22 phr. Further increase of T101 concentration led to slight increase of the grafting degree. A similar trend was observed with 6 phr GMA initially added.

Comparing the grafting degree between the GMA+T101 system and that of the GMA+TRIS+T101 system, it is clear that TRIS has obvious enhancing effect on the grafting of GMA onto EP. With 10 phr GMA initially added, a maximum value of 1.3% grafting degree was achieved by addition of 1.0 phr T101 in the absence of TRIS, whereas

as high as 2.5% grafting degree was measured in the presence of TRIS; that is nearly 100% improvement. At a low concentration of GMA (6 phr), similar maximum values were measured with and without TRIS, but the maximum value in GMA+T101 system was obtained at a high concentration of T101 (1.5 phr) and obvious crosslinking was formed (more than 10% gel) while much less T101 was needed and no gel was measured. Another feature of the addition of TRIS is that a very small amount of T101 was needed, especially with more TRIS and no gel was observed unless high amount of TRIS and T101 were added.

#### **3.2.5.4 Effect of TRIS Concentration on the Grafting Degree**

Figure 3-23 (a) shows the effect of TRIS concentration on the grafting degree. When T101/GMA+TRIS molar ratio was fixed at 0.005 (GMA=10 phr), the grafting degree initially increased with the increase of TRIS and then levelled off with further increasing TRIS above 2.5 phr. With a higher molar ratio of T101/GMA+TRIS, i.e. 0.01, raising TRIS concentration had little effect on grafting degree. However, when TRIS exceeded 4 phr, GMA-co-TRIS could be found in the reaction products. This is due to the high concentration of TRIS giving rise to higher possibility of the formation of GMA-co-TRIS which will interfere the grafting reaction. Further analysis of FTIR spectra of these samples showed that the carbonyl absorption peak at  $1730\text{ cm}^{-1}$  assigned to carbonyl group from both grafted GMA and grafted TRIS became stronger with increasing TRIS concentration. Figure 23 (b) shows the relation between area ratio of carbonyl absorption at  $1730\text{ cm}^{-1}$  to epoxy ring absorption at  $909\text{ cm}^{-1}$  ( $A_{1730\text{ cm}^{-1}}/A_{909\text{ cm}^{-1}}$ ). This indicates that the grafted TRIS increases at high TRIS concentration (initially added). The optimal concentration of TRIS was found to be GMA/TRIS=8/2.

#### **3.2.5.5 The Kinetics of Grafting Reaction in the Presence of TRIS**

As shown in the GMA system, the grafting reaction proceeded rapidly. However, in the presence of TRIS, the grafting reaction became faster. Figure 3-24 shows that the grafting was completed within 4 minutes with much higher grafting degree than that in the GMA system. It seemed that the higher amount of TRIS, the faster the grafting reaction. On the other hand, much less polyGMA was formed compared with GMA system and the amount of polyGMA levelled off after 2 min processing. In the presence of TRIS, it seems that the grafting reaction dominated.

### 3.2.5.6 Effect of Processing Temperature on Grafting Degree

In the presence of TRIS, the temperature effect on the grafting degree was quite different from that in the single monomer system without TRIS. Figure 3-25 shows the effect of the processing temperature on both grafting degree and the amount of polyGMA formed at a fixed concentration of reactants (10 phr GMA, 2.5 phr TRIS, 0.457 phr T101, TRIS/GMA ratio=2/8 and molar ratio of  $[T101]/[GMA]+[TRIS]=0.02$ ). It can be seen that the grafting degree increases slightly with decreasing temperature and reaches to the highest value at 160°C. The grafting degree decreases slightly with a further decrease of the temperature from 160°C to 140°C. Concerning the formation of polyGMA, very small amount of polyGMA was measured on the whole range of temperature examined (from 190°C to 140°C). Especially, no polyGMA was determined at a low temperature below 150°C. This is due to the high reactivity of TRIS towards GMA and EP as shown earlier. TRIS enhances the grafting reaction both with respect to grafting degree and the rate of grafting. TRIS can therefore enhance the grafting whereby initially TRIS onto the EP chains, then GMA grafts rapidly via the multi-functionality of TRIS. As a result, the chance of homopolymerisation of GMA would be reduced drastically.

It can be seen from the above results that the optimal processing temperature is at 160°C. At this temperature, the highest grafting was achieved with very little formation of polyGMA. A set of samples were prepared at this processing temperature with fixed concentrations of 10 phr GMA and 2.5 phr TRIS. When the peroxide concentration was decreased from a molar ratio of 0.02 ( $[T101]/[GMA]+[TRIS]$ ) to 0.003, the grafting degree just slightly decreased (see Figure 3-26). However, without any peroxide, the grafting degree dropped from 2.5% to 1%. Without any peroxide, a certain amount of GMA can also be grafted through a mechanism of macro-radicals formed by the shear force in the processing. The lower the temperature, the more macro-radicals are formed due to higher viscosity, but the shear-initiated grafting was not so effective. It was demonstrated that only very small amount of peroxide was required to initiate the grafting reaction in the presence of TRIS. 0.003 to 0.005 molar ratio of peroxide is high enough to initiate the grafting reaction. With higher concentration of peroxide, branching/crosslinking of EP became more severe, indicated by higher viscosity. Figure 3-27 shows the variation of MFI value for the above set of samples. High concentration of peroxide resulted in lower MFI. The overall melt rheological properties of functionalised EP was altered compared with the

virgin polymer. The functionalised EP has generally a lower MFI than the virgin EP. This indicates that the grade of EP used is likely to undergo branching though no gel was measured for most of the samples except when a very high concentration of peroxide was used leading to measurable crosslinking (insoluble gel).

### **3.2.6 Grafting GMA onto EPDM**

The primary aim of the overall project was to convert postconsumer PET bottles into a value-added thermoplastic elastomeric product with outstanding performance, especially with oil and heat resistant characteristics. This involves the reactive blending of PET with different functionalised elastomers. Functionalised EPDM has been used to blend with different engineering thermoplastics. For example, maleic anhydride functionalised EPDM has been used to toughen polyamides, such as nylon 6 [150]. GMA functionalised EPDM has been successfully blended with PBT to produce a thermoplastic elastomer [23]. As a result, an ethylene-propylene diene terpolymer (EPDM) was chosen in this study to be functionalised with GMA. EPDM used was a commercial grade, Buna AP 447 (purchased from Bayer). It has 74% ethylene and 5% 5-ethylidene-2-norbornene and remaining is propylene.

Based on the investigation of melt grafting of GMA onto EP in the absence and presence of TRIS, it was found that GMA could be grafted onto EP via a free radical grafting reaction using an organic peroxide as free radical initiator in the melt state, but strong side reactions, in terms of homopolymerisation of GMA and branching/crosslinking of EP, compete with the desired grafting reaction. The presence of a comonomer, e.g. TRIS, was shown to enhance the grafting reaction and reduce the side reactions. The melt grafting of EPDM with GMA was also carried out in an internal mixer (RAPRA-Hampden torque rheometer (TR)). Processing was conducted in a closed mixer at 180°C with a rotor speed of 65rpm for 10 minutes for all runs. The EPDM used was in the form of bale which was packed from crumble pellets so it was capable of absorbing a large amount of liquid monomer, thus facilitating material feeding and reducing monomer loss. Before processing, the mixture of GMA and peroxide T101 was mixed with the required amount of EPDM which was cut into small pieces in a cup for about 3 minutes in order that the liquid reagents were absorbed by the EPDM. They were charged into the preheated mixing chamber which was initially flushed with oxygen-free nitrogen. The mixing was conducted

under a close system by lowering the ram down (see Scheme 3-3). The processed polymer was cooled under a stream of nitrogen. When the comonomer TRIS was included in the formulation, a different addition sequence was adopted to avoid the formation of copolymer of TRIS-co-GMA during the melt grafting. Pre-weighed EPDM and TRIS were mixed in a cup to allow absorption of TRIS in the EPDM. Then they were introduced into the mixing chamber and mixed for 1 minute. The charge of a mixture of GMA and T101 was followed with a long needle syringe and the mixing was maintained for further 9 minutes. A set of GMA grafted EPDM (EPDM-g-GMA) with different compositions were prepared (see Table 3-2).

A similar purification procedure to that of GMA grafted EP products was applied. Due to the formation of gel during the melt grafting of GMA onto EPDM, all samples were subject to a precipitation purification procedure (see Scheme 3-3). Xylene was used as solvent because of its high boiling point and high solubility. About 3g sample was dissolved in refluxing xylene. Half of the solution was precipitated into 7 times of excess acetone and the other half was precipitated into 7 times of excess of methanol. Both precipitated polymers were filtered out, washed and dried in a vacuum oven at a temperature of 80-85°C for more 20 hours. The acetone purified sample was expected to contain grafted GMA only and the methanol purified sample was expected to contain both polyGMA and grafted GMA. Both purified samples were pressed into thin films and FTIR spectra were recorded. Similar to GMA grafted EP samples, the absorption area ratios  $909\text{ cm}^{-1}$  to  $720\text{ cm}^{-1}$  ( $A_{909\text{ cm}^{-1}}/A_{720\text{ cm}^{-1}}$ ) could be used to determine the concentration of GMA in the sample. The absorption area ratios  $909\text{ cm}^{-1}$  to  $720\text{ cm}^{-1}$  of the acetone purified and the methanol purified samples for each product were calculated and compared. It was found that they were the same for all samples prepared, indicating no measurable polyGMA was formed during the melt grafting. The grafting degree of GMA for all samples was determined by titration method as described in Section 2.5.1 and xylene was used as solvent instead of toluene. The results are listed in Table 3-2. The gel content in the GMA grafted EPDM samples were determined by Soxhlet extraction with xylene. The details of extraction procedure were described in Section 2.6 and the results are presented in Table 3-2.



FTIR was used to characterise GMA grafted EPDM. It was found that FTIR spectrum of virgin EPDM (see Fig. 2-2, p80) was similar to that of EP (see Fig. 2-1, p80) except a weak absorption at  $1685\text{cm}^{-1}$ , corresponding to the presence of C=C double bonds from a small amount of 5-ethylidene-2-norbornene (5%), was present in the FTIR spectrum of EPDM. Figure 3-28 shows the FTIR spectra of a purified EPDM-g-GMA sample and unmodified EPDM. The grafting of GMA onto EPDM can be confirmed by the appearance of the new absorptions at  $1730\text{cm}^{-1}$ , assigned to the ester carbonyl absorption of grafted GMA, and  $909\text{cm}^{-1}$  and  $844\text{cm}^{-1}$ , assigned to the epoxy ring of grafted GMA.

Figure 3-29 shows the effect of peroxide concentrations on the GMA grafting degree and gel formation with a fixed concentration of GMA (10 phr). It was found that increasing the peroxide concentration led to a proportional increase in grafting yield, while the gel content also increases significantly. For example, 0.3 phr T101 resulted in only 0.35% grafting degree with 2% gel, while 0.8 phr T101 led to 1.2% grafting degree with 18% gel. This may be attributed to the existence of 5% 5-ethylidene-2-norbornene. This small amount of double bonds incorporated in the EPDM chains can facilitate its vulcanisation for rubber industrial applications. That is why EPDM is very likely to crosslink during the melt free radical grafting, indicated by high gel content and high torque value during the processing. However, no measurable homopolymerised GMA (polyGMA) was determined. Though little polyGMA formed the overall grafting was low. Even at a high concentration of 1 phr T101, the GMA grafting degree did not exceed 1.7% - that is less than 20% of original GMA grafted, but the gel content reached to 36%. It was demonstrated that for the grade of EPDM used here, crosslinking was the main side reactions and the reactivity of GMA was low towards EPDM chains indicated by high percentage of gel and low GMA grafting degree.

In the GMA grafting of EP, it was shown earlier that the addition of comonomer TRIS led to enhancing of the desired grafting reaction and reducing the side reactions, especially the reduction of the formation of polyGMA in the melt grafting. In order to investigate the effect of TRIS in the GMA grafting of EPDM, a set of GMA grafted EPDM samples were prepared in the presence of TRIS. Table 3-2 lists the compositions, grafting degree and gel content. When GMA and TRIS were fixed at 10 phr and 1.11 phr respectively (GMA to TRIS ratio: 9/1), increasing T101 mole ratio to GMA and TRIS from 0.0025 to 0.02 resulted in gradual increase of grafting degree from 1.1% to 2.0%. Meanwhile, the gel

content also increased from 2% to 16% (see Figure 3-30). With the increase of TRIS to 2.5 phr (GMA to TRIS ratio: 8/2), increase T101 mole ratio to GMA and TRIS from 0.0025 to 0.01 led to gradual increase of grafting degree from 2.46% to 3.58%, but the gel content increased sharply from 6% to 69% (see Figure 3-31). It was obvious that high concentrations of TRIS and T101 led to both high grafting and also high gel content. With 2.5 phr TRIS, a very low concentration of peroxide was required to achieve high grafting and low gel. When 0.0025 mole ratio of T101 (actual T101: 0.057 phr in the formulation) was added to the system, about 2.5% GMA grafting degree was measured with only 6% gel. In the presence of TRIS, therefore a proper balance of compositions of TRIS to GMA and peroxide to GMA and TRIS was the key to achieving optimal grafting with minimum crosslinking of EPDM.

To get better understanding of GMA grafted EPDM in the presence of absence of TRIS, two samples were chosen for different solvent fractionation analysis. One sample was prepared with a composition of 100 phr EPDM, 10 phr GMA, and 0.8 phr T101 (referred to as EPDM-g-GMA<sub>T101</sub>) (sample DM-3 in Table 3-2), while another sample was prepared with a composition of 100 phr EPDM, 10 phr GMA, 2.5 phr TRIS and 0.057 phr T101 (referred to as EPDM-g-GMA<sub>TRIS</sub>) (sample DM-9 in Table 3-2). Differential solvent fractionation was performed in Soxhlet extractor devices under nitrogen atmosphere (see Scheme 3-4). A small amount of the polymer sample was pressed into thin films in a hot press at a temperature of 180°C. This sample was placed in a paper thimble and was subjected to sequential Soxhlet extraction with hexane, toluene and xylene (see Section 2.12, p76). To avoid degradation of polymer and oxidation of solvent during the extraction, a small amount of antioxidant Irganox 1076 (about 300 ppm) was added into the solvent. Hexane, toluene and xylene were used as a series of increasingly effective solvents with higher boiling points (boiling points are 69°C, 110°C, and 138°C, respectively). To keep the temperature in the extraction thimble as close to the boiling point of the solvent as possible, aluminium foil was used to wrap the extractors.

Unmodified EPDM (virgin EPDM) was found to be soluble in hexane completely. Using virgin EPDM as a control, no insoluble fraction was determined during the Soxhlet extraction with hexane. Figure 3-32 shows the fractionation results of two different GMA grafted EPDM samples. For the sample which was prepared in the absence of TRIS

(EPDM-g-GMA<sub>T101</sub>, sample DM-3), its grafting degree was 1.2% with 18% gel (determined by Soxhlet extraction with xylene). Its hexane soluble fraction was 62%. In the following extractions, the toluene and xylene soluble fractions were 7% and 12%, respectively. The insoluble gel obtained from the sequential extraction was 19%, and this is similar to the gel content measured with xylene extraction only. In the case of sample which was prepared in the presence of TRIS (EPDM-g-GMA<sub>TRIS</sub>, sample DM-9, 2.5% grafting degree with 6% gel (determined by Soxhlet extraction with xylene)), it is interesting to note that the hexane soluble fraction was only 35% (only half of that of EPDM-g-GMA<sub>T101</sub>, sample DM-3), whereas the toluene and xylene soluble fractions were 14% and 18%, respectively. The xylene insoluble fraction obtained from the sequential extraction was 33% and this was much higher than that determined by Soxhlet extraction with xylene only. Theoretically, they should be similar. To eliminate the possibility of experimental error, the experiments were repeated and the nitrogen atmosphere was insured during the whole process of extractions. The results were the same. The significant differences of fraction distribution in the three solvents between these two samples show that EPDM-g-GMA<sub>T101</sub>, sample DM-3, contains mainly a low temperature soluble fraction (hexane soluble fraction) and insoluble gel (accounting for 18% wt of all sample). For EPDM-g-GMA<sub>TRIS</sub>, sample DM-9, more soluble fraction distributes in the higher temperature soluble fraction and the insoluble fraction content after xylene extraction is much higher. The difference in the solubility behaviour arises from the difference of distribution of molecular weight of these two samples. A higher boiling point solvent is required to dissolve samples with higher molecular weight. This may be attributed to the nature of multifunctionality of TRIS.

The hexane soluble fractions for the above two samples were pressed into thin films and their FTIR spectra were recorded (see E in Scheme 3-4), meanwhile a very small amount of the hexane insoluble gel was taken from the thimbles and smeared into thin films between two KBr discs (see D in Scheme 3-4). The discs were placed in vacuum oven to dry the solvent and FTIR spectra were obtained. Figure 3-33 and 3-34 show both FTIR spectra of hexane soluble fraction and hexane insoluble fraction from the samples DM-3 and DM-9. It was found that 1730 cm<sup>-1</sup>, 909 cm<sup>-1</sup>, and 845 cm<sup>-1</sup> corresponding to the absorption of carbonyl and epoxy, respectively, were observed in both fractions but the absorption peak intensity in the insoluble fraction seemed to be stronger than that of soluble fraction, especially for sample DM-3. This indicates that more grafted GMA

distributes in the hexane insoluble fraction. Though the FTIR spectra of the hexane insoluble fractions were not so good due to the poor quality of the smeared film, the index ratio of  $A_{909\text{cm}^{-1}}/A_{720\text{cm}^{-1}}$  between hexane soluble fraction and hexane insoluble fraction for sample DM-3 and DM-9 were calculated to quantify the distribution of grafted GMA in each fraction. For sample DM-3, the area ratio of  $A_{909\text{cm}^{-1}}/A_{720\text{cm}^{-1}}$  in hexane soluble fraction was about 10% of that in hexane insoluble fraction, whereas for DM-9, the area ratio of  $A_{909\text{cm}^{-1}}/A_{720\text{cm}^{-1}}$  in hexane soluble fraction was about 50% of that in hexane insoluble fraction. Comparing with sample DM-9, it was clearly shown that more grafted GMA in DM-3 was distributed in hexane insoluble fraction. This can be attributed to the strong crosslinking reaction during the melt grafting in the EPDM+GMA+T101 system, indicating by high gel.

### **3.2.7 Grafting GMA onto a Mixture of EPDM and PP**

The results of grafting GMA onto EPDM demonstrated that GMA could be grafted onto EPDM, but the crosslinking of EPDM during the melt grafting constituted the main side reaction. Increasing concentration of peroxide gave rise to higher grafting accompanied by significant increase of crosslinking reflected by higher amount of insoluble gel. Crosslinking leads to significant alteration of rheological properties and can deteriorate the properties of EPDM. To minimise the crosslinking of EPDM, an attempt to graft GMA onto a mixture of EPDM and polypropylene (PP) (75/25) was made. EPDM used was the same as above, Buna AP 447. PP was a commercial grade of unstabilised PP (Propathene ICI, HF-26), white powder, supplied by ICI Plastics Division Ltd. It has a melt flow index (MFI) of 1.7g/10min (ASTM-1238 - 2.16Kg load, 230°C)

The melt grafting of EPDM/PP mixture with GMA was also carried out in an internal mixer (RAPRA-Hampden torque rheometer, TR). Processing was conducted in a closed mixer at 180°C with a rotor speed of 65rpm for 10 minutes for all runs. The weight ratio of EPDM to PP was fixed at 75/25. The PP used was in the form of fine white powders so it was capable of absorbing a large amount of liquid monomer, thus facilitating material feeding and reducing monomer loss. Before processing, the mixture of GMA and peroxide T101 was mixed with the required amount of EPDM and PP in a cup for about 3 minutes in order that the liquid reagents were absorbed by the EPDM and PP. They were charged into

the preheated mixing chamber which was initially flushed with oxygen-free nitrogen. The mixing was conducted under a close system by lowering the ram down (see Scheme 3-5). The processed polymer was cooled under a stream of nitrogen. When the comonomer TRIS was included in the formulation, a different addition sequence was adopted to avoid the formation of copolymer of TRIS-co-GMA during the melt grafting. Pre-weighed EPDM and TRIS were mixed in a cup to allow absorption of TRIS in the EPDM before they were introduced into the mixing chamber and mixed for 1 minute. This was followed by charging a mixture of GMA and T101 and the PP (mixed in a cup beforehand) and the mixing was maintained for further 9 minutes (see Scheme 3-5). A set of GMA grafted EPDM/PP (EPDM/PP-g-GMA) with different compositions were prepared (see Table 3-3).

A similar purification procedure as that of GMA grafted EPDM products was applied. Due to the fact that PP can be dissolved only with high boiling point solvent, such as xylene, all samples were subject to a precipitation-purification procedure using xylene (see Scheme 3-5). About 3g sample was dissolved in refluxing xylene. The solution was precipitated into 7 times of excess acetone. The precipitated polymer was filtered, washed and dried in a vacuum oven at a temperature of 80-85°C for more 20 hours. The purified sample was expected to contain only grafted GMA. The purified samples were pressed into thin films and FTIR spectra were recorded.

The grafting degree of GMA for all samples was determined by titration method as described in Section 2.5.1 and xylene used as solvent instead of toluene. The results list in Table 3-3. The amount of gel in GMA grafted EPDM/PP samples was determined by Soxhlet extraction with xylene. The details of extraction procedure was described in Section 2.6 and the results present in Table 3-3.

FTIR was used to characterised GMA grafted EPDM/PP. Due to the existence of both EPDM and PP in the grafted products, their FTIR spectra became more complicated. Figure 3-35 shows the spectrum of the blend of EPDM and PP at a weight ratio of 75/25. Characteristic absorption peaks of EPDM are at  $1685\text{ cm}^{-1}$ , corresponding to the existence of C=C double bonds from a small amount of 5-ethylidene-2-norbornene ( 5%), and  $720\text{ cm}^{-1}$  assigning to  $(-\text{CH}_2-)_n$  ( $n \geq 4$ ) rocking of EPDM chains. Absorption peaks at  $2717\text{ cm}^{-1}$  and  $898\text{ cm}^{-1}$  are assigned to PP chains. The grafting of GMA onto EPDM can be

confirmed by the appearance of the new absorptions at  $1730\text{ cm}^{-1}$ , assigned to the ester carbonyl absorption of grafted GMA, and  $909\text{ cm}^{-1}$ , assigned to the epoxy ring of grafted GMA. However, the peak at  $909\text{ cm}^{-1}$  is very close to the peak at  $898\text{ cm}^{-1}$  from PP. Depending on the intensity of grafted GMA in the product, one of these two peaks may appear as a shoulder, not a clear peak. It was clear that GMA had been grafted onto the mixture of EPDM/PP (see Figure 3-36).

Figure 3-37 shows the effect of peroxide concentrations on the GMA grafting degree and gel formation with a fixed concentration of 10 phr GMA. With 0.3 phr T101, 0.7% grafting degree and 0% gel were measured. Increasing the T101 concentration to 0.6 phr led to the increase of grafting degree to 1.5% with no gel measured. A further increase in the concentration of T101 resulted in levelling off the grafting degree, but the gel content reached to 11%. It is clear therefore that when comparing the grafting of GMA onto EPDM alone, the use of a small amount of PP resulted in reducing in the polymer crosslinking. During the melt grafting, the degradation of EPDM is dominated by crosslinking, while chain scission dominates the degradation of PP. As a result, a small amount of PP may suppress the crosslinking reaction during the melt grafting. However, the overall grafting degree remained low.

In order to investigate the effect of TRIS in the GMA grafting of EPDM/PP, a set of GMA grafted EPDM samples were prepared in the presence of TRIS. Table 3-3 lists the compositions, grafting degree and gel content. When GMA and TRIS were fixed at 10 phr and 1.11 phr, respectively, (GMA to TRIS ratio: 9/1), 0.0025 T101 mole ratio to GMA and TRIS led to an increase in the grafting degree to 2.2% and no gel formed. Increasing T101 mole ratio to GMA and TRIS from 0.0025 to 0.02 resulted in no obvious increase of grafting degree but a small amount of gel was measured (less than 5%) (see Figure 3-38). With increasing TRIS concentration to 2.5 phr (GMA to TRIS ratio: 8/2), an increase of T101 mole ratio to GMA+TRIS (from 0.0025 to 0.01) did not result in any change in the grafting level (about 3%). Increasing peroxide concentration has led to an increase in the gel content only. When the T101 concentration reached from 0.01 to 0.02 mole ratio, the gel content rose sharply from 6% to 46% (see Figure 3-39). It was obvious that high concentrations of TRIS and T101 led to high gel content. A very low concentration of peroxide was therefore required to achieve high grafting and low gel. Comparing with the grafting of EPDM with GMA, the gel content was much lower with or without TRIS.

Differential solvent fractionation analysis of GMA grafted EPDM/PP mixture was also carried out using the same procedure as the differential solvent fractionation analysis used for EPDM-g-GMA (see Section 3.2.6 and Scheme 3-4). Three samples were chosen for the analysis. First was a control sample which was a blend of EPDM/PP (weight ratio=75/25) processed under the same conditions as those used for grafting (temperature, 180°C; speed, 65 rpm; time, 10min, sample PM-0 in Table 3-3). The second sample was prepared with a composition of 75 phr EPDM, 25 phr PP, 10 phr GMA, and 0.6 phr T101 (referred as EPDM/PP-g-GMA<sub>T101</sub>) (sample PM-2 in Table 3-3), while the third sample was prepared with a composition of 75phr EPDM, 25phr PP, 10phr GMA, 2.5phr TRIS and 0.057phr T101(referred as EPDM-g-GMA<sub>TRIS</sub>) (sample PM-8 in Table 3-3 ). All three samples were subject to sequential extractions with the three solvent: hexane, toluene and xylene. Before extraction, all polymer samples were pressed into thin films (0.2-0.3mm).

EPDM is soluble in refluxing hexane, whereas PP is only partially soluble in refluxing toluene but completely soluble in refluxing xylene due to its crystalline characteristics. When unmodified EPDM (virgin) was Soxhlet extracted with hexane, no insoluble fraction was measured. For the unmodified PP, no insoluble fraction was determined in the extraction with xylene. Figure 3-40 shows the fractionation resulting from EPDM/PP (75/25 w/w) blend (sample PM-0). 77% of sample was measured as hexane soluble fraction - 2% more than the total part of EPDM in the blend. This is because a very small fraction of PP was also extracted with hexane. The toluene soluble fraction was 1.6% and xylene soluble fraction 21.4%. Though a small fraction of PP was extracted with toluene, the main part of PP was extracted in the xylene fraction. The hexane and xylene soluble fractions were analysed by FTIR and they were EPDM and PP respectively by comparing them with the spectra of virgin EPDM and PP (see Figures 3-41 and 3-42).

For the EPDM-g-GMA<sub>T101</sub> sample which was prepared in the absence of TRIS (EPDM-g-GMA<sub>T101</sub>, sample PM-2), its grafting degree was 1.5% with no gel determined by Soxhlet extraction with xylene. Its hexane soluble fraction was 59% (see Figure 3-43). In the following extractions, the toluene and xylene soluble fractions were 31.6% and 7% respectively. The xylene insoluble fraction was 2.4%. Figure 3-44 shows the FTIR spectra of different soluble fractions. It was found that the FTIR spectrum of the hexane soluble fraction matched that of virgin EPDM, indicating that this fraction extracted was

EPDM. Additional absorption peaks at  $909\text{ cm}^{-1}$  and  $845\text{ cm}^{-1}$  and  $1735\text{ cm}^{-1}$  were also observed, assigned to grafted GMA (see Figure 3-44 (b)). This means that grafted GMA exists in the low temperature hexane extraction fraction corresponding to relatively low molecular weight portion in the sample. The FTIR of the toluene soluble fraction shows that both EPDM and PP constitute this fraction by appearance of absorption peaks at  $2717\text{ cm}^{-1}$  and  $899\text{ cm}^{-1}$ , corresponding to PP, and absorption peak at  $720\text{ cm}^{-1}$  corresponding to EPDM (see Figure 3-44 (c)). Meanwhile, clear grafted GMA absorption peaks were also observed. Comparing the weight percentage of toluene soluble fraction of EPDM/PP blend, this fraction in the EPDM-g-GMA<sub>T101</sub> sample was much higher whereas the xylene soluble fraction became less. The xylene soluble fraction showed similar FTIR to that of toluene soluble fraction but its EPDM peak at  $720\text{ cm}^{-1}$  was much weaker, relating to less quantity of EPDM and higher quantity of PP in this fraction. Furthermore, the grafted GMA absorption peaks were much weaker, corresponding to less grafted GMA in this fraction. It can be seen that part of EPDM in the sample could not be extracted with hexane due to some crosslinking/ branching of EPDM chains leading to higher molecular weight. As a result, some EPDM fraction was found in the toluene and xylene soluble fraction. On the other hand, the PP fraction in sample could be extracted at lower temperature, e.g. from xylene extraction to toluene extraction. This may be due to the degradation of PP via chain scission leading to reduction in molecular weight. This may increase its solubility in lower boiling point solvent. From the FTIR analysis of soluble fractions, the distribution of the grafted GMA in the EPDM phase or PP phase could be reflected. It can be seen that all of these three soluble fractions contain a certain amount of grafted GMA. It seems that more grafting distributes in the toluene soluble fraction as indicated from the stronger intensity of GMA absorption peaks at  $1730\text{ cm}^{-1}$  and  $909\text{ cm}^{-1}$ . This means that more grafted GMA located in PP phase.

In the case of sample which was prepared in the presence of TRIS (EPDM-g-GMA<sub>TRIS</sub>, sample PM-9, 3.1% grafting degree with 0% gel determined by Soxhlet extraction with xylene), the hexane soluble fraction was 55%, whereas the toluene and xylene soluble fractions were 20 % and 7% respectively (see Figure 3-45). It was interesting to note that 18% insoluble fraction was detected. This result is different from that determined directly from Soxhlet extraction with xylene. Similar phenomena was observed in the differential solvent extraction of EPDM-g-GMA<sub>TRIS</sub> (sample DM-9). The FTIR analysis of soluble fractions is shown in Figure 3-46. The spectrum of hexane soluble fraction appeared





GMA was melt processed in EP in the presence of a peroxide (T101) and the GMA-grafted polymer was characterised by FTIR after purification of the reaction product. It was demonstrated that GMA is successfully grafted onto the EP confirmed by the appearance of new absorption peak  $1730\text{ cm}^{-1}$  ascribed to the formation of a saturated ester and absorptions at  $908\text{ cm}^{-1}$  and  $844\text{ cm}^{-1}$  ascribed to the presence of the epoxide ring. The formation of the homopolymerisation of GMA, polyGMA, during the melt grafting was determined by employing a set of purification procedures to separate the reaction products and then characterising the separated reaction products using FTIR (see Section 3.2.3). It was found that polyGMA indeed existed in the GMA grafted EP products (see Fig. 3-6).

Besides the desired grafting reaction and undesired formation of polyGMA during the melt grafting, crosslinking/branching or chain scission always accompanies the grafting reaction, which depends on the chemical structure of polymer substrates. Literature studies on the melt grafting of GMA and MA onto different polymers revealed that when PP was used the main polymer side reaction was the chain scission [73,75,90,91,119,120], whereas in the case of PE, EPR or EPDM, crosslinking predominates, resulting in low monomer grafting [73,105,106,113,118]. The EP used in this study contains much higher ethylene content than propylene (ethylene/propylene=4). Although both secondary and tertiary macroradicals are formed during the radical-initiated melt grafting reactions of GMA in ethylene-propylene copolymer (EP), the evidence suggests that crosslinking is the predominant reaction in the polymer examined in this study. This is reflected from both the torque-time curves which show that the final torque values increase (polymer becomes more viscous) with increasing initiator concentration, see Fig. 3-11 (a), and from the melt flow index results of GMA-grafted EP samples which become much lower than that of the virgin polymer, see Fig. 3-11 (b). Closer examination of the behaviour of the peroxide-initiated grafting system during the reactive processing step showed that, whereas lower peroxide concentrations have little effect on the torque characteristic of the polymer, higher peroxide levels were associated with much higher torque levels; associating with higher polymer viscosity and the formation of toluene insoluble gel (Fig. 3-11 (a)). However, it is important to point out that although the GMA-grafted polymer does become more viscous than the unmodified control, a crosslinked polymer fraction (defined as the toluene insoluble gel) was only detected at high peroxide concentrations (e.g. mole ratio:[T101]/[GMA]=0.12 ).

The results also show that homopolymerisation of GMA strongly competes with the desired grafting reaction. Increasing concentrations of T101 and GMA leads to an inproportionate increase in the grafting degree (see Figs. 3-10, 3-12) and the overall GMA grafting remains low. By contrast, the amount of polyGMA formed is proportional to the concentrations of GMA and T101. When the concentration of peroxide was fixed at 1 phr, increasing GMA concentration resulted in the sharply increase of the amount of polyGMA (see Fig. 3-14). At low concentration of GMA (below 10 phr), the grafting degree was higher than the amount of polyGMA, whereas the polyGMA exceeds the grafting degree when GMA was over 10 phr. It is clearly shown that high concentration of GMA makes the GMA homopolymerisation more favourable. This also reflects a lower reactivity of GMA towards EP giving rise to the low grafting level. It is interesting to note that the rate of grafting at the initial stage was faster than that of the homopolymerisation of GMA as observed from the kinetics of grafting in Fig. 3-15. This may be attributed to the faster rate of macroradical initiation by H-abstraction from polymer chains of EP once the radical formed from the decomposition of organic peroxide (see Scheme 3-6 Rn b). Temperature is another important factor which affects the formation of grafting and formation of polyGMA. In the presence of T101, the level of both grafting and polyGMA was low at low processing temperature (below 160°C) and very little polyGMA was formed. At higher temperature, the grafting degree increased rapidly and reached a peak, accompanied by gradual increase of polyGMA. A further increase in temperature led to sharp increase of polyGMA with decrease of grafting degree. This observation is closely related to the rate of decomposition of peroxide at the different temperatures. The halflife of T101 at 190°C is 1 min and a decrease in temperature by 5-10°C will double the halflife [73]. At a temperature of 160°C, the halflife is as long as about 6minutes [151]. That is why both grafting and homopolymerisation of GMA are low at the temperatures below 160°C. When the rate of decomposition of T101 is too slow, there are not enough free radicals to initiate the reactions. With the increase of temperature the rate of decomposition of T101 becomes faster so the rate of both grafting and polyGMA formation increase. When the temperature exceeds 180°C, the rate of reaction of homopolymerisation of GMA is significantly increased. As a result, it strongly competes with the grafting reaction so the grafting degree decreases at temperatures over 180°C.

### 3.3.1.2 The GMA-Grafting Mechanisms in the Absence of Comonomer

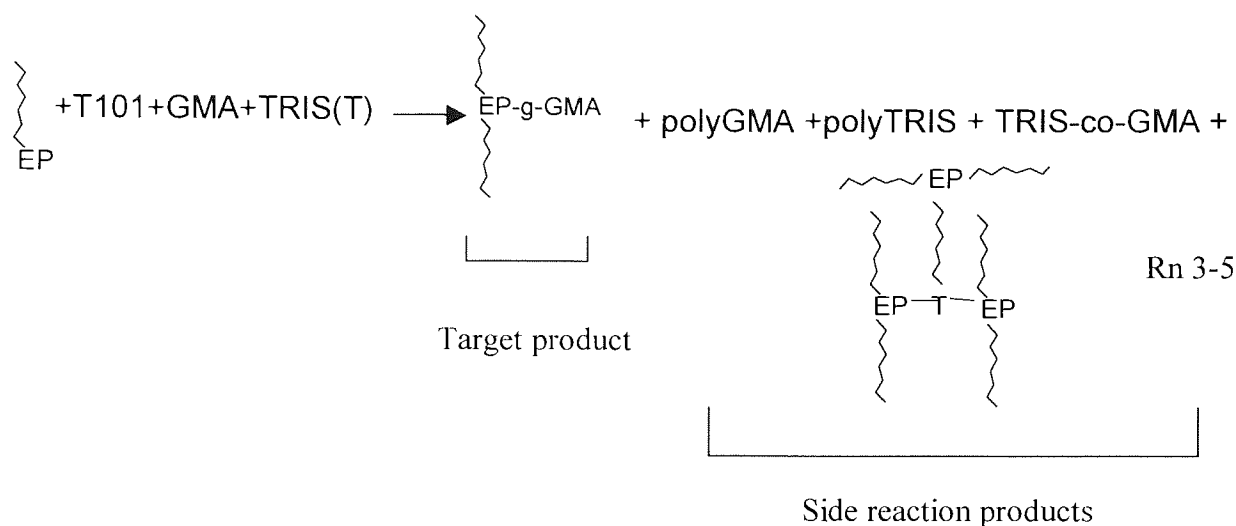
In the absence of a comonomer, the melt grafting of GMA onto EP in the presence of T101 follows a typical free radical grafting mechanism and is depicted in Scheme 3-6. During the melt processing, the peroxide would initiate both the target grafting reaction of GMA on EP-macroradicals (Scheme 3-6, rns b and e), via intra- and/or inter- molecular hydrogen abstraction (Scheme 3-6, rns g, h), and the undesirable homopolymerisation reaction of GMA, reaction f. Further grafting via reaction of the propagating GMA-radical with EPR-macroradical is unlikely due to its low H-abstrating ability, hence the GMA-graft length is expected to be short. The slightly higher torque level observed at higher peroxide concentrations (see Fig. 3-11 (a), T101=1phr), in samples where no toluene-insoluble gel was formed in the polymer, may be due to a certain degree of branching involving the branched macroradical, e.g. scheme 3-6 rn d. It is clear from Figs. 3-13 and 3-14 that the overall low grafting yield of GMA on EP is not only due to the known low free radical grafting reactivity of GMA [119], but also due to the competitiveness of GMA-homopolymerisation (scheme 3-6 rn f), especially at high initial GMA concentrations and high temperature, resulting in high poly-GMA formation in the grafting system.

### 3.3.2 Effect of the Presence of Comonomer, TRIS, on GMA Grafting onto EP

The above discussion shows that the overall grafting efficiency (conversion) of GMA on EP is low and that much higher peroxide concentrations are needed to achieve higher conversion rates, at the expense of degradation of the polymer. Meanwhile, homopolymerisation of GMA strongly competes with the desired grafting reaction and high amount of polyGMA is formed at high concentrations of peroxide and GMA. As discussed in Section 1.7, the use of a highly reactive comonomer can significantly enhance the desired grafting and reduce the undesired side reaction. In this work, in order to minimise the side reaction and increase the grafting degree of GMA onto EP, TRIS was used as a comonomer.

The presence of such a reactive multifunctional co-monomer in the GMA grafting system results in a number of additional side reactions involving the TRIS comonomer in addition to the formation of polyGMA. These reactions include the formation of ungrafted copolymer of TRIS and GMA (TRIS-co-GMA) as well as a homopolymer of the coagent

(polyTRIS), together with possible polymer crosslinking that may occur via reaction of the reactive functions of the comonomer with the polymer macroradicals, see Rn 3-5.



The results show clearly that the use of the comonomer, TRIS, leads to a significant improvement in grafting efficiency of GMA on EP and that higher levels of grafting can be achieved at much lower peroxide concentration resulting in negligible degradation of the polymer matrix (see Fig. 3-21). One of the features of grafting GMA onto EP in the presence of TRIS is that a very small amount of peroxide is required at a fixed concentration of TRIS. For example, when GMA and TRIS concentrations were fixed at 10 phr and 2.5 phr, it was enough to use 0.005 mole ratio of T101 to GMA+TRIS (T101= 0.123 phr) to achieve 2% grafting degree. A further increase of T101 concentration did not give rise to the increase of grafting level but the MFI of the processed EP dropped down significantly. This indicates that a certain level of peroxide is needed to initiate the grafting reaction. If the peroxide is above this level, the increase of peroxide concentration only leads to more branching/crosslinking of EP. Furthermore, the higher the TRIS concentration, the less the peroxide concentration needed. The optimal grafting in the presence of TRIS in terms of high grafting of GMA and minimum branching /crosslinking of EP can be achieved with a delicate balance between the molar ratios of the reagents (monomer, comonomer, initiator) and the process variables (e.g. temperature, processing time). One reason for this is the high reactivity of TRIS and its polyfunctional groups that can act as a linker to branch or crosslink the polymer chains. High concentration of

peroxide may give rise to fast and high grafting of TRIS onto polymer chains, resulting in high branching /crosslinking of EP indicated by low MFI value (see Table 3-1 (b)).

Examination of the kinetics of the grafting reaction in the presence of the comonomer, was carried out by taking out samples at different time intervals during the reactive processing followed by purification and analysis to determine the extent of the target and side reactions. It was found that samples processed in the presence of the comonomer did not contain measurable amounts of either the free TRIS-co-GMA copolymer or the polyTRIS. It was shown clearly that the rate of GMA-grafting is higher in the presence of TRIS when compared to the rate of grafting in the absence of TRIS and increased further with increasing comonomer concentration (see Fig. 3-24). Moreover, it was observed that the presence of TRIS leads to complete grafting reactions in shorter times. The presence of the comonomer in the grafting system leads not only to higher GMA grafting yield but also to less competition from side reactions. It is clear that the rate of formation of poly-GMA is very slow and its final yield is very low, especially when compared to the amount of poly-GMA formed in the absence of TRIS (at the same initial GMA concentration), see Fig. 3-24 a, b. It is interesting to note that a higher TRIS-to-GMA molar ratio results in slower initial rate of GMA-homopolymer formation, see Fig. 3-24 a, b, indicating that increasing concentration of TRIS results in a more favourable competition from the target grafting reaction of GMA (through TRIS) from the onset of the reaction with respect to that of GMA-homopolymer formation.

The fact that even when polyGMA does form (at the low concentrations measured) in the TRIS-containing systems, it builds up to a maximum at the early stages of the melt reaction but, subsequently, decreases to a much lower concentration on further processing. This behaviour contrasts with that of poly-GMA formed during the melt reaction of GMA in EP in the absence of TRIS where its concentration continues to increase with processing time, **Fig. 3-24 a,b** (see also Fig.3-15). This may suggest that the polyGMA formed in the absence of TRIS has a higher molar mass and is more stable for the duration of the grafting reaction whereas the poly-GMA formed in the presence of TRIS at the initial stages of the reaction is of a much lower molar mass and is relatively unstable and hence undergoes depropagation leading to a reduction in its final concentration in the polymer. The GMA-radicals produced from this depropagation reaction would then undergo further graft reaction through the intermediacy of the more reactive TRIS-graft-macroradical on further

processing resulting in the higher grafting efficiency observed in the presence of the comonomer.

### **3.3.3 The Mechanisms of GMA-Grafting on EP in the Presence of Comonomer, TRIS**

In order to minimise side reactions it is important that the radicals formed on the polymer backbone are trapped as rapidly as possible [75]. Some monomers are more effective than others at trapping such radicals. This may arise because of the relative solubility of the monomers in the polymer melt or it may be due to the inherent reactivity of the monomers. One strategy involves choosing a monomer combinations such that the comonomer is both effective in trapping the radicals formed on the polymer backbone and such that the propagating radical formed is highly reactive towards the desired monomer. As a electron-rich comonomer, styrene has been shown to be effective for improving grafting yields and reducing side reactions of electron deficient monomers, in particular MA [73,137] and GMA [118-120] onto polyolefins. For the case of the styrene-MA system, it was proposed that addition of an electron-donating monomer such as styrene can form a charge transfer complex (CTC) with MA. Cartier et. al. [119] recently investigated the reaction mechanism of GMA grafting onto PP with assistance of styrene. The effect of styrene on the increasing GMA grafting yield increase, the reduction of PP chain degradation and the grafting rate increase was studied in details. A reaction mechanism in the presence of styrene was proposed (see Fig.1-8 b) [119]. When styrene was added, styrene reacts first with PP macroradicals and the resulting free radicals then copolymerise with GMA. The higher reactivity of styrene towards PP macroradical compared to that of GMA was suggested to be due to the resonance effect between the double bond and the benzene ring of the former. The higher grafting yields obtained with styrene may be associated with longer chain grafts and more grafting sites [75]. Rates of copolymerisation of electron donor-electron acceptor pairs are substantially greater than that for homopolymerisation (of MA or GMA).

In this study, TRIS was used as a comonomer to enhance the grafting reaction of GMA onto EP. The incorporation of a small concentration of the highly reactive comonomer TRIS in the GMA-grafting system brings about important changes dominated by: a clear improvement in the grafting yields (Figs. 3-21, 3-22) which is achieved at a faster rate (Fig. 3-24), a substantial reduction in the main competing side reaction, the GMA-homopolymerisation (Fig. 3-24), and the absence of undesirable crosslinked/gel fraction

(no toluene insolubles). First of all, the high reactivity of TRIS towards EP-macroradicals was clearly illustrated from the distinct torque behaviour during the reactive processing (see Figs. 3-18, and 3-19). The presence of TRIS in EP resulted in a torque peak under both shear-initiated (without peroxide) and free radical-initiation (in the presence of a peroxide) (Figs.3-18, 3-19) indicating the occurrence of a reaction which leads to an increase in polymer melt viscosity. The height of the torque peak increases and the time for its onset decreases when the reaction is initiated by free radical, compared to that initiated by shear, and with increasing the TRIS concentration in the shear-initiated reaction. The much faster rate of formation of the torque peak (i.e. faster rate of reaction) under the free radical-initiated conditions indicates that the TRIS reactions, including grafting/branching or crosslinking, with the polymer (Scheme 3-7, rns k, m) are kinetically more favourable than is the case with shear-initiation. However, it is important to point out that in the case of TRIS, the mere fact of formation of a distinct peak, when TRIS is present, even in the absence of an added initiator (compared to the torque characteristics of GMA which does not show a peak even in the presence of the initiator, see Fig. 3-18, lends support to the high reactivity of TRIS towards macroradicals when compared to GMA. Another fact is that the high reactivity of TRIS towards GMA as demonstrated the formation of TRIS-co-GMA in the grafting when TRIS, GMA, T101 was added together. As a result, TRIS could be first grafted onto EP polymer chains and then GMA might be grafted onto EP via the reaction of GMA with grafted TRIS. This may be similar to the enhancing effect of styrene on the grafting of GMA onto PP or PE [119].

The mechanism of grafting of GMA in the presence of TRIS presents in the Scheme 3-7. Under the grafting conditions used in the presence of the comonomer, the extent of formation of a 'free' TRIS-co-GMA copolymer (Scheme 3-7, rn f) and polyTRIS (Scheme 3-7, rn e) was found to be negligible. However, due to the high reactivity of TRIS towards copolymerisation with GMA, the TRIS-containing branched macroradical (Scheme 3-7, rn i) rapidly formed at the onset of the melt processing operation is expected to react immediately with GMA (Scheme 3-7, rn l) resulting in the formation of a graft-(TRIS-co-GMA)-copolymer, see Scheme 3-7. But for the same reasoning, one should expect that a free TRIS-co-GMA copolymer would also form in the grafting system and would compete with the target grafting reaction. However, the experimental evidence presented shows that there was 'free' copolymer (after purification of the grafted polymer product) at the end of the grafting reaction. This does not necessarily mean, however, that



the propagation reaction between TRIS radicals and GMA does not occur during the melt reaction. In fact, it is almost certain (based on reactivities) that this reaction does occur during the initial stages of the grafting reaction, probably to a small extent, but the propagating TRIS-GMA copolymer radical would further react, on further processing, with a TRIS-containing-branched macroradical giving rise to further grafting.

On further high temperature processing of the polymer melt, chain scission of the graft-(TRIS-co-GMA)-copolymer chains might take place giving rise to restructuring of the branched/crosslinked graft copolymer. In the grafting of antioxidant onto PP in the presence of TRIS, the study of reaction mechanism suggested that the branching /crosslinking took place in the initial stage of processing [138]. Further processing leads to chain scission of the grafted polymer.

#### **3.3.4 Features of Grafting GMA onto EPDM**

Similar to other melt free radical grafting systems [28, 120], GMA could be grafted onto EPDM via melt free radical grafting reaction using an organic peroxide (T101) as a free radical initiator. Compared to the grafting system of GMA onto EP, significant differences could be found with respect to crosslinking of polymer, and the amount of polyGMA formed during the melt grafting. The results demonstrated that the desired grafting reaction was accompanied by obvious crosslinking of EPDM (see Figures 3-29, 3-30 and 3-31). High concentrations of peroxide resulted in high GMA grafting degree and also high gel formation. On the other hand, no measurable polyGMA was detected in the GMA grafted EPDM. It is clearly shown that different polymer substrates can lead to completely different grafting features and even different grafting mechanisms.

In the absence of TRIS, increasing peroxide concentration leads to the proportional increase of grafting yield, while the gel content also increases significantly (see Fig. 3-29). However, the overall grafting is low. This may be attributed to the presence of 5% 5-ethylidene-2-norbornene in EPDM, which consists of a pendant double bond. Unsaturation in the diene units of EPDM was acknowledged as the likely reactive centre, presumably via a free radical mechanism. The free radicals from the decomposition of organic peroxide can easily initiate macroradicals by H-abstracting via the double bond. These macroradicals may propagate the crosslinking reactions. That is why EPDM is very likely to crosslink during the melt free radical grafting, indicated by high gel content and high

torque value during the processing. No measurable homopolymerised GMA (polyGMA) may be also attributed to the existence of unsaturation of diene units of EPDM. If the free radical can initiate the macroradicals rapidly and the crosslinking reactions are fast, the chance of homopolymerisation of GMA would be reduced significantly.

In order to investigate the effect of TRIS in the GMA grafting of EPDM, a set of GMA grafted EPDM samples were prepared in the presence of TRIS. It was found that the addition of small amount of TRIS could increase the grafting degree, while crosslinking was also the main side reaction (see Figs. 3-30 and 3-31). It is clear that high concentrations of TRIS and T101 led to both high grafting and high gel content. For example, with 2.5 phr TRIS (GMA to TRIS ratio: 8/2), increase T101 mole ratio to GMA and TRIS from 0.0025 to 0.01 led to gradual increase of grafting degree from 2.5% to 3.6%, but the gel content increased sharply from 6% to 69% (see Figure 3-31). In the presence of TRIS, a very low concentration of peroxide was required to achieve high grafting and low gel. In the presence of TRIS, it was found that a proper balance of compositions of TRIS to GMA and peroxide to GMA and TRIS was the key to achieving optimal grafting with minimum crosslinking of EPDM.

One of the important aspects of free radical grafting is the changes of polymer structure and the microstructure of grafts. These may affect the physical and chemical characteristics of the modified polymers. Differential solvent fractionation was used to analyse the structure of GMA grafted EPDM in the absence and presence of TRIS. The results revealed the significant differences between these two types of GMA modified EPDM. The fractionation results show that the sample which was prepared in the absence of TRIS (EPDM-g-GMA<sub>T101</sub>, sample DM-3) has a higher low temperature soluble fraction (hexane soluble fraction), whereas the sample which was prepared in the presence of TRIS (EPDM-g-GMA<sub>TRIS</sub>, sample DM-9) has much less low temperature soluble fraction (hexane soluble fraction) but higher high temperature soluble fraction (that is toluene and xylene soluble fractions) (see Fig. 3-32). This clearly shows that EPDM-g-GMA<sub>TRIS</sub> has a high fraction of branched EPDM. This can be explained by the linker effect of TRIS. TRIS has multi-functional groups and is highly reactive towards EPDM chains. This certainly leads to high branching of EPDM.

The FTIR analysis of the hexane soluble and insoluble fractions for the above two samples revealed that grafted GMA is distributed in both fractions due to the appearance of absorption peaks at  $1730\text{ cm}^{-1}$ ,  $909\text{ cm}^{-1}$ , and  $845\text{ cm}^{-1}$  corresponding to the absorption of carbonyl, and epoxy groups, respectively (see Figures 3-33 and 3-34). However, it was found that the GMA absorption peak intensity in the insoluble fraction seemed to be stronger than that of soluble fraction, especially for EPDM-g-GMA<sub>T101</sub> (sample DM-3). This indicates that more grafted GMA distributes in the hexane insoluble fraction.

### 3.3.5 Effect of PP on GMA Grafting onto EPDM

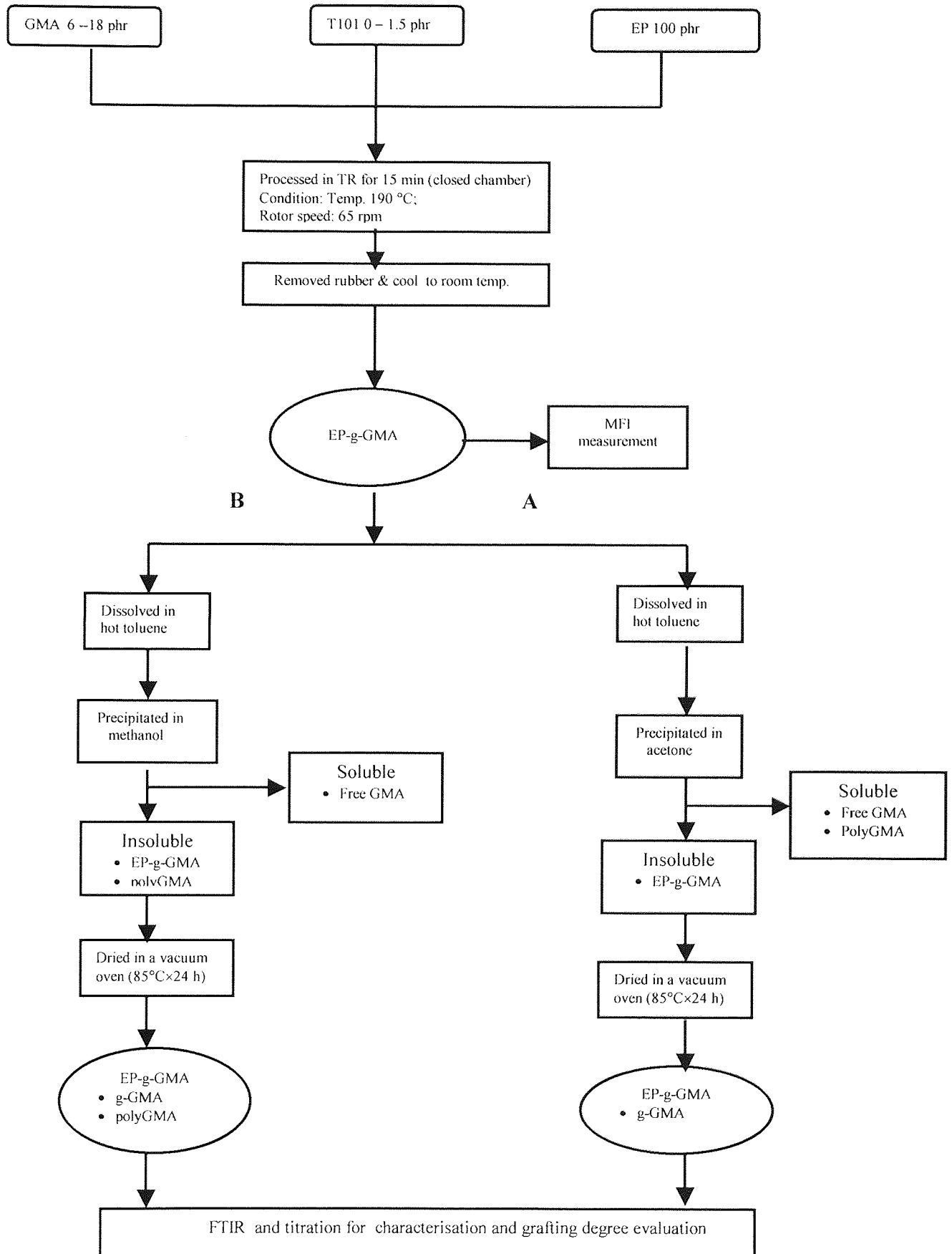
Crosslinking was shown to be the main side reaction in the GMA grafting system onto EPDM. An attempt has been made to reduce the crosslinking of EPDM during melt grafting by addition of small amount of polypropylene (PP) which undergoes primarily  $\beta$ -chain scission (via the tertiary macroalkyl radicals), leading to reduction in the molar mass [73].

When a small amount of PP was added to EPDM (EPDM/PP=75/25) during the melt grafting of GMA onto EPDM, the results demonstrated that the amount of gel could be significantly reduced compared to the grafting of GMA onto EPDM alone (see Figs. 3-37, 3-38 and 3-39). In the absence of TRIS, with a fixed concentration of GMA at 10 phr, increasing the concentration of peroxide, T101, from 0 to 0.6 phr led to an increase in the grafting degree while no gel was measured. When the concentration of peroxide, T101, was further raised to 1 phr, the GMA grafting degree levelled off, but more than 10% gel was determined (see Fig. 3-37). This clearly shows that the presence of PP does indeed decrease the extent of the crosslinking reaction of EPDM during the melt grafting. When the free radicals are formed with the decomposition of peroxide, macroradicals could be initiated by H-abstracting from the polymer chains of PP and EPDM. The macroradicals from PP might undergo both  $\beta$ -scission and grafting with GMA, while the macroradical from EPDM might undergo both crosslinking and grafting with GMA. Comparing with grafting GMA onto EPDM alone, the presence of PP can reduce the chance of crosslinking reaction of EPDM. The sequential solvent extraction (using hexane, toluene and xylene) results clearly show that the EPDM fraction is been branched or crosslinked and could be detected in the toluene soluble and xylene soluble fractions, whereas most of PP was

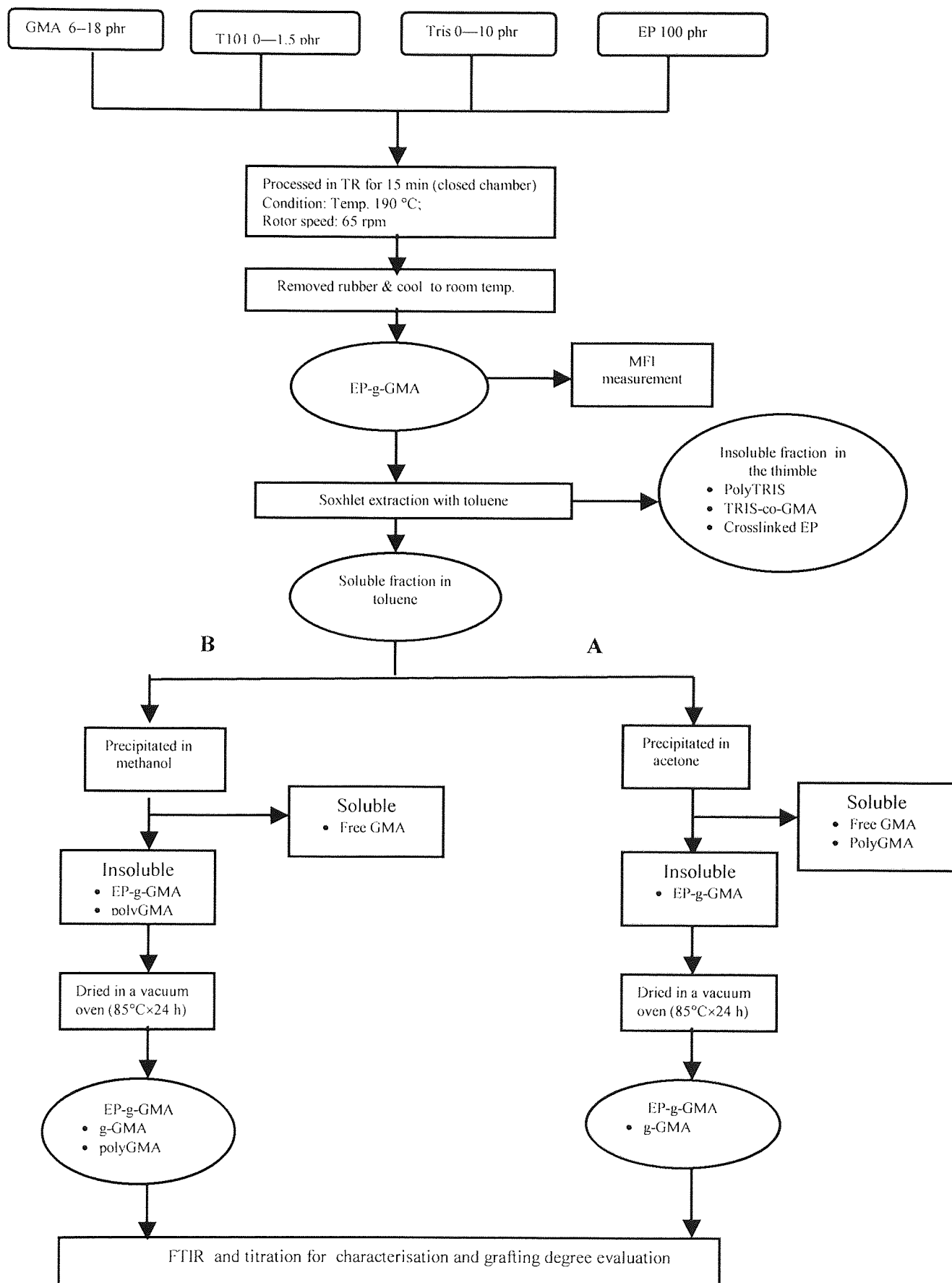
extracted in the toluene soluble fraction due to its degradation of PP during the melt grafting (see Figs. 3-43 and 3-44). It is interesting to note that all three soluble fractions contained grafted GMA which has been proved by FTIR analysis of the soluble fractions, but the toluene soluble fraction has higher grafted GMA than hexane and xylene soluble fractions. This may suggest that more grafted GMA distributes in the PP phase. This may be attributed to the fact that PP macroradicals may be initiated at a higher rate than that of EPDM.

In the presence of TRIS, the grafting mechanisms become more complicated. Due to the fact that TRIS can act as a crosslinking agent, the chain scission of PP could be reduced during the melt grafting [138, 141]. It is expected that the PP phase is less degraded and the EPDM might be branched or crosslinked. As a result, gel is more likely to form. Actually, a very low concentration of peroxide is needed to achieve a high grafting level without gel formation (see Figs 3-38, and 3-39). At a high concentration of TRIS and T101, high amount of gel could be determined. The differential solvent extraction results demonstrated that more xylene insoluble fraction was measured. This gives the evidence that TRIS led to the branching /crosslinking of EPDM and/or PP. Another fact is that no measurable grafted GMA distributes in the soluble fractions of hexane, toluene and xylene. All the grafted GMA was present in the high molecular weight fraction (see Figs 3-46 and 3-47). It can be proposed that TRIS grafts first onto EPDM and PP polymer chains, and then GMA grafts onto EPDM and PP via reaction with the grafted TRIS. Due to the multifunctionality of TRIS, branching and crosslinking are very likely to also take place. That is why nearly all the grafted GMA is contained in the xylene insoluble fraction.

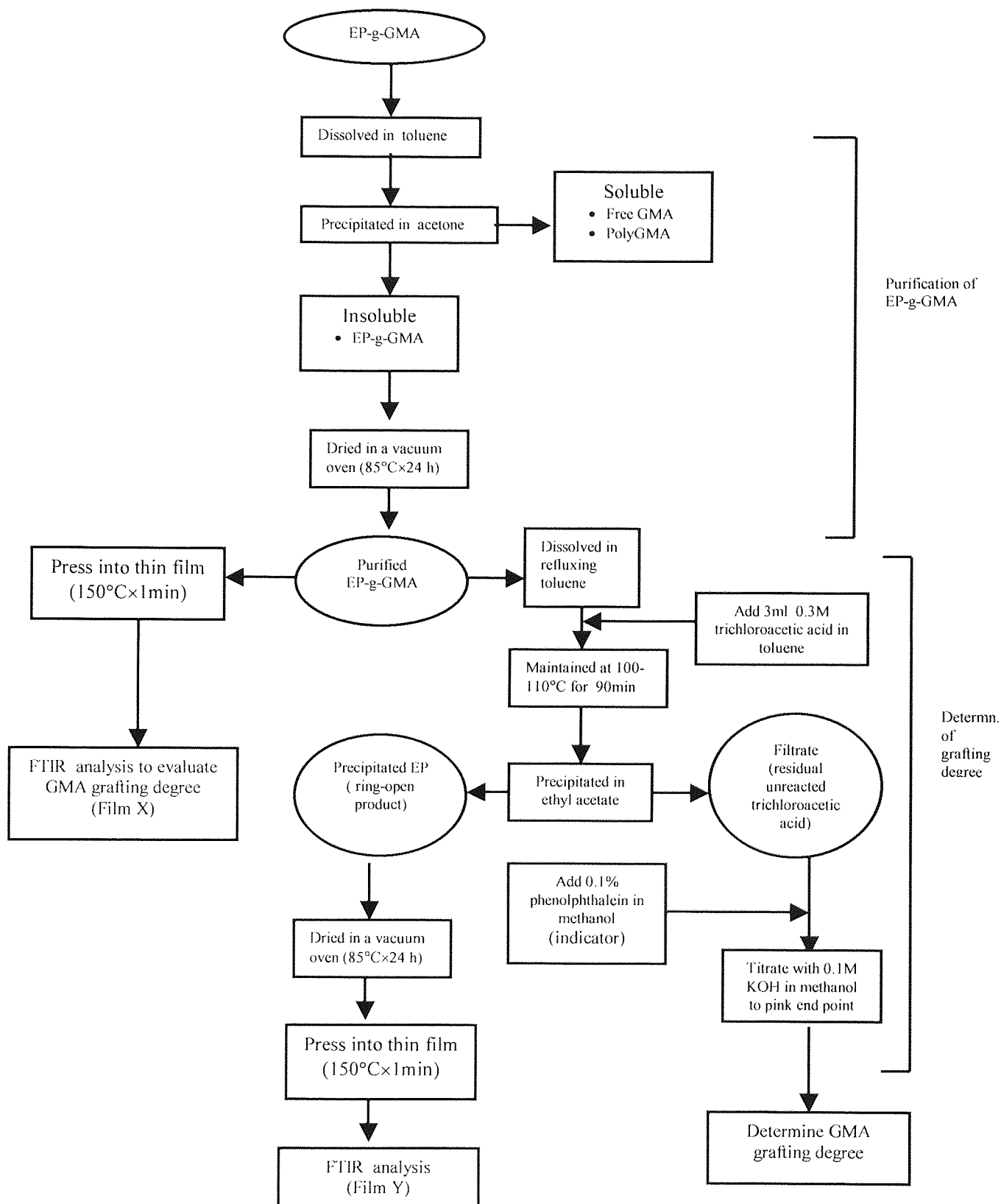
Scheme 3-1 a Methodology for grafting GMA onto EP in the absence of TRIS



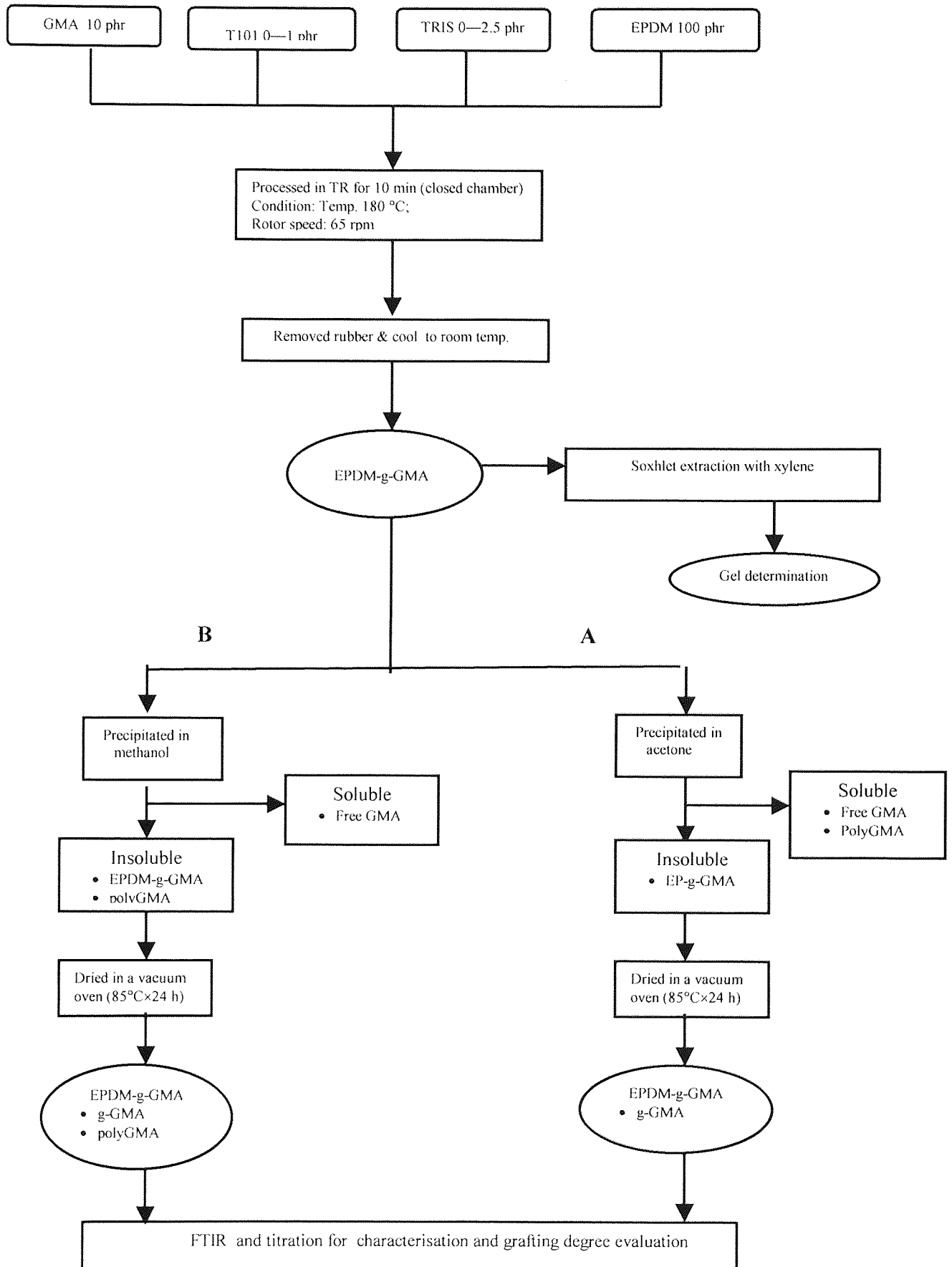
Scheme 3-1 b Methodology for grafting GMA onto EP in the presence of TRIS



Scheme 3-2 Flow chart for analysis of EP-g-GMA by titration and FTIR

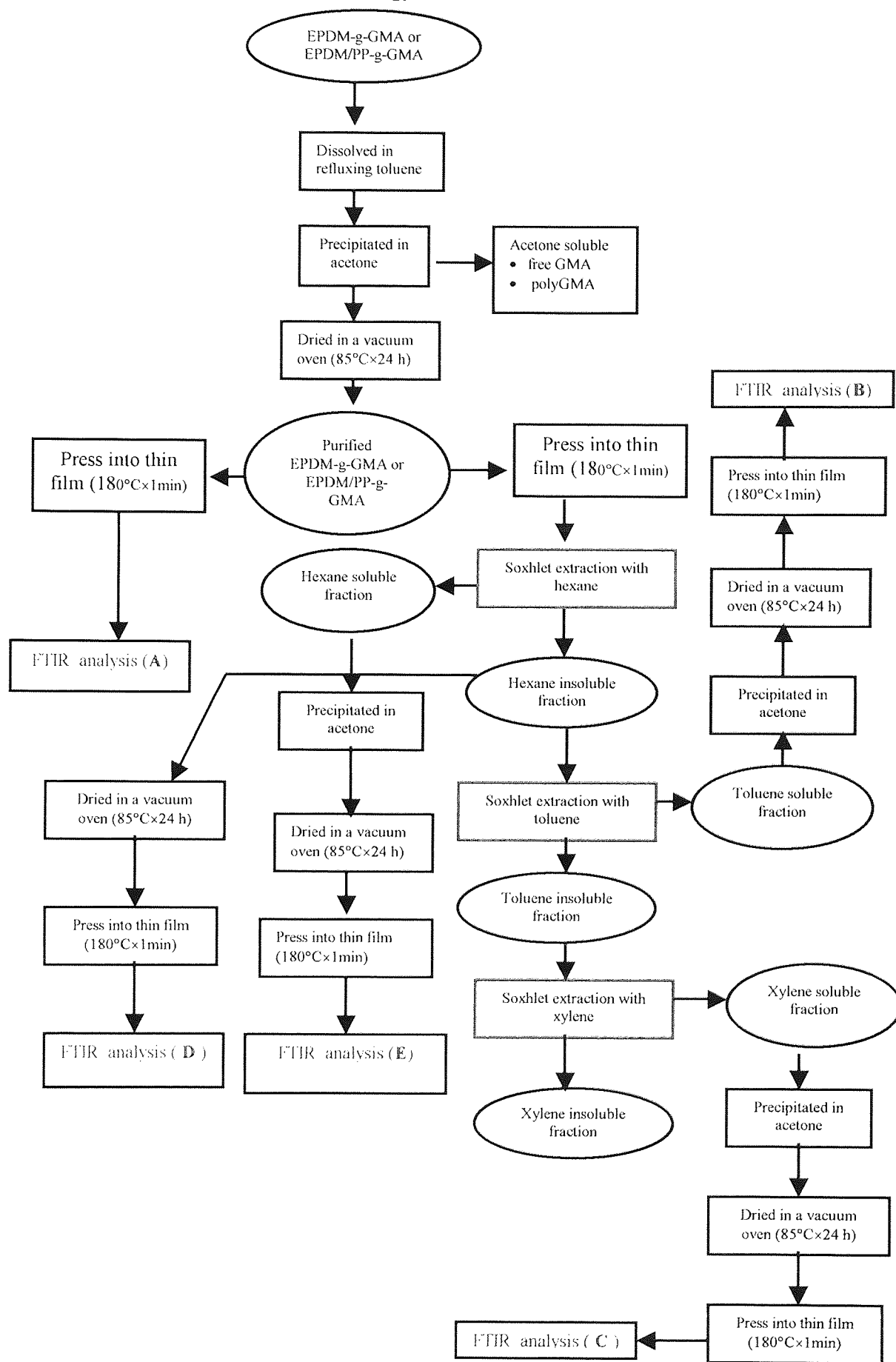


Scheme 3-3 Methodology for grafting GMA onto EPDM

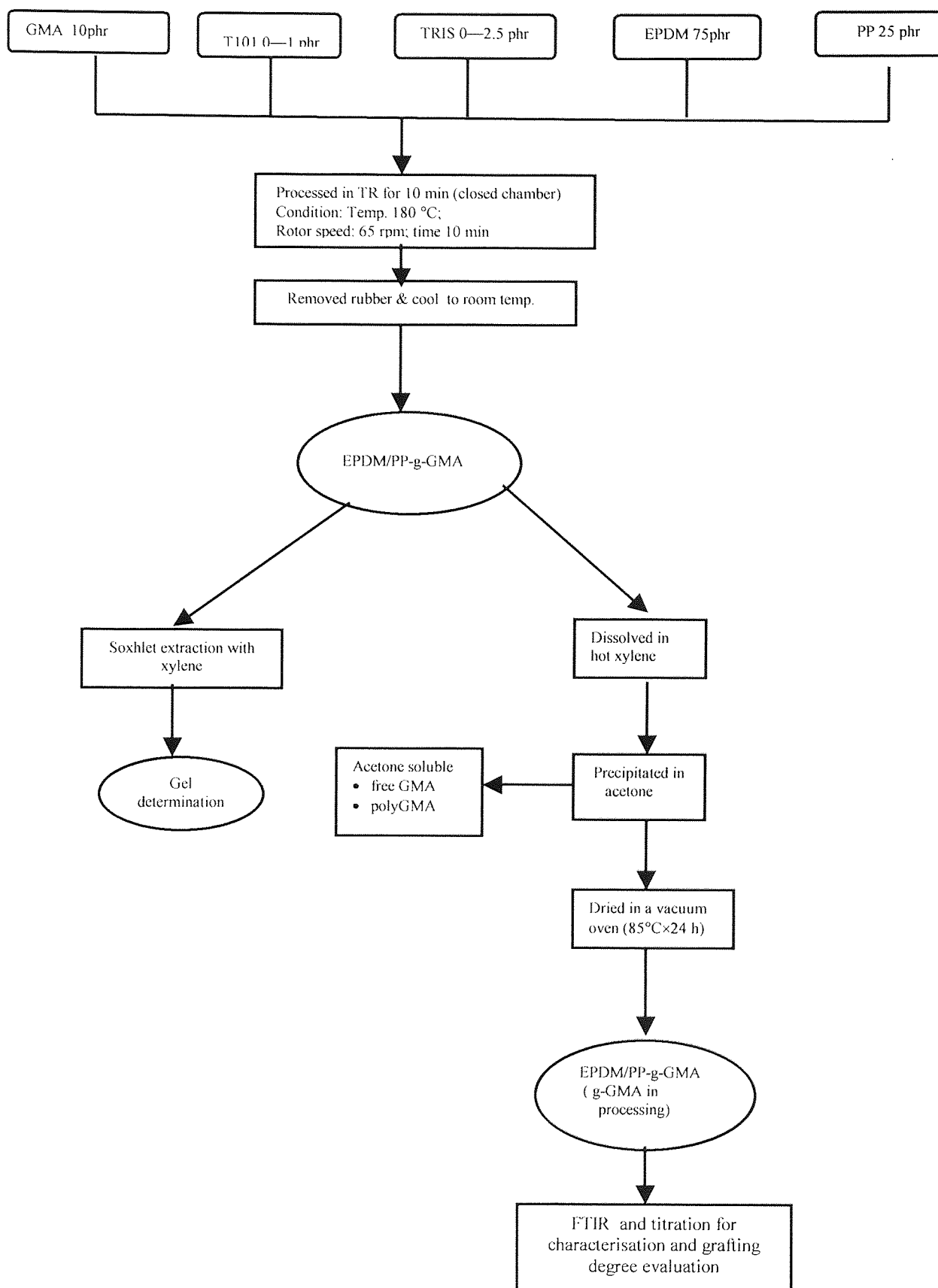




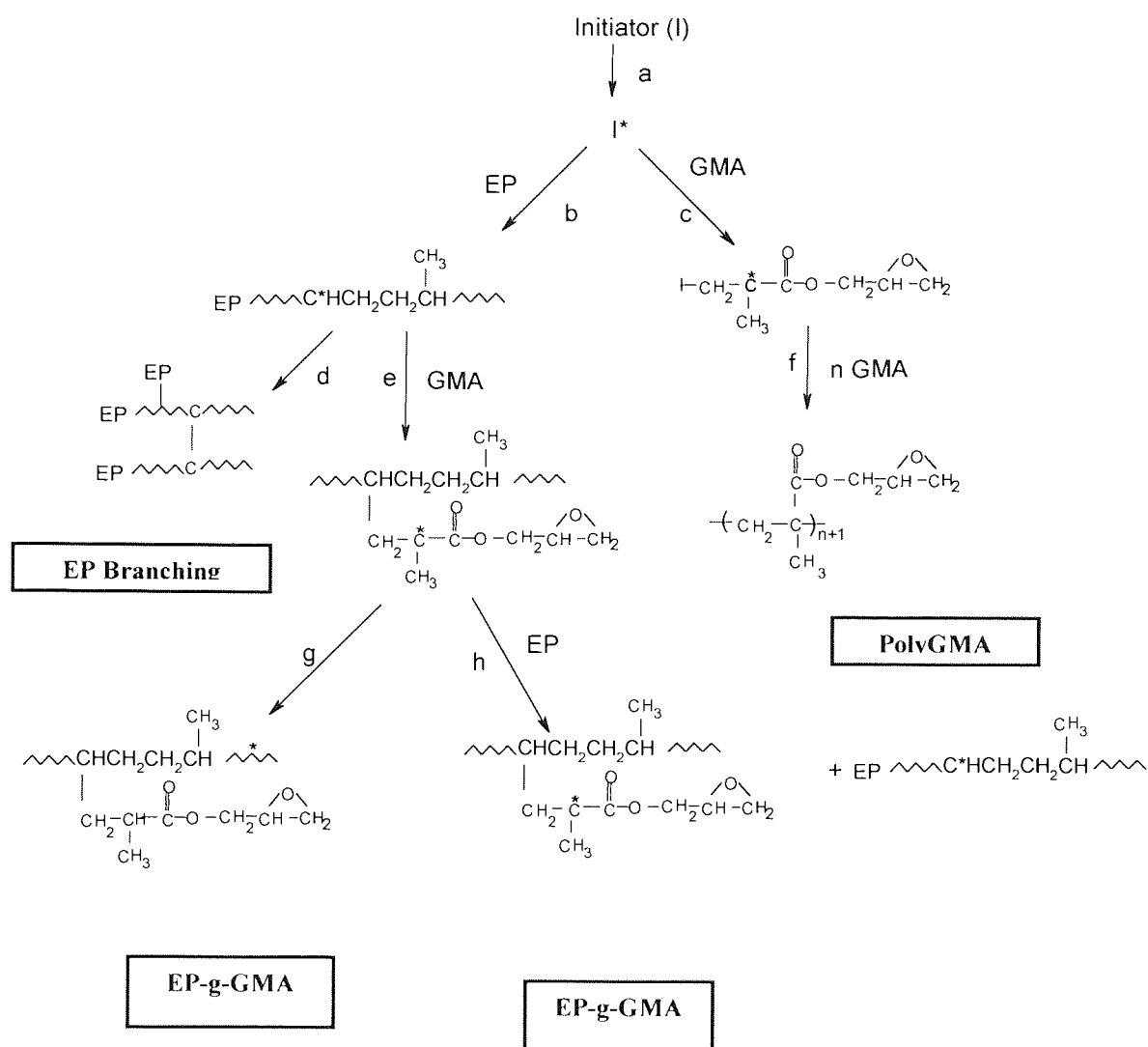
Scheme 3-4 Methodology for differential solvent extraction



Scheme 3-5 Methodology for grafting GMA onto EPDM/PP



Scheme 3-6 Grafting and homopolymerisation of GMA onto EP in the absence of TRIS



Scheme 3-7 Grafting of GMA onto EP in the presence of TRIS

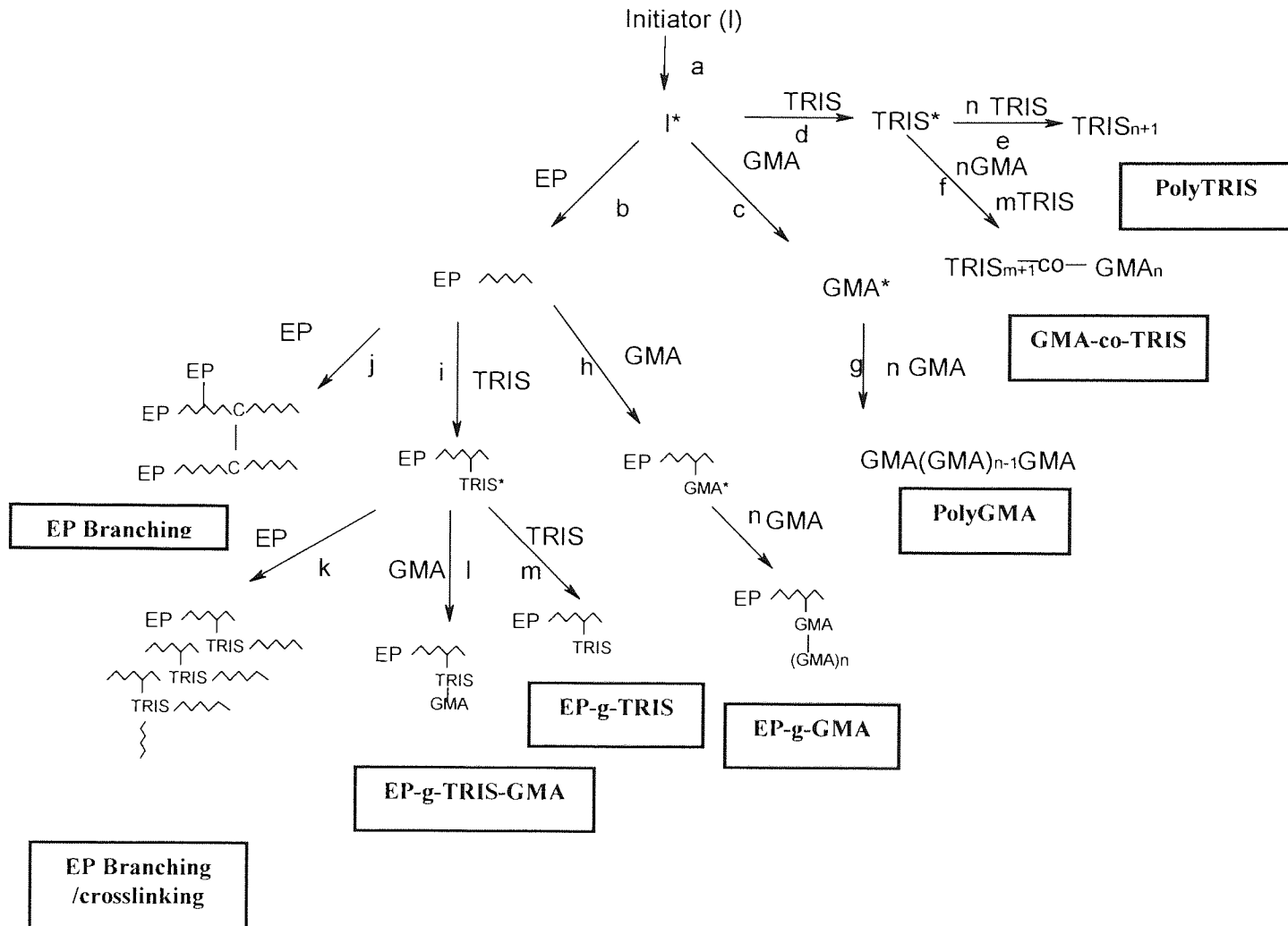


Table 3-1 The Experimental Composition and Results  
 GMA grafting onto EP system  
 (a) EP+GMA+T101 system (in the absence of TRIS)

Code	Compositions					Processing conditions				Grafting Degree (%)	Grafting Efficiency (%)	Poly-GMA wt(%)	MFI (g/10min)
	EP (phr)	GMA (phr)	TRIS (phr)	TRIS/GMA (w/w)	T101 (phr)	T101/[GMA]+[TRIS] MR*	Temp. (°C)	Rotor speed (rpm)	Time (min)				
GP-1	100	6	0	0	0.5	0.041	190	65	15	0.3	5		0.55
GP-2	100	6	0	0	1.0	0.082	190	65	15	0.6	9	0.2	0.10
GP-3	100	6	0	0	1.5	0.122	190	65	15	1.3	22		0
GP-4	100	10	0	0	0.5	0.024	190	65	15	0.8	8		0.73
GP-5	100	10	0	0	1.0	0.048	190	65	15	1.3	13	1.1	0.15
GP-6	100	10	0	0	1.5	0.073	190	65	15	1.3	13		0
GP-7	100	12	0	0	0.5	0.020	190	65	15	0.4	3	0.3	0.68
GP-8	100	12	0	0	1.0	0.040	190	65	15	1.4	12	1.6	0.18
GP-9	100	12	0	0	1.5	0.061	190	65	15	1.3	11	1.4	0.06
GP-10	100	18	0	0	0.5	0.014	190	65	15	0.6	3		0.79
GP-11	100	18	0	0	1.0	0.027	190	65	15	1.6	4	2.7	0.44
GP-12	100	18	0	0	1.5	0.041	190	65	15	1.8	10		0.05
GP-13	100	10	0	0	1.0	0.048	190	65	2	0.6	6	0.2	
GP-14	100	10	0	0	1.0	0.048	190	65	5	1.1	11	0.8	
GP-15	100	10	0	0	1.0	0.048	190	65	10	1.2	12	1.3	
GP-16	100	10	0	0	1.0	0.048	140	65	15	0.6	6		
GP-17	100	10	0	0	1.0	0.048	150	65	15	0.6	6		
GP-18	100	10	0	0	1.0	0.048	160	65	15	0.8	8	0.1	
GP-19	100	10	0	0	1.0	0.048	170	65	15	1.4	14	0.5	
GP-20	100	10	0	0	1.0	0.048	180	65	15	1.7	17	0.5	

Table 3-1 The Experimental Composition and Results  
 GMA grafting onto EP system  
 (b) EP+GMA+TRIS+T101 system (in the presence of TRIS)

Code	Compositions						Processing conditions				Grafting Degree (%)	Grafting Efficiency (%)	Poly-GMA wt(%)	MFI (g/10min)
	EP (phr)	GMA (phr)	TRIS (phr)	TRIS/GMA (w/w)	T101 (phr)	T101/[GMA]+[TRIS] MR*	Temp. (°C)	Rotor speed (rpm)	Time (min)					
GR-1	100	10	1.111	1/9	0.108	0.005	190	65	15	1.1	11		0.91	
GR-2	100	10	1.111	1/9	0.216	0.01	190	65	15	1.7	17	0.1	0.72	
GR-3	100	10	1.111	1/9	0.430	0.02	190	65	15	2.1	21	0.1	0.34	
GR-4	100	10	1.111	1/9	0.860	0.04	190	65	15	2.1	21		0.11	
GR-5	100	10	2.5	2/8	0.069	0.003	190	65	15	1.6	16	0.1	0.92	
GR-6	100	10	2.5	2/8	0.114	0.005	190	65	15	2.0	20	0.1	0.51	
GR-7	100	10	2.5	2/8	0.229	0.01	190	65	15	2.0	20	0.1	0.41	
GR-8	100	10	2.5	2/8	0.457	0.02	190	65	15	2.0	20	0.1	0.16	
GR-9	100	10	2.5	2/8	0.914	0.04	190	65	15	2.5	25		0.02	
GR-10	100	10	4.286	3/7	0.073	0.003	190	65	15	1.8	18			
GR-11	100	10	4.286	3/7	0.123	0.005	190	65	15	2.0	20			
GR-12	100	10	4.286	3/7	0.246	0.01	190	65	15	1.7	17			
GR-13	100	10	4.286	3/7	0.492	0.02	190	65	15	1.9	19			
GR-14	100	10	6.667	4/6	0.081	0.003	190	65	15	1.7	17			
GR-15	100	10	6.667	4/6	0.135	0.005	190	65	15	2.2	22			
GR-16	100	10	6.667	4/6	0.270	0.01	190	65	15	1.7	17			
GR-17	100	10	1.111	1/9	0.216	0.01	190	65	2	1.1	11	0.04		
GR-18	100	10	1.111	1/9	0.216	0.01	190	65	4	1.5	15	0.3		
GR-19	100	10	1.111	1/9	0.216	0.01	190	65	10	1.6	16	0.1		

Table 3-1 The Experimental Composition and Results  
 GMA grafting onto EP system  
 (b) EP+GMA+TRIS+T101 system (in the presence of TRIS) (continued)

Code	Compositions					Processing conditions				Grafting Degree (%)	Grafting Efficiency (%)	Poly-GMA wt(%)	MFI (g/10min)
	EP (phr)	GMA (phr)	TRIS (phr)	TRIS/GMA (w/w)	T101 (phr)	T101/[GMA]+[TRIS] MR*	Temp. (°C)	Rotor speed (rpm)	Time (min)				
GR-20	100	10	2.5	2/8	0.457	0.02	190	65	2	1.7	17	0.35	
GR-21	100	10	2.5	2/8	0.457	0.02	190	65	4	2.3	23	0.2	
GR-22	100	10	2.5	2/8	0.457	0.02	190	65	10	2.1	21	0.1	
GR-23	100	6	0.667	1/9	0.065	0.005	190	65	15	0.6	10		
GR-24	100	6	0.667	1/9	0.129	0.01	190	65	15	0.6	10		
GR-25	100	6	0.667	1/9	0.258	0.02	190	65	15	0.9	15		
GR-26	100	6	0.667	1/9	0.516	0.04	190	65	15	1.0	17		
GR-27	100	6	1.5	2/8	0.069	0.005	190	65	15	0.9	15		
GR-28	100	6	1.5	2/8	0.137	0.01	190	65	15	1.1	18		
GR-29	100	6	1.5	2/8	0.274	0.02	190	65	15	1.1	18		
GR-30	100	6	1.5	2/8	0.549	0.04	190	65	15	1.2	20		
GR-31	100	18	2	1/9	0.194	0.005	190	65	15	2.3	13		
GR-32	100	18	2	1/9	0.387	0.01	190	65	15	2.3	13	0.15	1.0
GR-33	100	18	2	1/9	0.774	0.02	190	65	15	1.9	11		
GR-34	100	18	2	1/9	1.548	0.04	190	65	15	2.4	13		
GR-35	100	10	2.5	2/8	0.457	0.02	140	65	15	2.3	23	0	
GR-36	100	10	2.5	2/8	0.457	0.02	150	65	15	2.4	24	0	
GR-37	100	10	2.5	2/8	0.457	0.02	160	65	15	2.6	26	0	0.18
GR-38	100	10	2.5	2/8	0.457	0.02	170	65	15	2.3	23	0.1	
GR-39	100	10	2.5	2/8	0.457	0.02	180	65	15	2.1	21	0	

Table 3-1 The Experimental Composition and Results  
 GMA grafting onto EP system  
 (b) EP+GMA+TRIS+T101 system (in the presence of TRIS) (continued)

Code	Compositions						Processing conditions			Grafting Degree (%)	Grafting Efficiency (%)	Poly-GMA wt(%)	MFI (g/10min)
	EP (phr)	GMA (phr)	TRIS (phr)	TRIS GMA (w/w)	T101 (phr)	T101/[GMA]+[TRIS] MR*	Temp. (°C)	Rotor speed (rpm)	Time (min)				
GR-40	100	10	2.5	2/8	0	0	160	65	15	1.0	10	1.34	
GR-41	100	10	2.5	2/8	0.069	0.003	160	65	15	2.4	24	1.05	
GR-42	100	10	2.5	2/8	0.114	0.005	160	65	15	2.5	25	1.0	
GR-43	100	10	2.5	2/8	0.229	0.01	160	65	15	2.1	21	0.73	
GR-44	100	18	2	1/9	0.097	0.0025	160	65	15	3.1	17	1.2	
GR-45	100	18	2	1/9	0.194	0.005	160	65	15	2.8	16	0.84	

\* MR — mole ratio of peroxide to monomer and comonomer

Table 3-1 The Experimental Composition and Results  
 GMA grafting onto EP system  
 (c) EP+GMA+T29B90 system (in the absence of TRIS)

Code	Compositions						Processing conditions			Grafting Degree (%)	Grafting Efficiency (%)	Poly-GMA wt(%)	MFI (g/10min)
	EP (phr)	GMA (phr)	TRIS (phr)	TRIS GMA (w/w)	T29B 90 (phr)	T101/[GMA]+[TRIS] MR*	Temp. (°C)	Rotor speed (rpm)	Time (min)				
BP-1	100	6	0	0	0.5	0.033	115	65	15	0	0	0.92	
BP-2	100	10	0	0	0.5	0.020	115	65	15	3.9	39	0.72	
BP-3	100	15	0	0	0.5	0.013	115	65	15	6.0	40	0.86	



Table 3-2 The Experimental Composition and Results

GMA grafting onto EPDM system (in the absence and presence of TRIS)

Code	Compositions					Processing conditions			Grafting Degree (%)	Grafting Efficiency (%)	Poly-GMA wt(%)	Gel (%)
	EPDM (phr)	GMA (phr)	TRIS (phr)	TRIS/GMA (w/w)	T101 (phr)	T101/[GMA]+[TRIS] MR*	Temp. (°C)	Rotor speed (rpm)				
DM-1	100	10	0	0	0	0	180	65	10	0	~0	2.1
DM-2	100	10	0	0	0.3	0.015	180	65	10	0.4	~0	2.2
DM-3	100	10	0	0	0.6	0.029	180	65	10	0.6	~0	10.6
DM-4	100	10	0	0	0.8	0.039	180	65	10	1.2	~0	18
DM-5	100	10	0	0	1.0	0.049	180	65	10	1.7	~0	36
DM-6	100	10	1.111	1/9	0.054	0.0025	180	65	10	1.1	~0	2
DM-7	100	10	1.111	1/9	0.108	0.005	180	65	10	1.3	~0	2.3
DM-8	100	10	1.111	1/9	0.216	0.01	180	65	10	1.7	~0	7.5
DM-9	100	10	1.111	1/9	0.430	0.02	180	65	10	2.0	~0	19
DM-10	100	10	2.5	2/8	0.058	0.0025	180	65	10	2.5	~0	6.1
DM-11	100	10	2.5	2/8	0.114	0.005	180	65	10	3.0	~0	2
DM-12	100	10	2.5	2/8	0.229	0.01	180	65	10	3.6	~0	69.5

\* MR — mole ratio of peroxide to monomer and comonomer

Table 3-3 The Experimental Composition and Results

GMA grafting onto EPDM/PP system (in the absence and presence of TRIS)

Code	Compositions						Processing conditions				Grafting Degree (%)	Grafting Efficiency (%)	Gel (%)	
	EPDM (phr)	PP (phr)	GMA (phr)	TRIS (phr)	TRIS GMA (w/w)	T101 (phr)	T101/[GMA]+[TRIS] MR*	Temp. (°C)	Rotor speed (rpm)	Time (min)				
PM-0	75	25	0	0	0	0	0	0	180	65	10	0		0
PM-1	75	25	10	0	0	0.3	0.015		180	65	10	0.7	7	0
PM-2	75	25	10	0	0	0.6	0.029		180	65	10	1.5	15	0
PM-3	75	25	10	0	0	1	0.049		180	65	10	1.6	16	11
PM-4	75	25	10	1.111	1/9	0.054	0.0025		180	65	10	2.2	22	0
PM-5	75	25	10	1.111	1/9	0.108	0.005		180	65	10	2.2	22	0
PM-6	75	25	10	1.111	1/9	0.216	0.01		180	65	10	2.9	29	2.4
PM-7	75	25	10	1.111	1/9	0.430	0.02		180	65	10	2.45	25	5.2
PM-8	75	25	10	2.5	2/8	0.057	0.0025		180	65	10	3.1	31	0
PM-9	75	25	10	2.5	2/8	0.114	0.005		180	65	10	3.1	31	6.4
PM-10	75	25	10	2.5	2/8	0.229	0.01		180	65	10	3.4	34	5.5
PM-11	75	25	10	2.5	2/8	0.457	0.02		180	65	10	3.1	31	46

\* MR — mole ratio of peroxide to monomer and comonomer

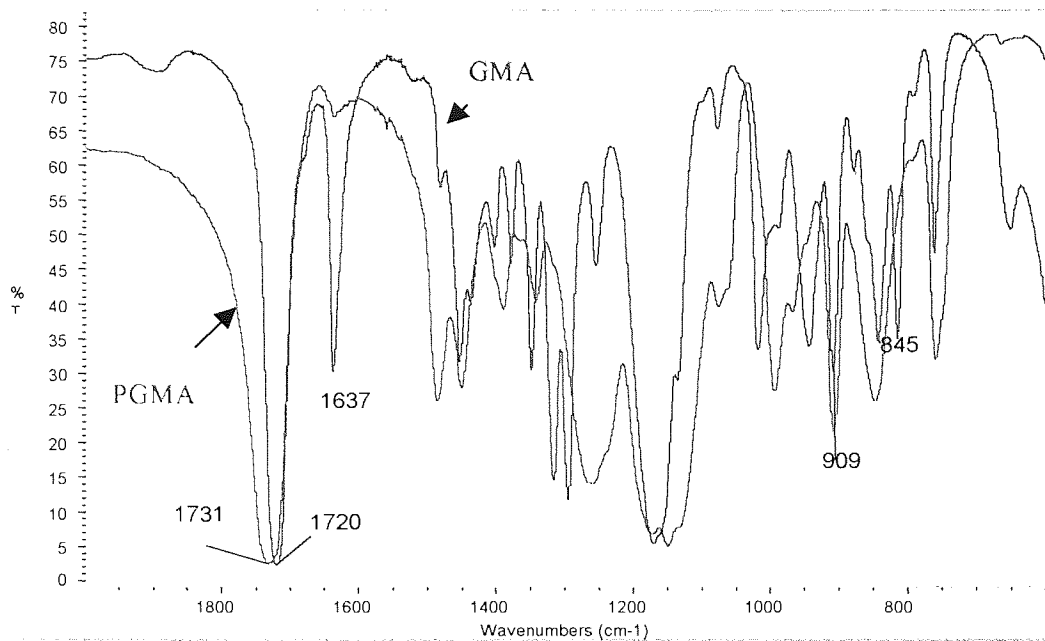


Figure 3-1 Comparison of FTIR spectra of polyGMA using KBr disc (red line) with GMA (black line)

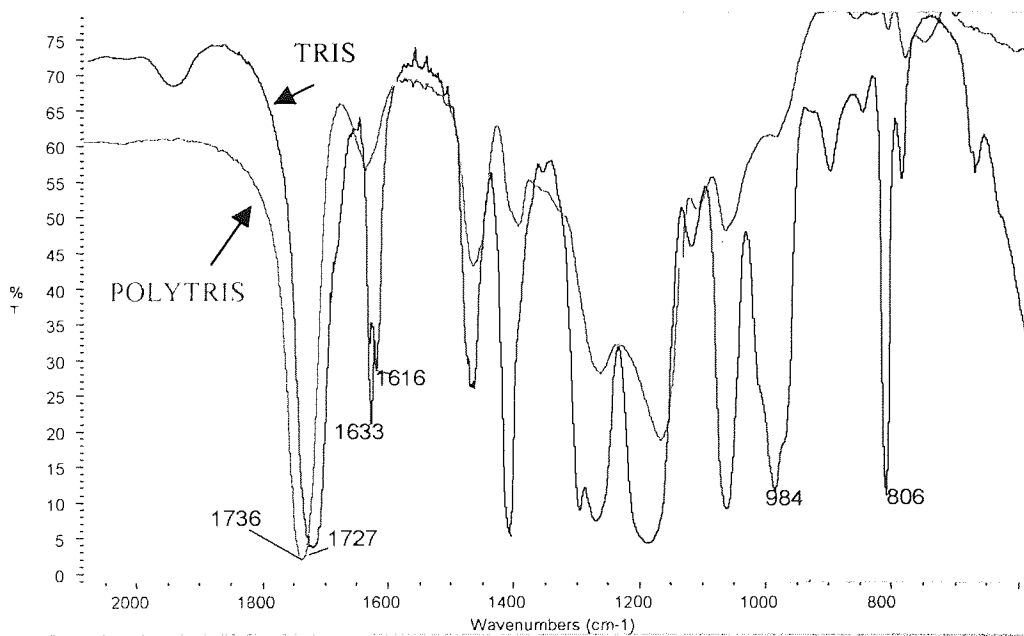


Figure 3-2 Comparison of FTIR spectra of polyTRIS using KBr disc (red line) with TRIS (black line)

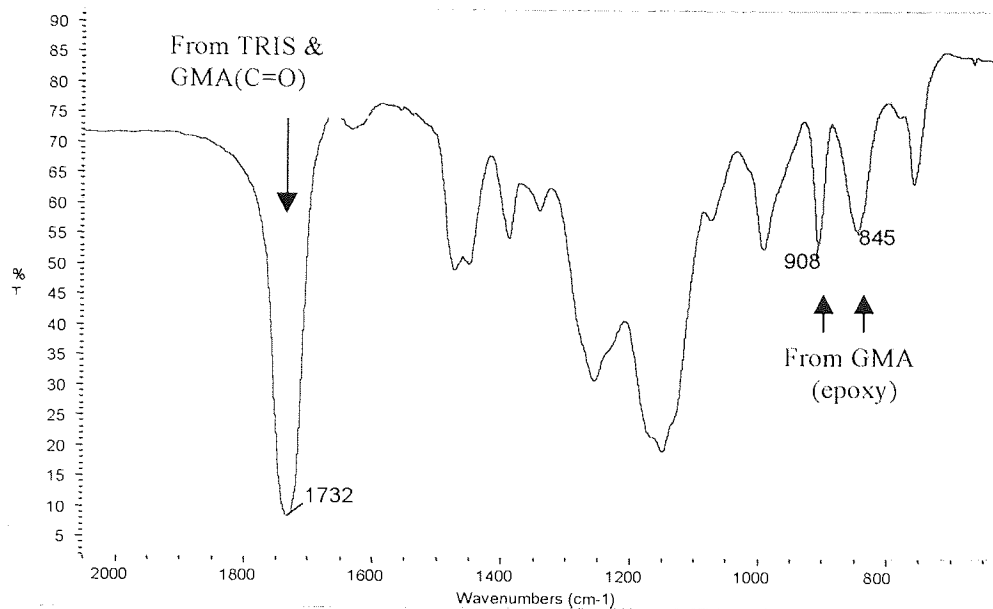


Figure 3-3 FTIR spectrum of copolymer GMA-co-TRIS using KBr disc

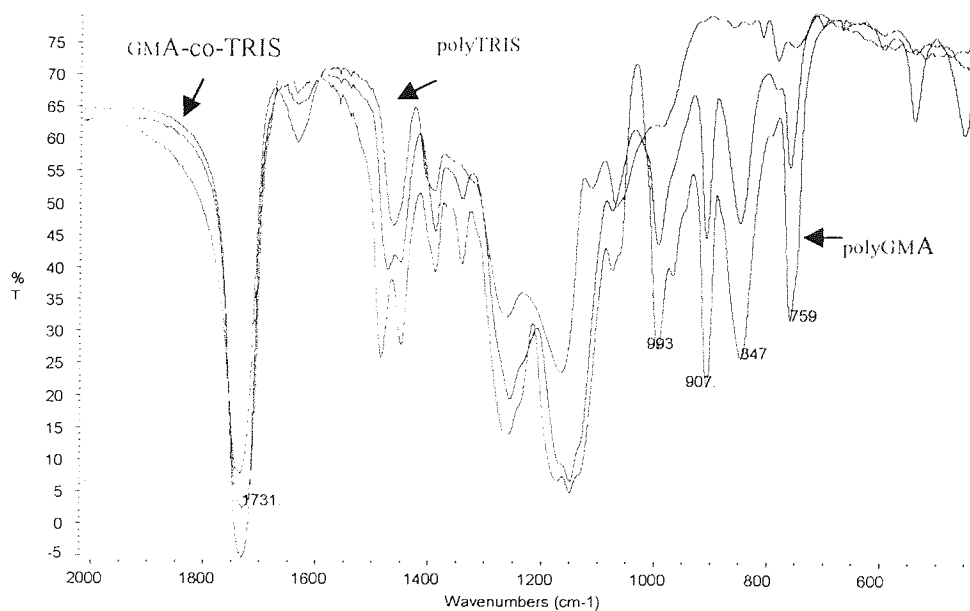


Figure 3-4 Comparison of spectra of polyGMA(red line), polyTRIS (green line), and PolyGMA-co-TRIS (blue line)

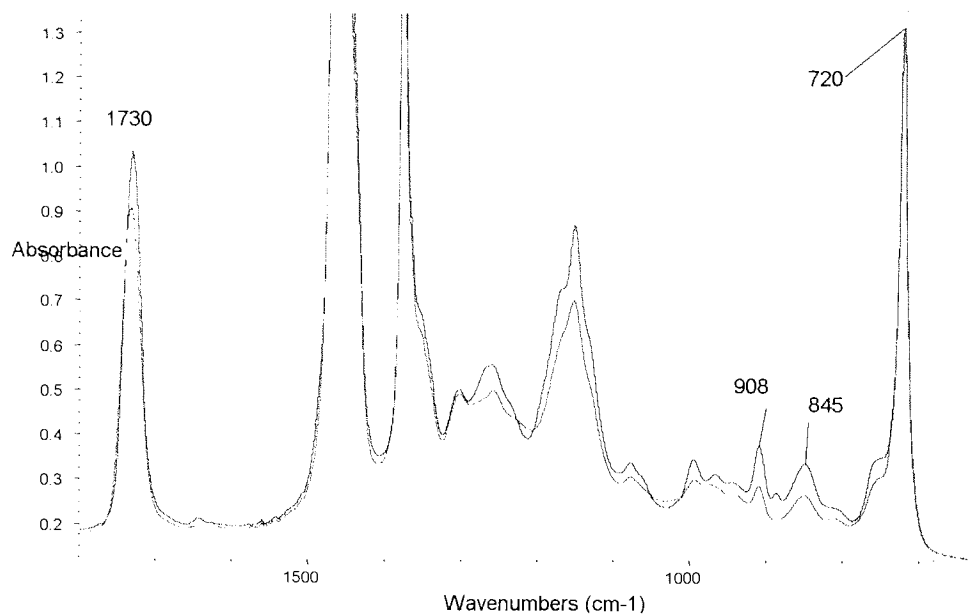


Figure 3-5 Spectra of EP-g-GMA(without TRIS) pressed films with different purification methods (red line: purified in acetone, blue line: purified in methanol) (sample GP-10: EP 100phr, GMA 18phr, T101 1.5phr, temp. 190°C, mixing time 15min, speed 65rpm)

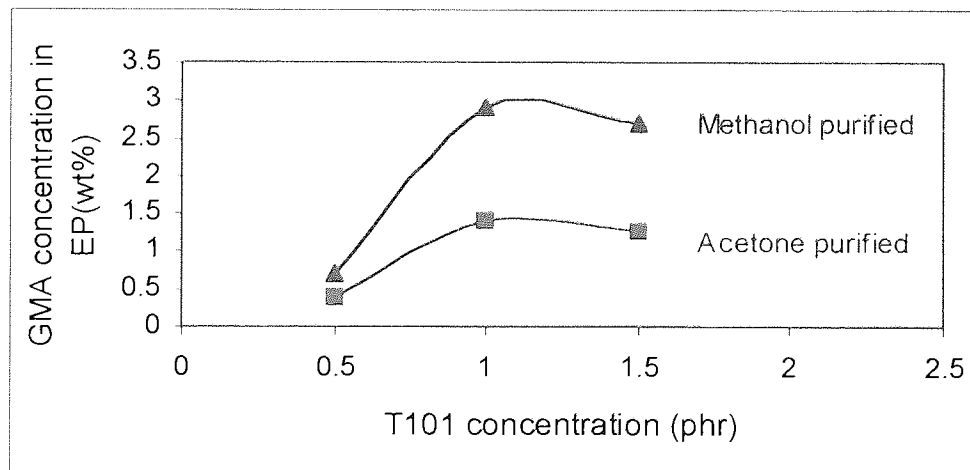


Figure 3-6 Variation of GMA concentration in polymer with different purification methods without TRIS (EP 100 phr, GMA 12 phr, temp. 190°C, mixing time 15min, speed 65rpm)

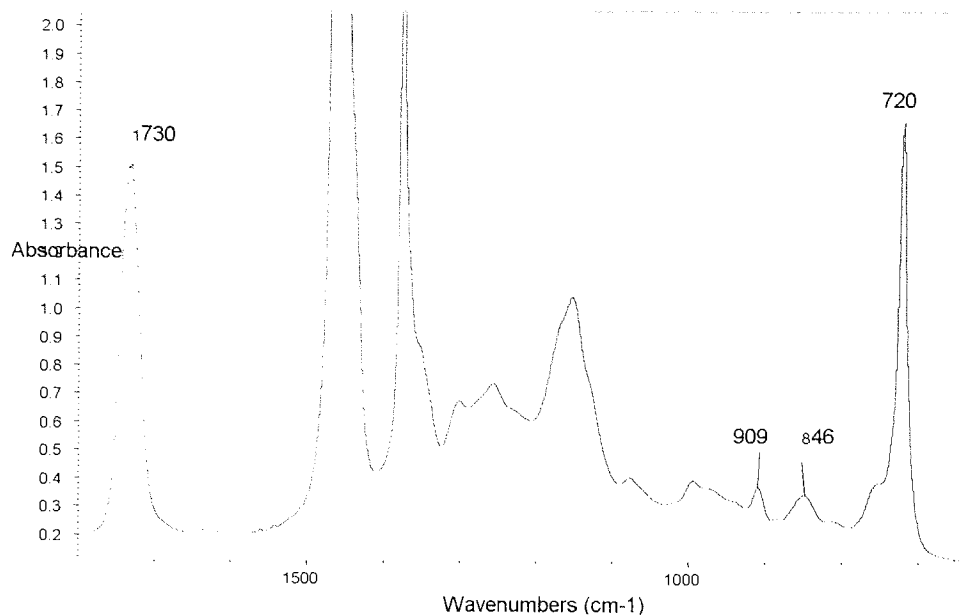
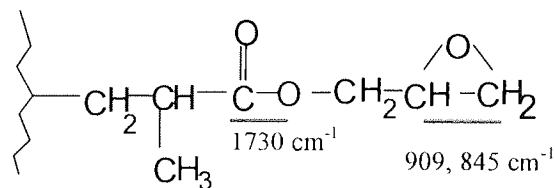
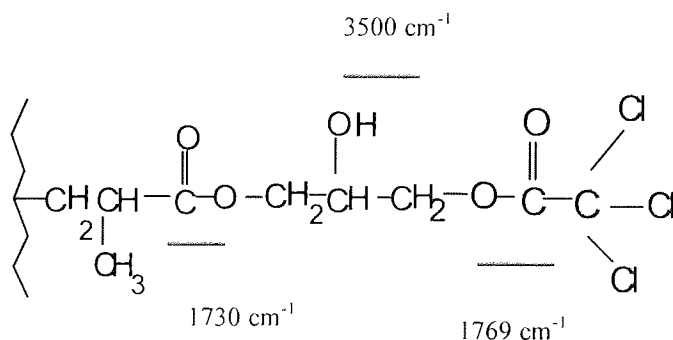


Figure 3-7 Spectrum of EP-g-GMA(with TRIS) pressed films ( purified in acetone) (sample GR-8: EP 100phr, GMA 10phr, TRIS 2.5phr, T101 0.45phr, temp. 190°C, mixing time 15min, speed 65rpm)



(a) Structure of GMA grafted EP



(b) Structure of ring open product

Figure 3-8 Structures of GMA grafted EP before and after the ring open reaction with trichloroacetic acid (a) structure of GMA grafted EP, (b) structure of ring open product after the ring open reaction with trichloroacetic acid

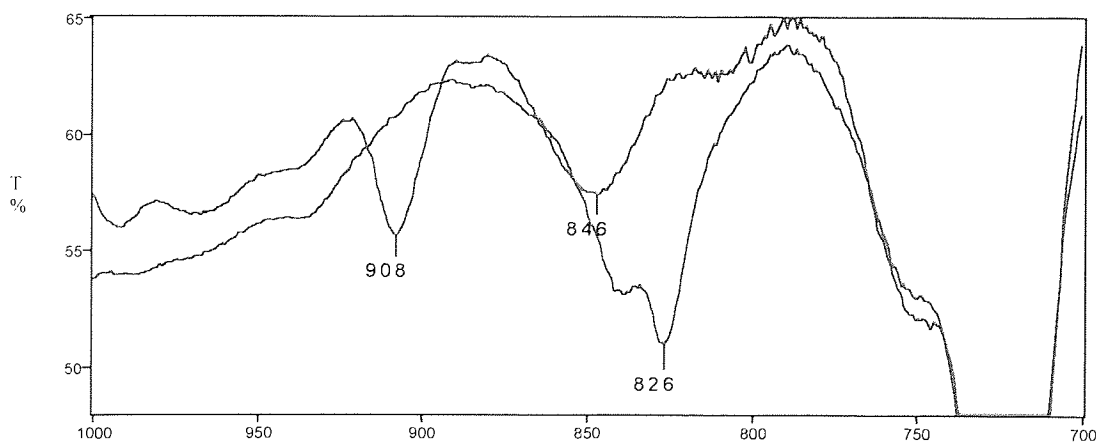
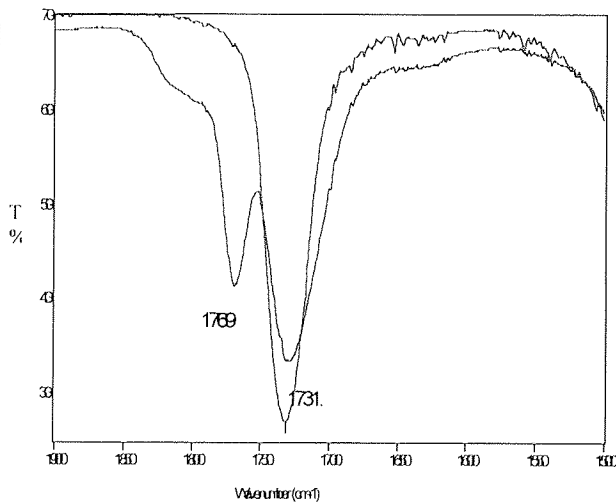
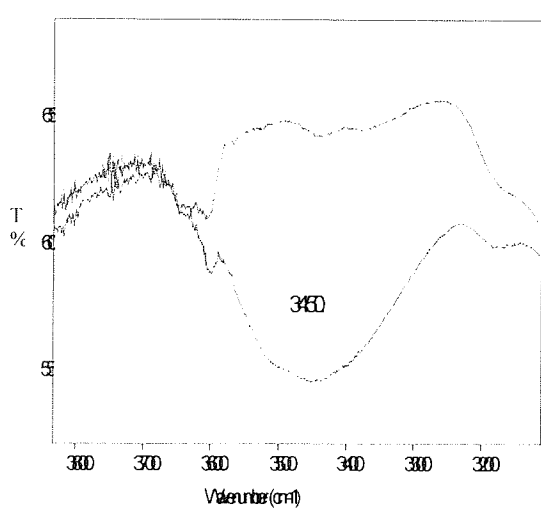
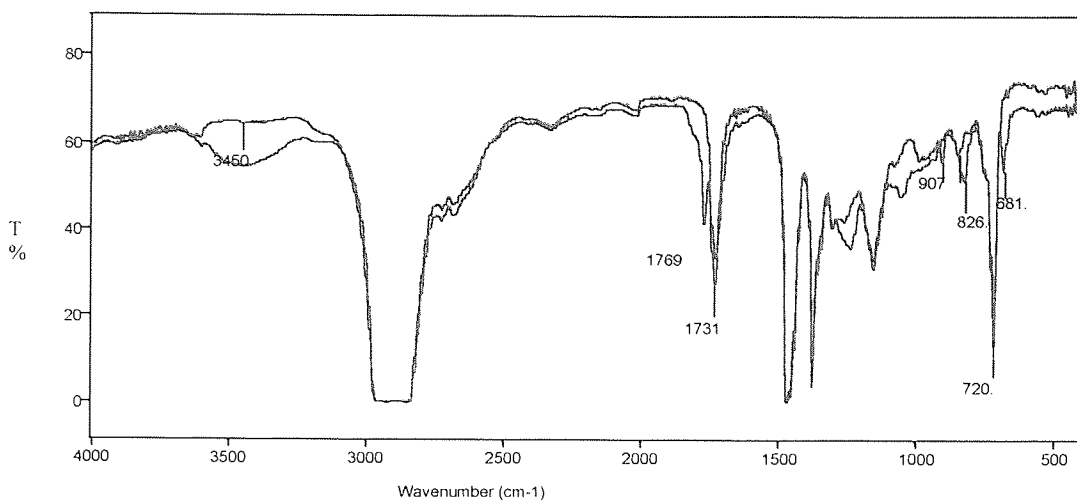


Figure 3-9 Comparison of spectra before and after the reaction of EP-g-GMA with trichloroacetic acid (red line: before reaction i.e. Film X; purple line: after reaction, i.e. Film Y)

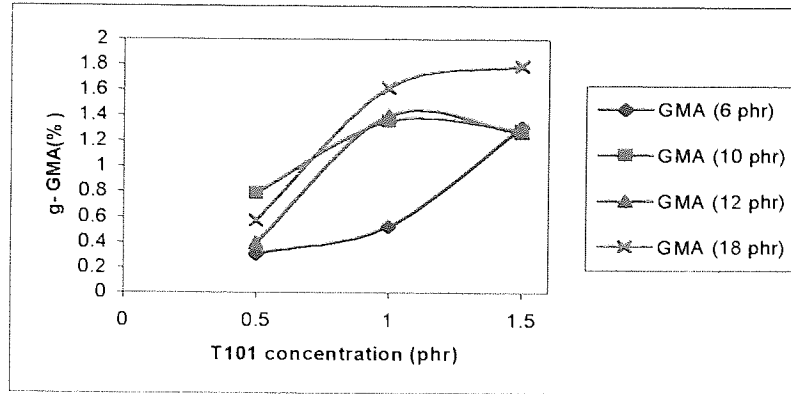
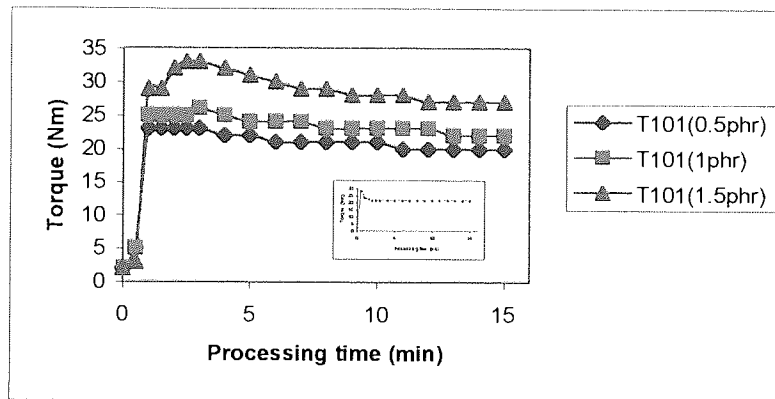
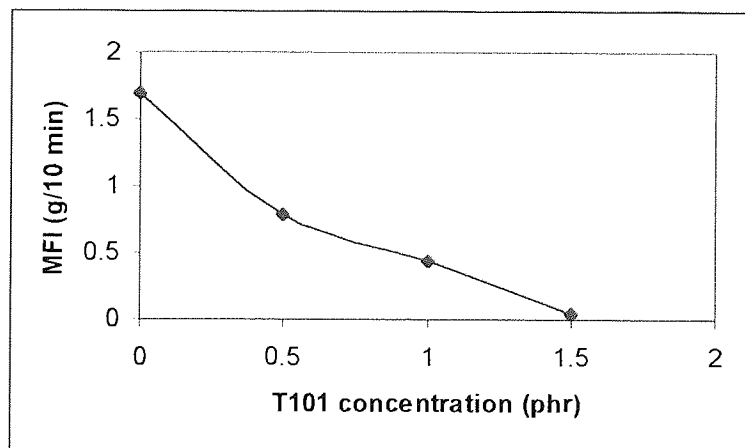


Figure 3-10 Effect of T101 concentration on grafting degree on EP with different amounts of GMA



(a) Torque-time curves (Inset: EP alone processed)



(b) Variation of MFI with different T101 concentrations

Figure 3-11 Effect of peroxide concentration on alteration of rheological properties (EP 100 phr, GMA 18 phr, Temp. 190°C, Rotor speed 65 rpm, time 15min)



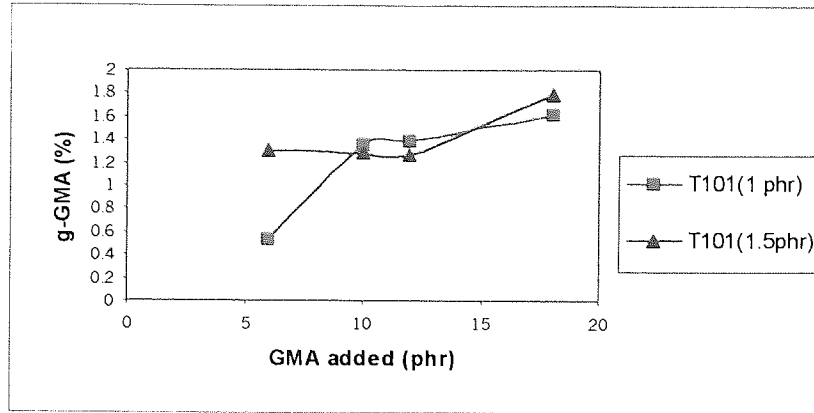


Figure 3-12 Effect of GMA concentration on grafting degree with different level of T101

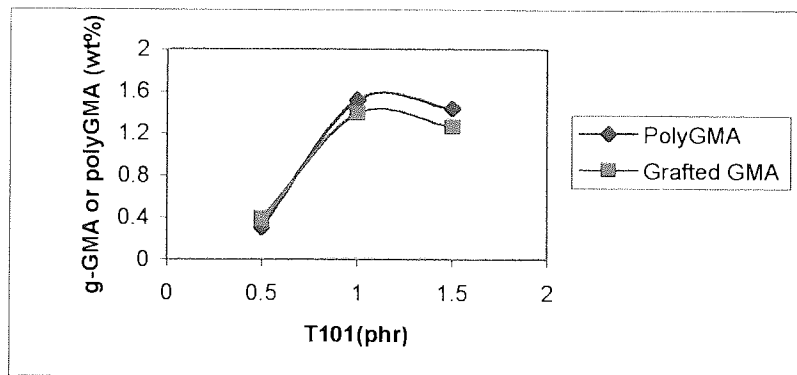


Figure 3-13 Effect of T101 concentration on amounts of grafted GMA and polyGMA formed in the melt grafting (EP 100 phr, GMA 12 phr, Temp. 190°C, rotor speed 65 rpm, time 15min)

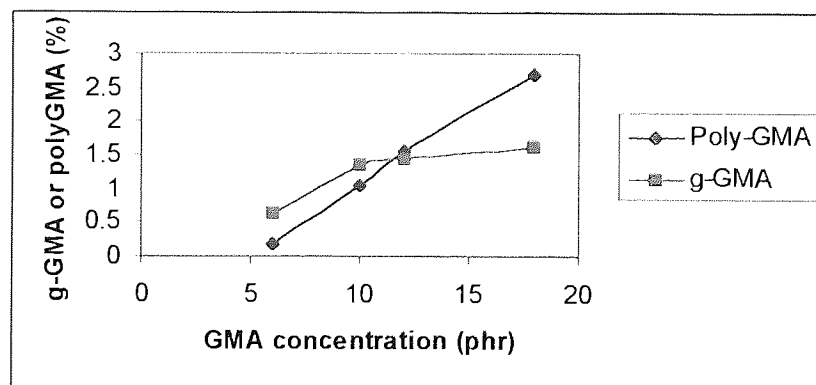


Figure 3-14 Effect of GMA concentration on amounts of grafted GMA and polyGMA formed in the melt grafting (EP 100 phr, T101 1 phr, Temp. 190°C, rotor speed 65 rpm, time 15min)

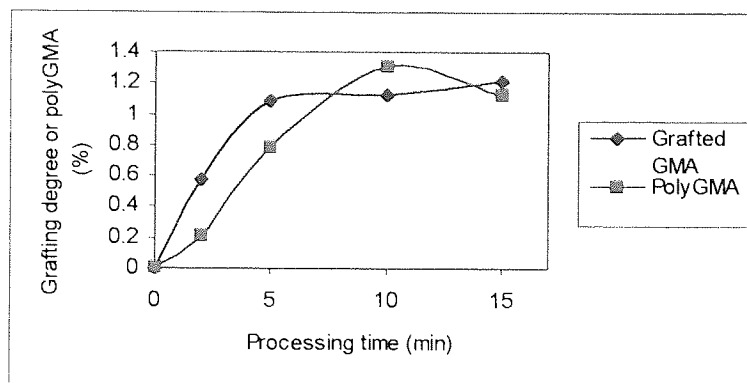


Figure 3-15 Effect of processing time on grafting degree (EP 100 phr, GMA 10 phr, T101 1.0 phr Temp. 190°C, Rotor speed 65 rpm)

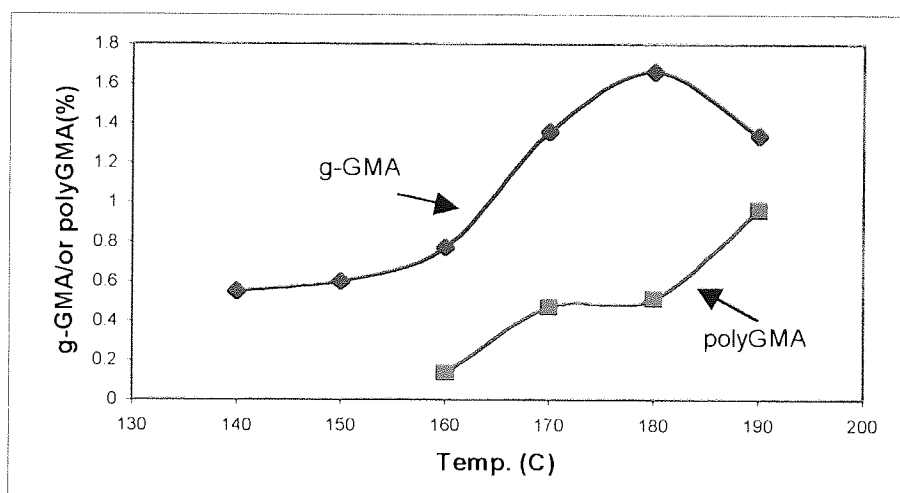


Figure 3-16 The effect of processing temperature on the grafting degree in GMA+T101 system (composition: PE 100phr, GMA 10phr, T101 1phr. Condition: speed 65rpm processing time 15 min)

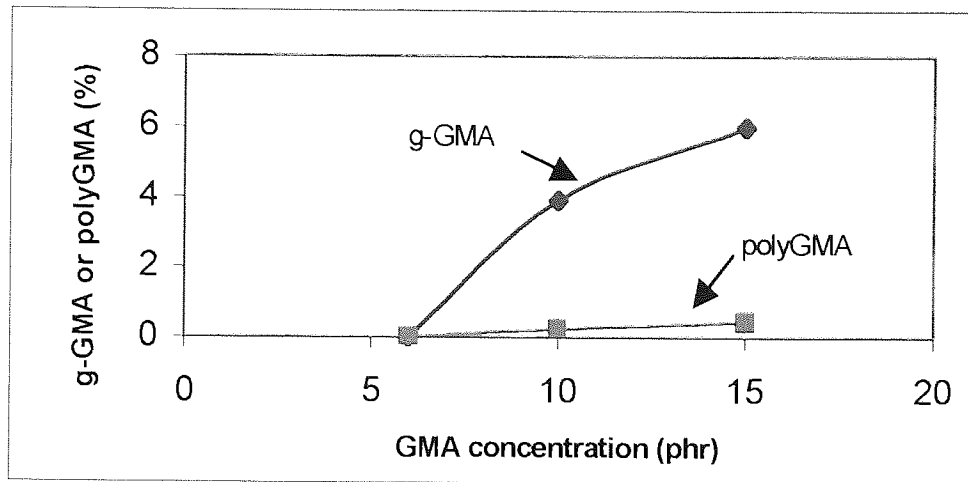


Figure 3-17 The effect of GMA concentration on the grafting degree in GMA+T29B90 system at low temperature

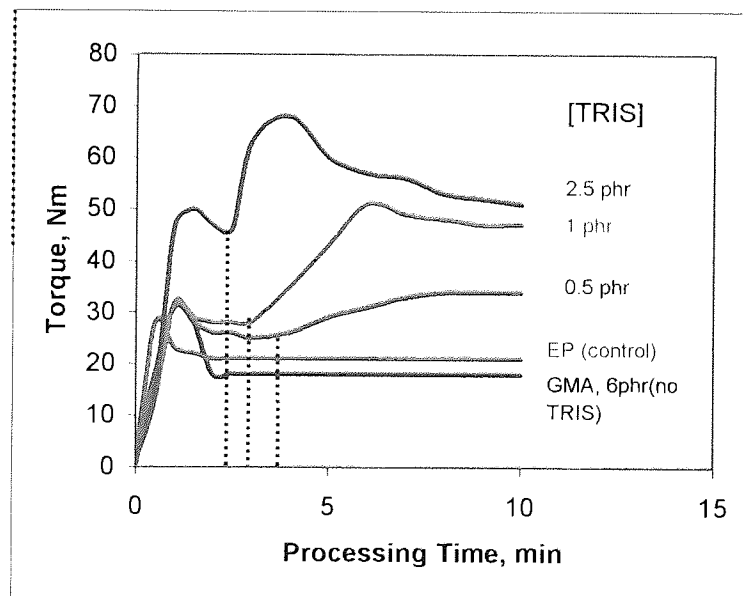


Figure 3-18 Variation of torque with processing time for shear-initiated reaction of TRIS in EP (with different level of TRIS) and curves of GMA alone (6phr) processed with EP and that of EP alone as control

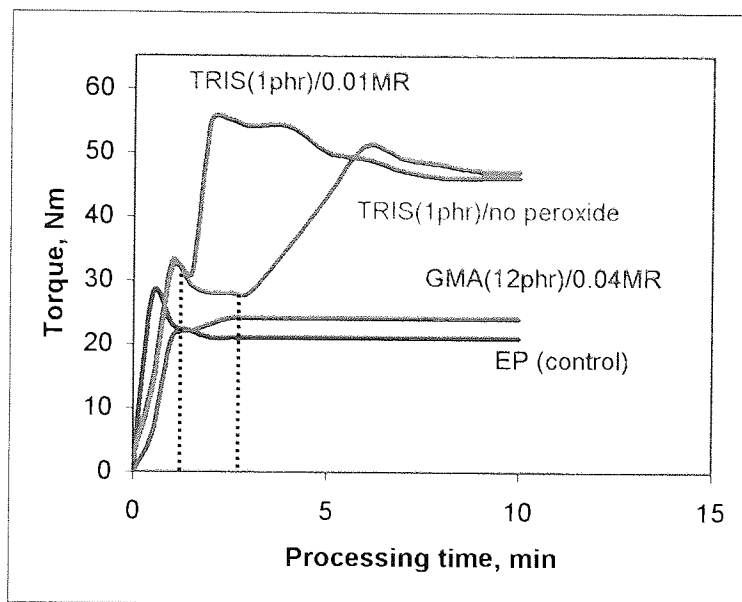


Figure 3-19 Variation of torque with processing time for peroxide-initiated reaction of TRIS in EP (T101/TRIS mole ratio=0.01 with TRIS=1phr) and curves of GMA (6phr) (T101/GMA mole ratio=0.04) processed with EP and that of EP alone as control

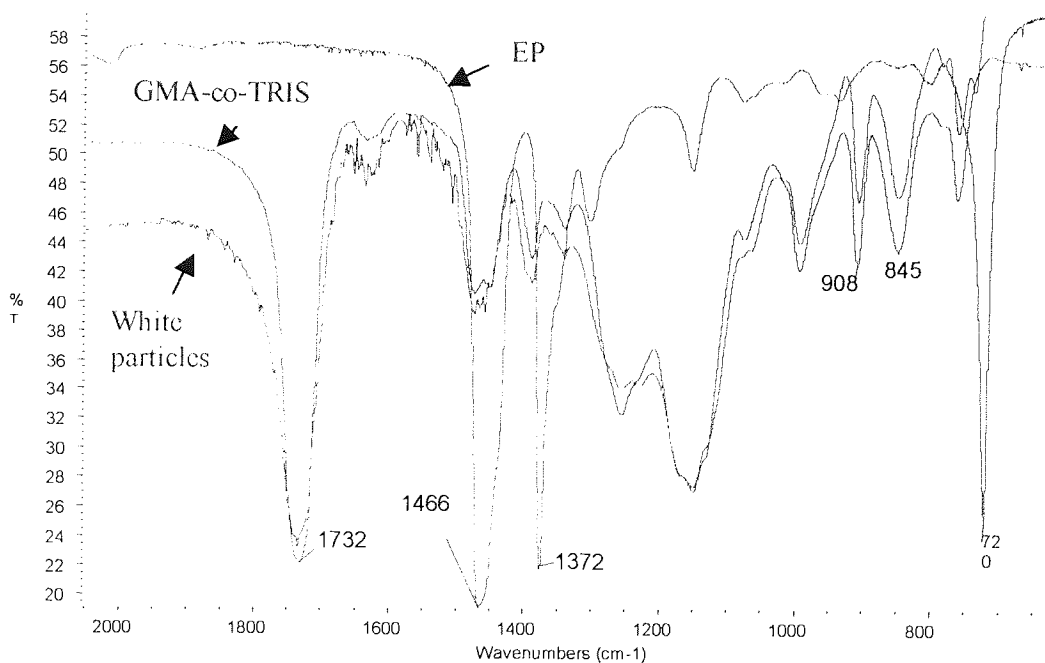


Figure 3-20 Comparison of FTIR spectra of white particle collected from the modified polymer (red line), GMA-co- TRIS (blue line) and EP (green line)

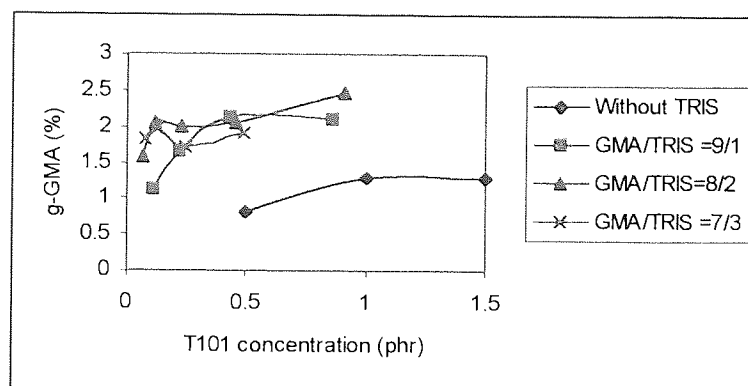


Figure 3-21 Effect of T101 concentration on the grafting degree (EP 100 phr, GMA 10 phr, Temp. 190°C, rotor speed 65 rpm, processing time 15min)

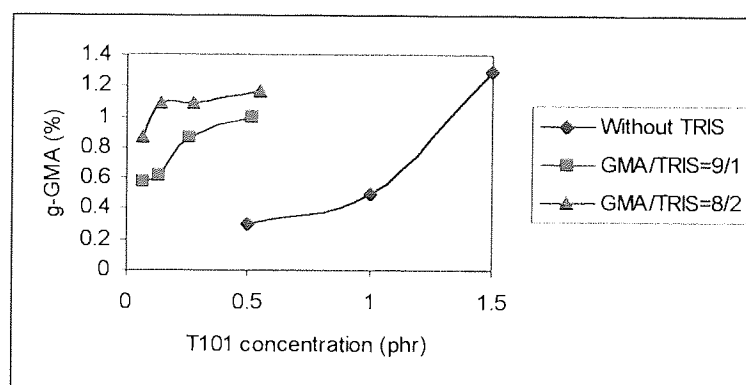
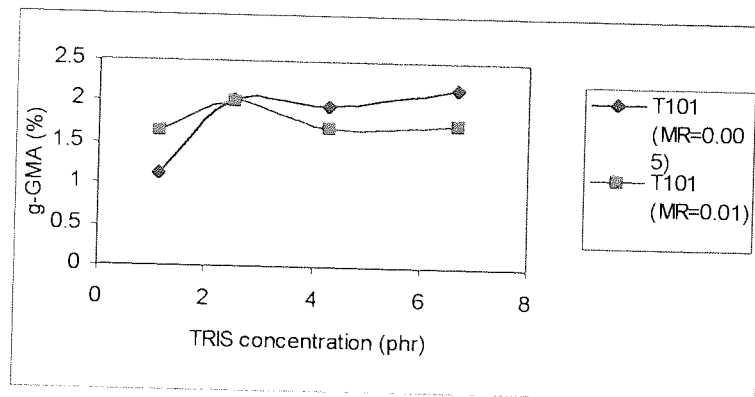
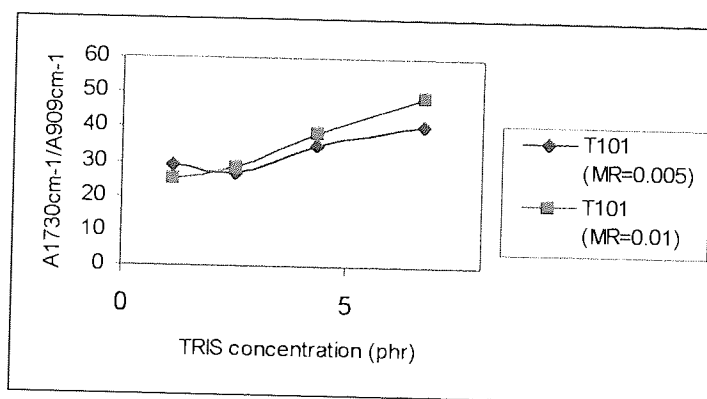


Figure 3-22 Effect of T101 concentration on the grafting degree (EP 100 phr, GMA 6 phr, Temp. 190°C, rotor speed 65 rpm, processing time 15min)

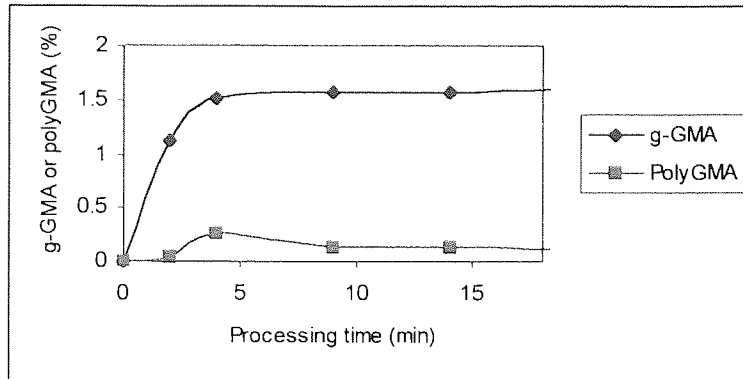


(a) Effect of TRIS concentration on the grafting degree (EP 100 phr, GMA 10 phr, Temp. 190°C, rotor speed 65 rpm, processing time 15min)

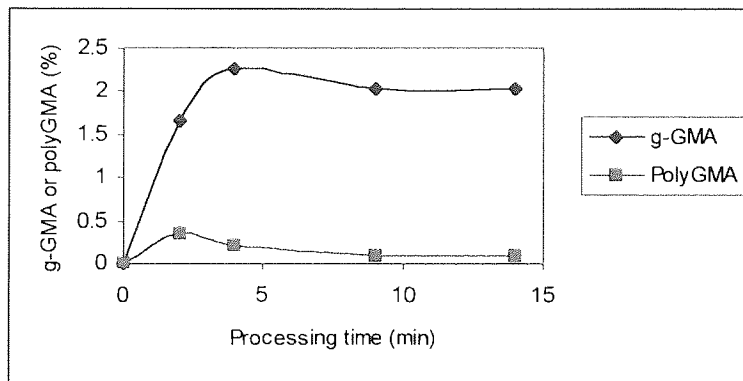


(b) Effect of TRIS concentration on area ratio  $A_{1730\text{cm}^{-1}}/A_{909\text{cm}^{-1}}$

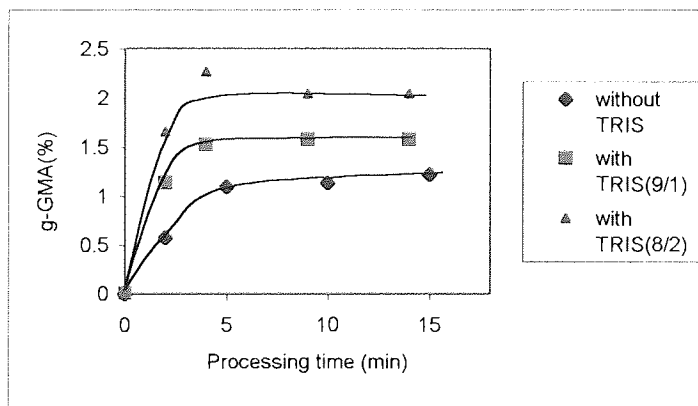
Figure 3-23 Effect of TRIS concentration on grafting degree and TRIS grafting (EP 100 phr, GMA 10 phr, Temp. 190°C, rotor speed 65 rpm, processing time 15min)



( a ) GMA/TRIS=9/1, T101=0.43 phr



( b ) GMA/TRIS=8/2 T101=0.46 phr



( C ) Comparison of grafting degree with and without TRIS

Figure 3-24 Effect of processing time on grafting degree (EP 100 phr, GMA 10 phr, Temp. 190°C, Rotor speed 65 rpm)

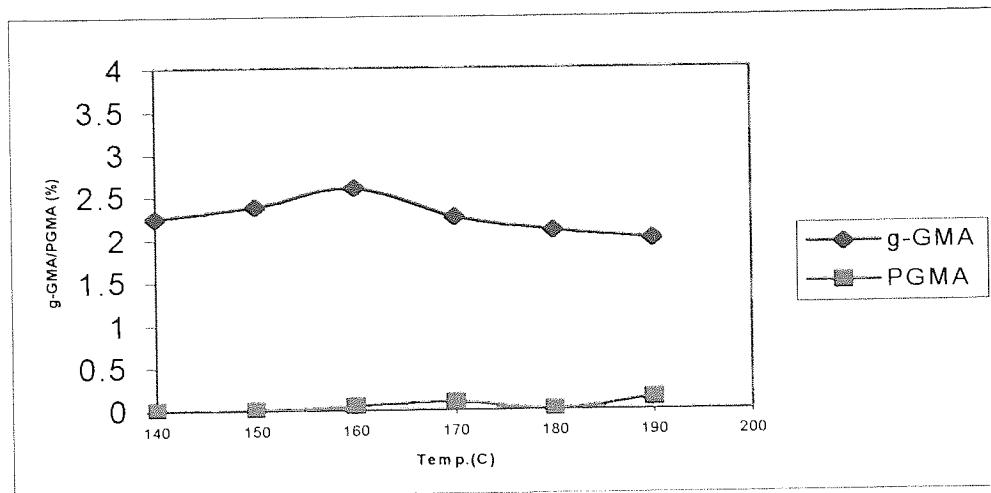


Figure 3-25 The effect of processing temperature on the grafting degree in the presence of TRIS (composition: EP 100phr, GMA10phr, TRIS 2.5 phr and T101 0.457 phr (TRIS/GMA =2/8 and molar ratio of [T101]/[GMA]+[TRIS]=0.02). Condition: speed 65rpm processing time 15 min)

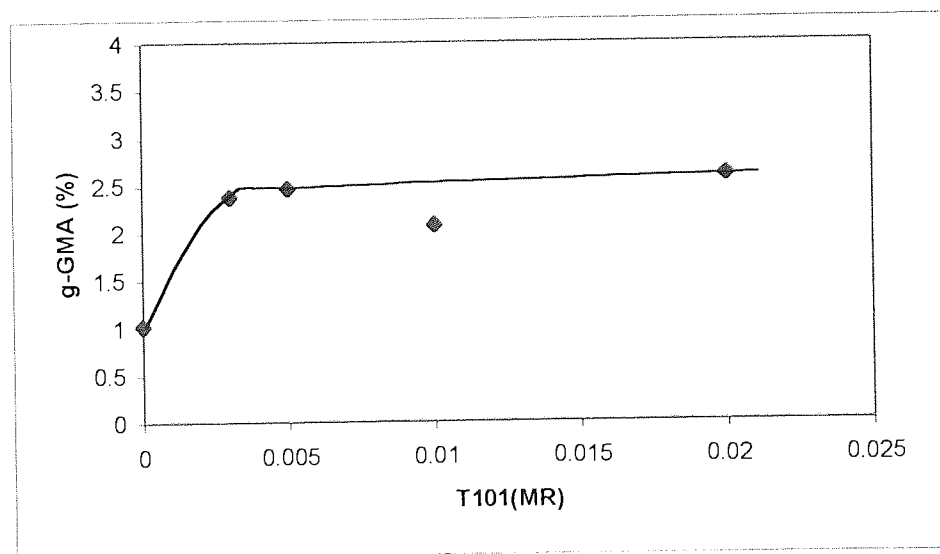


Figure 3-26 The effect of T101 concentration on the grafting degree in the presence of TRIS (Composition: PE 100phr, GMA10phr, TRIS 2.5 phr TRIS/GMA=2/8) Condition: speed 65rpm, processing temp. 160 °C, processing time 15 min)



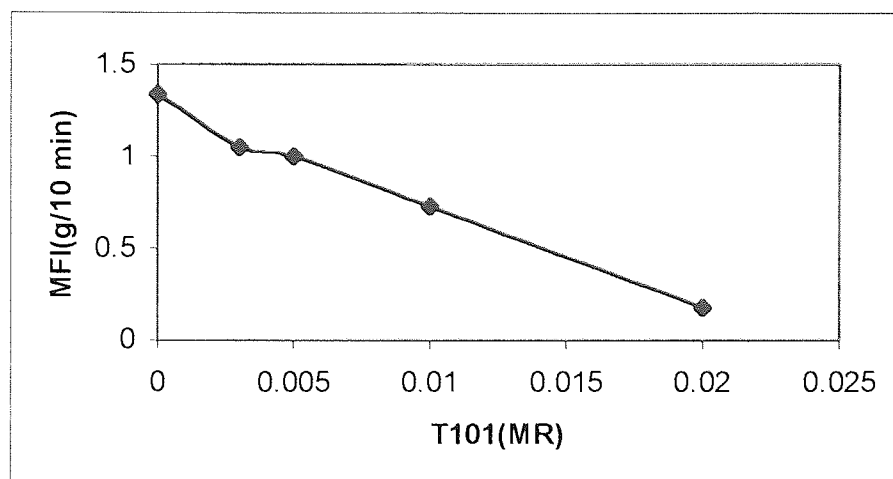


Figure 3-27 The effect of T101 concentration on MFI (Composition: EP 100phr, GMA10phr, TRIS 2.5 phr (TRIS/GMA=2/8), Condition: speed 65 rpm, processing temp. 160°C, processing time 15 min)

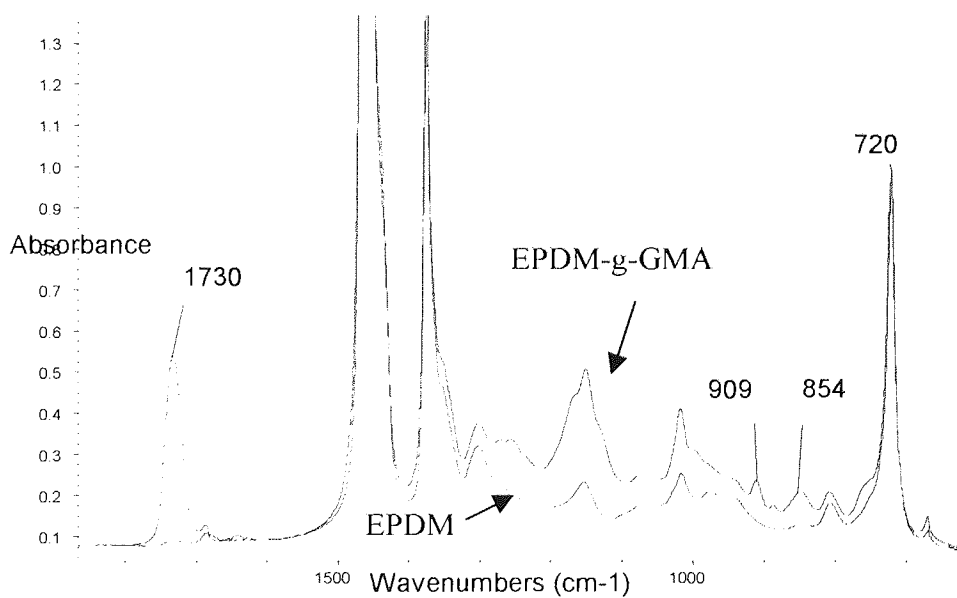


Figure 3-28 FTIR spectra of purified EPDM-g-GMA sample and unmodified EPDM

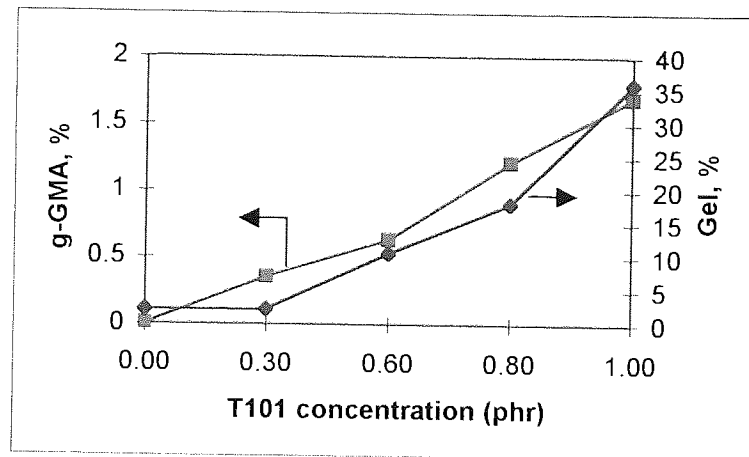


Figure 3-29 Effect of peroxide concentration on grafting degree and gel of GMA grafted EPDM in the absence of TRIS (EPDM, 100 phr; GMA, 10 phr)

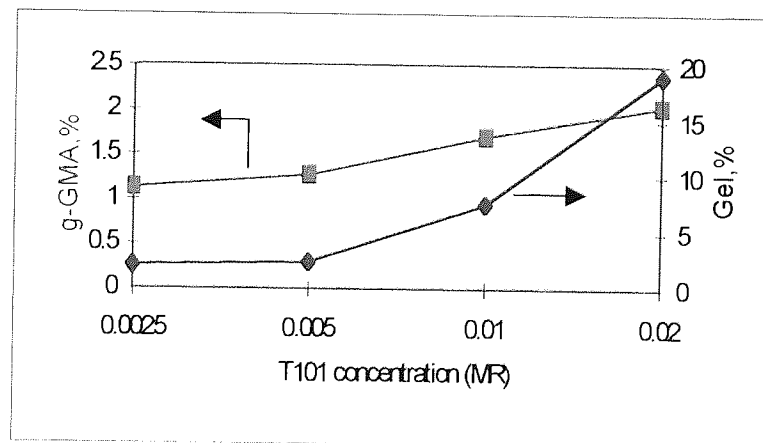


Figure 3-30 Effect of peroxide concentration on grafting degree and gel of GMA grafted EPDM in the presence of TRIS (EPDM, 100 phr; GMA, 10 phr ; TRIS, 1.11phr; GMA/TRIS=9/1)

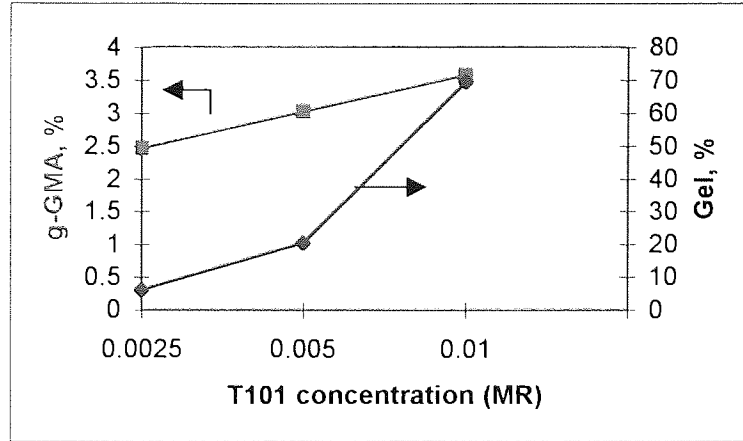


Figure 3-31 Effect of peroxide concentration on grafting degree and gel of GMA grafted EPDM in the presence of TRIS (EPDM, 100 phr; GMA, 10 phr; TRIS, 2.5 phr; GMA/TRIS=8/2)

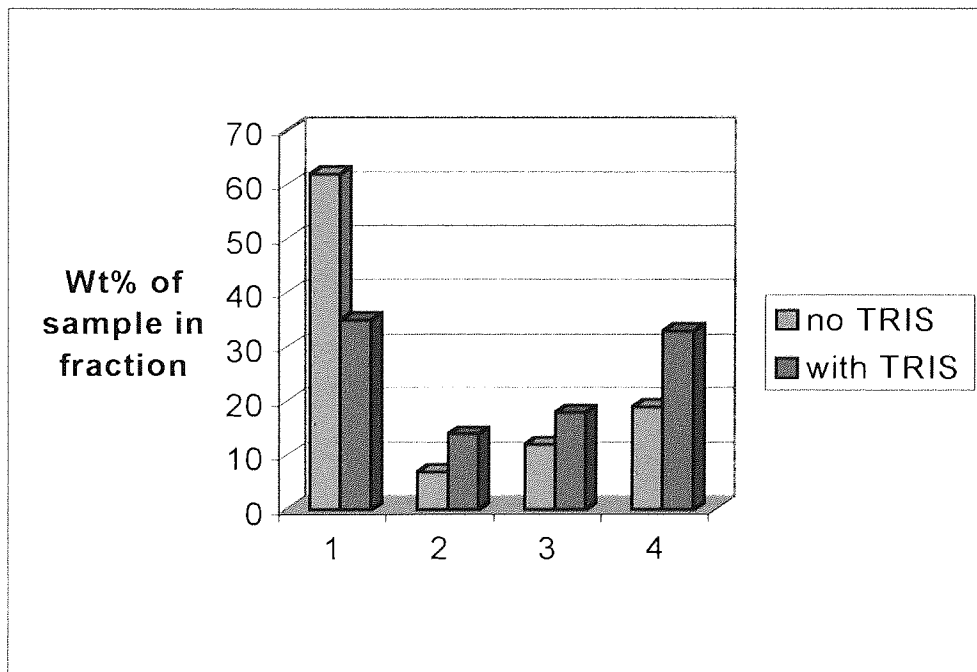


Figure 3-32 Comparison of weight percentage of separated fractions of two samples of EPDM-g-GMA which were prepared either in the presence of TRIS or in the absence of TRIS by differential solvent extraction (1-hexane soluble fraction; 2-toluene soluble fraction; 3-xylene soluble fraction; 4-insoluble gel)

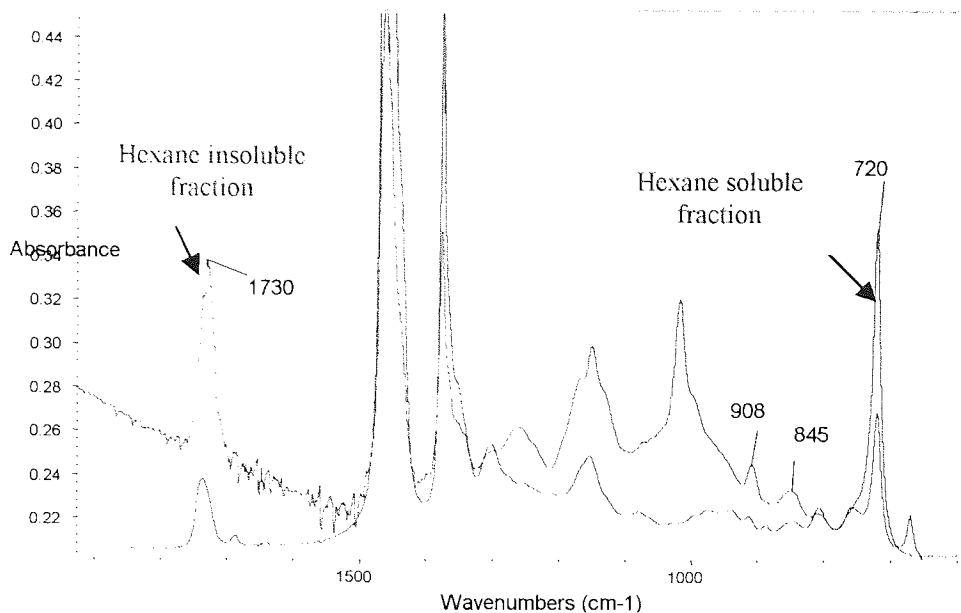


Figure 3-33 Comparison of FTIR spectra recorded from the hexane soluble fraction (see FTIR E in Scheme 3-4) and hexane insoluble fraction of EPDM-g-GMA<sub>101</sub> sample DM-3 (see FTIR D in Scheme 3-4)

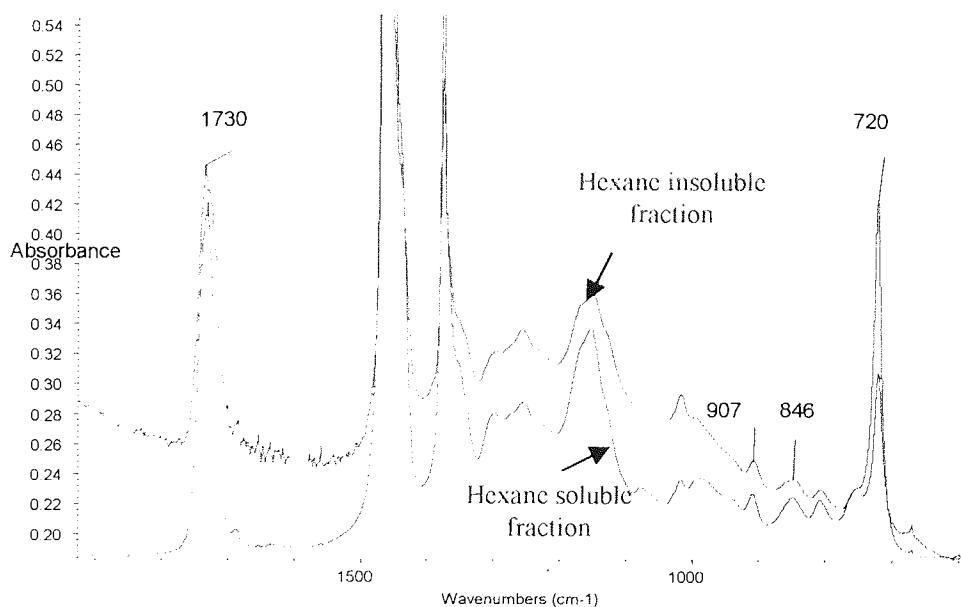


Figure 3-34 Comparison of FTIR spectra recorded from the hexane soluble fraction (see FTIR E in Scheme 3-4) and hexane insoluble fraction of EPDM-g-GMA<sub>101</sub> sample DM-9 (see FTIR D in Scheme 3-4)

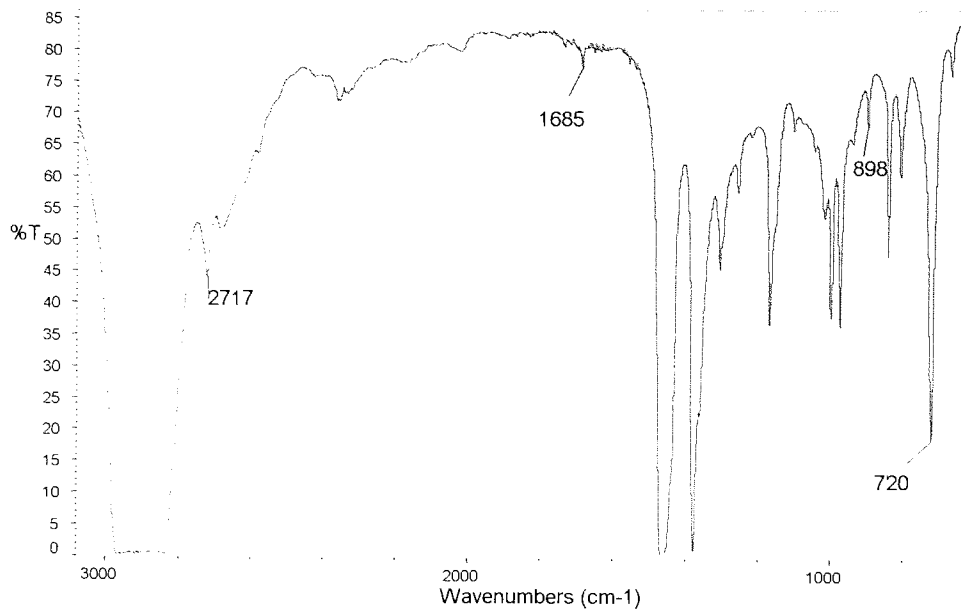


Figure 3-35 FTIR of the blend of EPDM/PP (weight ratio=75/25) ( conditions: temperature:180°C; speed: 65rpm; time: 10 min)

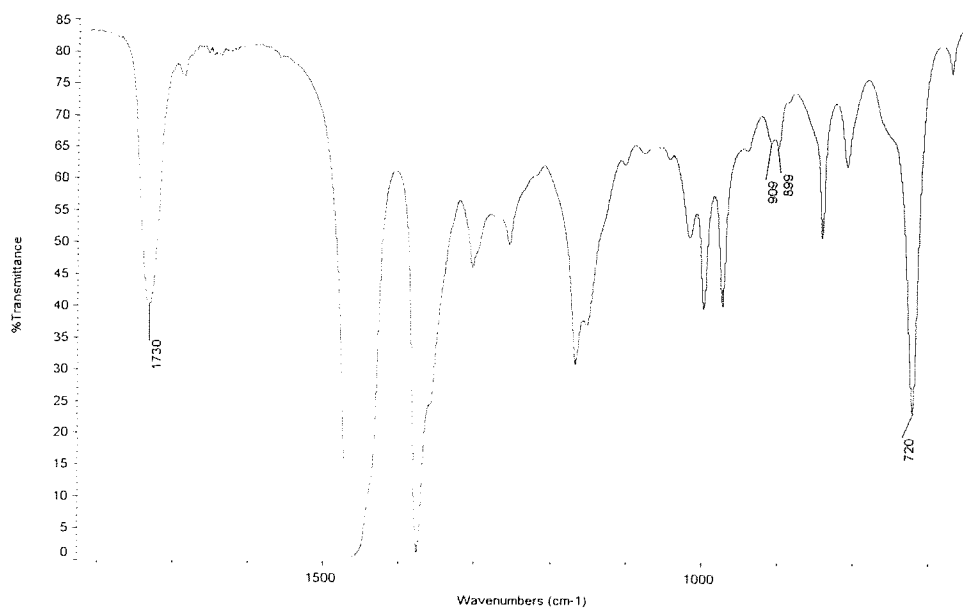


Figure 3-36 FTIR of EPDM/PP-g-GMA (EPDM: 75 phr; PP: 25phr; GMA: 10 phr; T101: 0.6phr) ( conditions: temperature:180°C; speed: 65rpm; time: 10 min)

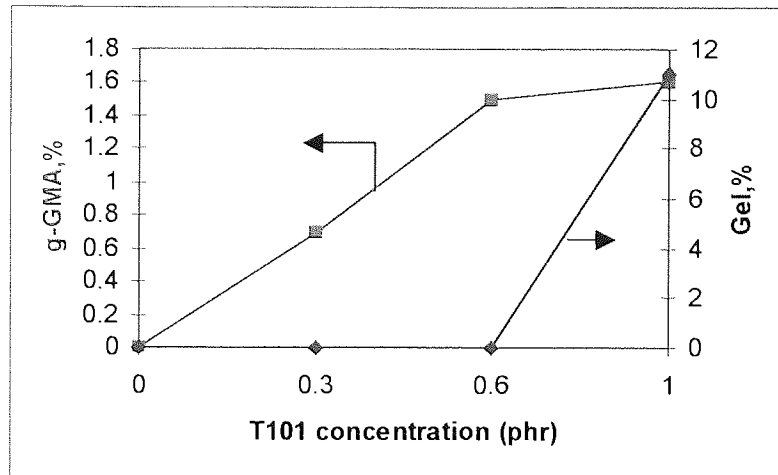


Figure 3-37 Effect of peroxide concentration on grafting degree and gel of GMA grafted EPDM/PP in the absence of TRIS (EPDM, 75 phr; PP, 25phr; GMA, 10 phr)

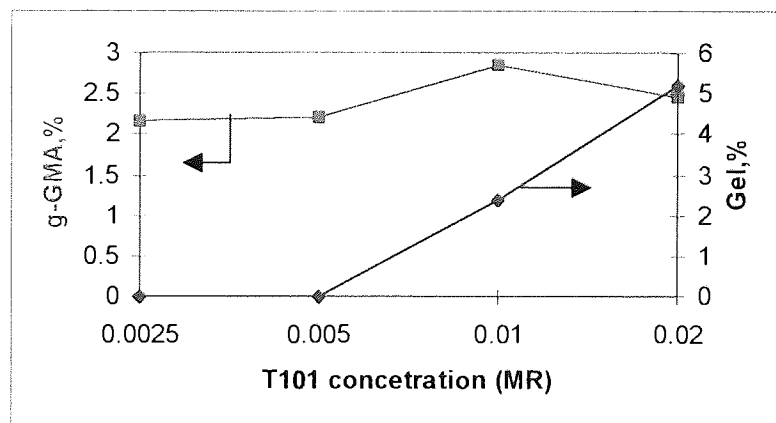


Figure 3-38 Effect of peroxide concentration on grafting degree and gel of GMA grafted EPDM/PP in the presence of TRIS (EPDM, 75 phr; PP, 25phr; GMA, 10 phr ; TRIS, 1.11phr; GMA/TRIS=9/1)

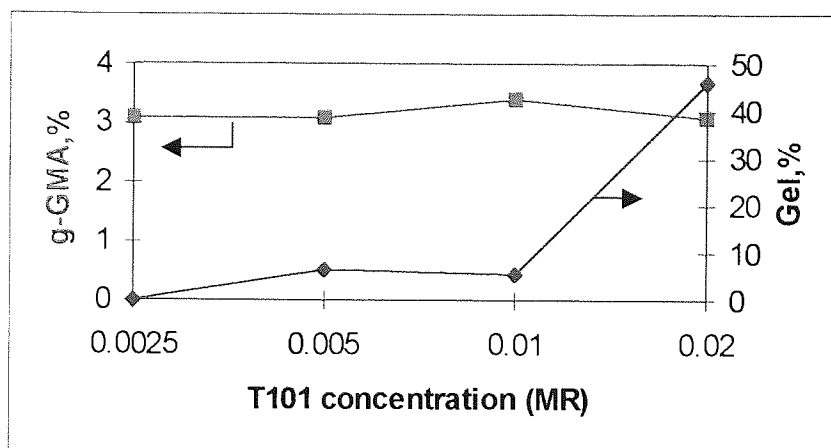


Figure 3-39 Effect of peroxide concentration on grafting degree and gel of GMA grafted EPDM/PP in the presence of TRIS (EPDM, 75 phr; PP, 25phr; GMA, 10 phr ; TRIS, 2.5phr; GMA/TRIS=8/2)

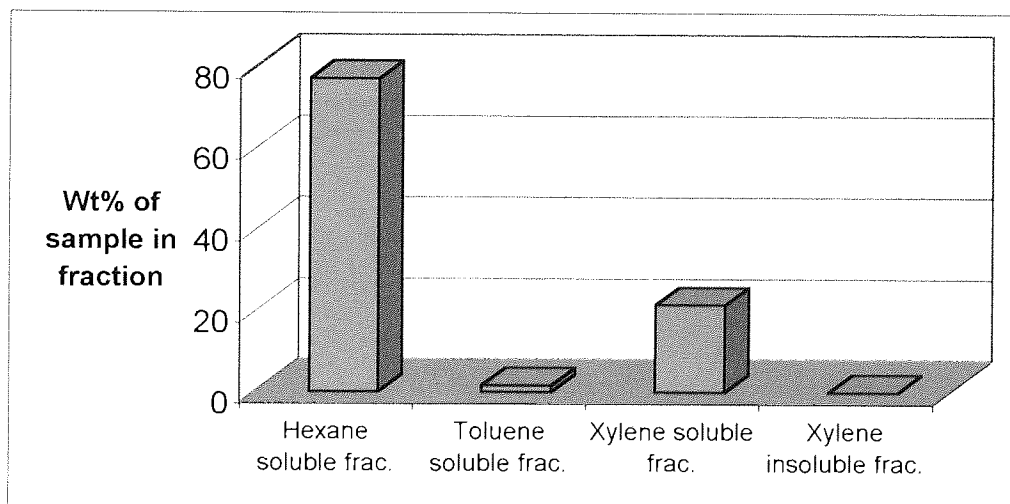


Figure 3-40 Weight percentage of separated fractions of the blend of EPDM/PP which were prepared under conditions of temperature, 180°C; speed, 65 rpm; time, 10minutes by differential solvent extraction (hexane, toluene, and xylene )

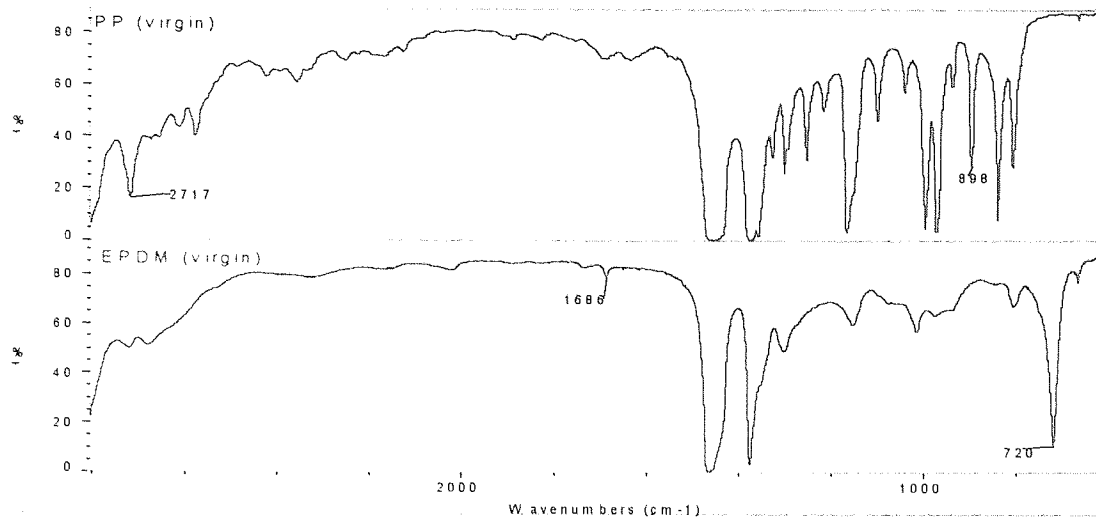


Figure 3-41 Comparison of FTIR spectra of virgin PP (top one) and virgin EPDM (bottom one)

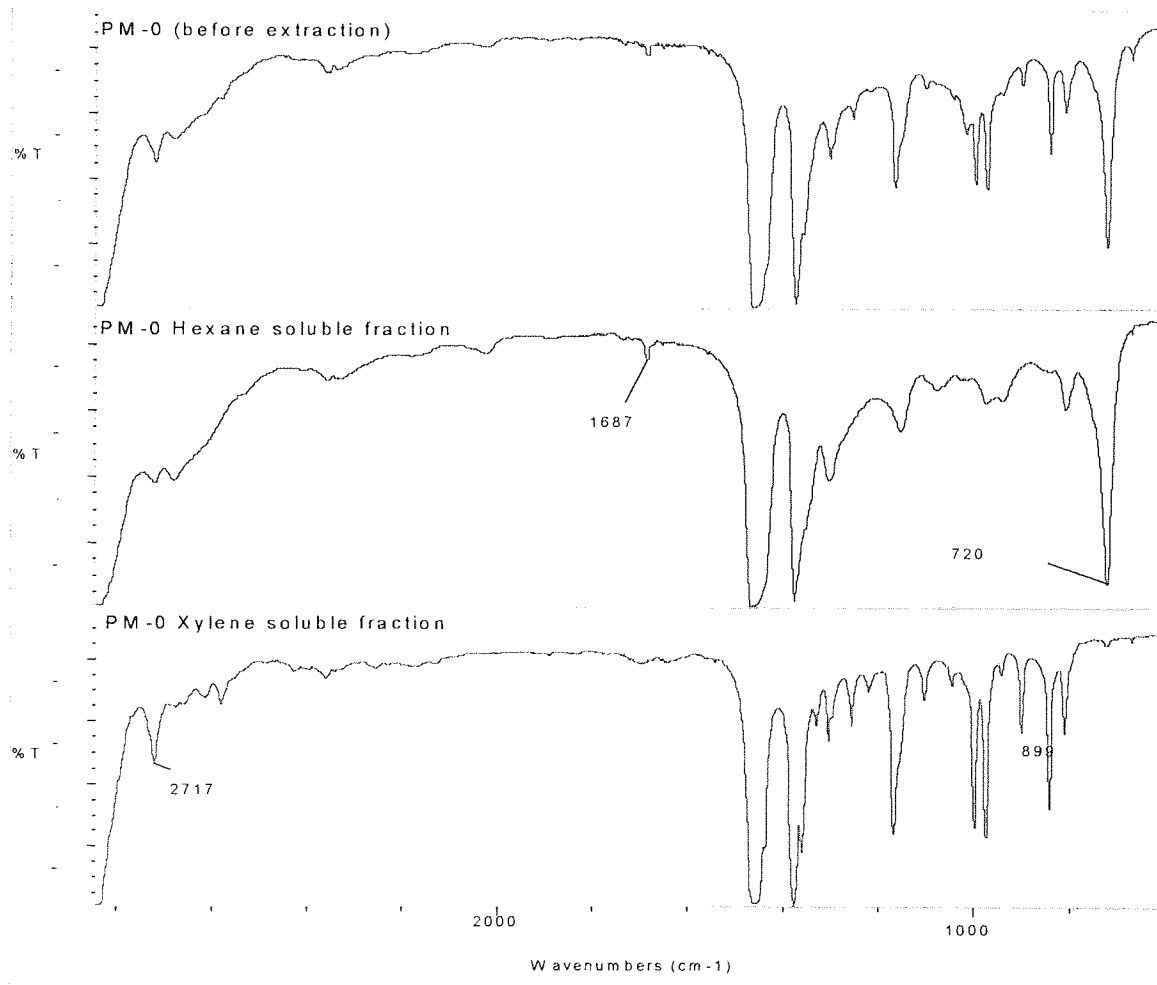


Figure 3-42 FTIR spectra of EPDM/PP blend (PM-0) (top one) and its hexane soluble fraction (middle one) and xylene soluble fraction (bottom one)



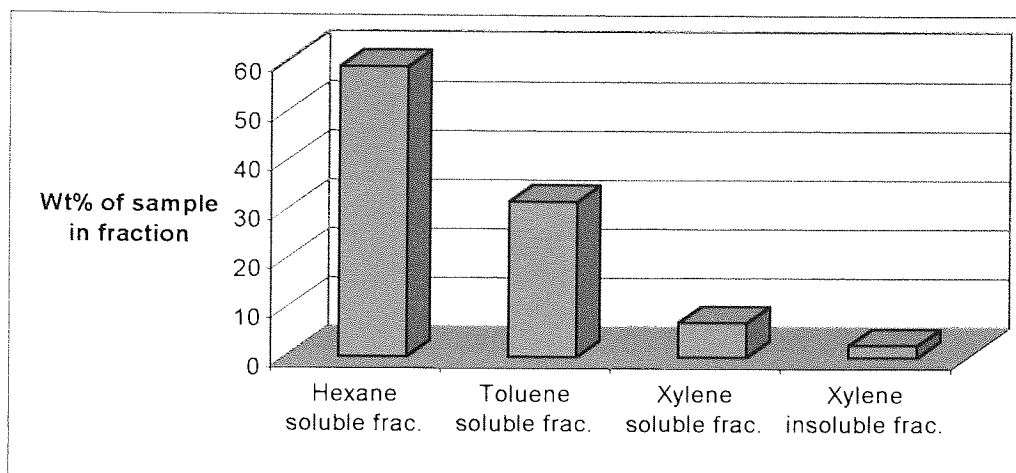


Figure 3-43 Weight percentage of separated fractions of EPDM/PP-g-GMA<sub>T101</sub> (sample PM-2 in Table 3-3 ) by differential solvent extraction (hexane, toluene, and xylene )

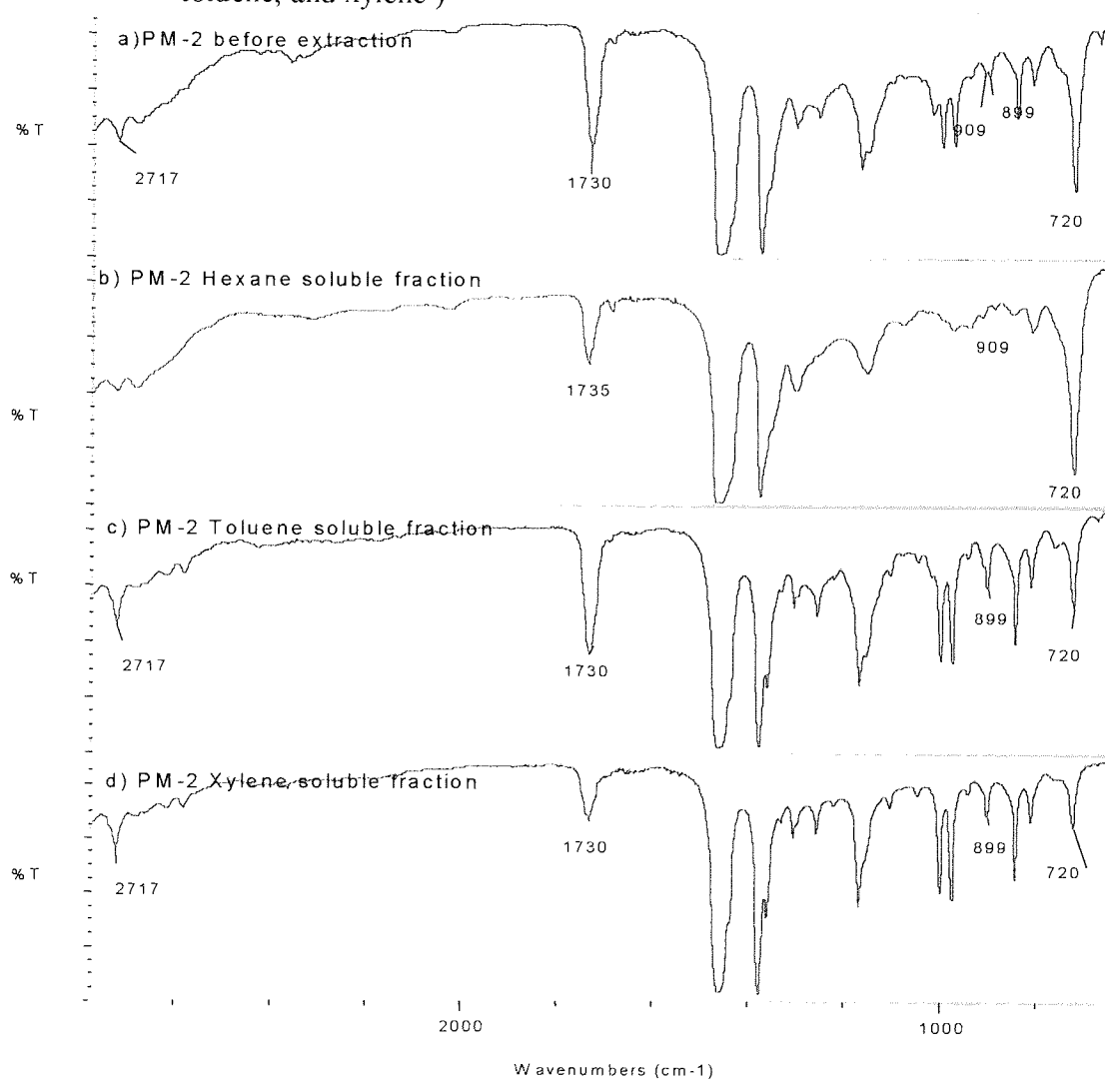


Figure 3-44 FTIR spectra of EPDM/PP g-GMA<sub>T101</sub> (PM-2) and its soluble fractions (a) before extraction, (b) hexane soluble fraction, (c) toluene soluble fraction, and (d) xylene soluble fraction

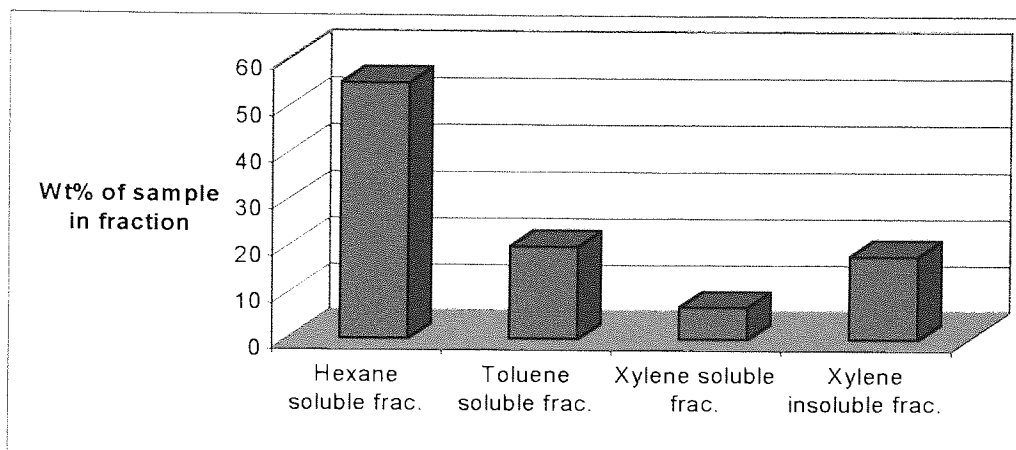


Figure 3-45 Weight percentage of separated fractions of EPDM/PP-g-GMA<sub>TRIS</sub> (sample PM-8 in Table 3-3 ) by differential solvent extraction (hexane, toluene, and xylene )

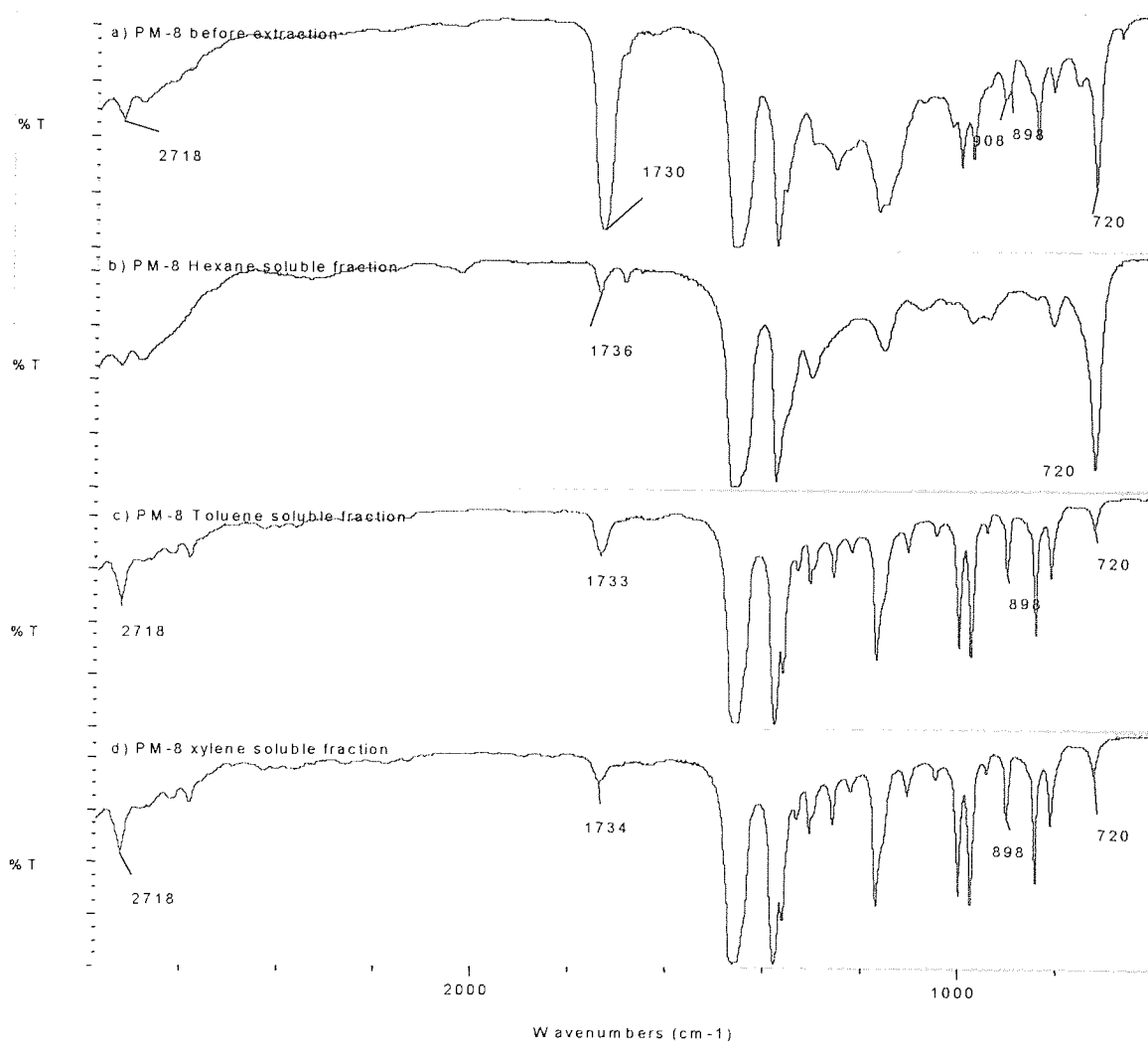


Figure 3-46 FTIR spectra of EPDM/PP g-GMA<sub>TRIS</sub> (PM-8) and its soluble fractions (a) before extraction, (b) hexane soluble fraction, (c) toluene soluble fraction, and (d) xylene soluble fraction

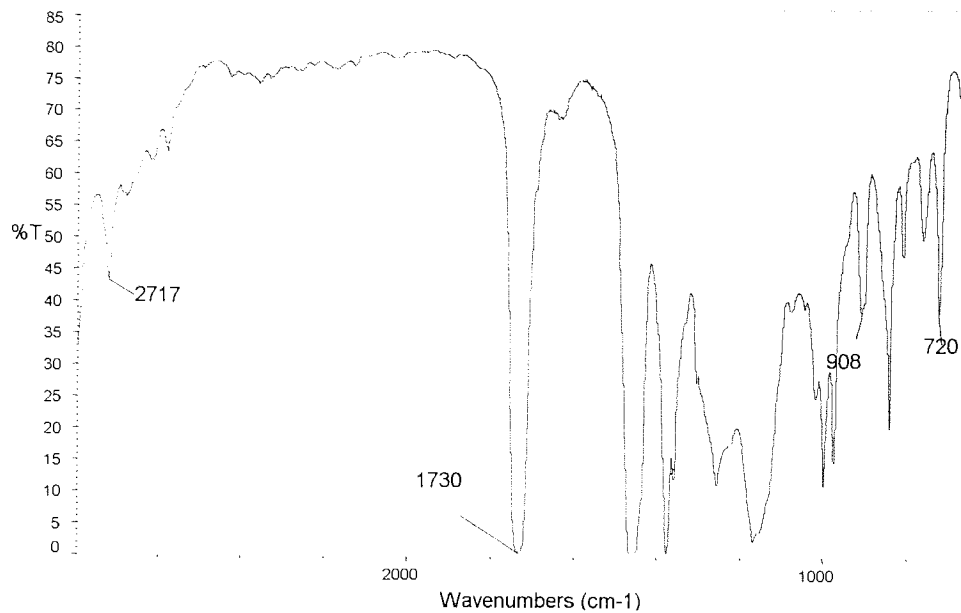


Figure 3-47 FTIR spectrum of the hexane insoluble fraction of EPDM/PP-g-GMA<sub>TRIS</sub> (sample PM-8)

## CHAPTER 4 FUNCTIONALISATION OF NATURAL RUBBER WITH MALEIC ANHYDRIDE

### 4.1 OBJECTIVE AND METHODOLOGY

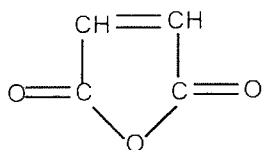
Maleation is one of the most widely used methods for the functionalisation of polymers. The maleation reaction takes advantage of the dual-functionality of maleic anhydride (MA) (I)—the 'ene' or radically active double bond and the nucleophilically reactive anhydride or ester group [76]. MA can be grafted onto either saturated or unsaturated polymers under a variety of conditions [77]. Considerable effort has been made to graft MA onto saturated polymers, particularly onto polyolefins, such as PE, PP, EPR, EPDM and ABS. This is due to the lack of reactive groups in these polymers that limits many of their end-uses, particularly those in which adhesion, dyeability, paintability or reactivity with other polymers is needed. MA is known to add readily to natural rubber (NR) or polyisoprene at elevated temperatures or in the presence of free radical initiators in solution [78-82]. This reaction can also be carried out in the solid state by thermal initiation and mastication [78,82-85].

In this study, natural rubber was selected to be functionalised with maleic anhydride in the solid state. A commercial grade of natural rubber e.g. SMR-L was used and the grafting of MA onto SMR-L was carried out in an internal mixer (e.g. a torque rheometer) either by thermal initiation or by free radical initiation. In the case of thermal initiation, maleic anhydride and natural rubber were mixed in a close system, whereas organic peroxides (bezoyl peroxide (BPO) (II) and 2,4-dimethyl-2,5-bis (t, butyl peroxy) hexane (T101) (III)) were used as initiators in the peroxide initiation (see Scheme 4-1). Before processing, the bale of natural rubber was cut down into small pieces. For some runs, the natural rubber was purified by using Soxhlet extraction with acetone before reactive processing. The reactive processing parameters below were developed and optimised, (see scheme 4-1) and the experimental conditions, compositions and grafting degree are shown in Tables 4-1 and 4-2:

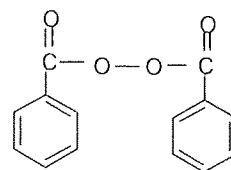
- a) Processing temperature (70°C—220°C);
- b) Processing time (2—15 min);
- c) Concentration of MA (0—14 phr);

- d) Type of peroxide (T101, and BPO) and their concentrations;
- e) Molar ratio of MA to peroxide;
- g) The addition sequence

The MA grafted natural rubber samples were purified and characterised by using FTIR spectroscopy. It was difficult to prepare thin films for FTIR measurement directly due to the tackiness and high viscosity of MA modified natural rubber samples, hence thin cured films were prepared. The rubber ingredients, zinc oxide, stearic acid, accelerator CBS (N-cyclohexyl-2-benzothiazole sulphamide), and sulfur were compounded on a two-roll mill (see Scheme 4-1 and Section 2.3.1). In order to eliminate any unreacted maleic anhydride from the reaction products and to ensure the correct measurement of maleic anhydride grafting level, Soxhlet extraction was adopted to purify the MA grafted natural rubber samples. The compounded rubbers were sheeted out as thin as possible and were vulcanised to thin films, referred to as **film A**. Films **A** are expected to include free maleic anhydride and grafted maleic anhydride during reactive processing, compounding and curing. **Film B** was obtained from extraction of the films **A** with acetone and expected to contain maleic anhydride grafted during reactive processing, compounding and curing (see Scheme 4-1). Another extraction procedure involves that the MA grafted natural rubber samples which were milled to thin sheets and then subject to Soxhlet extraction with acetone. The resultant rubber samples were compounded and cured into thin films, referred to as **film C**. These films are expected to contain only grafted maleic anhydride during reactive processing. The grafting degree of MA was examined by measuring absorption peak area ratio of the acid group at  $1710\text{ cm}^{-1}$  to the reference peak at  $2725\text{ cm}^{-1}$  ( $A_{1710\text{ cm}^{-1}}/A_{2725\text{ cm}^{-1}}$ ) (see Fig. 2-21).



(I) maleic anhydride



(II) benzoyl peroxide



From the FTIR spectra of both maleic anhydride and succinic anhydride, the most characteristic anhydride bands appeared at  $\sim 1780$  and  $1860\text{ cm}^{-1}$ , assigned to five members cyclic anhydrides due to symmetric and asymmetric C=O stretching respectively (Figures 2-7 and 2-15). The peak at  $1780\text{ cm}^{-1}$  is very strong and can be conveniently used to estimate the amount of grafted maleic anhydride by quantitative FTIR. For succinic acid, the acid group gives rise to a characteristic absorption peaks at  $1698\text{ cm}^{-1}$ , corresponding to the carboxylic acid symmetric C=O stretch (see Figure 2-14).

For the accurate characterisation of MA grafted natural rubber (NR-g-MA), it is of great importance to make sure of the total elimination of all the unreacted MA. This is because unreacted MA gives rise to absorption peaks in the same region as grafted anhydride ( $1780\text{ cm}^{-1}$ ). It was reported that the unreacted MA could be evaporated in vacuum oven at a temperature of  $120^\circ\text{C}$  if the grafted polymer was pressed into thin films [89]. Natural rubber contains unsaturated double bonds and can easily degrade at high temperature and the MA grafted natural rubber could not be pressed into thin films directly due to the tackiness and high viscosity of the MA grafted natural rubber. In order to prepare thin films for IR measurement, cure ingredients (zinc oxide, stearic acid, accelerator CBS and sulfur) were compounded in the reaction products on a two-roll mill and thin cured films were made by compression moulding at a temperature of  $150^\circ\text{C}$  for 20 minutes (see Section 2.3.1). The FTIR analysis showed that no difference was found between a pressed film without the curing ingredients and a cured film, indicating that the curing does not affect the FTIR analysis used here for the purpose of characterisation and determination of grafting level of MA on NR.

To check that maleic anhydride was really grafted on the polyisoprene chains of the natural rubber, the MA modified NR samples were purified by Soxhlet extraction with different solvents such as acetone, chloroform, and dichloromethane. Acetone was found to be the most suitable solvent both due to the high solubility of maleic anhydride in acetone and due to the good extraction ability for natural rubber. The adoption of the preparation of cured films for FTIR analysis gives rise to two possible purification procedures, e.g. either before the compounding or after compounding and curing. To determine the accurate purification procedures, three different films, which involved different extraction, methodologies and compounding procedures, were examined by FTIR (see Scheme 4-1

(route C)). After the MA modified NR samples were compounded with curing ingredients on a two-roll mill, thin cured films were prepared by compression moulding at a temperature 150°C for 20 minutes. These films were referred to as film A. Film A was not subjected to any extraction as a control, which was expected to include free MA, grafted MA during melt grafting processing, compounding and curing. After film A was extracted in acetone, the resulting film (referred to as film B) is expected to contain no free MA. Figures 4-2 and 4-3 compare the spectra recorded from both films A and B of two samples which were obtained at different processing temperatures. It can be seen that after 24 hours extraction (film B) a strong absorption band still appears at 1710  $\text{cm}^{-1}$  (assigned to a dimeric carboxylic acid), and a weak shoulder at 1780  $\text{cm}^{-1}$  (corresponding to cyclic anhydride with a 5-member ring), when the rubber was processed with MA at a high processing temperature (heating oil temp. 200°C) (Figure 4-2), whereas there are nearly no acid and anhydride bands observed after extraction for the sample obtained at a low processing temperature (temp. 90°C) (Figure 4-3). The grafted maleic anhydride mainly exists in the form of acid after vulcanisation. The extraction time was also examined. 24 hours extraction with acetone was found to be enough to eliminate all the free MA in the films.

By comparing FTIR spectra recorded from films A and B, it was found that the area of absorption bands at 1710  $\text{cm}^{-1}$  and 1772  $\text{cm}^{-1}$  after extraction (film B) were slightly different from those before the extraction (film A) as a result of the fact that only a small amount of free MA left in the films after processing and film preparation. This phenomenon attributes the characteristics of volatility and sublimation of MA under high temperatures during processing and curing so most of the free MA in the modified rubber disappeared during the processing and curing.

Another extraction procedure was also adopted to confirm the existence of grafted maleic anhydride on polyisoprene chain. The MA modified NR samples were milled into thin sheets and extracted in the Soxhlet extractor with acetone for 24 hours (see Scheme 4-1 (route d)). After being dried in vacuum oven at a room temperature for more than 20 hours, curing agents were compounded on a two-roll mill and thin films were prepared by compression moulding. This is referred to as film C, which was expected to contain the grafted MA produced only during the reactive processing stage. The spectrum recorded



from films C shows the same absorption bands as those from observed in films B. The difference is that the absorption area ratio ( $A_{1710\text{ cm}^{-1}} / A_{2725\text{ cm}^{-1}}$ ) from film C is slightly smaller than that from films B. This demonstrates that free MA in the reaction products may further react with the rubber during the milling for compounding. In order to prove the further reaction of unreacted MA remained in the samples during the compounding and curing vulcanisation, one sample was prepared by mixing 30g SMR-L with 1.8g MA on a cold two-roll mill for 20 minutes. The same Soxhlet extraction procedure was adopted to prepare film D (see scheme 4-2). Their FTIR spectra also show strong absorption bands at  $1710\text{ cm}^{-1}$  and  $1780\text{ cm}^{-1}$ , indicating the grafting of MA onto natural rubber (see Figure 4-4). The grafting reaction of MA onto natural rubber can also be initiated by mastication. Macro-radicals can be formed by mechanical shear force while the rubber passes through a cold two roll mill. However, the rubber became dry and ragged as reported [83-84] and could not be processed easily. This demonstrated that if there is any unreacted MA in the processed NR, the processing of compounding on the two-roll mill leads to further reaction of MA with NR.

Comparing these three kinds of films (films A, B, and C), it is clear that film C should be used to evaluate the amount of grafted MA during the melt grafting in the internal mixer. On the other hand, the free MA in the rubber can affect the film quality adversely. Films C were generally more smooth and transparent than films A and B hence the results from films C are more accurate. The film C was used for all samples to determine the MA grafting degree by quantitative FTIR analysis.

The spectra of the purified MA grafted natural rubber via both thermal initiation (see Figure 4-5) and peroxide initiation (see Figure 4-6) show new bands at  $1710\text{ cm}^{-1}$  (strong) and a shoulder at  $1772\text{ cm}^{-1}$  (shoulder) by comparing it with that of unmodified natural rubber. The absorption band at  $1710\text{ cm}^{-1}$  is assigned to the characteristic band of succinic acid group and band at  $1772\text{ cm}^{-1}$  is assigned to the characteristic band of the anhydride function. Figure 4-7 shows the comparison of FTIR spectra of MA, SA, SAN and MA grafted NR. The results confirm that the reaction products contain mainly grafted acid function and to a much lesser extent anhydride function. The grafting degree of MA onto the NR for each sample was determined by examining the FTIR spectrum of the film C. The absorption peak area ratio of the acid group at  $1710\text{ cm}^{-1}$  to the reference peak at  $2725$

$\text{cm}^{-1}$  ( $A_{1710 \text{ cm}^{-1}}/A_{2725 \text{ cm}^{-1}}$ ) was calculated and the actual grafting degree was obtained by comparison of the area ratio to a calibration curve (see Section 2.5.1).

The processed natural rubber with MA in the presence or absence of peroxide show a significantly different physical appearance from raw natural rubber. The products obtained at a temperature above  $180^{\circ}\text{C}$  without peroxide have a brown colour and become tacky whereas no obvious colour change was observed when the reaction was carried out below  $160^{\circ}\text{C}$  with or without peroxide. The more MA grafted, the deeper was the brown colour of the reaction products, especially at a high temperature above  $200^{\circ}\text{C}$ . Natural rubber is soluble in ordinary hydrocarbon solvents, such as benzene, toluene, xylene, and becomes swelled in polar solvents, such as acetone, chloroform, and dichloromethane. The solubility of the reaction products became lower in hydrocarbon solvents. The rubber with a very small amount of grafted MA can only become like 'jelly' or partially soluble in these solvents even at a temperature of  $100^{\circ}\text{C}$ . If purified SMR-L was used and the processing temperature was kept below  $160^{\circ}\text{C}$ , the discharged rubber mixtures were very crumble.

Generally, the reaction products obtained using raw natural rubber under the conditions studied in this work exist in a normal rubbery state. However, if purified natural rubber was used, with or without peroxide, and the processing temperature was below  $160^{\circ}\text{C}$ , the mixtures became crumbled. They were rough, dry and ragged when they were sheeted on a two-roll mill. They were similar to the mixture obtained directly from mixing of natural rubber with maleic anhydride on a cold two-roll mill [83-84]. When the temperature was above  $160^{\circ}\text{C}$ , the products show a normal state.

#### **4.2.2 Grafting MA onto NR by Thermal Initiation**

Maleic anhydride (MA) is known to add readily to natural rubber or polyisoprene at elevated temperatures or in the presence of free radical initiators in solution [78-82]. This reaction can also be carried out in the solid state by three techniques: thermal initiation, peroxide initiation, and initiation by mastication [78, 82-84]. In the case of thermal

initiation, the rubber maleination reaction requires a temperature higher than 160°C and preferably about 220-240°C, along with a considerable excess of maleic anhydride [78].

In the case of thermal initiation, the required amount of SMR-L was cut into small pieces and mixed with MA in the torque rheometer under inert atmosphere. To establish the optimal processing conditions and compositions, the effects of processing temperature, processing time, purification of raw SMR-L, and the concentrations of MA on the grafting degree were examined. Table 4-1 lists the experimental results.

The FTIR spectra show that MA can be grafted onto the rubber when the rubber and MA were mixed in the internal mixer at a high temperature. The processing temperature is a key parameter to achieve the thermal initiation. Figure 4-8 shows the relationship of grafting level to the processing temperature (heating oil temperature). When raw SMR-L was processed with 6 phr MA, no MA was grafted onto the rubber until the processing temperature rose to 140°C. Increasing the temperature was from 140°C to 220°C led to a rapid increase in the MA grafting level. This is similar to what observed in solution studies [87].

However, significant difference can be found when MA was mixed with purified natural rubber which was Soxhlet extracted with acetone before the grafting reaction. Much higher grafting degree was measured when purified natural rubber used compared to raw natural rubber. Even at low temperature, below 160°C, a certain amount of MA could be grafted onto the rubber but the reaction products became crumbled. The products were rough, dry and ragged when they were sheeted on a two-roll mill. They were similar to the mixture obtained directly from mixing of natural rubber with maleic anhydride on a cold two-roll mill. When the temperature was above 180°C, however, the products show a normal rubbery state. The grafting degree decreased initially to a minimum value with increasing the temperature from 90°C to 110°C, and then increased sharply when the temperature rose to 150°C followed by a plateau from 150°C to 180°C. At the temperatures over 180°C, the grafting degree increased further with increasing temperature (see Figure 4-8).

The reason of the much higher amount of MA grafted onto purified SMR-L compared to the unpurified SMR-L, may be due to the reduction of the contents of some natural

substances, such as natural protein, in the rubber which were removed by extraction. These substances may inhibit the grafting reaction. Furthermore, extraction of the low molecular fractions of natural rubber, may lead to easier to production (by shear force) of macroradicals during mixing, especially at low temperature. Both grafting of MA onto the rubber chains and cross-linking may take place at same time hence the reaction products show a crumble state which indicates formation of crosslinking to some extent.

The grafting reaction is clearly reflected from the torque-time curves. When SMR-L alone was processed, the torque increased immediately to a maximum value after addition of SMR-L due to the low temperature of rubber (see Figure 4-9 (inset)). The mechanical force and oxidation under high temperature reduces the molecular weight and the rubber becomes more plastic and the torque decreases gradually. When MA was added to the rubber, a different torque-time curve was observed. In the two-minute premixing of SMR-L, the torque decreased from the first peak which was measured after the introduction of the rubber. After MA was charged into the mixing chamber, further torque drop to a minimum value could be observed due to melting of MA and lubrication effect on rubber (see Figure 4-9). This process can become much shorter at a high temperature so the torque peak shifted to short times. With dispersion of MA in the rubber the torque increases sharply to a peak value. In the case of raw SMR-L used without purification, the processing temperature exerts a strong influence on the time to reach the peak value (see Figure 4-10 (a)). The lower the processing temperature, the longer time is needed to disperse MA in the rubber. Very short time is needed at a temperature above 200°C. Increasing the processing temperature could significantly improve the dispersion of MA in the rubber. This may be due to the higher solubility of MA in the rubber at higher temperatures. There are no obvious peaks after the dispersion of MA at temperatures below 150°C and a steady torque is obtained until the discharge (see Fig.4-9 (b)). When using a higher amount of MA at a temperature of 200°C, the torque peak value becomes slightly higher and the peak area are expanded. Compared to the torque-time curves when raw SMR-L was used, significant differences can be found when purified SMR-L was used (see Figure 4-11). In the range of processing temperatures used from 90-220°C, an obvious peak was observed despite the change in the processing temperature.

When purified SMR-L was used, much longer time was needed to reach the peak and the peak value was much higher than that with raw SMR-L (see Figure 4-10) at a low temperature. This longer time for the dispersion of MA in the purified rubber may be attributed to the extraction of some natural substances from the rubber, which may be helpful for dispersing MA into the rubber. Under a temperature of above 180°C the peak torque value with the purified rubber was slightly lower than that with the unpurified rubber.

It is obvious that high temperatures could lead to higher grafting of MA. However, at such high temperatures (above 200°C), the rubber can easily oxidise so the properties of MA modified NR could be adversely affected. The reaction, therefore, should be preferably carried out at a temperature of about 200°C under inert atmosphere (nitrogen). When the reaction was carried out at the preferable temperature (i.e. 200°C) without peroxide, the grafting degree increased with increasing MA concentration (see Figure 4-12). In the case of unpurified SMR-L, the relation between the grafting degree and the amount of MA initially added was linear. About 30% of total MA initially added was grafted onto the rubber. When purified SMR-L was used, the grafting degree increased gradually with increasing the MA concentration and levelled off when MA initially added was over 10 phr. Compared with unpurified SMR-L, more MA was grafted onto the purified rubber.

Figure 4-13 shows the effect of processing time on the grafting degree with 6 phr MA at 200°C. It can be seen that the reaction takes place rapidly at a processing temperature of 200°C and is nearly finished within 10 minutes.

#### **4.2.3 Grafting MA onto NR by Free Radical Initiation**

The reaction of MA with natural rubber is readily initiated in solution at a temperature around 130°C by several peroxides: e.g. BPO, AIBN (azo bisisobutyronitrile), paramentane hydroperoxide [87]. In this study, organic peroxides were also used to initiate the grafting reaction of MA onto NR. The grafting reaction was carried out in the internal mixer in the presence of peroxide. Two different peroxide were used; benzoyl peroxide (BPO) and 2,5-dimethyl-2,5-bis(t-butyl peroxy) hexane (T101). The effects of concentrations of peroxides, MA, addition sequence, processing temperature, and

processing time on the grafting degree of MA were investigated in detail. The experimental conditions and results are present in Table 4-2.

The grafting reaction was found to be much more difficult to initiate by peroxides in the solid state. When BPO was used, the maleic anhydride modified natural rubber was in its normal rubbery state, e.g. there was no sign of crosslinking, but the grafting degree was found to be low. Figure 4-14 shows the effect of BPO concentration and temperatures on MA grafting level. The reaction was conducted with a fixed amount of MA (6 phr) under a fixed mixing conditions (50 rpm, 15 min, mixing temp. 110, 130, and 140°C) to investigate the effect of BPO concentration. At a temperature of 110°C, at least 0.3 phr BPO was needed to initiate any grafting and the maximum grafting degree was only 0.4%. When the temperature was raised to 130°C, the grafting degree increased slightly and the maximum value was 0.6%. With further increase of temperature to 140°C, the grafting degree decreased further. This may be due to the short half-life of BPO ( $t_{1/2}$  = 11 minutes at 110°C and  $t_{1/2}$  = 4.5 minutes at 120°C [151]) at such a high temperature. Concerning the grafting efficiency, the overall relatively low grafting levels under the most favourable grafting conditions suggest that the BPO is not the ideal peroxide in this case.

Another peroxide, T101, which has longer half-life time at higher temperatures ( $t_{1/2}$  = 14 minutes at 150°C) [151], was used (temperatures and concentration were varied) (see Figure 4-15). It was found that this peroxide could initiate the reaction of MA with natural rubber at a temperature above 150°C quite efficiently leading to much higher overall grafting levels than BPO. The grafting degree increases rapidly to a peak value with increasing the T101 concentration to 0.4 phr at a fixed temperature of 150°C and then decrease with further increase of T101. When the temperature was raised to 160°C, the grafting reaction was initiated quite efficiently by T101 and the grafting degree of MA increased strongly with increasing T101 concentration. For example, 2.2 % grafting degree was achieved with only 0.2 phr T101. This value exceeds that obtained at 200°C without peroxide when 6phr MA was added to unpurified SMR-L. However, with the increase of T101 concentration or processing temperature, the degree of crosslinking during mixing becomes obvious and unacceptable. Through a series of experiments, the optimum temperature was found to be between 150-160°C and concentration of T101 less than 0.04 phr.

The MA concentration has a different effect on the grafting level with different initiation techniques. When the reaction was carried out at a preferable temperature (200°C) without peroxide, the grafting level increased with increasing MA concentration (see Figure 4-12). If a peroxide was used to initiate the reaction, the grafting level was found not to be a monotonic function of its initial concentration. Figure 4-16 shows that MA grafting level increases initially with increasing MA concentration and reaches a maximum at about 6 phr MA introduced at a temperature of 150°C and then decreases with a further increase in MA concentration. When the processing temperature was increased to 160°C, a slight difference was found. The grafting level maintains a high value when MA concentration was changed from 6 phr to 10 phr before reduction in the grafting level. This may be due to the limited solubility of MA in the molten rubber. This could be observed from the torque-time curves during the processing and Figure 4-17 shows the strong influence of MA concentration on the torque in the presence of T101. When the concentration of MA added exceeded a certain amount, e.g. 10 phr, the torque increased slowly and no obvious peak was recorded. If more than 14 phr MA was introduced, the mixing became quite difficult and a very low torque value was maintained. This may be attributed to the low solubility of MA in the rubber. However, higher temperatures can enhance the mixing process. The addition sequence can also influence the mixing efficiency. If more than 14 phr MA was added in two portions, the second portion will be difficult to disperse into the rubber. The mixing efficiency plays a very important role in reactive processing. If chemicals can not be dispersed into the rubber thoroughly, the reaction rate will be lowered greatly and some side reactions may occur so the mixing process must be optimised. This phenomenon was reported for grafting MA onto PP [73, 88], and EPDM [102]. It was proposed that with increasing MA content, the mixture changes from a single phase to a biphasic system with MA droplets dispersed in the molten polymer. The formation of MA droplets not only reduces the effective concentrations of MA and the peroxide for grafting, but also promotes MA homopolymerisation [73]. High temperature can increase the solubility of MA in the natural rubber so the torque during the mixing increases quickly to a high value at a temperature of 200°C when more than 14 phr MA was used.

In the case when T101 is used, the reaction rate was much slower than in the case with thermal initiation at a high temperature (Figure 4-18). The grafting level increased rapidly

initially within 5 minutes and then increased gradually with continuing mixing. T101 is usually used at a high temperature. It can be decomposed slowly at a temperature of 150°C ( $t_{1/2}$  =14 minutes at 150°C,  $t_{1/2}$  =5.5 minutes at 160°C) [151] so the reaction progressed gradually within 20 minutes.

#### 4.2.4 Optimal Conditions

The results show that maleic anhydride could be grafted onto natural rubber via melt grafting by using both thermal and peroxide initiation techniques. The functionalised rubber should have enough functional groups to react and crosslinking should be minimised.

It is clear that when the reaction was carried out at a high temperature using purified SMR-L without any peroxide much higher grafting degree was achieved than that via free radical initiation using peroxide T101 (see Figure 4-19). Furthermore, at a temperature around 200°C, MA can be rapidly grafted onto natural rubber without any peroxide.

#### 3.2.5 Analysis of the Reaction Products

To get a better understanding of the grafting reaction of MA with NR using different initiation techniques, the MA modified NR samples were subjected to separation of soluble and insoluble fractions by Soxhelt extraction with toluene. Scheme 4-3 describes the steps used to analyse the reaction products. Three samples were chosen to be analysed:

A3-9 (obtained at a temperature of 200°C without any peroxide)

D3-42 (obtained at a temperature of 140°C without any peroxide)

D3-51 (obtained at a temperature of 150°C in the presence of T 101, 0.04 phr)

After being extracted in acetone with Soxhlet extractor to eliminate the unreacted MA, the samples were placed in toluene for more than 12hours, allowing them to swell or dissolve completely. Extraction was then performed in toluene with Soxhlet extractor for 12 hours. During the extraction, nitrogen was introduced into the flask to prevent the rubber from oxidation and the solvent was refilled once. The amount of the insoluble fraction (remaining in thimbles) was determined after drying in a vacuum oven at room



temperature (see Table 3-4). The soluble fraction in toluene was casted directly from the solution into thin films on KBr discs and their FTIR spectra were recorded for the analysis.

As a control, it was found that unmodified NR with MA was completely soluble in toluene so no gel was measured when NR was Soxhlet extracted with toluene. For the MA modified NR samples, insoluble gel was detected after the extraction with toluene. The results show that the amount of gel was roughly proportional to the MA grafting degree (see Table 4-4). The sample D-42 in which 0.4% grafting degree was measured had 35% gel, while samples D-51 and A3-9 with 2% have a similar amount of gel at around about 70%. This clearly shows that the grafting reaction of MA with NR is accompanied by crosslinking reactions of NR chains.

However, significant difference was found in the FTIR analysis of the toluene soluble fractions between samples D-51 and A3-9, which represent two types of NR-g-MA. Sample D-51 was prepared via peroxide initiation whereas the sample A3-9 via thermal initiation. Three obvious characteristic absorption peaks at  $1862\text{ cm}^{-1}$ ,  $1787\text{ cm}^{-1}$  and  $1711\text{ cm}^{-1}$  were recorded in the case of the soluble fraction of sample A3-9, whereas there was only one obvious peak at  $1784\text{ cm}^{-1}$  from sample D3-51 (see Figures 4-20 and 4-21). The peaks at  $1862\text{ cm}^{-1}$ ,  $1787\text{ cm}^{-1}$  correspond to the grafted anhydride and the peak at  $1711\text{ cm}^{-1}$  to the grafted acid which might be hydrolysed from the grafted anhydride during the melt grafting. This means that the soluble fraction from A3-9 contains both grafted anhydride and acid whereas no acid was found in D3-51. Furthermore, the soluble fraction from A3-9 has much stronger peak absorption at  $1787\text{ cm}^{-1}$  compared to that of D-51. It demonstrates that at similar level of MA grafting, more grafted MA in the form of grafted anhydride and acid distribute in the low molecular weight fraction when using thermal initiation to prepare NR-g-MA.

#### 4.3 DISCUSSION

The results clearly show that the grafting of MA onto natural rubber can be achieved either by thermal initiation or peroxide initiation in the solid state. In case of thermal initiation, processing temperature plays the most important role. When raw natural rubber was used, the grafting reaction took place at a temperature of over  $150^{\circ}\text{C}$ . The higher the

temperature, the more efficient the grafting of MA onto the natural rubber was. It has been proposed that the addition reaction of MA onto natural rubber takes place via a Diels-Alder type reaction as shown in Scheme 4-4 (a). The high temperature makes the reaction more favourable. Actually, the grafting reaction of MA onto natural rubber in the solid state using the internal mixer as a reactor is very complicated due to the high viscosity of the natural rubber. Even at a high temperature, the natural rubber does not behave like a normal plastic melt, and hence high shearing forces would be exerted onto the rubber during the mixing. Macroradicals could be formed as a result of when the breaking of polymer chains. This factor is more obvious when the rubber was processed at a low temperature.

The analysis of the MA grafted natural rubber shows that the grafted MA could be either in the form of anhydride or in the form of acid as observed in the toluene soluble fraction. The existence of the insoluble gel in solvents such as toluene suggests that the natural rubber has been crosslinked to a certain extent. This indicates that crosslinking reactions accompany the grafting reaction. It was proposed that MA was substituted on one of the neighbouring methylenes of the polyisoprenic double bond [86,87]. This includes intramolecular reaction and intermolecular reaction (Diagram 1, 2). Under a thermal condition, the transposition of the isoprenic double bond to vinylidene double bonds induced by thermal energy was also reported (Diagram 3) [86-87]. The intramolecular reaction can contribute to crosslinking effects. Another factor contributing to crosslinking is due to the macroradicals produced by shearing forces. These macroradicals could not only initiate the grafting reaction of MA onto the polymer chains, but can also lead to branching and crosslinking of the polymer.

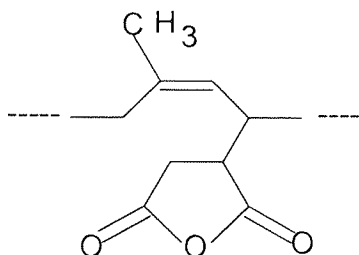


Diagram 1 Intramolecular grafting

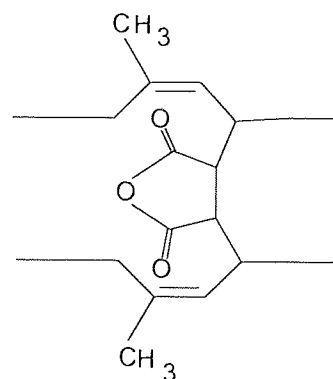


Diagram 2 Intermolecular grafting

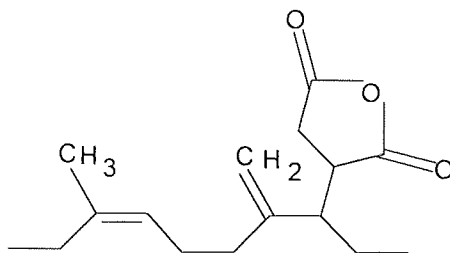


Diagram 3 Rearrangement of the isoprene double bond

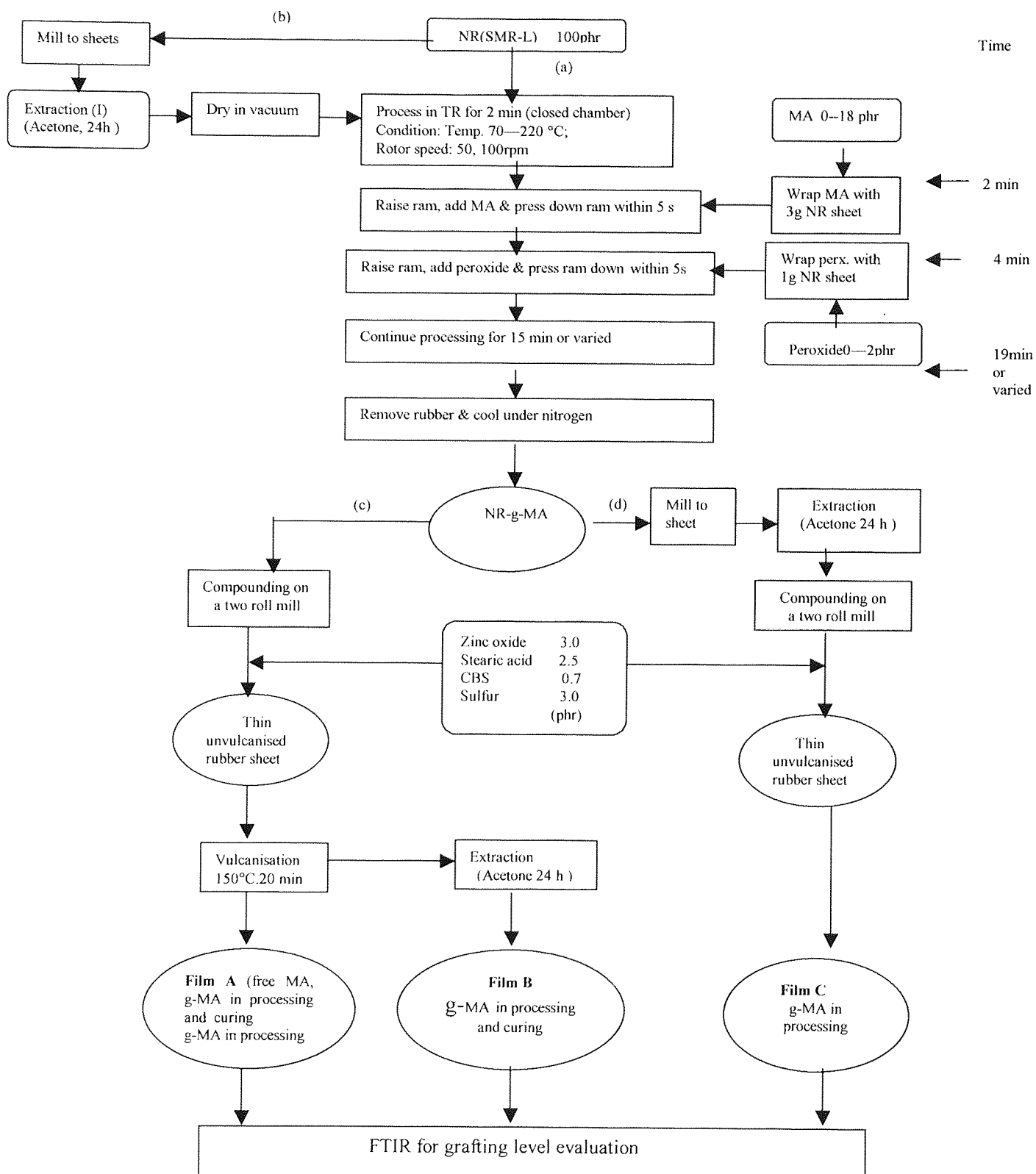
It was found that the purity of the natural rubber also affected the grafting efficiency. Compared to raw natural rubber, acetone purified natural rubber samples gave rise to higher grafting degree and the grafting reaction was shown to take place at lower temperature. The MA modified natural rubber obtained at low temperature (below 160°C) was crumble, indicating high degree of crosslinking. This may be attributed to the fact that the natural rubber contains 5-8% non-rubber constituents such as proteins [87]. Furthermore, it possesses certain “abnormal” chemical groups attached to the main chain (aldehydes, hydroperoxides). The fraction of non-rubber in the natural rubber can compete or interfere with many reactions [152]. The purification by Soxhlet extraction with acetone can reduce the amount of non-rubber substances giving rise to higher grafting. The reason for that a small amount of MA could graft onto NR when purified natural rubber was mixed with MA at a temperature between 90-160°C can be due to the loss of low molecular weight fraction of natural rubber during the acetone extraction. It was found that a small fraction of the low molecular weight rubber was also soluble in the acetone and was extracted. During the mixing in the internal mixer, the fraction of low molecular weight rubber can act as lubricant so it is not so easy to break the rubber chain by shearing forces when raw natural rubber was used. In contrast, the shear forces may break the rubber chain more efficiently to form more macro-radicals at a low processing temperature when the low molecular weight fraction was removed. As a result, a small amount of MA could graft onto natural rubber via free radical grafting at a low processing temperature (90-160°C). Meanwhile, crosslinking reactions also take place which make the MA modified natural rubber appear crumble.

In the presence of peroxide, the grafting reaction can be carried out via a free radical initiation mechanism (see Scheme 4-4 (b)). The decomposition of peroxide generates free radical and then the macroradicals could be initiated by the H-abstraction from the double bonds of the rubber chains. These macroradicals would not only initiate the grafting MA onto the rubber chains, but also lead to crosslinking due to the radically active double bonds of the rubber chains. The high radically activity of these double bonds makes the crosslinking much more prevalent in the presence of peroxides [76]. When the high concentrations of the peroxide, T101, was used or the processing was carried out at higher temperature, the crosslinking of the rubber became dominated and unacceptable. The crosslinking should be avoided or minimised. This was achieved by carefully balancing the concentration of peroxide and processing temperature.

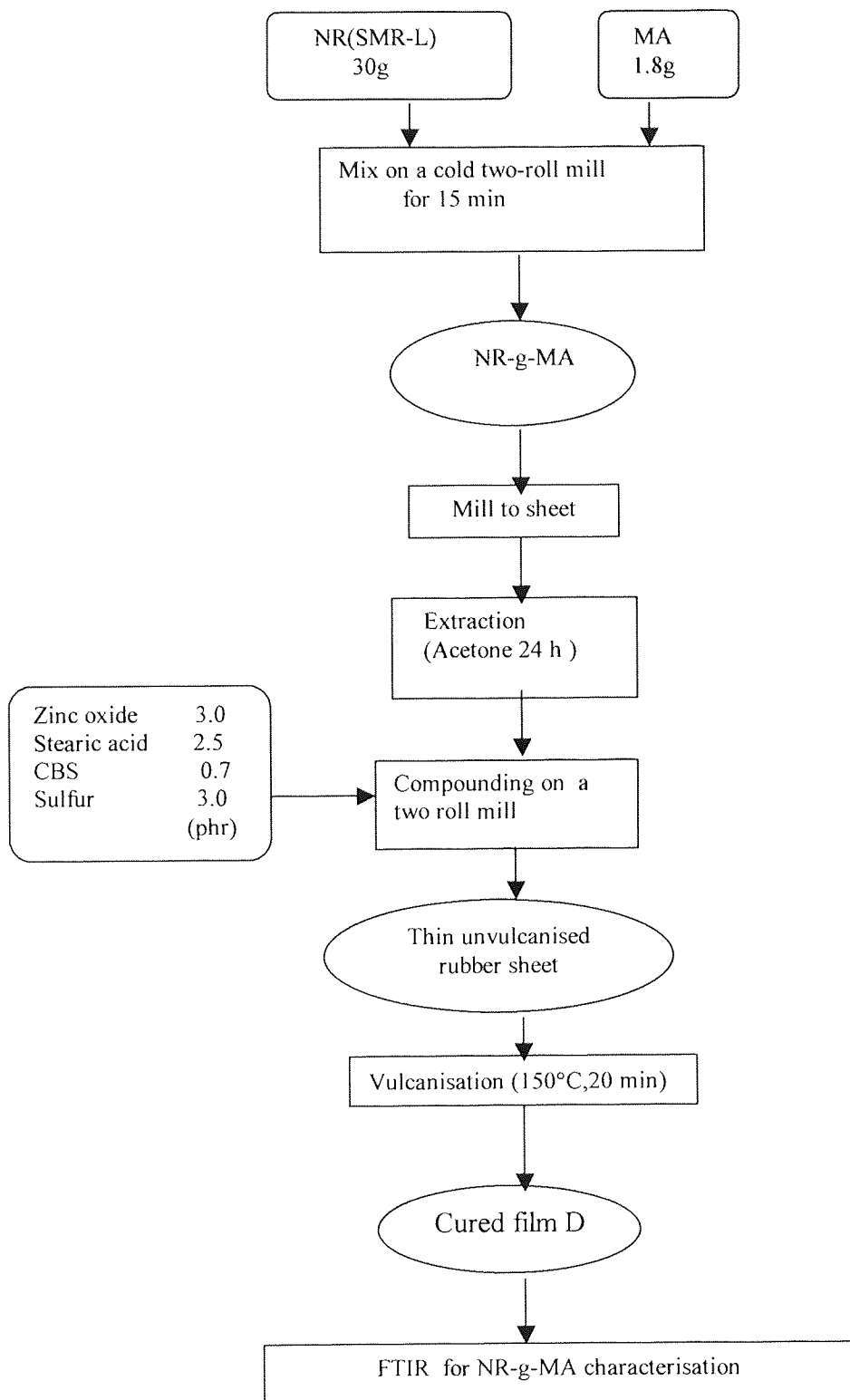
The initial analysis results showed that the reaction products obtained by peroxide initiation and thermal initiation via melt processing are different. When the reaction was carried out at a high temperature without peroxide, about one third of the reaction product was soluble in toluene and its FTIR spectrum showed a strong anhydride absorption bands at 1780, 1850  $\text{cm}^{-1}$  and acid band at 1710  $\text{cm}^{-1}$  (Figure 4-21). This confirms that a partial hydrolysis accompanies the maleation reaction. The reaction product obtained at a temperature of 150°C in the presence of T101 has also about 30% soluble fraction in toluene, but its FTIR spectrum (from the soluble fraction) was shown to have only a weak anhydride absorption band at 1780  $\text{cm}^{-1}$  (Figure 4-20). This indicates that its MA grafting level in the soluble fraction of the peroxide-initiated product is much less than that in the soluble fraction of the thermally maleated rubber. The spectrum of the 'normal' reaction product has an obvious absorption band at 3280  $\text{cm}^{-1}$ , which corresponds to the oxidation of polyisoprene [86], but no oxidation band was found in the soluble fraction of these MA-modified samples. All samples have high amounts of gel and even 0.4 % grafting degree of MA led to about 34 % gel. This indicates that crosslinking accompanies the grafting reaction of MA onto the rubber chains which may have resulted from the intermolecular structures of grafted MA, especially by peroxide initiation.

The MA-modified NR samples were not used further in this work for the purpose of reactive blending with PET due to the fact that MA-modified NR generally has high viscosity and high oxidation at the temperature of 260°C for blending with PET.

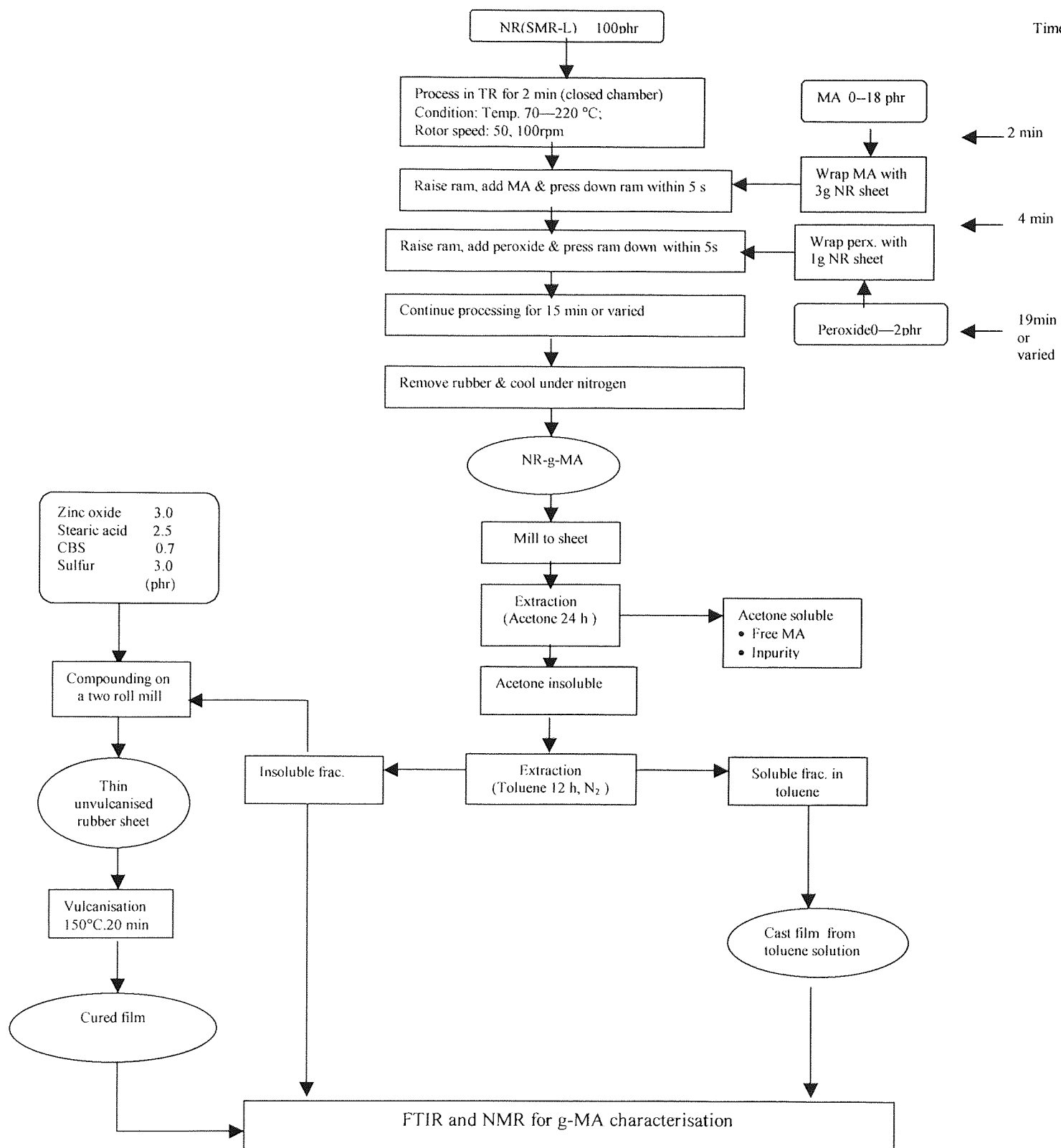
Scheme 4-1 Flow chart for grafting maleic anhydride(MA) onto natural rubber



Scheme 4-2 Flow chart for analysing MA grafted natural rubber by mixing on a cold two-roll mill

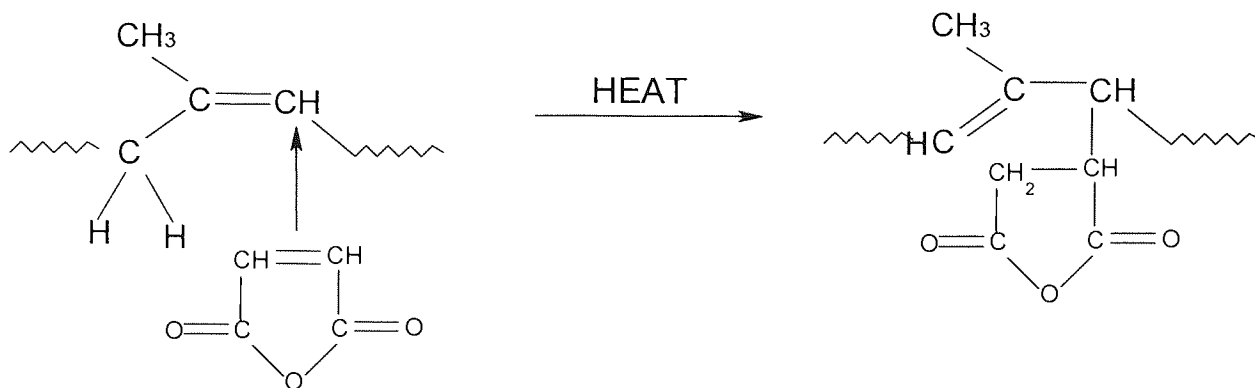


Scheme 4-3 Flow chart for analysing MA grafted natural rubber



Scheme 4-4 The mechanisms of grafting MA onto natural rubber

(a) Thermal initiation



(b) Peroxide initiation

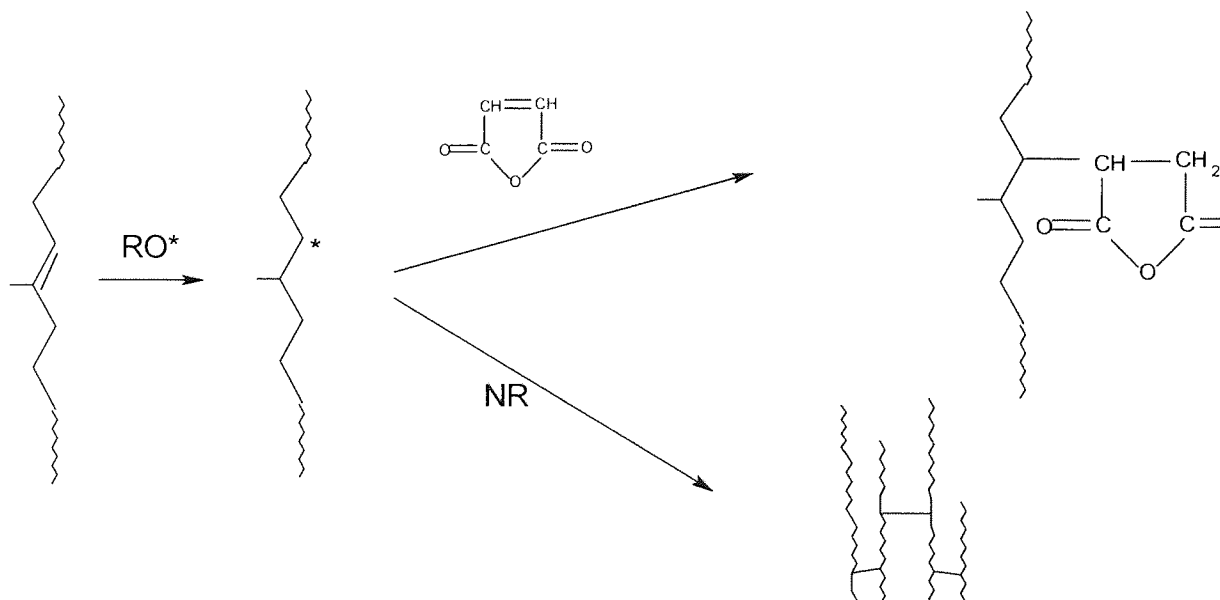




Table 4-1 The Experimental Conditions and Results

(a) Thermal Initiation in the absence of peroxide  
( Raw SMR-L without purification used)

Code	Composition		Processing Conditions			Grafting Degree (%)	Grafting Efficiency (%)
	SMR-L (phr)	MA (phr)	Rotor Speed (rpm)	Oil Temp. (C)	Mixing Time (min)		
A3-5	100	6	50	74	15	0	0
A3-6	100	6	50	90	15	0	0
A3-7	100	6	50	110	15	0	0
A3-8	100	6	50	150	15	0.4	6
A3-9	100	6	50	200	15	1.9	32
A3-10	100	6	50	220	15	2.5	42
A3-11	100	6	50	200	5	1.2	21
A3-12	100	6	50	200	10	1.9	32
A1-1	100	2	50	200	15	0.4	22
A2-1	100	4	50	200	15	1.4	35
A4-1	100	8	50	200	15	2.8	35
A5-1	100	10	50	200	15	2.9	29
A6-1	100	12	50	200	15	3.6	30
A7-1	100	14	50	200	15	4.1	30
A3-14	100	6	50	170	15	0.6	10

(b) Thermal Initiation in the absence of peroxide  
(Purified SMR-L used)

Code	Composition		Processing Conditions			Grafting Degree (%)	Grafting efficiency (%)
	Extracted SMR-L (phr)	MA (phr)	Rotor Speed (rpm)	Oil Temp. (C)	Mixing Time (min)		
AE3-2	100	6	50	90	15	1.2	20
AE3-3	100	6	50	110	15	0.6	10
AE3-4	100	6	50	130	15	1.3	21
AE3-5	100	6	50	150	15	2.1	36
AE3-6	100	6	50	180	15	2.2	37
AE3-7	100	6	50	200	15	2.9	48
AE3-10	100	2	50	200	15	1.2	61
AE3-11	100	4	50	220	15	2.0	49
AE3-12	100	8	50	200	15	3.8	48
AE3-13	100	10	50	200	15	4.5	45
AE3-14	100	12	50	200	15	5.0	42

Table 4-2 The Experimental Conditions and Results

(a) Peroxide initiation using BPO

Code	Composition			Processing Conditions			Grafting Degree (%)	Grafting Efficiency (%)
	SMR-L (phr)	MA (phr)	Peroxide (BPO) (phr)	Rotor Speed (rpm)	Oil Temp. (°C)	Mixing Time (min)		
C3-5	100	6	0.20	50	110	15	0	0
C3-6	100	6	0.40	50	110	15	0.2	4
C3-7	100	6	0.60	50	110	15	0.4	6
C3-8	100	6	0.80	50	110	15	0.3	5
C3-9	100	6	1.00	50	110	15	0.4	6
C3-10	100	6	0.20	50	130	15	0.3	6
C3-11	100	6	0.40	50	130	15	0.4	6
C3-12	100	6	0.60	50	130	15	0.6	10
C3-13	100	6	0.80	50	130	15	0.6	10
C3-14	100	6	1.00	50	130	15	0.5	8
C3-16	100	6	0.20	50	140	15	0.3	5
C3-17	100	6	0.40	50	140	15	0.2	4
C3-18	100	6	0.60	50	140	15	0.2	3
C3-20	100	6	1.00	50	140	15	0.5	9

Cont. Table 3-1 (b) Peroxide initiation using T101

Code	Composition			Processing Conditions			Grafting degree (%)	Grafting efficiency (%)
	SMR-L (phr)	MA (phr)	Peroxide (T101) (phr)	Rotor Speed (rpm)	Oil Temp. (°C)	Mixing Time (min)		
D3-42	100	6	0	50	140	15	0.4	7
D3-43	100	6	0.02	50	140	15	0.5	8
D3-44	100	6	0.04	50	140	15	0.7	12
D3-45	100	6	0.06	50	140	15	0.6	10
D3-46	100	6	0.08	50	140	15	0.6	10
D3-47	100	6	0.10	50	140	15	1.1	18
D3-48	100	6	0.12	50	140	15	1.0	17
D3-49	100	6	0	50	150	15	0.6	9
D3-50	100	6	0.02	50	150	15	1.0	16
D3-51	100	6	0.04	50	150	15	2.0	33
D3-52	100	6	0.06	50	150	15	1.7	28
D3-53	100	6	0.08	50	150	15	1.6	27
D3-55	100	6	0	50	160	15	1.1	18
D3-56	100	6	0.02	50	160	15	2.2	36
D3-57	100	6	0.04	50	160	15	2.5	41
D3-59	100	2	0.04	50	150	15	0.3	14
D3-60	100	4	0.04	50	150	15	0.6	15
D3-61	100	8	0.04	50	150	15	1.6	20
D3-62	100	10	0.04	50	150	15	1.5	15
D3-63	100	14	0.04	50	150	15	1.1	8
D3-65	100	2	0.02	50	160	15	0.3	16
D3-66	100	4	0.02	50	160	15	0.9	21
D3-67	100	8	0.02	50	160	15	2.2	28
D3-68	100	10	0.02	50	160	15	2.2	22
D3-69	100	14	0.02	50	160	15	1.7	12
D3-71	100	6	0.04	50	150	5	0.4	7
D3-72	100	6	0.04	50	150	10	0.5	9

Table 4- 3 Major absorption bands and probable functional assignments in the FTIR spectra of NR, MA, SA, SAN, MA-g-NR

Name	Peak (cm-1)	Intensity	Assignment	FTIR
NR	3033	weak	=CH stretching	Fig. 2-4
	2958,2852	very strong	CH <sub>2</sub> , CH <sub>3</sub> stretching	
	2725	weak	CH <sub>2</sub> stretching	
	1662	medium	C=C stretching	
	1448,1375	strong	CH <sub>2</sub> ,CH <sub>3</sub> deformation	
MA	1856	weak	C=O asymmetric stretching	Fig. 2-7
	1780	very strong	C=O symmetric stretching	
SAN	1860	medium	C=O asymmetric stretching	Fig. 2-15
	1782	very strong	C=O symmetric stretching	
SA	1698	strong	C=O stretching	Fig. 2-14
MA-g-NR	2725	Weak	CH <sub>2</sub> stretching (from NR chains) C=O symmetric stretching ( anhydride group from grafted MA) C=O stretching (acid group from grafted MA) C=C stretching (from NR chains)	Fig. 2-19 & Fig. 4-2
	1772	Shoulder		
	1710	Strong		
	1662	Strong		

Table 4-4 Determination of the amount of insoluble fraction in toluene

Sample	Composition NR/MA/T101 (phr)	Condition Speed (rpm) /temp.(°C) /time(min)	Grafting degree (%)	Extraction in toluene Insoluble fraction(%)
D3-42	100/6/0	50/140 /15	0.4	35
D3-51	100/6/0.04	50/150/15	2.0	74
A3-9	100/6/0	50/200/15	2.0	71

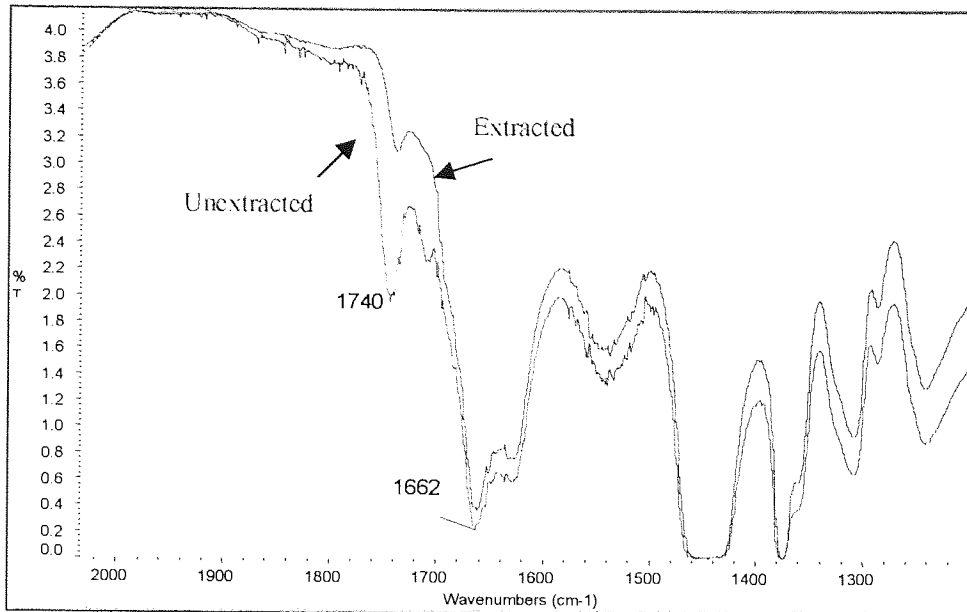


Figure 4-1 FTIR spectrum of extracted SMR-L (Extracted for 24 hours with acetone , pressed film: 150°C × 15 seconds)

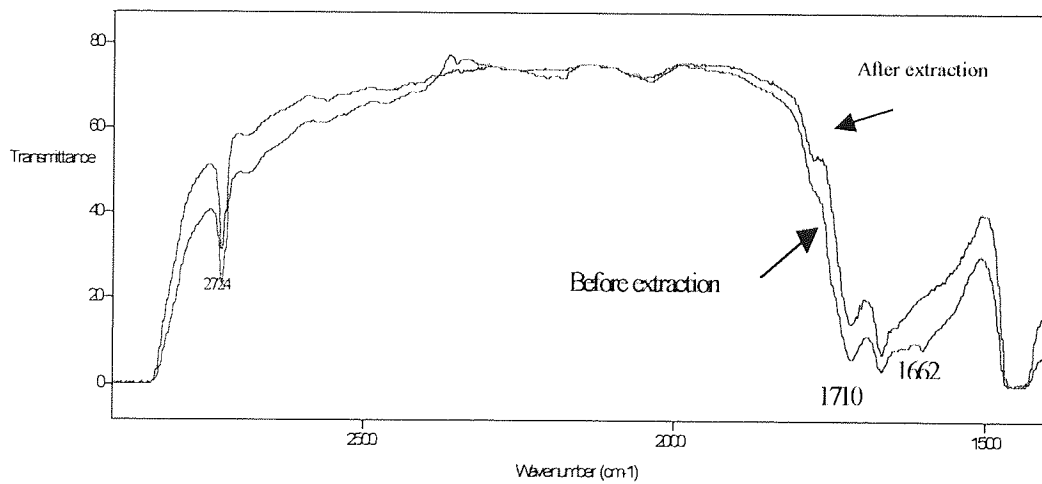


Figure 4-2 Comparison of spectra obtained from cured film both before extraction (film A) and after extraction (film B) with acetone for 24 hours (Sample A3-10: SMR-L 100 phr; MA 6phr; Temp. 220°C ; time 15 min )

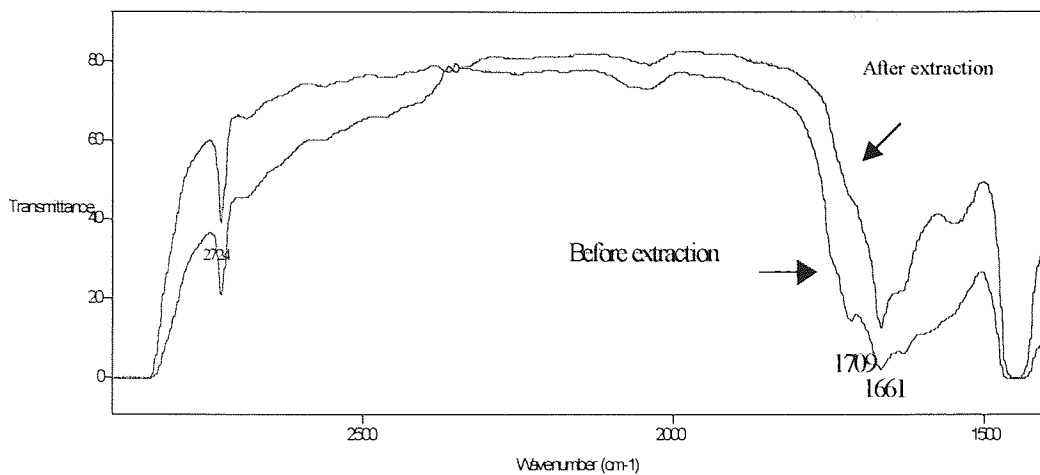


Figure 4-3 Comparison of FTIR spectra obtained from cured films both before extraction (film A) and after extraction in acetone (film B) for 24 hours (Sample A3-6: SMR-L 100 phr; MA 6 phr; Temp. 90 °C ; time 15 min)

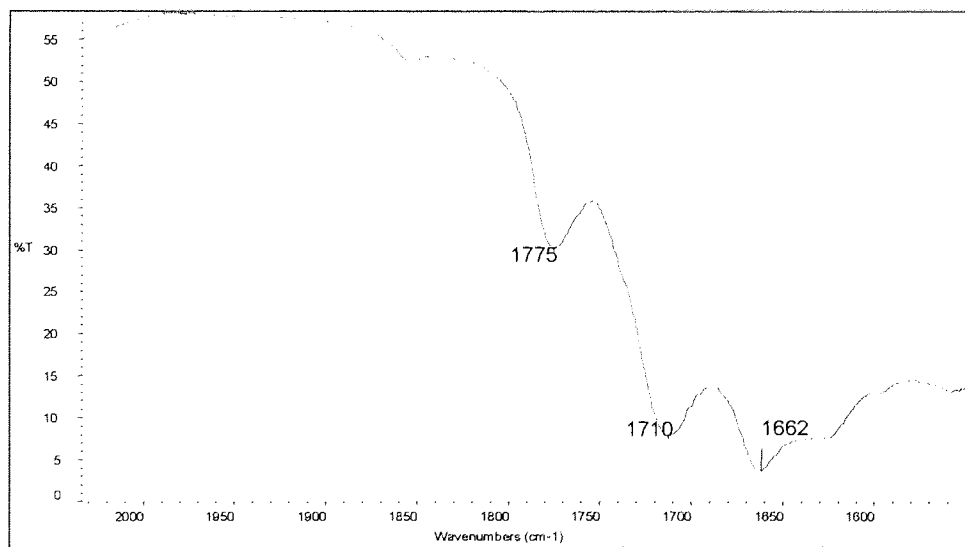


Figure 4-4 FTIR spectrum of MA modified natural rubber prepared by mixing MA and natural rubber on a two-roll mill

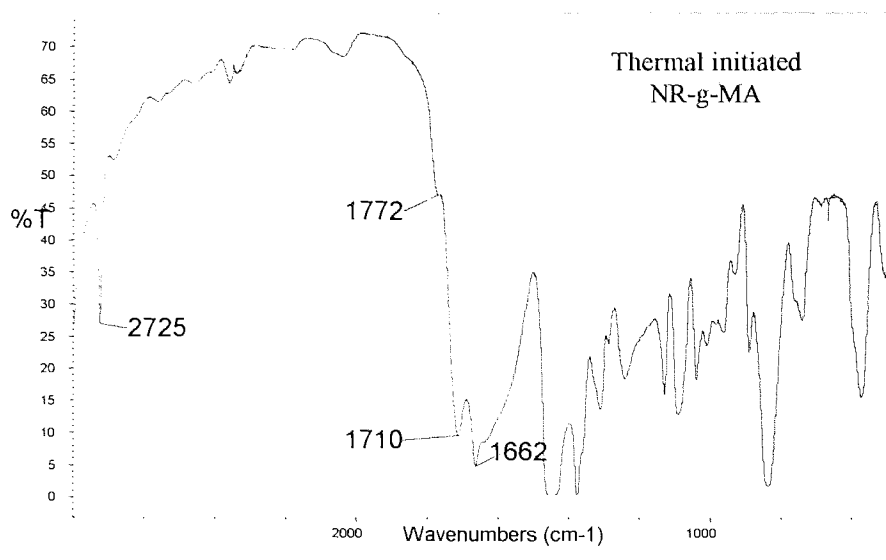


Figure 4-5 FTIR spectrum of MA grafted natural rubber (Thermal initiated—sample A3-9: SMR-L 100 phr; MA 6 phr; Temp. 200 °C ; time 15 min)

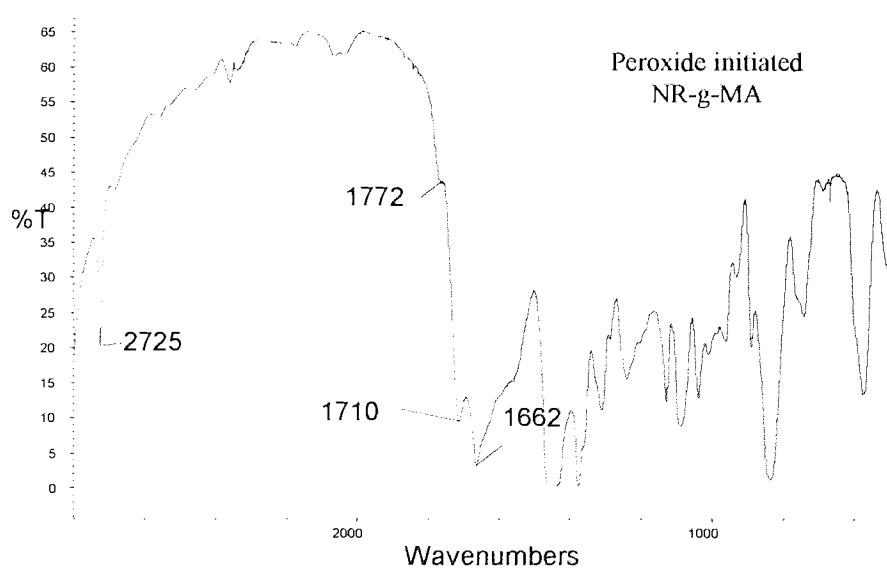


Figure 4-6 FTIR spectrum of MA grafted natural rubber (Peroxide initiated—sample D3-51: SMR-L 100 phr; MA 6 phr; T101 0.04phr, Temp. 150 °C ; time 15 min)



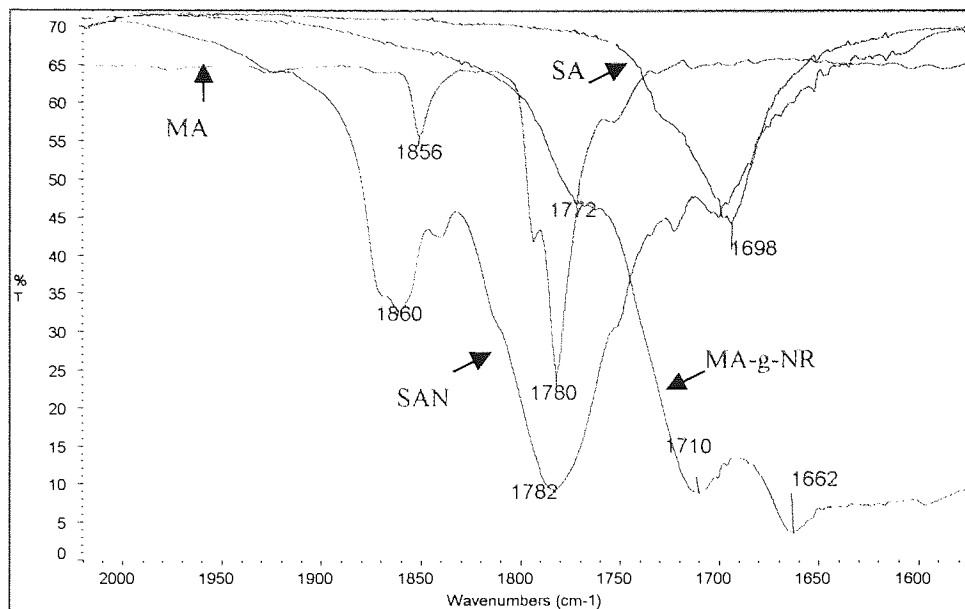


Figure 4-7 Comparison of FTIR spectra of MA grafted rubber with maleic anhydride, succinic anhydride and succinic acid)

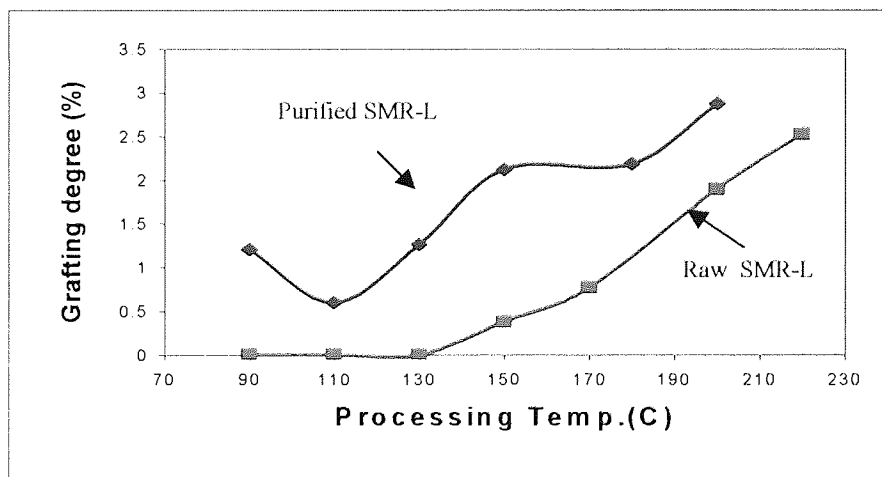
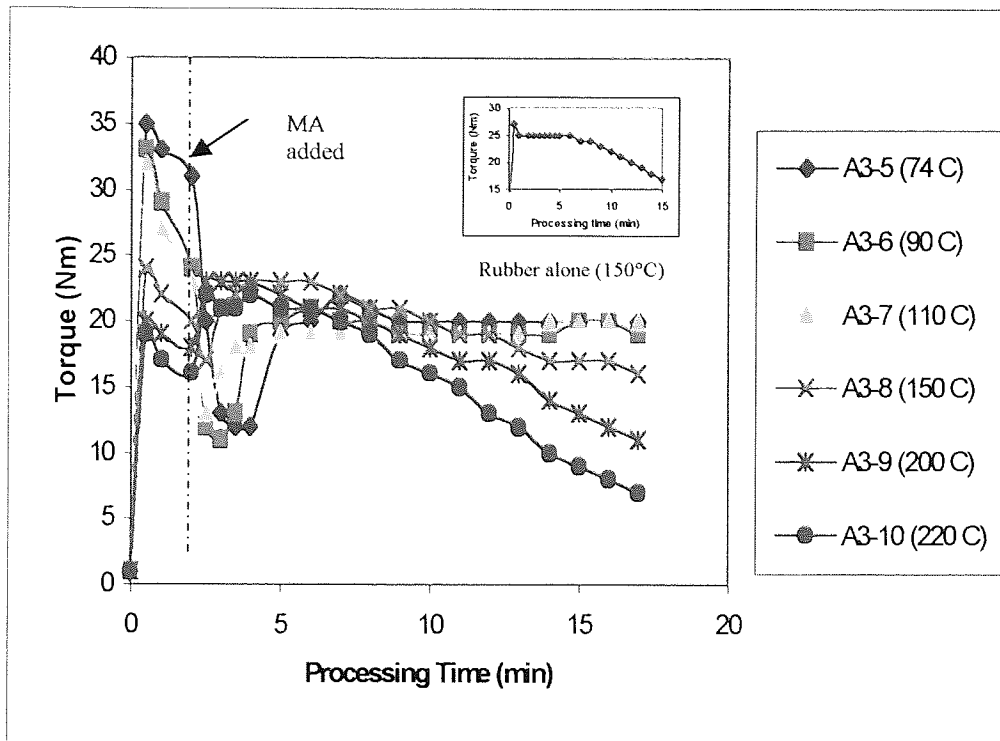
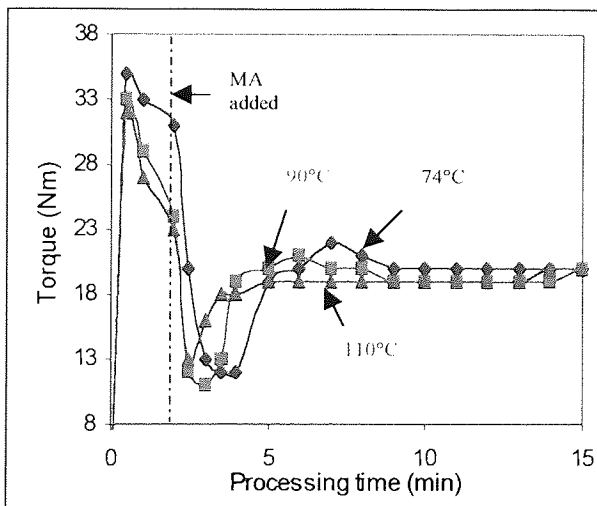


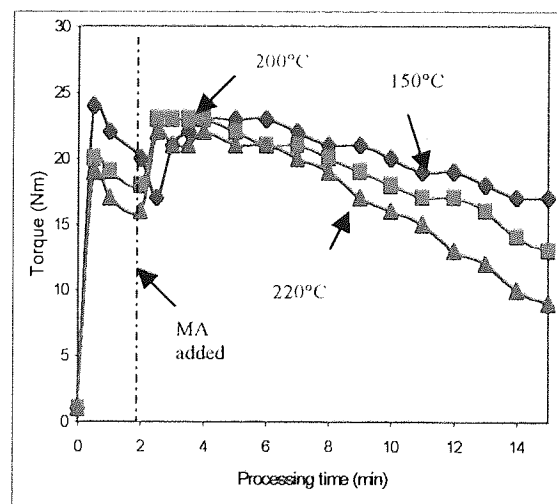
Figure 4-8 Effect of processing temperature on MA grafting degree (processing condition: SMR-L: 100 phr; MA: 6phr; no peroxide, mixing time: 15 min, speed: 50 rpm)



(a)

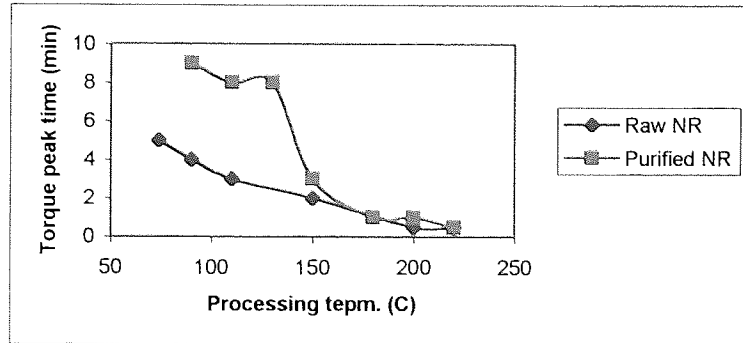


(b)

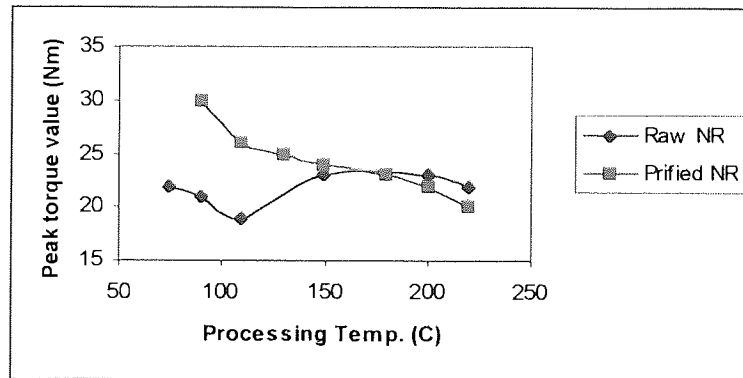


(c)

Figure 4-9 Torque-time curves— (a) samples A3-5 ~ A3-10 (Raw SMR-L (100phr), MA(6phr), no peroxide, 15 min, (A3-5 74°C, A3-6 90°C, A3-7 110°C, A3-8 150°C, A3-9 200°C, A3-10 220°C) ), (b) low processing temperature (samples A3-5 ~ A3-7), (c) high processing temperature (samples A3-8 ~ A3-10)



(a) Effect of processing temperature on peak time (from the addition of MA)



(b) Effect of processing temperature on peak torque value

Figure 4-10 Effect of processing temperature on peak time and peak torque value of raw and purified NR processed with MA (6 phr) and no peroxide for 15 min effect of processing temperature on peak time, (b) effect of processing temperature on peak torque value

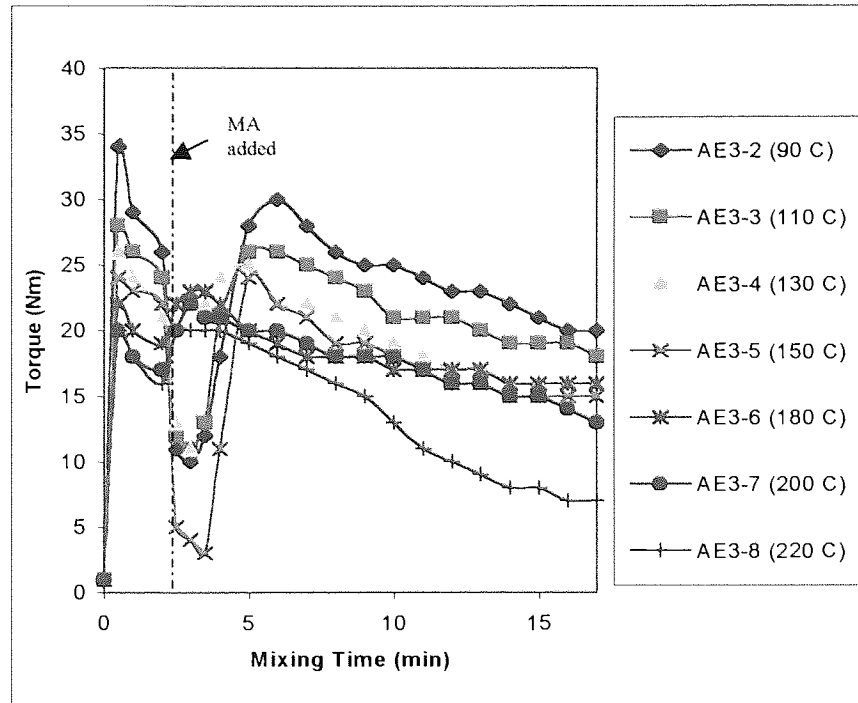


Figure 4-11 Torque-time curves—Purified SMR-L(100phr), MA(6 phr), no peroxide, 15 min. (AE3-2 90°C, AE3-3 110°C, AE3-4 130°C, AE3-5 150°C, AE3-6 180°C, AE3-7 200°C, AE3-8 220°C)

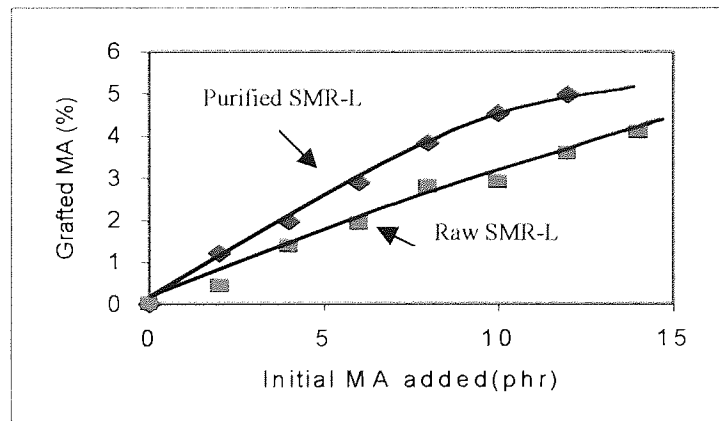


Figure 4-12 Effect of MA concentration on MA grafting degree (Processing conditions: processing temp. 200°C, mixing time: 15 min, speed: 50rpm)

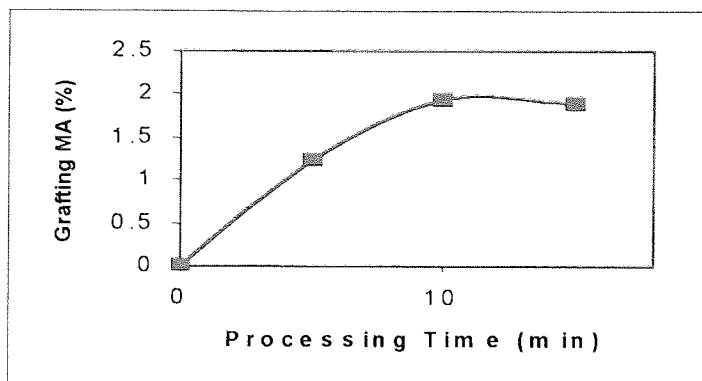


Figure 4-13 Effect of processing time on MA grafting degree (Processing conditions: raw SMR-L 100phr, MA 6phr, processing temp. 200°C, speed: 50rpm)

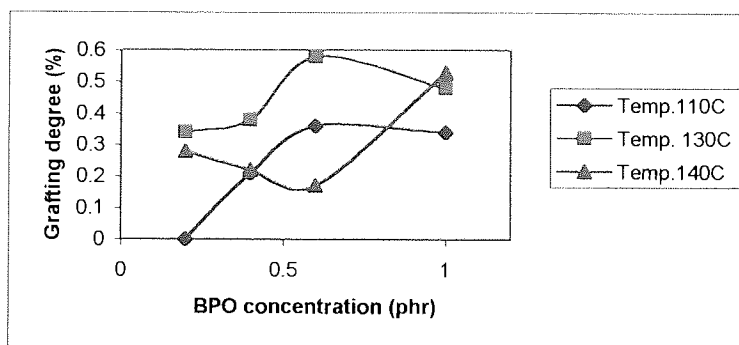


Figure 4-14 Effect of BPO concentration on MA grafting degree( Raw SMR-L 100 phr, MA 6 phr, processing time 15 min, speed: 50rpm)

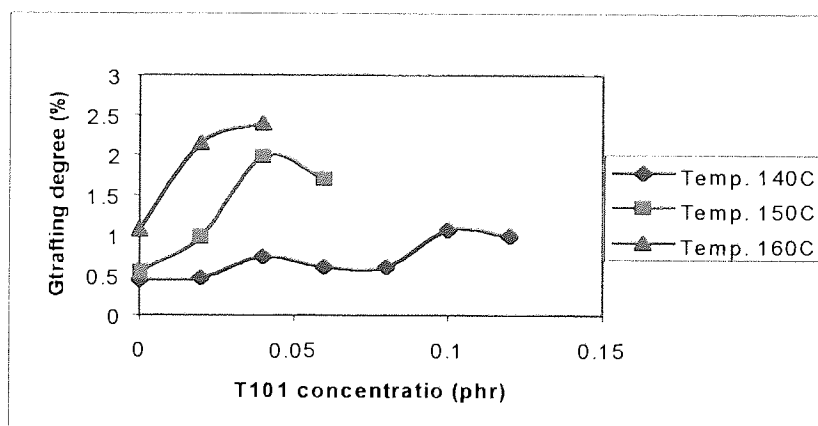


Figure 4-15 Effect of T101 concentration and processing temperatures on MA grafting degree( raw SMR-L 100phr, MA 6 phr, processing time 15 min, speed: 50rpm)

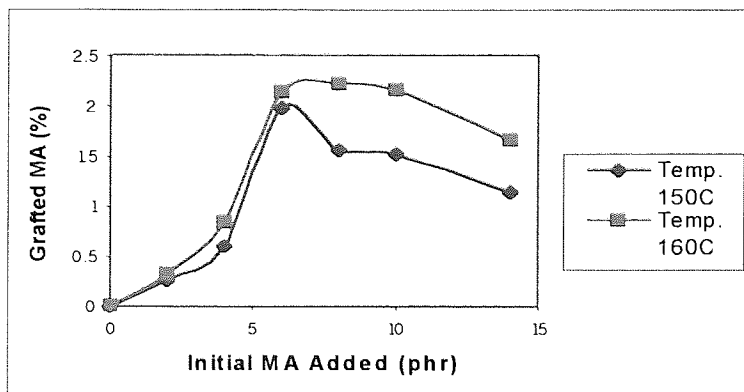


Figure 4-16 Effect of MA concentration on MA grafting degree (Processing conditions: raw SMR-L 100 phr , and T101 0.04 phr for processing temp. 150 °C, 0.02 phr for 160°C, mixing time: 15 min, speed: 50rpm)

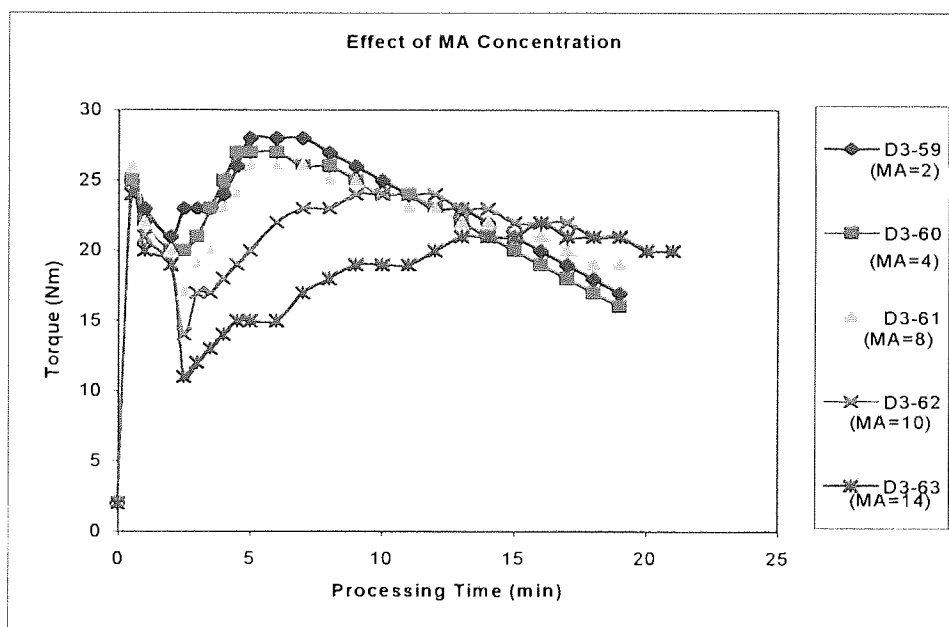


Figure 4-17 Torque-time curves—Raw SMR-L:100phr, T101: 0.04 phr, temp.: 150°C, time:15 min. (D3-59, 2 phr MA; D3-60, 4 phr MA; D3-61, 8 phr MA; D3-62, 10 phr MA; D3-63, 14 phr MA)

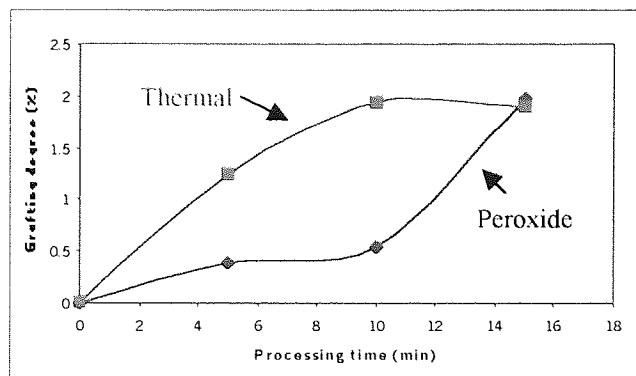


Figure 4-18 Effect of processing time on MA grafting degree (by peroxide: raw SMR-L 100 phr, MA 6phr, T 101 0.04phr, temp. 150°C, speed 50rpm; by thermal: raw SMR-L 100 phr, MA 6phr, temp. 150°C, speed 50rpm)

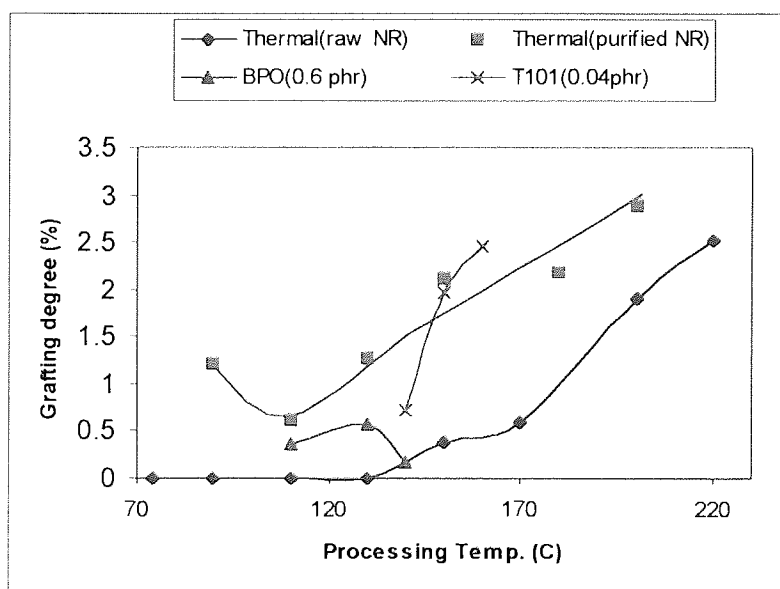
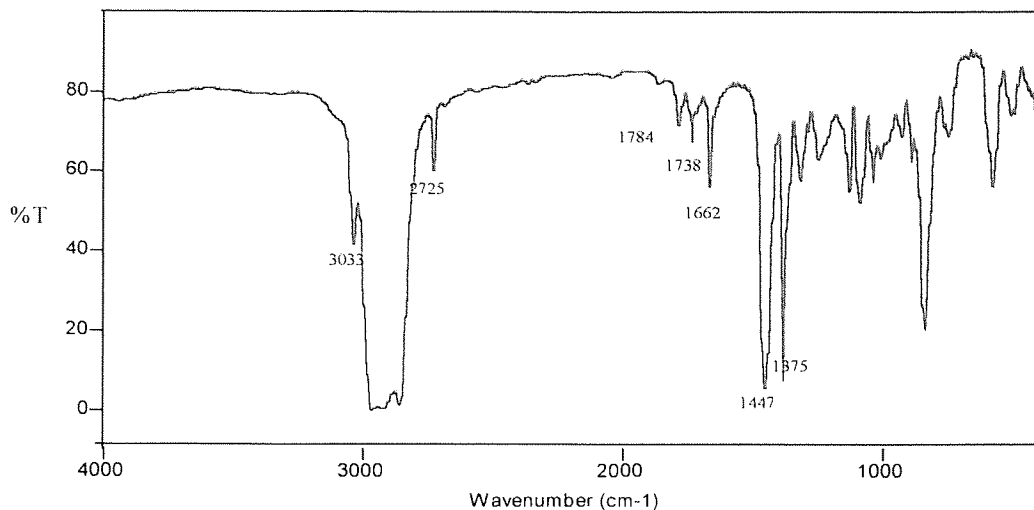
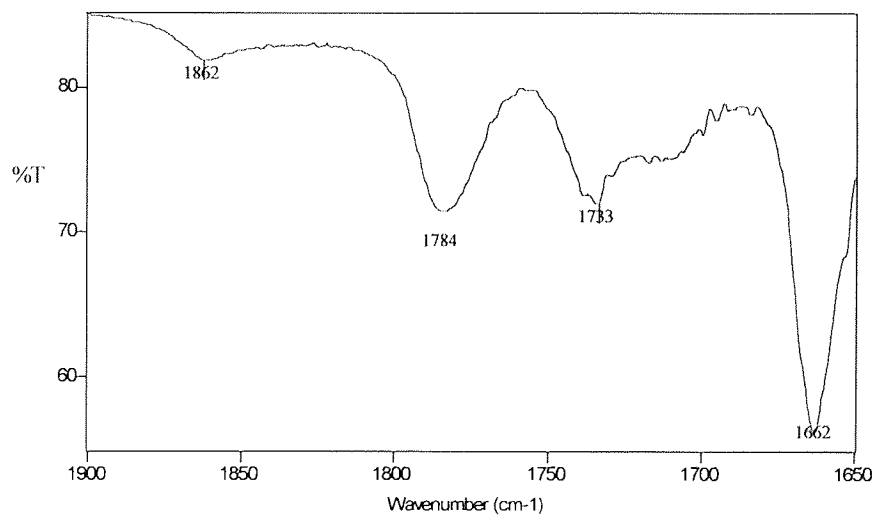


Figure 4-19 Comparison of effect of processing temperature on MA grafting degree by different initiation techniques (processing condition: SMR-L 100 phr, MA 6phr, processing time 15min, speed 50rpm)



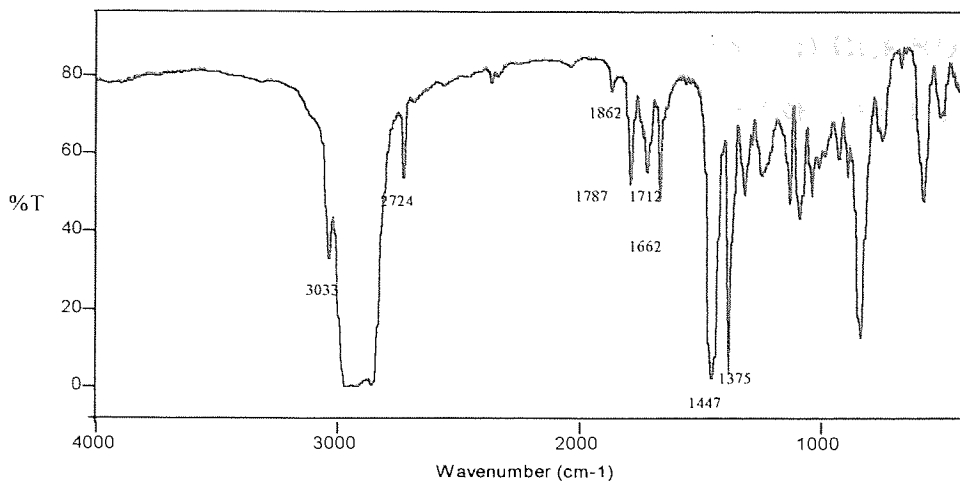
(a) Full spectrum



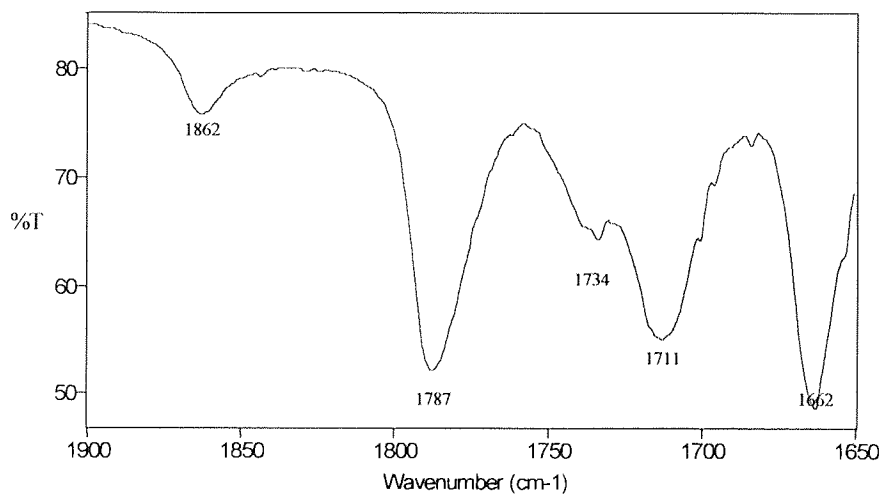
(b) Enlarged portion

Figure 4-20 FTIR spectrum of soluble fraction in toluene of reaction product casted from solution using KBr disc(Sample D3-51)(peroxide initiated product; T101 (0.04phr), MA (6 phr), 150°C )





(a) Full spectrum



(b) Enlarged portion

Figure 4-21 FTIR spectrum of soluble fraction in toluene of reaction products cast from solution using KBr disc(Sample A3-9) (thermal initiated product; MA 6 phr, 200°C)

## CHAPTER 5 REACTIVE COMPATIBILISATION OF POLY(ETHYLENE TEREPHTHALATE) BASED BLENDS USING GLYCIDYL METHACRYLATE FUNTIONALISED POLYOLEFINS

### 5.1 OBJECTIVE AND METHODOLOGY

Blending of two or more polymers has been an effective and powerful technique to obtain a new polymeric material with desirable mechanical properties [17,18] and poly(ethylene terephthalate) (PET) has been used recently in blends with other polymer, especially polyolefins, for the purpose of property modification, new materials or recycling have received considerable interest [4-8]. As discussed in Chapter 1 Sections 1.3 and 1.4, the compatibilisation of polymer blends is the key to achieving the required properties and performance and the reactive blending has attracted great attention and has been used widely for this purpose. In-situ copolymers are produced through interfacial reactions between reactive polymers directly during blending and these act to compatibilise polymer blends. The morphology of incompatible polymer blends with an in-situ compatibiliser becomes very fine, since copolymers formed by the reaction between functional groups existing in constituent components in the blend can reduce the interfacial tension between the dispersed phase and the matrix. This finer morphology can persist even at higher shear stresses [33,34]. The in-situ, or reactive, compatibilisation method is more attractive and cost-effective because it allows to produce compatibilisers in-situ at the interfaces without separate preparation step. When two polymers are to be compatibilised and only one contains functional groups and the other one is chemically inert, the inert polymer must be functionalised so that it becomes compatible with the functional polymer that bears reactive groups capable of chemical reaction with the functionalised polymer.

PET and PBT polymers contain two types of terminal groups: carboxylic and hydroxyl ( $-\text{COOH}$ ,  $-\text{OH}$ ) which can readily react with many functional groups such as anhydride, epoxy, oxazoline, isocyanate and carbodiimide attached onto a second polymer leading to graft copolymers formation during melt blending [16]. This approach has gained great success for the in situ compatibilisation of PET or PBT blends with polyethylene [7, 10, 32, 36, 49, 54-56], polypropylene [26, 29-31, 40,41, 45-48, 57-62], polystyrene [33-35,50],

EPDM [22,23,63]. It was reported that polyester-based reactively compatibilised blends are the second largest group of blends after polyamide-based blends [64].

To achieve the second objective of this work, compatibilisation of PET blends (based on virgin PET) with GMA-functionalised rubbers via reactive blending was examined. The compatibilisation strategy involved the in situ formation of copolymers through the reactions between the end groups (carboxyl and hydroxyl) of PET and the functional groups grafted onto the rubbers, e.g. grafted GMA, during melt blending. The functionalisation of rubbers, e.g. EP-g-GMA, EPDM-g-GMA, and EPDM/PP-g-GMA, had been carried out in an internal mixer in the absence and presence of the comonomer, TRIS, as discussed in Chapter 3. In this part of the study, the compatibilising effects of these GMA functionalised-rubbers with PET was investigated. The PET blends were characterised in terms of morphology, dynamic mechanical properties, tensile properties and the interfacial reactions.

Blending PET with EP, EPDM and GMA functionalised EP and EPDM was carried out in the torque rheometer. The mixing temperature, rotor speed and mixing time were fixed at 275°C, 65rpm and 10 minutes. A series of GMA functionalised rubber samples with different grafting degrees, different melt viscosities (e.g. different MFI values) and different grafting systems, were used to blend with PET at ratios of 50/50, 60/40 and 80/20 PET/rubbers. Table 5-1, 5-3 lists the blends' compositions and blending conditions. The compatibilisation of these blends was then assessed in terms of morphology, dynamic mechanical properties, tensile properties and interfacial reaction characterisation (see Scheme 5-1). To get better understanding of the effect of the interfacial reactions between PET end groups and grafted functional groups (GMA) of the functionalised rubbers on compatibilisation, the blends were fractionated by using different solvents and the copolymers formed during melt blending were isolated and characterised by FTIR spectroscopy.

## 5.2 RESULTS

### 5.2.1 Compatibilisation of PET with GMA Grafted EP

#### 5.2.1.1 Processing Characteristics

The processing characteristics of the blends have been studied from the torque-time curves recorded during the blending. In this study, three types of GMA functionalised EP were used, i.e. 1) prepared in single monomer system (GMA+T101) at high temperature; 2) prepared in the presence of TRIS (GMA +TRIS+T101); 3) prepared in single monomer system at low temperature (GMA+T29B90) (For details, see Chapter 3.2.4-3.2.5). A series of EP-g-GMA samples were prepared (see Table 5-1 (a) for the composition and processing condition) and blended with PET in three weight ratios (PET/EP-g-GMA: 80/20, 60/40, 50/50) (see Table 4-1 (b) for compositions). For all runs, the rotor speed, processing temperature (heating oil temperature) and blending time were kept at 65 rpm, 275°C and 10 min.

In all cases, the mixing torque falls rapidly within 1 minutes with the melting of PET and the rubbers and then decreases gradually. Figures 5-1 and 5-2 show the torque-time curves for PET with virgin EP and EP-g-GMA (GR-42) (prepared in the presence of TRIS) in three different weight ratios. When PET was blended with virgin EP, the torque level was just slightly higher than that with PET alone. No big difference was observed with the three different weight ratios of PET to virgin EP (PET/EP=80/20, 60/40, 50/50) (see Figure 5-1). Though virgin EP has a higher viscosity than PET, the degradation of EP may reduce the effect of viscosity of EP so higher portion of EP did not lead to an obvious increase in torque. Even when EP-g-GMA sample (GP-32) was blended with PET, the increase of the rubber weight ratio from 20% to 50% (PET/EP-g-GMA weight ratios: 80/20, 60/40, 50/50) only slightly increased the torque (see Figure 5-2).

Generally, the torque value became higher when EP-g-GMA was blended with PET compared to blends of PET with virgin EP. It is proposed that the increase of torque results from the reaction of epoxy group (grafted GMA onto the rubber chains) with the functional groups from PET (–COOH, –OH) during the reactive blending at a high temperature (see Scheme 5-2). Such reactions lead to the formation of copolymer of PET-co-EP as a type of

branching reaction or even crosslinking. As a result, higher torque values were observed during the mixing, indicating an increase in the viscosity of the blends. Other research workers have also reported such a phenomena [37,38,39,40]. So the torque curves can reflect the extent of reactions which takes place during the reactive blending step. However, it is shown that the three different types of EP-g-GMA samples, (i.e. GMA+T101 system, denoted as EP-g-GMA<sub>T101</sub>, GMA+T101+TRIS system, denoted as EP-g-GMA<sub>TRIS</sub>, and GMA+T29B90 at low temperature system, denoted as EP-g-GMA<sub>T29B90</sub>), have different effects on the torque curves due to their different grafting structure characteristics resulting from different grafting mechanisms.

### ***PET/EP-g-GMA<sub>T101</sub> blends***

When GMA was grafted onto EP in GMA+T101 system, it was found that homopolymerisation of GMA was a strongly competing with the desired GMA grafting reaction, especially at a high processing temperature in systems containing high concentrations of GMA and T101. As a consequence, both grafted GMA and polyGMA are present in these samples. When these samples were used for blending with PET, the torque dropped sharply within the first minute, then increased slightly but stayed at this value for a couple of minutes. Following this plateau, the torque decreased gradually and levelled off (see Figure 5-3). It was observed that the blend was very viscous after 10 minutes mixing and was not easily compression moulded into thin sheets with the rough surfaces of the sheets, especially when higher weight ratio of the rubber phase (50/50) in the blend was used. It is obvious that a significant branching or even crosslinking does take place during the blending with PET due to the presence of polyGMA in the EP-g-GMA<sub>T101</sub>. The multi-epoxy groups from polyGMA can also react with the end groups of PET and may cause branching or/and crosslinking of PET phase. To prove the reaction of polyGMA with PET, 4% synthesised polyGMA was added to PET and processed under the same condition as those used for blending. The torque level was significantly higher than PET alone, especially in the first couple of minutes' mixing (see Figure 5-3). After the mixing, the polymer became very viscous and looked like becoming crosslinked. To further analysis the effect of poly GMA in the EP-g-GMA<sub>T101</sub> on the compatibilisation of PET with EP-g-GMA<sub>T101</sub> blends, the purified EP-g-GMA<sub>T101</sub> (sample GP-11) in which the polyGMA was removed by precipitation method was used to blend with PET. This sample which was prepared with 18 phr GMA and 1 phr T101 at 190°C (grafting degree: 1.6%, polyGMA: 2.7 %) was dissolved in toluene and

then precipitated into 7 times excess acetone. After drying, the purified sample did not contain any polyGMA. When this sample was blended with PET (PET/ EP-g-GMA<sub>T101</sub> =80/20), the torque level is shown to be lower than that of unpurified EP-g-GMA<sub>T101</sub>, and no torque increase and plateau were observed (see Figure 5-3). The torque decreased gradually and finally levelled off. The blend looked like a normal molten polymer when the chamber was opened after mixing. It was demonstrated that polyGMA in the EP-g-GMA samples has a very adverse effect on the blends' melt properties and processing properties so polyGMA should be removed from the samples or the processing conditions should be optimised to avoid the formation of polyGMA in the reactive grafting process of GMA. Furthermore, these experiments illustrate that the reaction of epoxy group of polyGMA with carboxylic acid group of PET must be quite fast at such a high temperature during the blending.

#### ***PET/EP-g-GMA<sub>TRIS</sub> blends***

When the functionalised EP samples were prepared in the presence of TRIS (EP-g-GMA<sub>TRIS</sub>), very low amount of polyGMA was measured or even no polyGMA was detected at the optimised processing conditions while high grafting degree was achieved (see Chapter 3 Section 3.2.5, p106). Two sets of samples were prepared by varying the concentrations of GMA, T101 and TRIS to obtain different grafting degree or different melt viscosity. One set of samples was chosen to have similar viscosity (e.g. similar MFI value) but different grafting degree (see Table 5-1 (a), samples GR-40, GR-41, GR-42, GR-44), whereas another set was chosen to have similar grafting degree but different melt viscosities (different MFI value) (see Table 5-1 (a), samples GR-32, GR-6, GR-8). It was found that PET/EP-g-GMA<sub>TRIS</sub> blends did not show any sign of crosslinking. However, the GMA grafting level and MFI of EP-g-GMA<sub>TRIS</sub> samples have certain effect on the torque level. If EP-g-GMA samples have similar MFI value, but different level of grafting, higher grafting level gave rise to higher torque during the blending with PET (see Figure 5-4). Higher grafting levels can result in more reaction of the epoxy group of the functional rubber with PET and may produce more copolymer of PET-co-EP. This interfacial reaction increases the viscosity of the blends.

### *PET/EP-g-GMA<sub>T29B90</sub> blends*

As mentioned before, the structure of the grafted GMA in samples which were prepared with GMA+T29B90 system at low temperature (115°C) may be quite different from that of the grafted GMA in the samples prepared at high temperature via melt free radical grafting mechanism. Indeed, these samples gave rise to much lower torque level during the blending was measured (see Figure 5-5) though the rubber samples had much higher grafting level (see Chapter 3 Section 3.2.4, p102).

#### **5.2.1.2 Morphology Observation**

The morphology is a very important factor to determine the blends' mechanical properties. Morphology of the blends was characterised from a cross-section of cryogenically fractured surfaces of compression moulded plaques by using a scanning electron microscope. To get better observation, the fractured surfaces were all subjected to etching in boiling toluene to extract the EP phase before SEM observation.

#### ***Morphology of PET/EP Blends***

The morphology of heterogeneous polymer blends depends on blend composition, viscosity of individual components and processing history. With the same processing history, the morphology is determined by the melt viscosity ratio and the composition. Generally, the least viscous component is likely to form the continuous phase. The SEM micrographes of the blends of PET with virgin EP in the ratios of 80/20 and 60/40 are shown in Figure 5-6 (a) and Figure 5-9 (a). In the PET/EP=80/20 blend, EP was found to be the dispersed domains in the continuous PET matrix (Figure 5-6 (a)). This is due to the higher viscosity and lower content of EP compared to PET in the blends. As the rubber content of EP in the blends increases from 20 to 40 w%, the EP was found to be still present as the dispersed phase but the domain size varied greatly (Figure 5-9 (a)) and becomes unstable. Coarse dispersion and poor adhesion at phase boundaries were observed. This is due to their immiscibility and significant difference of chemical and physical properties. When the EP content was increased to 50wt%, the fractured samples could not be etched in boiling toluene because they were dissolved in the hot toluene and

resulted in cloudy solution with some white particles (i.e. PET particles). This demonstrates that in 50/50 w/w blends the EP is not the dispersed phase anymore, it may have become the continuous phase.

### *Morphology of PET/EP-g-GMA (80/20 w/w) blends*

When 20 wt% EP-g-GMA samples were blended with 80 wt% PET, the rubber phase was dispersed finely in the continuous PET matrix. Fine dispersion and good adhesion at phase boundaries could be observed but their effectiveness depends on many factors including the GMA grafting level, melt viscosity, amount of polyGMA.

#### a) Effect of GMA grafting degree on the dispersion of EP-g-GMA in the blends

In this particular blending system of PET/EP-g-GMA, the compatibilisation mechanism is based on the reaction of the epoxy group from grafted GMA with the end groups of PET ( $-\text{COOH}$ ,  $-\text{OH}$ ) to form copolymer of PET and EP during the reactive blending. The copolymer can act as an emulsifier which locates at the interface so the interfacial tension in the melt can be reduced leading to an extremely fine dispersion of one phase in another. This can also increase the adhesion at the phase boundaries, giving an improved stress transfer and a stabilised dispersed phase against growth during annealing, again by modifying the phase boundaries interface. The grafting degree of GMA in the EP-g-GMA should play a very important role in the reactive blending of PET with EP-g-GMA. The size of the particles of the dispersed phase is expected to depend on the melt viscosities of the dispersed and matrix phases, the shear rate applied during processing, and interfacial tension [22,39]. When a set of samples of EP-g-GMA<sub>TRIS</sub> with similar MFI value but different GMA grafting degrees (samples GR-40, GR-41, GR-42, GR-44 in Table 5-1 (a)) were blended with PET at a weight ratio of 80/20, the effect of GMA grafting degree on the morphology of the 80/20 PET/EP-g-GMA blends is clearly shown by the scanning electron micrographs of Figure 5-6. Figure 5-6 (a) shows SEM of PET blended with unmodified EP (virgin). It is clearly seen that EP is dispersed as spherical particles (semi-spherical holes observed after the EP was etched) in the continuous PET phase. Due to the high interphase tension and coalescence, EP domains were in spherical form and the interfacial boundaries were very clear and sharp. The coarse dispersion and poor adhesion



at phase boundaries indicate its immiscibility and incompatibility due to the significant difference of chemical and physical properties between PET and EP.

Figure 5-6 (b-e) shows the SEM of blends of PET with GMA modified EP containing different levels of grafting with similar melt viscosity. Four samples of GMA grafted EP prepared in the presence of TRIS had similar MFI value of about 1.0 with GMA grafting levels of 1%, 2.4%, 2.5% and 3.1%, respectively (samples GR-40, GR-41, GR-42, GR-44 in the Table 5-1 (a)) and blended with PET. The more functionality in the rubber phase, the more reaction should take place between EP and PET phases during the reactive blending and more copolymers of EP-co-PET might be formed. It is clear from the SEM pictures that the higher the GMA grafting degree, the finer the dispersed rubber phase is. Compared with PET/EP blend, a significant reduction of the domain size of the rubber phase was observed in PET/EP-g-GMA blends. When the sample with grafting degree of 1% was blended with PET, an obvious reduction of the rubber domain size could be observed (Figure 5-6 (b)). As the grafting increases to 2.4 %, a significant improvement of the dispersion of rubber phase in the PET was achieved (Figure 5-6 (c)). With further increase of the grafting degree to 3.1%, no additional reduction in the domain size of the rubber phase could be observed (Figure 5-6 (d-e)). It can be concluded that about 2% grafting of GMA in the rubber phase is enough for the interfacial chemical reaction. Though high amount of grafted GMA enhances the reaction between the two phase, the formed EP-co-PET may not be certainly located at the interfaces so the emulsifying effect of copolymer is limited and the particle size also depends on other factors, such as the viscosity ratio of the blending components [39].

#### b) Effect of viscosity of EP-g-GMA on the dispersion of EP-g-GMA in the blends

During the functionalisation of EP with GMA, the viscosity of EP can be increased in the presence of peroxide. However, the viscosity of the rubber component is a very important factor for the dispersion of rubber in the PET blend. The main mechanism governing the morphology development is believed to be the results of both droplet breakup and coalescence. In studies on nylon/rubber blending, Wu suggested a minimum particle size when the viscosities of the two phases were closely matched [22]. In PET/EP blending system, EP has a higher viscosity than PET. The increase of viscosity of modified EP during the melt grafting resulted in much bigger difference of viscosity between the two

phases. A set of EP-g-GMA samples with different viscosities (MFI from 1.0 to 0.1) but containing a similar grafting level (about 2.0%) (see Table 5-1 (a), samples GR-32, GR-6, GR-8 )) were prepared in the presence of TRIS and the morphology of their blends with PET is shown in Figure 5-7. It was found that the higher the viscosity of the rubber phase, the larger the rubber domain size is (see Figure 5-7). The higher viscosity (lower MFI) of functionalised EP increases the viscosity difference between the two polymers so the higher viscosity polymer becomes more difficult to disperse in the lower viscosity polymer matrix under the same blending condition.

### c) Effect of polyGMA on the dispersion of EP-g-GMA in the blends

It was found that polyGMA was formed in GMA modified EP (EP-g-GMA<sub>T101</sub>) as a result of side reaction of grafting of GMA in the presence of the peroxide, T101. To investigate the effect of polyGMA on the dispersion of rubber phase in PET matrix, one sample of EP-g-GMA<sub>T101</sub> was prepared, in which 3% of polyGMA was formed with 1.6% grafting degree (sample GP-11 in the Table 5-1 (a)). Part of this sample was purified to remove the polyGMA using a precipitation procedure as developed for the determination of grafting degree of GMA in EP-g-GMA. Both the unpurified and purified samples were blended with PET under the same condition and their SEM micrographes are shown in Figure 5-8. It was demonstrated that both blends had finer dispersion of the rubber phase when compared to physical PET/EP blends, but the dispersion of the purified samples with no polyGMA was much finer than that of the unpurified sample. It is clear that the polyGMA has an adverse effect on the dispersion of the rubber phase of the blend. The reason for this may be attributed to the fact that polyGMA can also react with the end groups of PET (-COOH, -OH) like the grafted epoxy groups. The torque-time curves of the blending give a clear evidence of the reaction as shown in Figure 5-3. If the GMA modified EP contains polyGMA, it will compete with the desired reaction of grafted epoxy groups with the end groups of PET to form PET-co-EP copolymer and reduce the compatibilising effect as observed from SEM (Figure 5-8). The crosslinking effect of polyGMA adversely affect the rheological properties of the blends for sequent moulding or further processing performance. Based on the results of morphology and torque-time curves, removal of polyGMA from the EP-g-GMA samples or avoiding its formation in the reactive grafting process is very critical measure to ensure a better compatibilisation of EP with PET.

### ***Morphology of PET/EP-g-GMA (60/40 w/w) blends***

As the unmodified EP contents in the blends increases from 20% to 40%, the rubber phase is shown still to be dispersed in the continuous PET phase, but the domain size significantly increases and size distribution vary significantly (see Figure 5-9 (a)). This is attributed to the reagglomeration or coalescence of the dispersed rubber particles. Sharp and clear interfacial boundaries also indicate the immiscibility and incompatibility. When GMA grafted EP (samples GP-20, GR-42, GR-44 and BP-3 in the Table 5-1 (a)) was blended with PET, much finer dispersion of the rubber phase was observed (see Figure 5-9 (b)-(d)). However, great difference in the morphology of the blends with different types of GMA grafted EP was found. When PET was blended with EP-g-GMA<sub>T101</sub> prepared in GMA+T101 system (sample GP-20: grafting: 1.3%, polyGMA: 1.1%), EP-g-GMA was dispersed with smaller domain size but the interfacial boundaries were very clear. Lower grafting level and the presence of polyGMA in the rubber phase can reduce the interfacial reaction. In contrast, EP-g-GMA<sub>TRIS</sub> prepared in GMA+TRIS+T101 system (sample GR-44: grafting: 3%, polyGMA: ~0%) had higher grafting level with no measurable polyGMA. The SEM of the blends shows rough interfacial boundary surface and good adhesion at interfaces. This may be due to the high grafting level of GMA leading to strong interphase reaction. It was noted that when EP-g-GMA<sub>T29B90</sub> was blended with PET, rubber phase dispersed as well defined spherical particles (semi-spherical holes observed after the EP was etched) in the continuous PET phase and the interface was very clear. Though this EP-g-GMA<sub>T29B90</sub> sample has extremely high grafting degree of 6%, it seems that no obvious interfacial reaction does take place. This is reflected from the low torque values observed during the mixing (see Figure 5-5) and smooth and clear interface (see Figure 5-9 (d)).

#### **5.2.1.3 Dynamic Mechanical Properties**

Dynamic mechanical thermal analysis (DMTA) is a good technique for the study of the compatibilisation of polymer blends and the effect of compatibilisation on the dynamic mechanical properties of various polymer blends have been reported [8,142-145]. Generally, for an incompatible blend, the  $\tan\delta$  Vs temperature curve shows the presence of two  $\tan\delta$  or damping peaks corresponding to the glass transition temperatures of the

individual polymers [146]. For a highly compatible blend the curve shows only a single peak in between the transition temperatures of the component polymers, whereas there are still two separate peaks corresponding to the individual polymers in the case of partially compatible polymer blends, but the position of the peaks should be shifted to higher or lower temperature as a function of compositions [144].

The dynamic mechanical properties such as storage modulus ( $E'$ ) and  $\tan\delta$  of the pure components and the blends were measured from  $-80^\circ\text{C}$  to  $180^\circ\text{C}$ . Figures 5-10 and 5-11 show the variation of  $E'$  and  $\tan\delta$  Vs temperature for the virgin EP and virgin PET. The  $\tan\delta$  curve of EP shows a peak at  $-24.5^\circ\text{C}$  corresponding to the glass transition of EP, whereas a peak of  $\tan\delta$  curve for PET was recorded at  $94^\circ\text{C}$  corresponding to the glass transition of PET. The  $E'$  curve of EP shows the typical viscoelasticity properties of unvulcanised elastomer. At low temperature below glass transition, high modulus was measured. The storage modulus dropped 2-3 orders of magnitude in the glass transition zone from  $-50$  to  $-10^\circ\text{C}$ . A narrow rubbery state was maintained from  $-10$  to  $50^\circ\text{C}$ , followed by a softening area indicated by the continuous decrease of storage modulus and continuous increase of  $\tan\delta$ . In contrast,  $E'$  of PET within the glass transition zone only dropped 1 order, followed by an increase of  $E'$  around  $100^\circ\text{C}$ . This may be due to crystallisation of PET during the heating. PET is highly crystallized polymer. If the molten PET was cooled rapidly as the preparation of DMTA samples did, the PET can be partially amorphous. Reheating the polymer can lead to further crystallization of the polymer. The GMA modified EP samples, regardless of EP-g-GMA<sub>T101</sub> or EP-g-GMA<sub>TRIS</sub>, have a similar dynamic mechanical properties compared with virgin EP. However, a slight shift of the glass transition temperature ( $2^\circ\text{C}$ ) was detected.

The variation of  $\tan\delta$  with temperature of the PET/unmodified EP blends with a wt ratio of 80/20, 60/40 and 50/50 is shown in Figure 5-12. The blends with 80/20 and 60/40 ratios show two  $\tan\delta$  peaks corresponding to the glass transition of PET and EP, while only one peak of  $\tan\delta$  shows for 50/50 PET/EP blend related to the glass transition of EP. The PET peak could not be measured at this ratio because EP was the continuous phase. When the temperature rose to above  $50^\circ\text{C}$ , the EP phase started to soften and  $\tan\delta$  increased continuously. The PET phase peak was overlapped. Table 5-2 lists the  $\tan\delta$  peaks for those blends. The peak positions of  $\tan\delta$  varied with the variation of the composition. With

an increase in EP content in the physical blends of PET/EP, the peak of  $\tan\delta$  corresponding to EP shifted to higher temperature, while the peak for PET to lower temperature. The variation of  $\tan\delta$  peak depending on the weight ratios of individual polymers was also reported by others [7,143,144]. This is due to phase formation and the morphology of the blends. The value of  $\tan\delta$  peak for EP also increase with increasing the EP content.

For blends of PET with GMA modified EP, two typical samples of GMA modified EP were chosen and blended with three ratios: PET/EP-g-GMA=80/20, 60/40, 50/50. One sample was EP-g-GMA<sub>T101</sub> prepared in the GMA+T101 system containing 1.6% polyGMA with 0.5% grafting (sample GP-20 in the Table 5-1) and the other sample was EP-g-GMA<sub>TRIS</sub> prepared in the GMA+TRIS+T101 containing no polyGMA with higher grafting (2.5%) (sample GR-42 in the Table 5-1). The variation of  $\tan\delta$  as a function of temperature for 80/20 PET/EP-g-GMA is shown in Figure 5-13. The PET/EP-g-GMA blends also show the same behaviour for the  $\tan\delta$  curve as that of PET/EP, i.e. the compatibilised blends show the presence of two separate maximas corresponding to the glass transition temperature of PET and EP-g-GMA. This indicates the existence of two separated phases as observed from SEM of the blends. However, the position of  $\tan\delta$  corresponding to T<sub>gs</sub> of PET and EP-g-GMA was shifted to certain extent according to the difference of the rubber phase. The largest shifts were observed for PET/EP-g-GMA<sub>TRIS</sub> blends, i.e. PET peak shifted from 94 to 88.6°C; that is more than 5°C shift. For PET/EP-g-GMA<sub>T101</sub> blends, similar peak shift was observed. At this blending ratio, the  $\tan\delta$  peak for the rubber phase was very small and no obvious difference could be found. However, comparing the peak values of  $\tan\delta$  for PET phase for these three blends, a significant difference was found. For the PET/EP-g-GMA<sub>T101</sub> blends, the peak value of  $\tan\delta$  for PET was much lower than those for PET/EP and PET/EP-g-GMA<sub>TRIS</sub>, while the peak value of  $\tan\delta$  for PET phase of PET/EP-g-GMA<sub>TRIS</sub> blend was much higher than that of PET/EP blend. The corresponding difference was also found in E' vs temperature curve at this PET glass transition zone (see Figure 5-14). The value of storage modulus E' of PET/EP-g-GMA<sub>TRIS</sub> dropped sharply to the lowest value of about  $10^{7.5}$  pa and then rose rapidly to a plateau as the temperature increased from 60 to 120°C. In this range of temperature variation, the E' of PET/EP-g-GMA<sub>T101</sub> blend only decreased to its lowest value of  $10^{8.5}$  pa and followed by a slight increase. This phenomena may be due to the differences in crystallinity of PET

phase in those blends. The polyGMA crosslinking effect might reduce the crystalline extent of PET phase in the blends of PET/EP-g-GMA<sub>T101</sub>.

When the weight ratio of the rubber phase increased from 20% to 40%, similar  $\tan\delta$  vs temperature curves were measured, but the peak value of  $\tan\delta$  for the rubber phase increased while the peak value of  $\tan\delta$  for PET phase corresponding decreased due to the variation of composition (see Figures 5-15, and 5-16). Comparing those three blends, PET/EP-g-GMA<sub>TRIS</sub> gave rise to the highest peak value of  $\tan\delta$  for both PET and rubber phase, whereas PET/EP-g-GMA<sub>T101</sub> showed the lowest value for both phases. Corresponding differences in storage modulus were also clear. PET/EP-g-GMA<sub>T101</sub> blends had the highest  $E'$  value for the all temperature range as well as lower  $E'$  drops in two glass transition zones of the individual polymers. On the contrary the PET/EP-g-GMA<sub>TIRS</sub> blends had the highest  $E'$  reduction in those two zones. Obvious  $\tan\delta$  peak shifts were observed for PET/EP-g-GMA blends (see Table 5-2). Comparing with the PET/EP blend, EP-g-GMA<sub>TIRS</sub> led to a bigger peak shift, i.e. PET phase peak shifted from 98°C in PET/EP blend to 94.1°C and the rubber phase from -31.8°C to -27.3°C. From the extent of  $\tan\delta$  peak shifts, it is obvious that EP-g-GMA<sub>TRIS</sub> has a better compatibilising effect. This can be explained from the morphology observation of the 60/40 PET/EP-g-GMA<sub>TIRS</sub> blend, in which a better interfacial adhesion was clearly detected.

Figures 5-17 and 5-18 show the DMTA curves for the 50/50 PET/EP and PET/EP-g-GMA blends. At this wt ratio,  $\tan\delta$  curve of PET/EP shows only EP peak due to the formation of EP continuous phase and the big difference in Tgs. For PET/EP-g-GMA blends, separate peaks corresponding to the glass transition of PET and EP-g-GMA were observed. Comparing the  $\tan\delta$  peaks of the rubber phase, the peak value for PET/EP blend is shown to be much higher than that of PET/EP-g-GMA. It was noted that the  $\tan\delta$  peak of the rubber phase for PET/EP-g-GMA<sub>T101</sub> blends shifted to lower temperature, while the rubber phase peak in PET/EP-g-GMA<sub>TRIS</sub> blend became broad and shifted to higher temperature. The big difference in the  $\tan\delta$  peak of PET phase may reflect the difference of the phase structure of these three blends. At this weight ratio, PET in PET/EP-g-GMA<sub>T101</sub> blend is still the continuous phase as indicated by normal  $\tan\delta$  peak of PET phase and steady value of  $E'$  within the temperature range from 0°C to 80°C. The  $\tan\delta$  and  $E'$  curves of PET/EP-g-GMA<sub>TRIS</sub> blend on the other hand show that the PET phase is not the continuous phase; it

may be the co-continuous phase. This has been confirmed from the solubility test of the blends. The 50/50 PET/EP blend was dissolved in boiling toluene to form cloudy solution because PET phase was in the form of small particles and insoluble in the boiling toluene, whereas the 50/50 PET/EP-g-GMA<sub>T101</sub> blend could not be dissolved. The 50/50 PET/EP-g-GMA<sub>TRIS</sub> blend however could be dissolved at a very slow rate.

#### **5.2.1.4 Interphase reaction between PET and EP-g-GMA during the reactive blending**

Determination of the interface reaction between PET and EP-g-GMA can help characterise the PET blends. The initial analysis results showed that the reaction of epoxy group with the end groups of PET did indeed take place in the reactive blending.

##### **5.2.1.4.1 Solubility test**

It was reported that the solubility test (called as “Molau test”) could be used to qualitatively investigate a graft copolymerisation during the blending process [42,142]. In this investigation, 3g sample of the blends (PET/EP or PET/EP-g-GMA=80/20) was dissolved in 90 ml of the mixed solvents of phenol/tetrachloroethane (60/40 w/w) at a temperature of 85-90°C for 3-4 hours. The optical aspect of the dispersion was observed. The PET phase is, in principle, soluble in the mixture of the solvents, whereas the rubber phase is insoluble. In PET/EP blending system, no common solvent for both PET and EP could be found. PET is soluble in the mixture of phenol/tetrachloroethane, whereas the rubber phase is soluble in hot toluene. For the non-reactive blend of 80/20 PET/EP, PET formed as the continuous phase and was dissolved in the mixture of solvents within 3-4 hours, but the insoluble EP was isolated in the form of coarse, white flakes which floated on the top of the solution. In the case of 80/20 PET/EP-g-GMA<sub>TRIS</sub>, a white milky colloidal suspension was observed without any floated rubber flakes on the top of the solution. This indicates that the presence of PET-co-EP graft copolymer has acted as an emulsifier and is responsible for the formation of the white, colloidal suspension instead of formation of the floating rubber flakes on the top of the solution.

#### 5.2.1.4.2 FTIR Analysis of PET Blends

When the blends of PET/EP-g-GMA were pressed into thin films and then were analysed by FTIR, no peaks at  $909\text{ cm}^{-1}$  corresponding to the characteristic absorption of epoxy group was recorded. This may not necessarily mean the disappearance of epoxy group in the rubber phase due to the reaction of epoxy ring with the end groups of PET ( $-\text{COOH}$ ,  $-\text{OH}$ ) as this peak can be overlapped by PET peaks. When the rubber phase was Soxhlet extracted with toluene in the blends of PET/EP or EP-g-GMA (50/50) and analysed by FTIR,  $909\text{ cm}^{-1}$  peak was still observed, but the intensity was obviously much lower than the original one. This is due to the fact that a part of the grafted GMA which is located at the interface boundaries reacts with PET so the remaining grafted GMA would be expected to be less than the original. To prove the presence of a graft copolymer due to the interpolymer reaction, a solvent extraction procedure was used to separate the blend components. Two samples were used. PET1-0 was the physical blend of 80wt% PET with 20wt% virgin EP and PET1-7 was the blend of 80wt% PET with 20wt% EP-g-GMA containing 3.1% grafted GMA prepared in the presence of TRIS. 1.5g of each sample was dissolved into a mixed solvent of phenol/chlorobenzene/xylene (40/40/20 w/w) at  $80^\circ\text{C}$  for 3-4 hours. After the solution was filtered off to remove any impurity, the solution was added into warm toluene to precipitate PET. The PET fraction was separated and the remaining solution was added into methanol to precipitate the EP fraction. The precipitated PET and EP were dried in a vacuum oven at  $80^\circ\text{C}$  for more than 20 hours. About 0.1g of separated PET were pressed into thin films using a press at a temperature of  $275^\circ\text{C}$  and characterised by FTIR. By comparing the FTIR spectra of their PET fraction with those of virgin PET and EP, it was found that the PET fraction from PET1-0 was nearly the same as virgin PET, whereas obviously EP peaks could be observed in the PET fraction from PET1-7 (see Figure 5-19). Figure 5-19 (a) shows the spectrum of virgin EP which was obtained by casting thin film from toluene solution onto KBr disk. It has strong peaks at  $2916\text{ cm}^{-1}$  and  $2850\text{ cm}^{-1}$ , corresponding to  $-\text{CH}_2$ ,  $-\text{CH}_3$  absorption. The spectrum of virgin PET gives one strong peak at  $2955\text{ cm}^{-1}$  and one weak peak at  $2883\text{ cm}^{-1}$ . The FTIR spectrum of PET fraction from PET1-7 show three peaks at  $2955$ ,  $2916$ ,  $2850\text{ cm}^{-1}$  and a shoulder at  $2883\text{ cm}^{-1}$ , indicating that a fraction of EP exists in the separated PET fraction (see Figure 5-19 (b)). This may be an evidence of the formation of graft copolymer of



PET-co-EP in the reactive blending. More analysis will need to be conducted to separate the graft copolymer.

## 5.2.2 Compatibilisation of PET with GMA Grafted EPDM

### 5.2.2.1 Processing Characteristics of PET/EPDM-g-GMA Blends

As discussed in Chapter 3.2.6, GMA could be grafted onto EPDM via melt free radical grafting reaction using an organic peroxide (TI01) as a free radical initiator. Compared to the grafting of GMA onto EP, a significant difference could be found with respect to crosslinking of the polymer and the amount of polyGMA formed during the melt grafting. The results demonstrated that the desired grafting reaction was accompanied by obvious crosslinking of EPDM during the grafting (see Figures 3-29, 3-30 and 3-31 in Chapter 3). High concentrations of peroxide resulted in high GMA grafting degree and high gel formation, indicating the extent of crosslinking of EPDM. On the other hand, no measurable polyGMA was detected in the GMA grafted EPDM. The presence of TRIS as a comonomer could enhance the grafting and reduce the crosslinking. To investigate the compatibilisation effect of GMA grafted EPDM with PET, a set of samples were chosen to blend with PET. Table 5-3 lists the blending compositions and conditions.

When these EPDM-g-GMA samples (DM-2 to DM-5 and DM-10) were blended with PET at a weight ratio of 20/80 in a batch mixer, the torque values were monitored. Figure 5-20 compares the torque versus time curves of PET/EPDM and PET/EPDM-g-GMA (samples PEM-1-PEM-5 in Table 5-3) during reactive blending. When virgin EPDM was blended with PET, the torque dropped sharply in the first 2 minutes' mixing with the melting of PET, followed by gradual decrease to 10 Nm at the end of mixing. This may be due to the degradation of both PET and EPDM at a high temperature (275°C). Compared with PET/EPDM blend, blending EPDM-g-GMA samples prepared in the presence of peroxide only (i.e. EPDM-g-GMA<sub>TI01</sub>) with PET resulted in much higher torque. The viscosity increase (torque increase) can be attributed to the overall molecular weight increase from the anticipated epoxy coupling reaction with the end groups of PET (-COOH, -OH) to form EPDM-g-PET copolymers during the melt blending. This phenomenon was also observed in the blending of PET/EP-g-GMA. The possible reactions of grafted GMA with

PET is present in Scheme 5-2. However, this torque increase effect is much stronger than in the case of PET/EP-g-GMA system.

The GMA grafting degree has a strong effect on the pattern of torque-time curves of blending (see Figure 5-20). With 0.35% GMA (sample DM-2) in EPDM-g-GMA, the torque value reached to the lowest value within initial 1.5 minutes' mixing, and the low torque value was maintaining for further 30 seconds. Then, a sharp increase of torque from 18Nm to 22.5Nm was observed, followed by a slightly decrease of the torque until the end of mixing (see Figure 5-20 (PEM-20)). This sharp increase of the torque might be due to the start of interfacial reactions. With the increase of GMA grafting level, this sharp increase of the torque shifted to forward and the torque gradually increased with the proceeding of the mixing until the end of mixing. The higher the GMA grafting in the EPDM-g-GMA, the higher the torque was at the end of mixing. It is clearly seen that more GMA grafting leads to more vigorous reactions between epoxy groups and the end groups of PET. This can also be reflected in the ternary blending of PET/EPDM/EPDM-g-GMA (see Figure 5-21). The less EPDM-g-GMA added (keep total EPDM and EPDM-g-GMA at 20% and PET 80%), the less increase of torque observed. The torque increase is proportional to the amount of grafted GMA in the rubber phase.

However, when EPDM-g-GMA prepared in the presence of TRIS (i.e. EPDM-g-GMA<sub>TRIS</sub>) was blended with PET, no obvious torque increase was observed during the melt blending (see Figure 5-22). The torque sharply dropped to 19.4Nm in the first 1.5 minutes' mixing, and then a slight increase was observed within the next 30 seconds mixing. From this peak, the torque went down gradually until the end of mixing. The final torque value was practically equivalent to that of PET/EPDM blend. This may imply that though high grafting could be achieved in the presence of TRIS, the reactivity of its grafted GMA is low. In the following section, the effectiveness of EPDM-g-GMA on the compatibilisation of PET blends will be further discussed.

#### **5.2.2.2 Morphology of PET/EPDM or PET/EPDM-g-GMA Blends**

Figure 5-23 (a-e) shows the SEM micrographs of the physical blend of PET/EPDM and PET/EPDM-g-GMA blends at a weight ratio of 80/20. To get better observation, the fractured surfaces were all subjected to etching in boiling xylene to extract the rubber

phase (leaving holes on the fractured surfaces when PET as the continuous phase) before the morphology observation. The SEM micrograph is the most convenient approach to differentiate the morphologies between a compatibilised blend and an uncompatibilised counterpart. Generally, an immiscible and incompatible blend usually results in coarse morphology due to a high interfacial tension and gross phase separation. The physical blend of PET/EPDM is incompatible due to the significant difference in physical and chemical properties and coarse morphology was observed. It is clearly seen that EPDM was dispersed as spherical particles (semi-spherical holes observed after the EPDM was etched) in the continuous PET phase (Figure 5-23 (a)). Sharp and narrow interfaces and coarse dispersion of rubber particles in the PET matrix confirmed the incompatibility of the physical blend.

When PET was blended with GMA grafted EPDM, interfacial reactions between the two phases can be expected to take place as shown in Scheme 5-2. The formation of copolymers during the melt blending can act as emulsifier to reduce the interfacial tension and to improve interfacial adhesion leading to fine and stable morphology. In the SEM micrographs of PET/EPDM-g-GMA blends (see Figure 5-23 (b)-(e)), a significant reduction of the domain size of the rubber phase was observed. The much finer morphology indicates the compatibilisation of PET/EPDM-g-GMA. The graft degree of GMA in the EPDM-g-GMA phase has an obvious effect on the domain size of rubber phase and the shape of particles of the rubber phase. The sample with lowest grafting (sample DM-2: g-GMA =0.35 %) has the finest dispersion in the blend. The rubber phase dispersed in very uniform spherical particles as similar size of semi-spherical holes observed after the rubber phase was etched. With the increase of GMA grafting in the rubber phase, the domain size of the rubber phase became bigger and more uneven. This can be attributed to two reasons. Firstly, the high grafting of GMA was accompanied by an increase in viscosity of EPDM-g-GMA due to higher peroxide concentration. The higher viscosity of the rubber phase makes its dispersion more difficult. The other reason may be the stronger reactions between two phases with the increase of GMA grafting leading to higher viscosity of the blends as discussed before (Section 5.2.1.1). The high viscosity of the blends can decrease the mixing efficiency. On the other hand, the high GMA grafting degree leads to more interfacial reaction between the two phases and more in situ copolymers will certainly be formed. This may decrease the coalescence force of the rubber phase so the shape of the particles were not well-defined spherical and the size of

particles was not uniform (see Figure 5-23 (c, d)). It becomes clear that a high GMA grafting in the rubber phase can have an adverse effect on the dispersion of rubber phase. It seems that 0.35% of GMA grafting degree in the EPDM-g-GMA is high enough to result in an efficient compatibilisation of the blends.

EPDM-g-GMA can be added as a compatibiliser in PET/EPDM blends. Figure 5-24 compares the SEM micrographs of binary blend of PET/EPDM-g-GMA and ternary blends of PET/EPDM/EPDM-g-GMA with the same weight ratio of PET phase as 80% (EPDM-g-GMA sample DM-4 used). The addition of a small amount of EPDM-g-GMA led to significant improvement in rubber phase dispersion. The rubber phase in the ternary blends is dispersed as well-defined fine spherical particles. Changing EPDM-g-GMA weight ratio in the blends from 10% (PET/EPDM/EPDM-g-GMA=80/10/10) to 5% (PET/EPDM/EPDM-g-GMA=80/15/5) made no obvious difference on the morphologies of both blends. Actually, the addition of 5% EPDM-g-GMA (1.2% GMA grafting) in the blend of PET/EPDM (80/15) is equivalent to 0.3% of GMA grafting in the rubber phase. It is clearly seen that when the extent of grafted GMA level reaches a certain level, a further increase of the amount of grafted GMA does not have any further positive effect on the dispersion of the rubber phase. This can be attributed to the effect of the amount of in-situ copolymers formed during the melt blending. The higher the GMA grafting level in the rubber phase, the more the in situ copolymer formation is. However, it has been reported that only ~2 wt% in-situ formed copolymers were enough to stabilise the blend morphology [153,154]. It was suggested that when a blend with an in situ compatibiliser was prepared by a commonly used melt blending method, all the in situ formed copolymers were not guaranteed to be located at the interface and some parts existed in the matrix as micelles with sizes of 20-50nm [35].

Though EPDM-g-GMA can be added as an effective compatibiliser in blends of PET/EPDM, the extent of improvement on the morphology is not as good as that of the binary blends of PET/EPDM-g-GMA. At a similar level of GMA grafting in the rubber phase, a blend of PET/EPDM (sample: DM-2, g-GMA=0.35%) exhibits a much finer morphology than that of the ternary blend of PET/EPDM/EPDM-g-GMA (80/15/5) with 5% EPDM-g-GMA (sample: DM-4, g-GMA=1.2%) (see Figure 5-23 (b) and Figure 5-24 (c)). The effectiveness of the compatibiliser depends not only the level of functionality but also the molecular structure and molecular weight of functionalised rubber. It is not easy

to disperse a small amount of EPDM-g-GMA which has higher viscosity and has undergone some crosslinking, efficiently and evenly in the unmodified EPDM phase. As a result, the efficiency of the reaction of grafted GMA towards PET end groups in the ternary blends might be decreased.

However, when EPDM-g-GMA prepared in the presence of TRIS (DM-10 used) was used in the ternary blends, it was not as effective as EPDM-g-GMA prepared without TRIS. Figure 5-25 shows the effect of amount of EPDM-g-GMA<sub>TRIS</sub> (DM-10) on the morphology of the blends. In the SEM micrographs of three blends of PET/EPDM/ EPDM-g-GMA<sub>TRIS</sub>, the decrease of weight ratio of EPDM-g-GMA (DM-10) from 20 % to 5% led to larger domain size of rubber phase. Addition of 5% EPDM-g-GMA<sub>TRIS</sub> only slightly reduced the domain size of rubber phase with a coarse morphology. The explanation for this phenomenon might be the difference of EPDM-g-GMA molecular structure, especially the microstructure of grafted GMA. Due to the high reactivity of TRIS towards both EPDM and GMA and multi-functionality, the presence of TRIS as a comonomer may lead to long grafts of GMA. This will decrease the efficiency of the reactions of grafted GMA. A similar phenomena was reported for GMA grafted PP (PP-g-GMA) in the presence of styrene as a comonomer [27]. It was found that PP-g-GMA prepared in the presence of styrene was less effective in compatibilising PP/NBR blends than PP-g-GMA prepared just in the presence of peroxide.

### 5.2.2.3 Tensile Properties

Examination of mechanical properties is important for the evaluation for the compatibility of the blends. The properties of rubber-plastic blends are determined by (1) material properties of rubber and plastic phase, (2) rubber/plastic proportions, (3) the phase morphology, and (4) the interaction at the interface. For immiscible pair of polymers, high interfacial tension and lack of interfacial adhesion in the blends lead to coarse and unstable morphology and poor overall physical and mechanical performance. At first, the tensile properties of the virgin polymers, PET and EPDM, were measured. The measurement results show that PET has a very high modulus and high strength, similar to typical plastics (see Table 5-4). After reaching the yielding point under stretching, PET sample was necking until the break. In contrast, virgin EPDM gave the typical properties of an elastomeric material. It has a high elongation at break but low overall strength. They are

totally different in physical properties (see Figure 5-26). When virgin PET and EPDM were blended at a ratio of 80/20, the yielding strength, strength at break and elongation at break were measured as 26.9 Mpa, 17 Mpa and 27 % (see Figure 5-27). Compared with virgin PET, the strength is much lower. The low tensile properties of the PET/EPR blend can be related essentially to the larger size of EPDM domains with poor adhesion to the matrix as observed from its SEM micrograph in Figure 5-23 (a). These domains act as gross material defects, causing premature rupture of the specimen soon after the beginning of the yield.

In the case of PET/EPDM-g-GMA (80/20) blends, the tensile properties were strongly dependent on a particular EPDM-g-GMA sample used (see Table 5-4). When EPDM-g-GMA sample with the lowest grafting of GMA (DM-2) was blended with PET, the blend exhibited the best tensile properties (see Figure 5-27 (b)). Its strength at break and elongation at break reached to 32.1 Mpa and 347%, which are much higher than the physical blend of PET/EPDM. This result is consistent with the observation of morphology of this blend (see Figure 5-23 (b)). The fine and uniform morphology resulted in high tensile properties, particularly in elongation at break. The good adhesion at interfaces can also contribute to the excellent tensile properties. With the increase of the GMA grafting level (sample DM-2—DM-5), the tensile properties of PET/EPDM-g-GMA blends decreased, especially the elongation at break (see Figure 5-28). This may be related to the low uniformity of the domain sizes of the rubber phase in the blends when high GMA grafting EPDM-g-GMA samples were used. Comparing with binary blends of PER/EPDM-g-GMA, the ternary blends of PET/EPDM/EPDM-g-GMA exhibited even better tensile properties (see Table 5-4). This indicates that EPDM-g-GMA can be used to compatibilise PET/EPDM blends effectively. It is important to point out that existence of grafted GMA in the rubber phase results certainly in the interfacial reactions with the end groups of PET to form in-situ copolymer, hence fine morphology and good interfacial adhesion can be achieved. However, if grafted GMA exceeds a certain level in the PET blends, too stronger reactions between the two phases could lead to high viscosity of the blends, lower uniformity of morphology and poor tensile properties. Therefore, a reasonable level of GMA grafting in the rubber phase is required for the compatibilisation of PET/EPDM blends.

#### 5.2.2.4 Dynamic Mechanical Properties

The glass transition temperatures ( $T_g$ ) determined by DMTA for pure blend components and blends of PET/EPDM, PET/EPDM-g-GMA and PET/EPDM/EPDM-g-GMA with a fixed weight ratio of 80% PET in the blends are reported in Table 5-5. Curves of  $\tan\delta$  vs temperature for all blends show two  $\tan\delta$  peaks corresponding to the glass transition of PET and EPDM or EPDM-g-GMA. This indicates the presence of two separated phases as observed from SEM of the blends. In the case of physical blend of PET/EPDM, the  $T_g$ s of EPDM phase and PET phase are different from that of pure blend components. The  $T_g$  of rubber phase is 6°C lower than that of the pure EPDM, while the  $T_g$  of PET phase is 11°C higher than that of pure PET. This is due to the phase formation and the morphology of the blends. However, the  $T_g$ s of PET and EPDM-g-GMA in the compatibilised blends were shifted to certain extent according to the difference of the rubber phase. Figure 5-29 shows the  $\tan\delta$  vs temperature curves of PET/EPDM and PET/EPDM-g-GMA. The  $T_g$  of the rubber phase in the blends of PET/EPDM-g-GMA slightly shifted to lower temperature (about 2°C) than physical blend, whereas the  $T_g$  shift of PET phase depended on the type and the GMA grafting level of EPDM-g-GMA. When EPDM-g-GMA prepared in the presence of TRIS was used, the  $T_g$  of PET phase remained practically unchanged. In contrast, the use of EPDM-g-GMA prepared just in the presence of peroxide in the blends led to up to 11°C shift of  $T_g$  of PET phase to lower temperature. These observations are closely related to the intensity of interphase reactions during the melt blending as characterised by torque increase. No torque increase was measured during the blending of PET with EPDM-g-GMA (sample DM-10) (see Figure 5-22) so the  $T_g$ s of both phase remained practically unchanged. The stronger interphase reactions during blending, the bigger the shift of  $T_g$  of PET phase measured. The  $T_g$  shift can be another evidence of improved interactions between the phases. However, it should be noted that the improved interactions suggested by DMTA analysis are not always reflected in improved mechanical properties if other factors, such as morphology, are more dominant than the increased interactions between phases.

### 5.2.2.5 Characterisation of Interphase Reactions by FTIR Analysis

The analysis of the interfacial reaction of PET with epoxy group containing in the polymer by using FTIR technique have been reported by several researchers [7,35,41]. Jeon et al. studied the in-situ formation of the graft copolymers of PS-g-PBT in blends of PS-g-GMA/PBT by using solvent extraction followed by FTIR analysis [35]. To prove the presence of graft copolymer due to the interpolymer reaction in the blending system examined in this work, a solvent extraction procedure was also used to separate the blend components. Three samples were analysed: 80/20 PET/EPDM and 80/20 PET/EPDM-g-GMA (sample DM-4 and DM-10) blends. About 1g of each sample was pressed into thin films and then dissolved into a mixed solvent of phenol/chlorobenzene/xylene (40/40/20 w/w) at 80°C for 3—4 hours. After the solution was filtered off to remove any impurity, the solution was added into warm toluene to precipitate PET. The precipitated PET was dried in a vacuum oven at 80°C for more than 20 hours. About 0.1 g of separated PET was pressed into thin film using a press at a temperature of 275°C and characterised by FTIR. By comparing the FTIR spectra of their PET fraction with those of virgin PET and EPDM, it was found that the PET fraction from PET/EPDM blend was the same as virgin PET, whereas obvious EPDM peaks could be observed in the PET fraction from PET/EPDM-g-GMA blends (see Fig. 5-30). This can be an evidence of formation of copolymer during the melt blending through the reactions between the two phases. Figure 5-30 (a) shows the spectrum of virgin EPDM which was obtained by casting thin film from toluene solution onto KBr disk and spectrum of virgin PET thin film. EPDM has strong peaks at 2916  $\text{cm}^{-1}$  and 2848  $\text{cm}^{-1}$ , corresponding to  $-\text{CH}_2$ ,  $-\text{CH}_3$  absorption. The spectrum of virgin PET gave one strong peak at 2957  $\text{cm}^{-1}$  and one weak peak at 2887  $\text{cm}^{-1}$ . The FTIR spectrum of PET fraction separated from PET/EPR-g-GMAT<sub>101</sub> (sample DM-4) blend shows three strong peaks at 2957, 2920, 2848  $\text{cm}^{-1}$ , indicating that a fraction of EPDM exists in the separated PET fraction (see Fig. 5-29 (b)), whereas the FTIR spectrum of PET fraction from PET/EPDM-g-GMA<sub>TRIS</sub> (sample DM-10) blend only shows a strong peak at 2955  $\text{cm}^{-1}$ , a weak peak at 2918  $\text{cm}^{-1}$ . Significant difference on the intensity of the peak absorptions at 2918, and 2850  $\text{cm}^{-1}$  corresponds to the significant difference on the quantity of the trace of EPDM in the PET fraction for these two blends. It is clear that the EPDM-g-GMA<sub>TRIS</sub> prepared in the presence of TRIS has a lower reactivity towards the end groups of PET



regardless of its higher grafting level than the EPDM-g-GMA<sub>T101</sub> prepared just in the presence of peroxide so the less amount of copolymer EPDM-PET formed.

### 5.3 DISCUSSION

#### 5.3.1 Compatibilisation of EP-g-GMA with PET

As observed from the morphology of PET/EP 80/20 blends (see Figure 5-6 (a)), rubber phase was dispersed as spherical particles (semi-spherical holes observed after the EP was etched) in the continuous PET phase. Due to the high interphase tension and coalescence, the EP domains were in spherical form and the interfacial boundaries were very clear and sharp (see Figure 5-6 (a)). When the blending weight ratio of PET/EP was changed to 60/40, the morphology of the physical blends became clear, coarse and unsteady, indicating the incompatibility of these two polymers (see Figure 5-9 (a)). When GMA grafted EP was blended with PET, a significant improvement on the dispersion of the rubber phase could be achieved (see Figure 5-6 (b)-(e)). This is resulted from the formation of copolymer of PET-co-EP through the interfacial reactions of grafted GMA groups in the rubber phase with the carboxylic and hydroxyl end groups of PET, supporting by the solubility test and the FTIR analysis of the blends (see Figure 5-19). The formation of the copolymer can reduce the interfacial tension leading to fine dispersion of rubber phase in the PET phase and improve the interfacial adhesion as the copolymer locates at the interfaces acting as linker between phases.

However, it was found that the properties and structure of the GMA grafted rubber samples play a very important role on the efficiency of the compatibilisation of the PET/rubber blends. The properties of GMA grafted rubbers relate mainly to the rheological properties, while the structure of GMA grafted rubbers can be affected by the microstructure of the grafts (grafting sites, graft length, graft sequence distribution) and the structure of the rubber chains which result from different grafting mechanisms.

As described in the mechanism of free radical grafting reaction (see Section 1.5, p43, and Figure 1-2, p45), the chemistry of melt free radical grafting is complicated due to the high temperature, high viscosity and heterogeneity of the reacting medium. First of all, the desired grafting reaction is always accompanied by degradation, crosslinking of polymer

substrates and homopolymerisation of monomers which can significantly alter their valuable mechanical properties and processing characteristics. In the case of PE, EP, or EPDM, crosslinking was revealed as a common problem during the melt grafting [73]. The results demonstrated that the homopolymerisation of GMA and the branching/crosslinking of EP constitute the main side reactions encountered during the grafting of GMA onto EP. The branching/crosslinking results in a significant increase of the melt viscosity of the GMA modified EP (see Figure 3-11, p155). It was found that the higher viscosity of the rubber phase has led to large rubber domain size (see Figure 5-7) in the blends of PET/EP-g-GMA. The main mechanism governing the morphology development is believed to be the results of both droplet breakup and coalescence. In studies on nylon/rubber blending, it was suggested that a minimum particle size could be achieved when the viscosities of two phases are closely matched [22]. In PET/EP blending system, the virgin EP already has a higher viscosity than PET. The increase of viscosity of the GMA modified EP during the melt grafting resulted in much bigger difference of viscosity between the two phases. The higher viscosity (lower MFI) of functionalised EP (see Table 5-1 b) makes the viscosity difference between the two polymers even larger hence the larger rubber domains were observed.

The presence of polyGMA in the EP-g-GMA samples has a significant effect on the compatibilisation of the PET/EP-g-GMA blends. As revealed from the functionalisation of EP in the presence and absence of the comonomer, TRIS, (see Chapter 3 Section 3.2.4, p102, and 3.2.5, p106), the formation of polyGMA during the grafting of GMA onto EP is the main side reaction which competes strongly with the desired grafting reaction in the absence of the comonomer. The use of the comonomer could greatly enhance the grafting reaction and reduce the formation of polyGMA. At the optimal compositions and the optimal processing conditions, no measurable polyGMA was detected in the EP-g-GMA<sub>TRIS</sub> in the GMA+TRIS+T101 system (see Chapter 3 Section 3.2.5.5, p112, and Figure 3-24, p162). During the melt blending with PET, the presence of polyGMA in the EP-g-GMA<sub>T101</sub> samples could result in obvious crosslinking of the PET phase and could reduce the efficiency of the compatibilisation effect, i.e. larger domain size of EP-GMA phase was dispersed in the PET phase (see Figure 5-8). It was demonstrated that the epoxy group of polyGMA could react with carboxylic acid groups of PET as the epoxy group of the grafted GMA does (see Figure 5-3). The presence of polyGMA in the rubber samples will almost certainly decrease the possibility of the desired interfacial reaction hence

decrease the compatibilisation efficiency. As a result, the presence of polyGMA in the EP-g-GMA<sub>T101</sub> samples has an adverse effect on the rubber dispersion and the rheological properties of the blends.

In contrast, the EP-g-GMA<sub>TRIS</sub> samples gave rise a better compatibilisation with PET in terms of the finer dispersion of the rubber phase and the better interfacial adhesion as observed from the SEM micrographs (see Figures 5-6 and 5-9) due to the higher GMA grafting and the absence of the polyGMA (see Table 5-1 b) in the EP-g-GMA<sub>TRIS</sub> samples. It can be concluded therefore that minimising or avoiding the homopolymerisation reaction of GMA monomer during the grafting process of EP is a key to preparation of GMA functionalised EP, to achieve a better compatibilisation with PET during the reactive blending. The use of the comonomer, TRIS, has been shown in this study to enhance the grafting of GMA and decrease the homopolymerisation of GMA monomer efficiently (see Chapter 3 Section 3.2.5, p106).

It is very important to note that the microstructure of the grafts also affects the efficiency of the compatibilisation. In the blending of PET with EP-g-GMA<sub>T29B90</sub>, it was found that the interfacial reactions occurred to a lower extent and this is reflected by the low torque values (see Figure 5-5) during blending and the sharp and smooth interfaces observed in SEM of PET/ EP-g-GMA<sub>T29B90</sub> 60/40 blend (see Figure 5-9). As for the grafting of GMA onto EP using T29B90 as the free radical initiator processed at a low temperature (115°C), it was interesting to notice that the grafting of GMA depended on the concentration of the initial GMA added at such a low processing temperature. Nearly no GMA was grafted onto the EP when 6 phr GMA was added initially, whereas the grafting degree increased sharply to 6% when 15 phr GMA was added (see Figure 3-17, p158). It seems that a critical value of the initial GMA concentration is needed for the grafting reaction. In this case the amount of polyGMA also increased with the increase of initial GMA, but was relatively low. At such a low temperature, the grafting mechanism and the structure of the grafted GMA may be different from that which takes place at high temperatures due to the high viscosity of EP. GMA might graft onto the EP forming long grafts. Though high grafting could be achieved in the presence of the peroxide, T29B90, the efficiency of the interfacial reaction is low and the interfacial adhesion is poor. Better understanding of the structure of the grafted GMA will be very useful to explain the interfacial reactions during the reactive

blending. It can clearly be seen that the microstructure of the grafts can certainly be a very important factor in the reactive compatibilisation of PET blends.

### 5.3.2 Compatibilisation of EPDM-g-GMA with PET

The different characteristics of grafting GMA onto EPDM from that of grafting GMA onto EP lead to significant difference on their compatibilisation effect with PET. When GMA was grafted onto EPDM in the absence of TRIS, no polyGMA was detected in the EPDM-g-GMA samples, but crosslinking accompanied the grafting (see Figure 3-29, p165). The overall grafting was shown to be low. The presence of TRIS during the grafting results in the high GMA grafting and the less crosslinking (see Figures 3-30, p165, and 3-31, p166). However, the results illustrate that the EPDM-g-GMA<sub>T101</sub> prepared in the GMA+T101 system give rise to much more efficient compatibilisation effect with PET when compared to the EPDM-g-GMA<sub>TRIS</sub> prepared in the GMA+TRIS+T101 system in terms of the very fine dispersion of the rubber phase (see Figure 5-23) and the excellent tensile properties (see Figure 5-28). Another factor is the microstructure of grafts which affect the efficiency of compatibilisation. The reasons may be the difference of the nature of the interfacial reactions. As indicated by the lower torque value during the blending of PET with EPDM-g-GMA<sub>TRIS</sub> (see Figure 5-22), less interfacial reactions might be expected between the PET phase and the EPDM-g-GMA<sub>T101</sub> phase. Though the presence of TRIS enhanced the grafting reaction, resulting in a higher grafting degree, the microstructure of the grafted GMA in this case may have made the interfacial reaction less efficient. Analysis of EPDM-g-GMA<sub>TRIS</sub> sample and EPDM-g-GMA<sub>T101</sub> shows the significant difference in the features of the grafted GMA (see Chapter 3 Section 3.2.6, p114). The differential solvent fractionation was used to analyse the structures of GMA grafted EPDM prepared in the absence and presence of TRIS. The results revealed the significant differences between these two types of GMA modified EPDM. The fractionation results showed that the sample which was prepared in the absence of TRIS (EPDM-g-GMA<sub>T101</sub>, sample DM-3) had a higher low temperature soluble fraction (hexane soluble fraction), whereas the sample which was prepared in the presence of TRIS (EPDM-g-GMA<sub>TRIS</sub>, sample DM-9) had much less low temperature soluble fraction (hexane soluble fraction) but higher high temperature soluble fraction (that is toluene and xylene soluble fractions) (see Figure 3-32, p166). This clearly shows that EPDM-g-GMA<sub>TRIS</sub> has a high fraction of branched EPDM. This can be explained by the linker effect of TRIS. TRIS has multi-functional groups and is highly

reactive towards EPDM chains. This certainly leads to high branching of EPDM. It can be assumed that grafted GMA may be in a multibranch form of copolymer with TRIS due to the high reactivity of GMA toward TRIS and the multifunctionality feature of TRIS. In contrast, the grafts of GMA in EPDM-g-GMA<sub>T101</sub> may be short grafts generating more graft sites on the EPDM chains. During reactive blending, grafted GMA groups with short grafts and more graft sites will almost certainly have more chance for reacting with the end groups of PET.

On the other hand, EPDM-g-GMA<sub>T101</sub> could also lead to very efficient interfacial reactions during the reactive blending with PET. It was found that only about 0.3% GMA grafting degree is high enough to result in the finer dispersion and the excellent mechanical properties in the PET/EPDM-g-GMA 80/20 blends (see Figure 5-23 and 5-28). When the GMA grafting degree exceeds this level, the strong interfacial reaction has an adverse effect on the compatibilisation, i.e. a significant increase in the melt viscosity of the PET blends and the uneven domain size distribution of the rubber phase (see Figure 5-23).

### **5.3.3 Interfacial Reactions between PET and GMA grafted EP or EPDM**

Due to the significant difference between PET and EP or EPDM rubbers in terms of both physical and chemical properties, these polymer pairs are completely incompatible. If these polymers are blended directly, the high interfacial tension and lack of interfacial adhesion will lead to coarse, unstable morphology and poor overall physical and mechanical performance. Generally, the compatibilisation of immiscible blends is achieved by: 1) reducing the interfacial tension in the melt, causing an emulsifying effect and leading to an extremely fine dispersion of one phase in another; 2) increasing the adhesion at phase boundaries, giving improved stress transfer; 3) stabilising the dispersed phase against growth during annealing, again by modifying the phase boundaries interface [12]. To achieve the compatibilisation of PET with EP or EPDM, the reactive blending is a relatively new and versatile approach. In this compatibilisation method, desired copolymers are produced through interfacial reactions between reactive polymers directly during blending. Copolymers can act as an emulsifier which locate at the interface so the interfacial tension in the melt can be reduced leading to an extremely fine dispersion of one phase in another. This can also increase the adhesion at phase boundaries, giving improved stress transfer and stabilise the dispersed phase against growth during annealing, again by

modifying the phase boundaries interface. Such graft copolymers strengthen the interface between domains, but perhaps more importantly they provide steric stabilisation to reduce rate of coalescence all of which shift the balance between drop break up and coalescence to give a finer dispersion and more stable morphology [37-39].

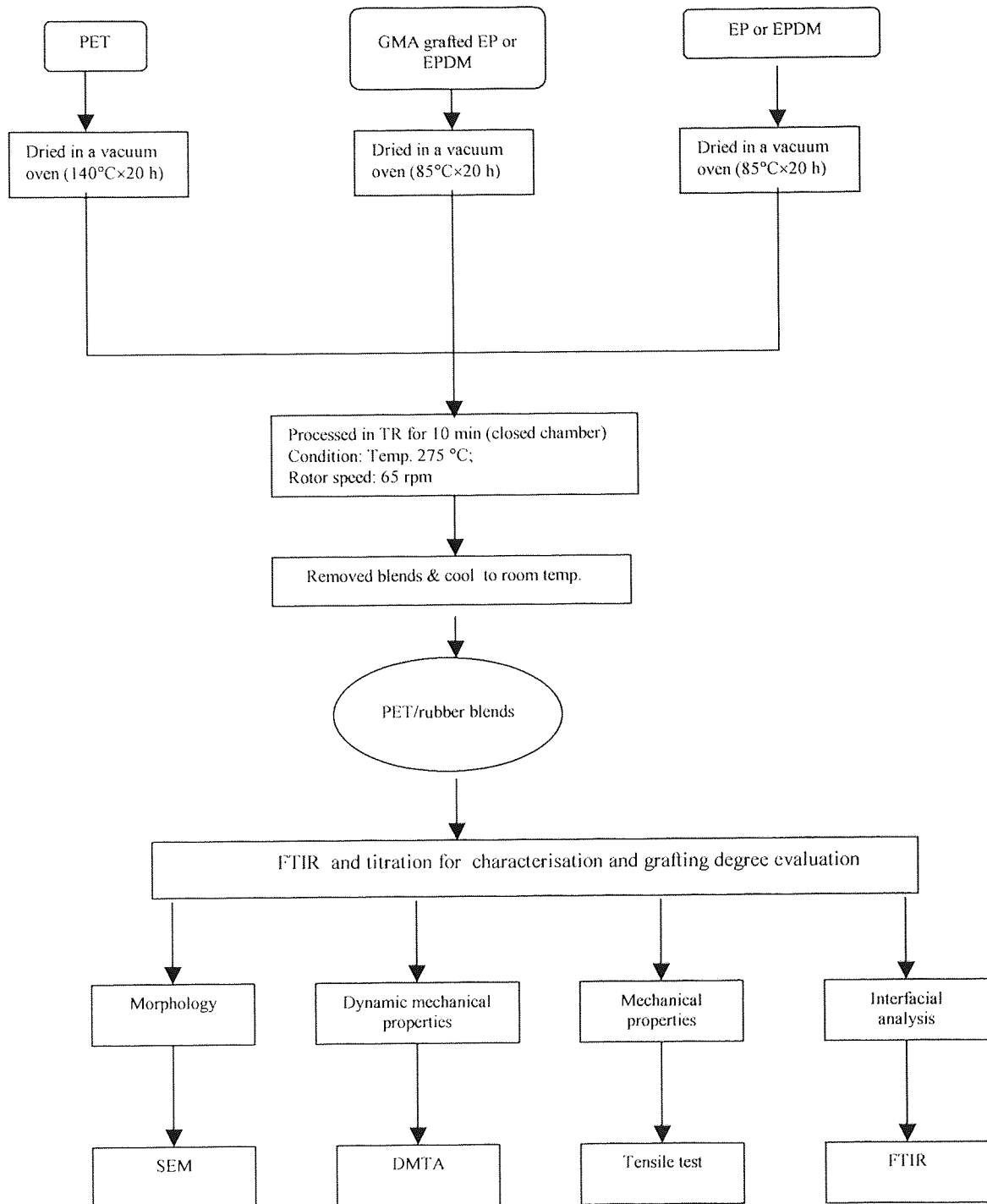
For PET blends, the important characteristics of chemical structure of PET phase is the presence of carboxylic and hydroxyl terminal groups, which can readily react with other functions such as anhydride, epoxy, oxazoline, isocyanate and carbodiimide groups [16]. Some studies have already demonstrated that epoxy containing polymers are very effective for the compatibilisation of PET blends [63]. For example, ethylene-co-glycidyl methacrylate (E-GMA) copolymer has been widely used as compatibiliser in PET/PE blends [32,36,63]. Efforts had been made to prove the formation of copolymer from the reactions of epoxy groups and the end groups of PET or PBT [35,37-39,63]. Evidence from blending ethylene-glycidyl methacrylate copolymer (E-GMA) with low molecular weight compounds which were monofunctional or multifunctional in terms of the hydroxyl or carboxyl group content showed that carboxyl groups react with the epoxide contained in the EGMA copolymer, but hydroxyl groups did not. It was concluded that only the PBT carboxyl but not the hydroxyl end groups had the potential to react with the epoxide functionality found in the terpolymer of methyl methacrylate, glycidyl methacrylate and ethyl acrylate (MGE) under the processing conditions they used [38].

In the compatibilisation of PET and GMA grafted EP or EPDM, it is very important to verify the reactions between the grafted GMA with the end groups of PET. In this study, it was difficult to isolate the copolymer formed during the reactive blending, but the evidence clearly indicates that reactions do take place between the PET phase and the rubber phase (see Sections 5.2.2.1 and 5.2.2.5). The torque-time curves clearly reflect the interfacial reactions by the increase of torque value when PET was blended with either EP-g-GMA or EPDM-g-GMA (see Figure 5-4 for PET/EP-g-GMA blends and Figure 5-20 for PET/EPDM-g-GMA blends). The fact that the higher grafting degree of GMA in the EPDM-g-GMA<sub>T101</sub> phase resulted in the higher torque values further supports the occurrence of the interfacial reactions (see Figure 5-20). EPDM-g-GMA samples have stronger effect on the increase of torque value during the melt blending with PET than EP-g-GMA samples. It is clearly shown that when the GMA grafting degree of EPDM-g-GMA<sub>T101</sub> reaches to 0.6%, the gradual increase of the torque with the proceeding of the

blending indicates the branching or/and crosslinking reaction during the blending of PET with EPDM-g-GMA<sub>T101</sub> at a weight ratio of 80/20 (see Figure 5-20). The solubility test and FTIR analysis of the blends also gave more evidence of the interfacial reaction leading to the formation of copolymer (see Section 5.2.1.4).

The possible reactions between epoxy groups and the end groups of PET, e.g. carboxyl group and hydroxyl group are presented in Scheme 5-2. The strong polarisation of the O-H bond of carboxylic acids of PET end groups ensures fast reaction between epoxy and carboxylic acid groups (see Scheme 5-2 (Rn 1)). This could be proved by the reaction of polyGMA with PET. It seems that the reaction starts already within 1 minute by comparing the torque-time curves of PET alone and PET + polyGMA (see Figure 5-3). For the processing of PET alone, the torque drops sharply to about 25 Nm within the first minute of processing, whereas the torque value kept at 32 Nm in the presence of 4% synthesised polyGMA during the processing (see Figure 5-3). The fast reactions between the interfaces are essential for reactive blending, since the residence time is normally short when an extruder is used as the processing reactor. This reaction creates free OH groups which, again, are reactive with epoxy groups (see Scheme 5-2 (Rn 3)). During the mixing, the described reaction may lead to considerable branching [18]. This is particularly true for the blending of PET with EPDM-g-GMA. When the EPDM-g-GMA having a GMA grafting degree above 0.6% was blended with PET, an obviously continuous torque increase was observed after the torque value reached to a plateau from 1 minute to 6 minutes, indicating the obvious crosslinking with the going of interfacial reaction. Other possible reactions are esterification (see Scheme 5-2 (Rn 2)) of secondary hydroxyl groups and hydrolysis of the epoxy group. The branching or crosslinking will lead to higher viscosity during the mixing.

Scheme 5-1 Methodology for compatibilisation of PET/rubbers blends





Scheme 5-2 Possible interfacial reactions of GMA grafted rubbers with end groups of PET

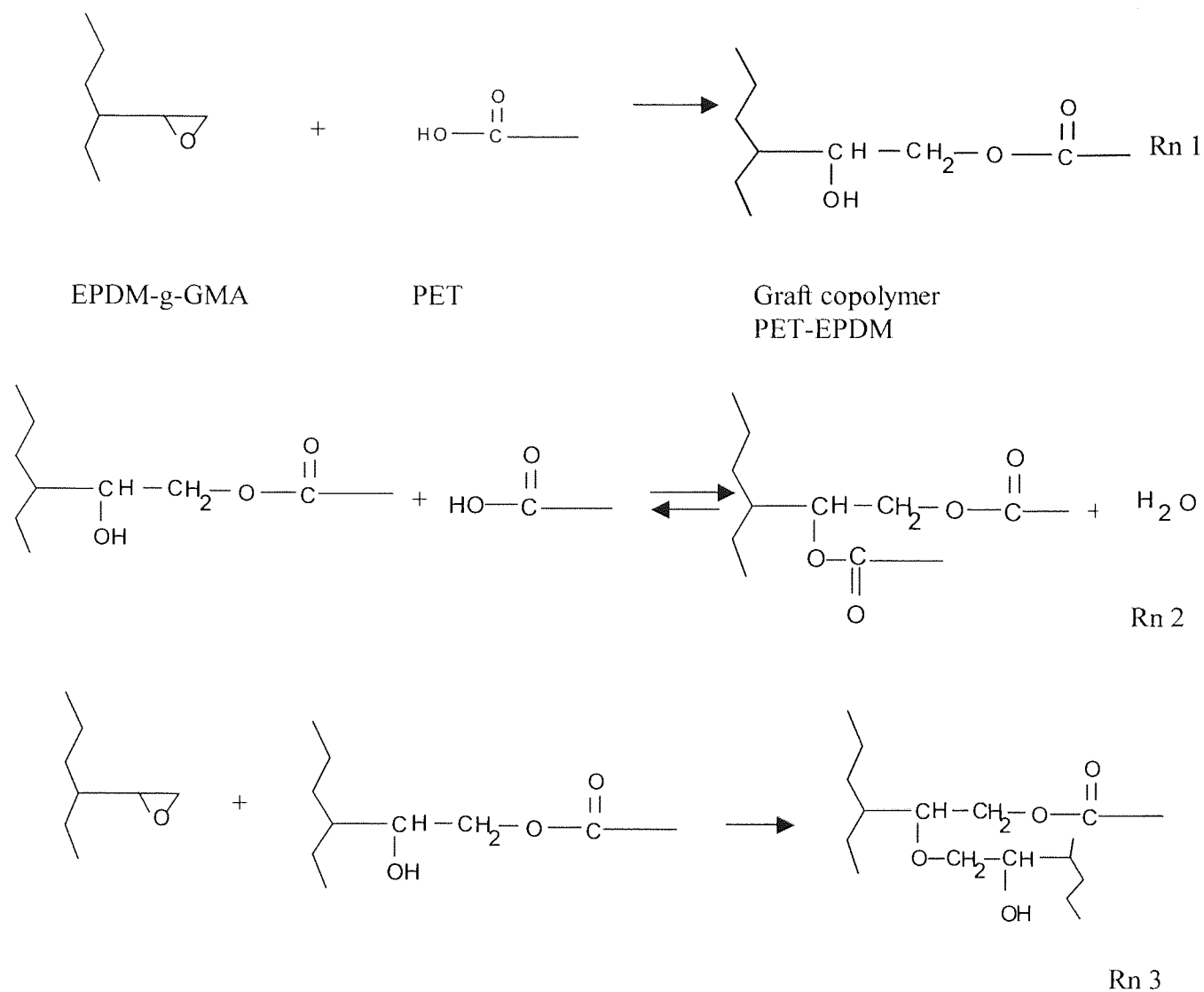


Table 5-1 Compositions and conditions for preparation of PET/EP-g-GMA blends

(a) Composition and condition for EP-g-GMA samples preparation

Code	Compositions						Conditions Temp.(°C)/speed (rpm) /time (min)	Grafting Degree (%)	PolyGMA (%)
	EP (phr)	GMA (phr)	TRIS (phr)	T101 (phr)	GMA /TRIS	[T101]/ [GMA+ TRIS]			
GP-11	100	18	0	1.0			190/65/15	1.6	2.7
GP-11 (purified)	100	18	0	1.0			190/65/15	1.6	0
GP-20	100	10	0	1.0			180/65/15	1.7	0.5
GR-40	100	10	2.5	0	8/2	0	160/65/15	1.0	~0
GR-41	100	10	2.5	0.069	8/2	0.003	160/65/15	2.4	~0
GR-42	100	10	2.5	0.114	8/2	0.005	160/65/15	2.5	~0
GR-44	100	18	2	0.097	9/1	0.002 5	160/65/15	3.1	~0
GR-32	100	18	2	0.384	9/1	0.01	190/65/15	2.3	0.15
GR-6	100	10	2.5	0.114	8/2	0.005	190/65/15	2.0	0.1
GR-8	100	10	2.5	0.457	8/2	0.02	190/65/15	2.0	0.1
BP-2	100	10	0	T20B90 0.5			115/65/15	3.9	0.3
BP-3	100	15	0	T20B90 0.5			115/65/15	6.0	0.4

(b) PET/EP-g-GMA blend compositions and conditions

Code	Compositions		Conditions Temp(°C)/speed (rpm)/time (min)	Feature of EP-g-GMA components			
	Components	Weight ratio		Grafting degree (%)	PolyGMA (%)	MFI	Remarks
PET0-0	PET/EP	100/0	275/65/10				
PET1-0	PET/EP	80/20	275/65/10	0	0	1.7	Virgin EP
PET1-1	PET/GP-20	80/20	275/65/10	1.7	0.5		GMA+T101
PET1-2	PET/GP-11	80/20	275/65/10	1.6	2.7	0.44	GMA+T101
PET1-3	PET/GP-11 (purified)	80/20	275/65/10	1.6	0	0.44	GMA+T101
PET1-4	PET/GR-40	80/20	275/65/10	1.0	~0	1.34	With TRIS
PET1-5	PET/GR-41	80/20	275/65/10	2.4	~0	1.05	With TRIS
PET1-6	PET/GR-42	80/20	275/65/10	2.5	~0	1.0	With TRIS
PET1-7	PET/GR-44	80/20	275/65/10	3.1	~0	1.2	With TRIS
PET1-8	PET/GR-32	80/20	275/65/10	2.3	0.15	1.0	With TRIS
PET1-9	PET/GR-6	80/20	275/65/10	2.0	0.1	0.5	With TRIS
PET1-10	PET/GR-8	80/20	275/65/10	2.0	0.1	0.1	With TRIS
PET1-11	PET/BP-2	80/20	275/65/10	3.9	0.24	0.72	GMA+T29B 90
PET1-12	PET/BP-3	80/20	275/65/10	6.0	0.43	0.86	GMA+T29B 90
PET2-0	PET/EP	60/40	275/65/10	0	0	1.7	Virgin EP
PET2-1	PET/GP-20	60/40	275/65/10	1.6	0.5		GMA+T101
PET2-2	PET/GR-42	60/40	275/65/10	2.5	~0	1.0	With TRIS
PET2-3	PET/GR-44	60/40	275/65/10	3.1	~0	1.2	With TRIS
PET2-4	PET/BP-3	60/40	275/65/10	6.0	0.43	0.86	GMA+T29B 90
PET3-0	PET/EP	50/50	275/65/10	0	0	1.7	Virgin EP
PET3-1	PET/GP-20	50/50	275/65/10				GMA+T101
PET3-2	PET/GR-42	50/50	275/65/10	2.5	~0	1.0	With TRIS
PET3-3	PET/BP-3	50/50	275/65/10	6.0	0.43	0.86	GMA+T29B 90
PET0-1	PET/poly- GMA	100/4	275/65/10				Synthesised polyGMA

Table 5-2 Peaks of  $\tan\delta$  curves corresponding to the glass transition of individual component for different types of PET/EP (or EP-g-GMA) blends

Blend ratio PET/EP (or EP-g-GMA) w/w	PET/EP		PET/EP-g-GMA <sub>T101</sub> *				PET/EP-g-GMA <sub>TRIS</sub> **				
	EP phase	PET phase	EP phase		PET phase		EP phase		PET phase		
	Tg (°C)	Tg (°C)	Tg (°C)	Shift (°C)	Tg (°C)	Shift (°C)	Tg (°C)	Shift (°C)	Tg (°C)	Shift (°C)	
100/0	—	93.6	—	—	93.6	—	—	—	—	93.6	—
80/20	-32.6	94.1	-33.2	-0.6	89.6	-4.5	-32.1	+0.5	88.6	-5.5	
60/40	-31.8	98	-29.2	+2.6	95.4	-2.6	-27.3	+4.5	94.1	-3.9	
50/50	-21.0	—	-23.2	-2.2	87.2	—	-18.6	+2.4	91.7	—	
0/100	-24.5	—	-22.5	+2	—	—	-22.4	+2.1	—	—	

\* EP-g-GMA<sub>T101</sub> used – sample GP-20

\*\* EP-g-GMA<sub>TRIS</sub> used – sample GR-42

Table 5-3 Compositions and conditions for preparation of PET/EPDM-g-GMA blends

Code	Compositions		Conditions Temp(°C)/ speed (rpm)/ time (min)	Preparation of EPDM-g-GMA components			
	Components	Weight ratio		Composition EPDM/GMA/TRIS/T101 (phr)	Temp(°C)/speed (rpm)/time (min)	Grafting degree (%)	Gel (%)
PEM-1	PET/EPDM	80/20	275/65/10				
PEM-2	PET/DM-2	80/20	275/65/10	100/10/0/0.3	180/65/10	0.45	2
PEM-3	PET/DM-3	80/20	275/65/10	100/10/0/0.6	180/65/10	0.6	10
PEM-4	PET/DM-4	80/20	275/65/10	100/10/0/0.8	180/65/10	1.2	18
PEM-4-1	PET/DM-4/EPDM	80/10/10	275/65/10	100/10/0/0.8	180/65/10	1.2	18
PEM-4-2	PET/DM-4/EPDM	80/5/15	275/65/10	100/10/0/0.8	180/65/10	1.2	18
PEM-5	PET/DM-5	80/20	275/65/10	100/10/0/1.0	180/65/10	1.7	36
PEM-6	PET/DM-10	80/20	275/65/10	100/10/2.5/0.06	180/65/10	2.5	6
PEM-6-1	PET/DM-10/EPDM	80/10/10	275/65/10	100/10/2.5/0.06	180/65/10	2.5	6
PEM-6-2	PET/DM-10/EPDM	80/5/15	275/65/10	100/10/2.5/0.06	180/65/10	2.5	6

Table 5-4 The tensile properties of different PET blends

Code	Sample composition	Yield strength (MPa)	Strength at break (Mpa)	Elongation at break (%)	Energy to break point (J)
PET-V	PET (virgin)	54.0±1.2	59.0±3.3	402 ±12	
EPDM-V	EPDM (virgin)		7.3 ±0.7	570 ±21	
PEM-1	PET/EPDM (80/20)	26.9 ±1	19.0±0.5	27±7	0.5±0.2
PEM-2	PET/EPDM-g-GMA(DM-2) (80/20)	29.5±0.1	32.1±2	347±60	7.0±1.5
PEM-3	PET/EPDM-g-GMA(DM-3) (80/20)	30.1±0.1	24.5±5.0	319±62	6.6±1.6
PEM-4	PET/EPDM-g-GMA(DM-4) (80/20)	27.7±0.5	19.3±0.3	94±62	1.8±1.2
PEM-5	PET/EPDM-g-GMA(DM-5) (80/20)	26.3±0.3	19.5±0.4	34±15	0.6±0.3
PEM-6	PET/EPDM-g-GMA(DM-10) (80/20)	26.3±1.7	18.3±1	217±47	3.6±0.7
PEM-4-1	PET/EPDM-g-GMA(DM-4) /EPDM (80/10/10)	29.1±0.3	33.9±0.8	402±12	8.5±0.2
PEM-4-2	PET/EPDM-g-GMA(DM-4)/ EPDM (80/5/15)	29.3±0.2	28.6±2.6	374±17	7.4±0.6

Table 5-5 Glass transition temperatures (T<sub>g</sub>) of different blends measured by DMTA

Sample composition	Glass transition temperature (°C)	
	EPDM or EPDM-g-GMA phase	PET phase
PET	----	93.6
EPDM	-21.4	----
PET/EPDM (80/20)	-27.5	104.7
PET/EPDM-g-GMA (DM-2) (80/20)	-29.1	100.9
PET/EPDM-g-GMA (DM-4) (80/20)	-31.8	92.9
PET/EPDM-g-GMA (DM-10) (80/20)	-29.1	105.7
PET/EPDM/EPDM-g-GMA (DM-4) (80/10/5)	-30.2	104.0

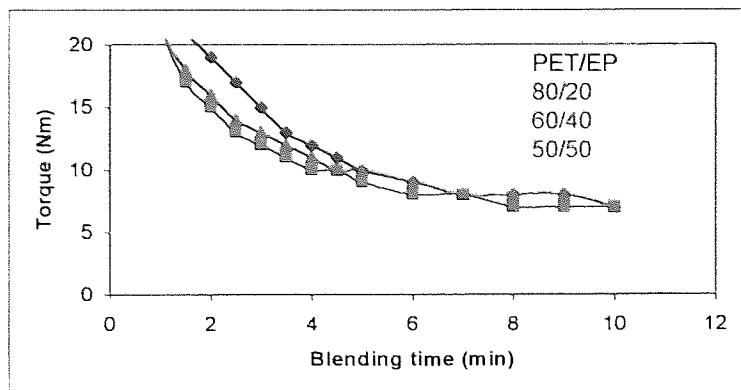


Figure 5-1 The torque-time curves of blending of PET/EP with three weight ratios: 80/20, 60/40, 50/50

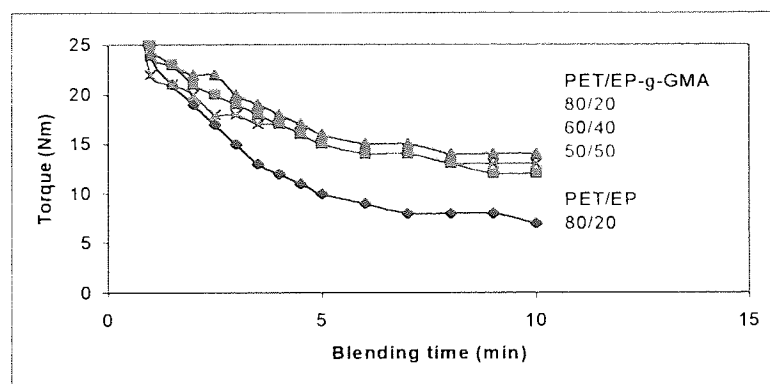


Figure 5-2 The torque-time curves of blending of PET/EP-g-GMA (EP-g-GMA sample G-42) with three weight ratios : 80/20 (PET1-6), 60/40 (PET2-2, 50/50 (PET3-2)

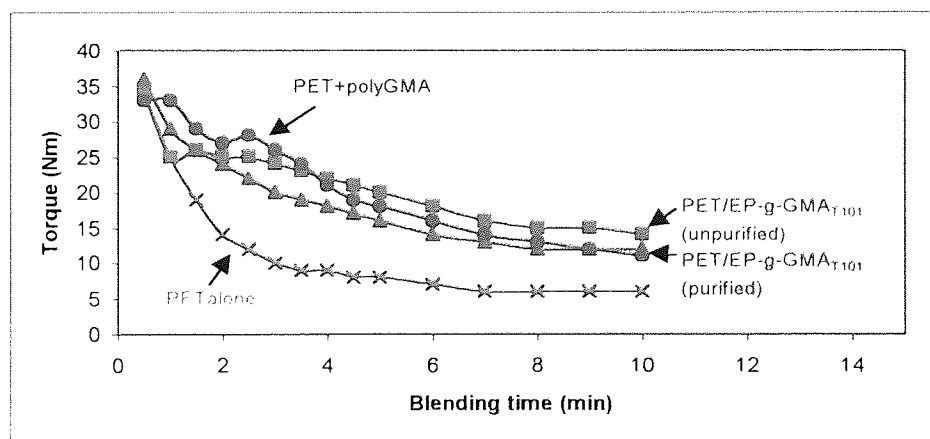


Figure 5-3 The torque-time curves of blending PET with EP-g-GMA<sub>T101</sub> (unpurified containing grafted GMA and polyGMA, sample GP-11, and purified containing only grafted GMA) at a weight ratio of 80/20, and PET with and without polyGMA (see Table 5-1 (b) for detailed compositions)

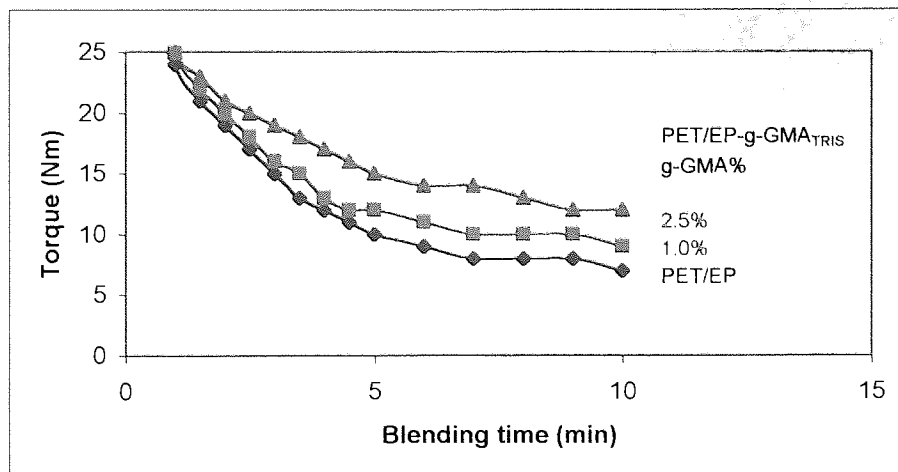


Figure 5-4 The torque-time curves of blending PET with EP-g-GMA<sub>TRIS</sub> –effect of grafting degree of EP-g-GMA<sub>TRIS</sub> on the torque value at a weight ratio of 80/20 (see Table 5-1 (b) for sample PET1-0, PET1-4, PET1-6)

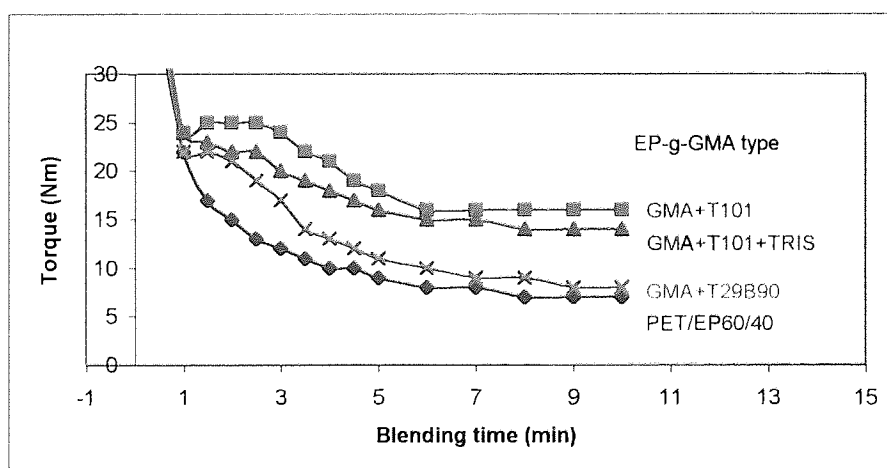
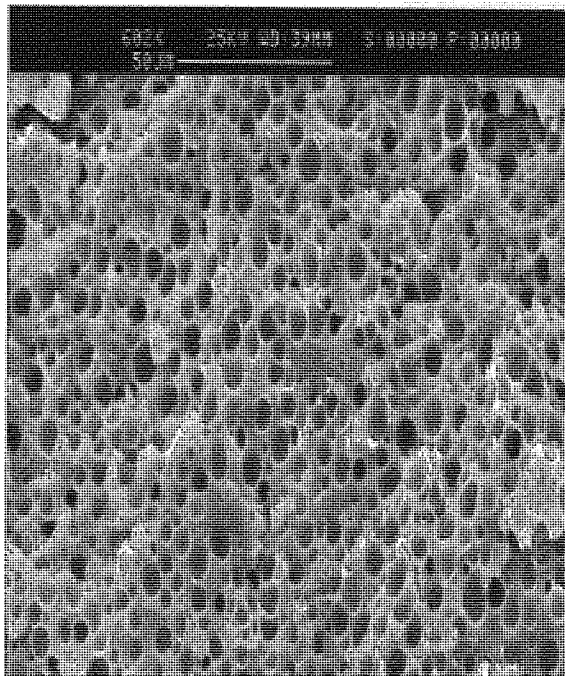
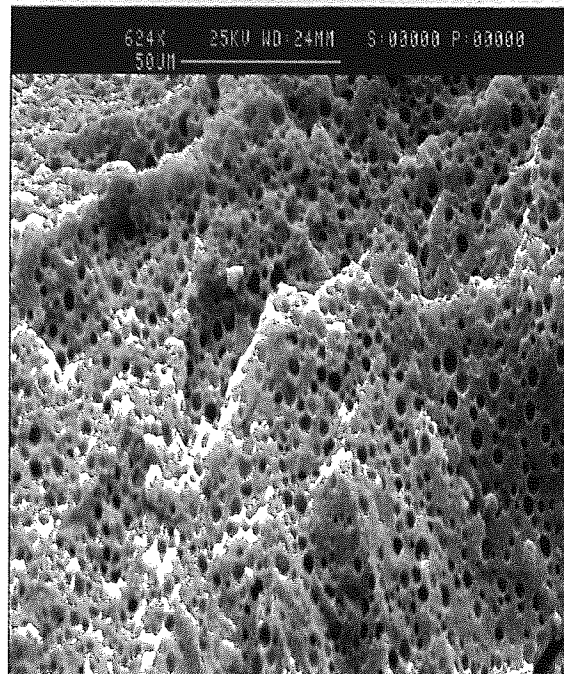


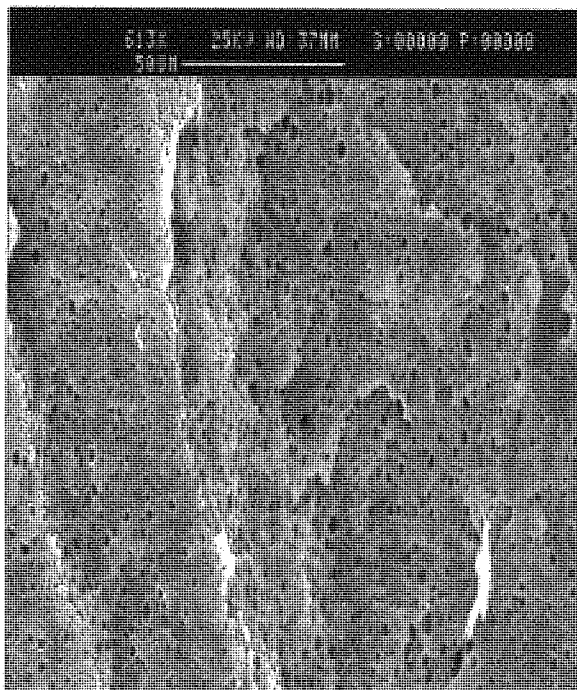
Figure 5-5 The torque-time curves of blending PET with different types of EP-g-GMA at a weight ratio of 80/20 (see Table 5-1 (b) for sample PET2-0, PET2-1, PET2-2 and PET2-4)



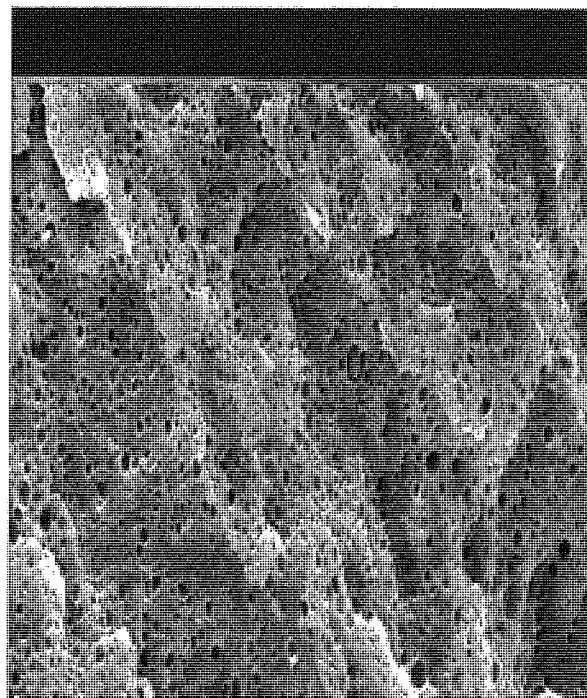
(a)PET/EP (PET1-0)



(b)PET/EP-g-GMA (PET1-4)  
g-GMA=1%

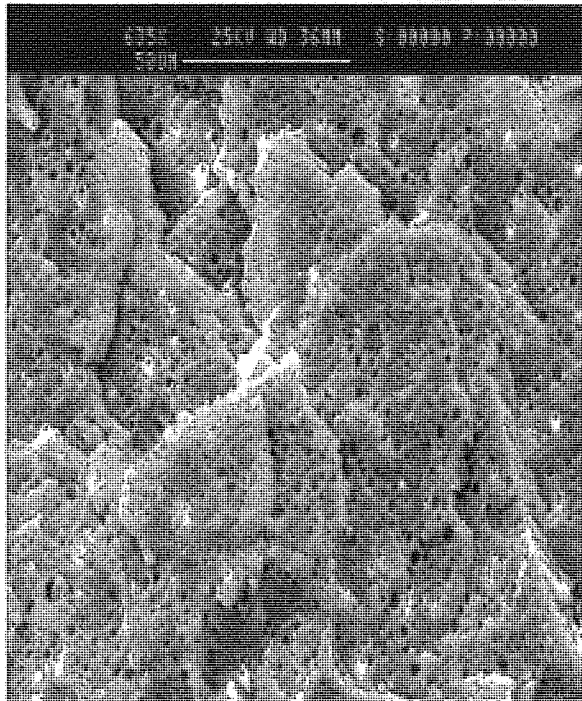


(c) PET/EP-g-GMA (PET1-5)  
g-GMA=2.4%



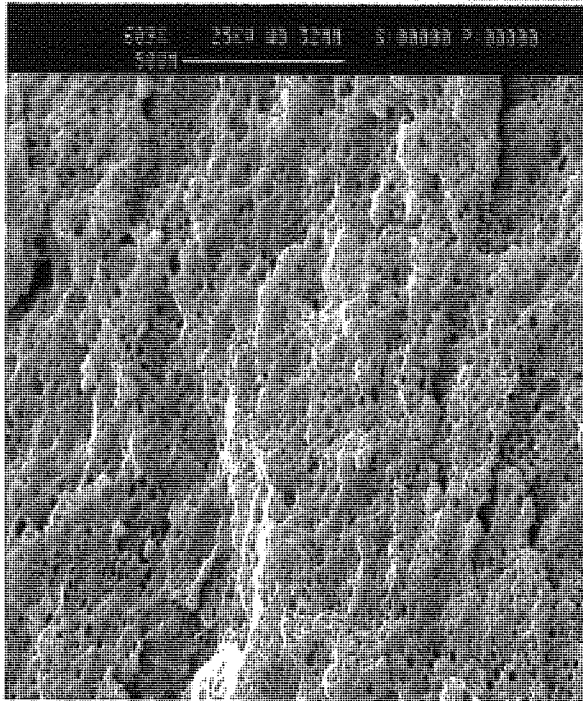
(d) PET/EP-g-GMA (PET1-6)  
g-GMA=2.5%



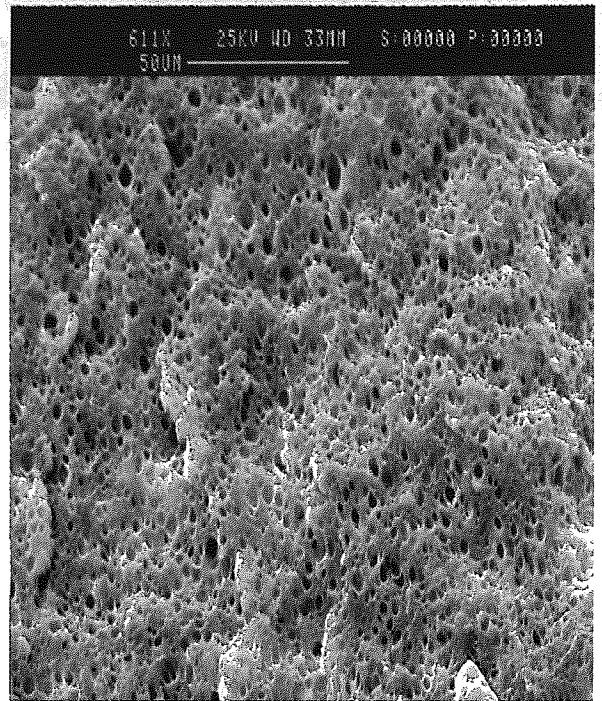


(e)PET/EP-g-GMA (PET1-7)  
g-GMA=3.1%

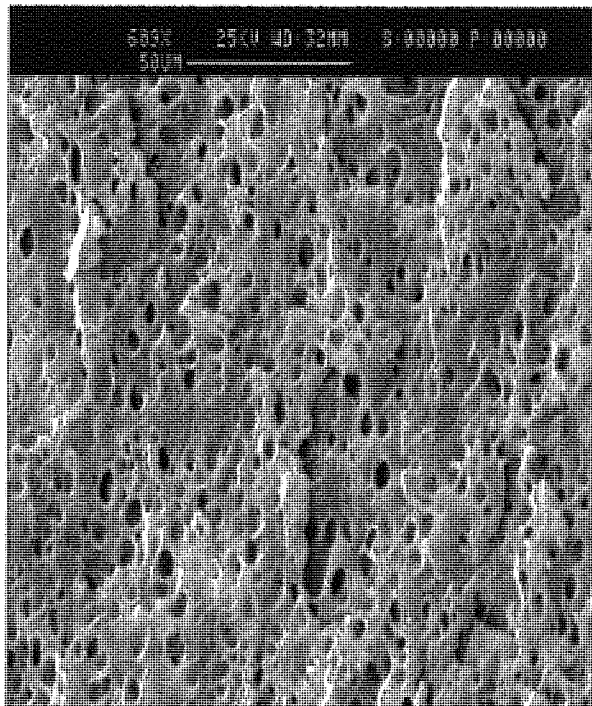
Figure 5-6 SEM of 80/20 PET/EP or EP-g-GMA<sub>TRIS</sub> blends: the effect of grafting degree of EP-g-GMA on the morphology (all these EP-g-GMA<sub>TRIS</sub> samples have similar MFI value: about 1.1 g/10min)



(a)PET/EP-g-GMA (PET1-8)  
MFI=1

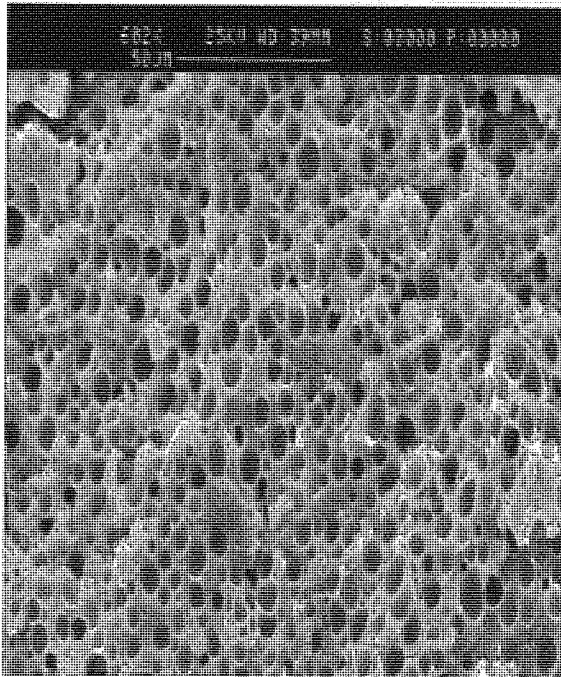


(b)PET/EP-g-GMA (PET1-9)  
MFI=0.5

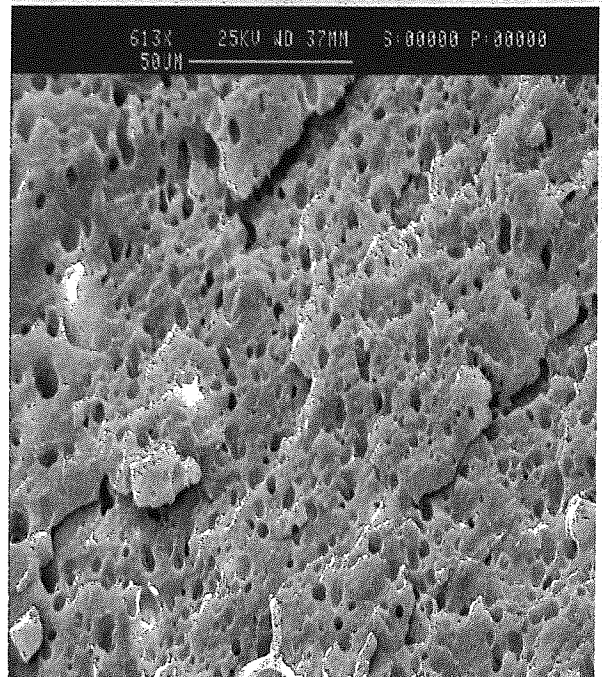


(c)PET/EP-g-GMA (PET1-10)  
MFI=0.1

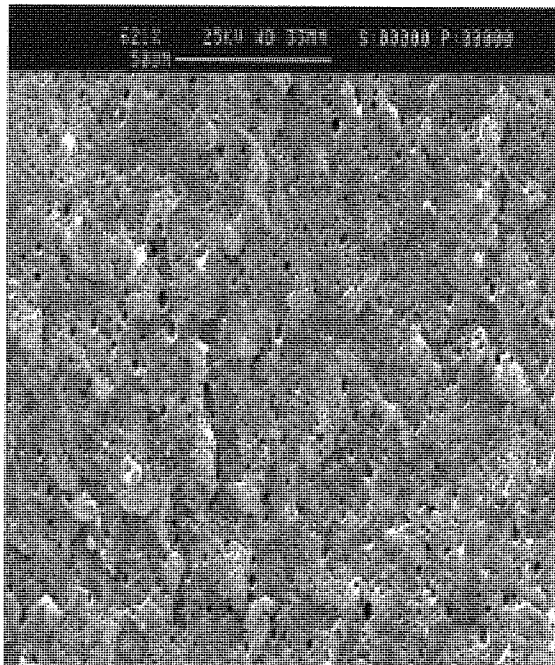
Figure 5-7 SEM of 80/20 PET/ EP-g-GMA<sub>TRIS</sub> blends: the effect of viscosity of EP-g-GMA on the morphology of the blends (all these EP-g-GMA<sub>TRIS</sub> samples have similar grafting level of GMA: about 2.0%)



(a)PET/EP (PET1-0)



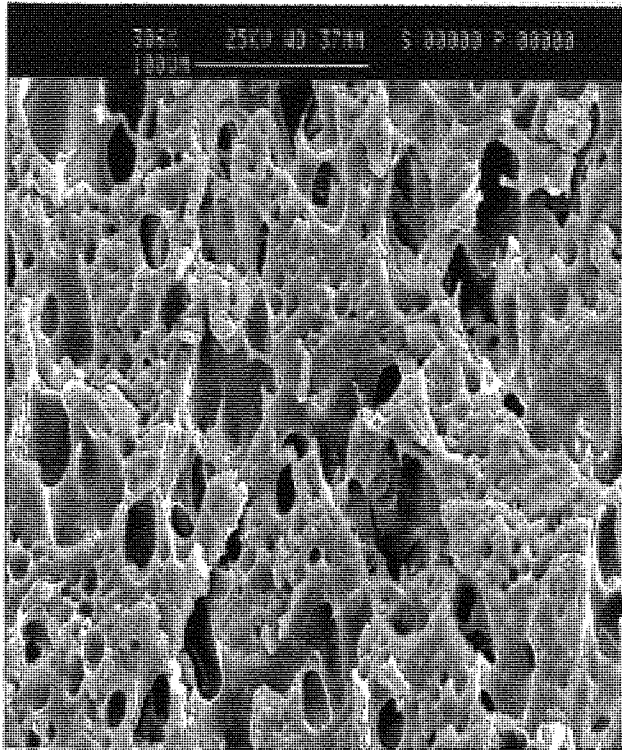
(b)PET/EP-g-GMA<sub>T101</sub> (PET1-2)  
unpurified GP-11 used :  
g-GMA=1.6% polyGMA=2.7%



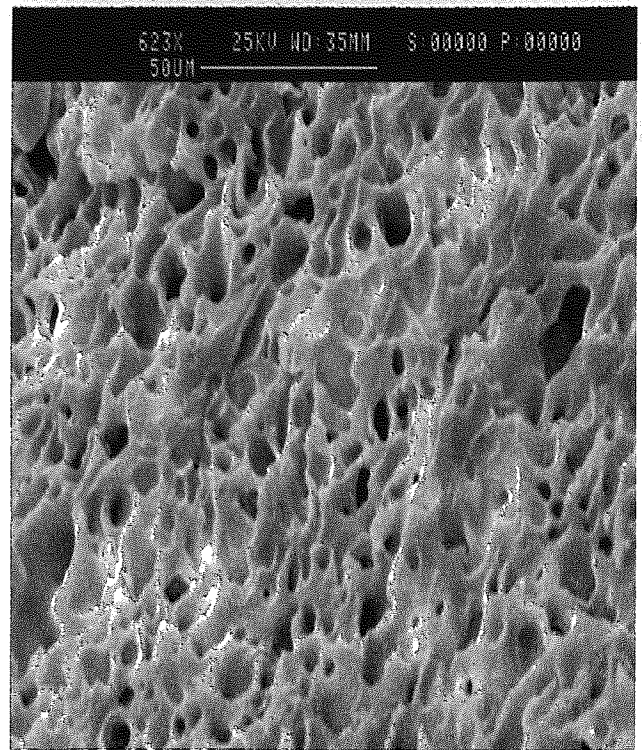
(c) PET/EP-g-GMA (PET1-3)  
purified GP-11 used :  
g-GMA=1.6% polyGMA=0%

Figure 5-8 SEM of 80/20 PET/EP-g-GMA<sub>T101</sub> blends: the effect of polyGMA of EP-g-GMA on the morphology of the blends

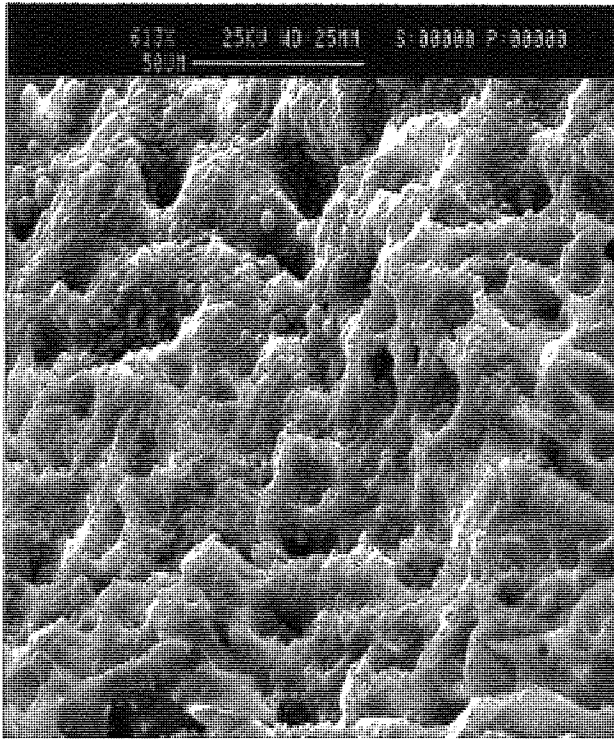




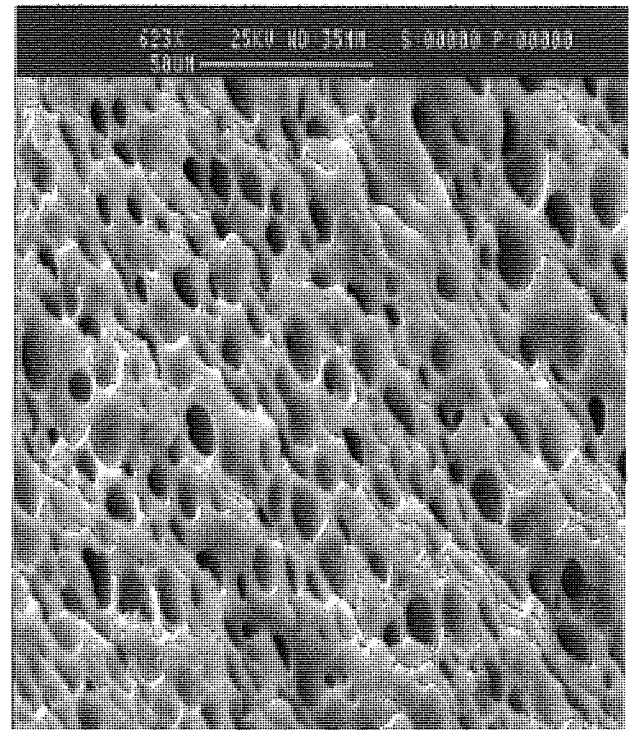
(a) PET/EP (PET2-0)



(b) PET/EP-g-GMA<sub>T101</sub> (PET2-1)  
GP-20 used: g-GMA=1.6%  
polyGMA=0.5%



(c) PET/EP-g-GMA<sub>TRIS</sub> (PET2-3)  
GR-44 used: g-GMA=3.1%  
polyGMA=0.0%



(d) PET/EP-g-GMA<sub>T29B90</sub> (PET2-4)  
BP-3 used: g-GMA=6.0%  
polyGMA=0.4%

Figure 5-9 SEM of 60/40 PET/EP or EP-g-GMA: the effect of different types of EP-g-GMA on the morphology of the blends (Note the scale difference for (a) PET/EP)

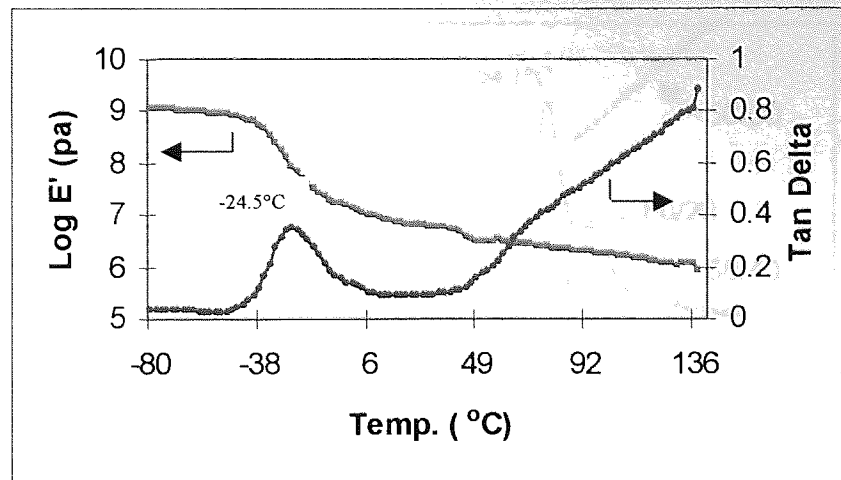


Figure 5-10 DMTA curves for EP (virgin) as a function of E' and Tan $\delta$

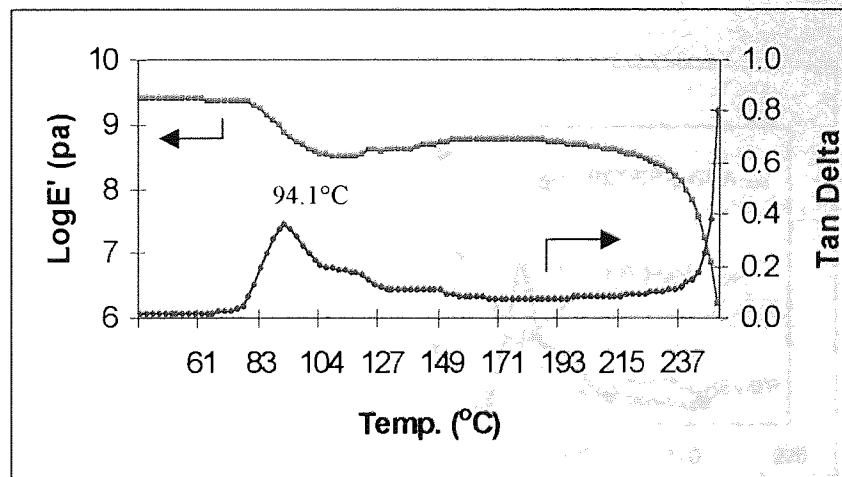


Figure 5-11 DMTA curves for PET (virgin) as a function of E' and Tan $\delta$

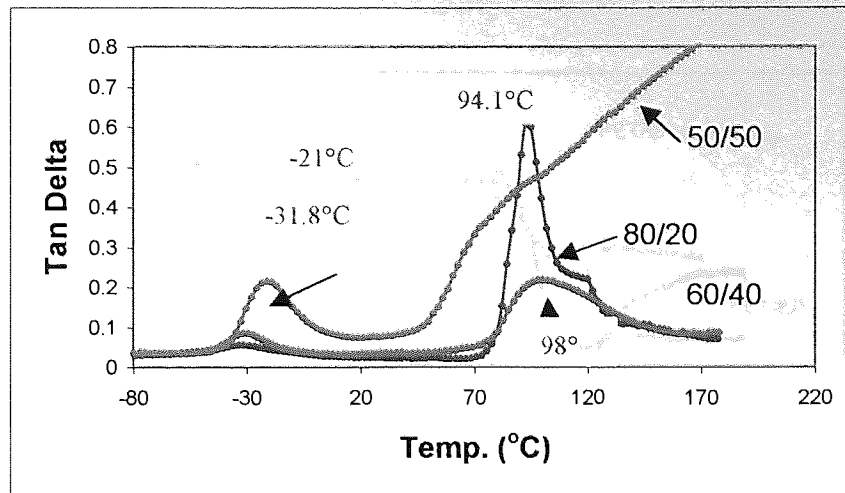


Figure 5-12 DMTA curves for PET/EP (80/20, 60/40, and 50/50) blends as a function of  $Tan\delta$

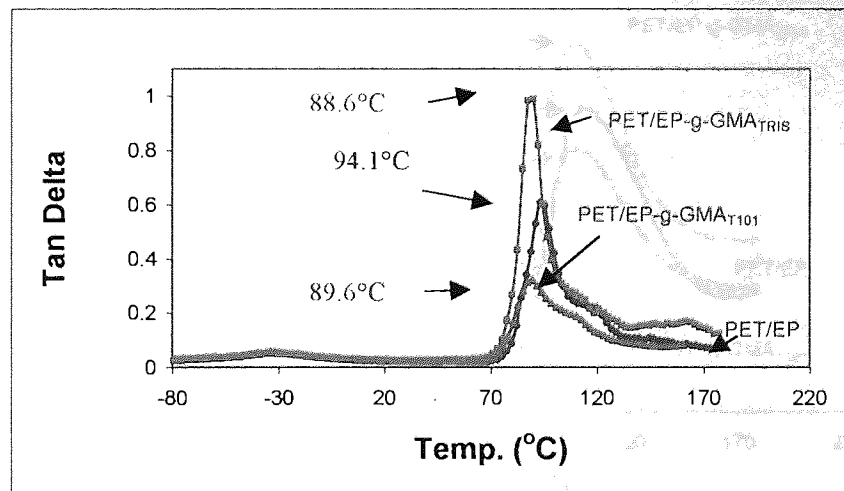


Figure 5-13 Comparison of DMTA curves between PET/EP blend and PET/EP-g-GMA (80/20) blends as a function of  $Tan\delta$

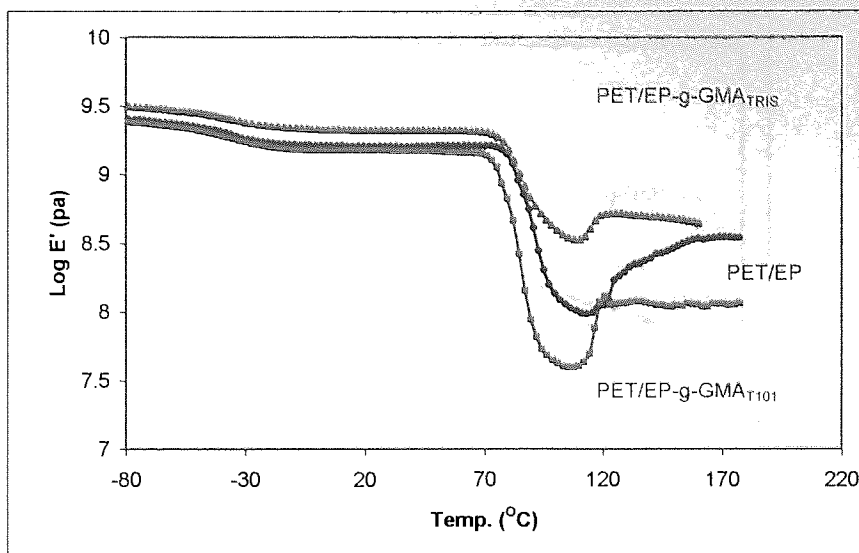


Figure 5-14 DMTA curves for PET/EP (EP-g-GMA) 80/20 blends as a function of E'

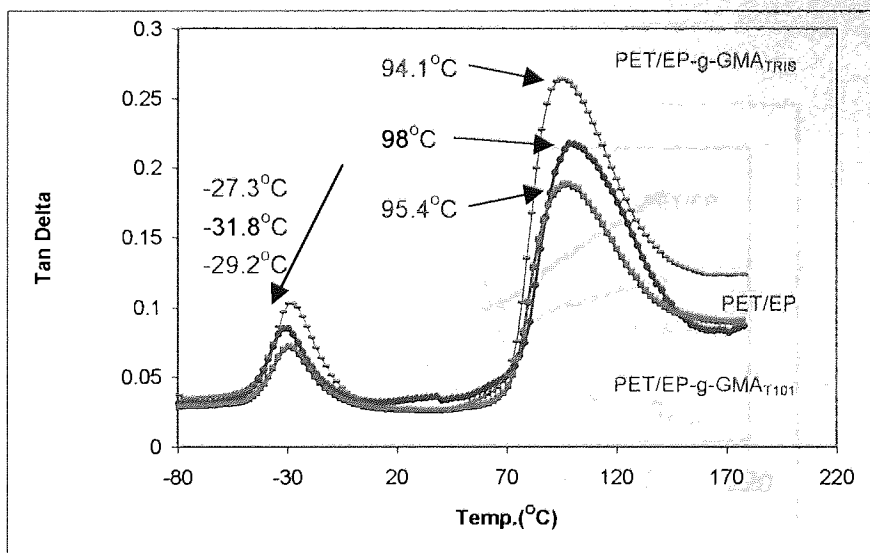


Figure 5-15 DMTA curves for PET/EP (EP-g-GMA) 60/40 blends as a function of Tanδ

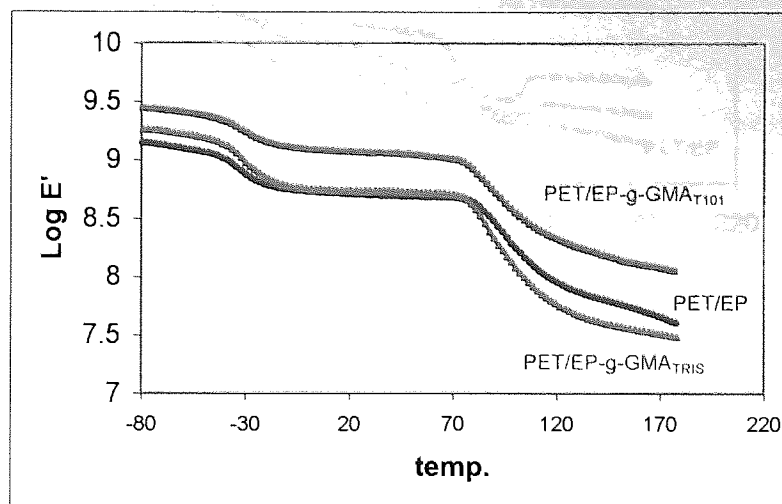


Figure 5-16 DMTA curves for PET/EP (EP-g-GMA) 60/40 blends as a function of E'

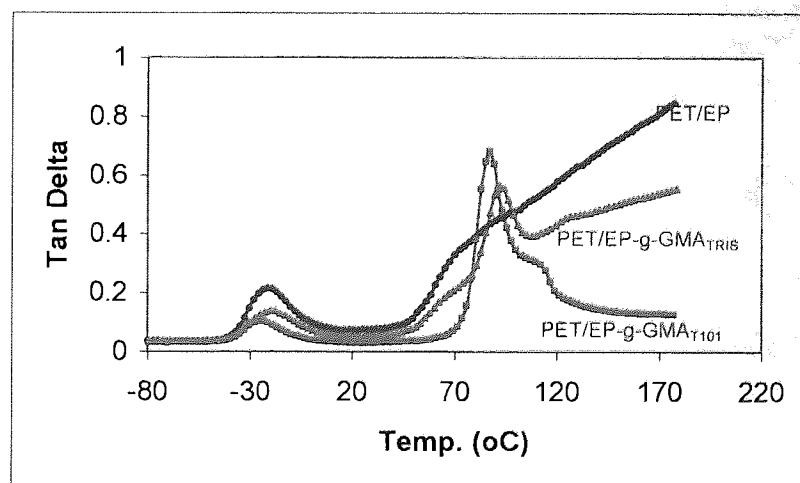


Figure 5-17 DMTA curves for PET/EP (EP-g-GMA) 50/50 blends as a function of tanδ



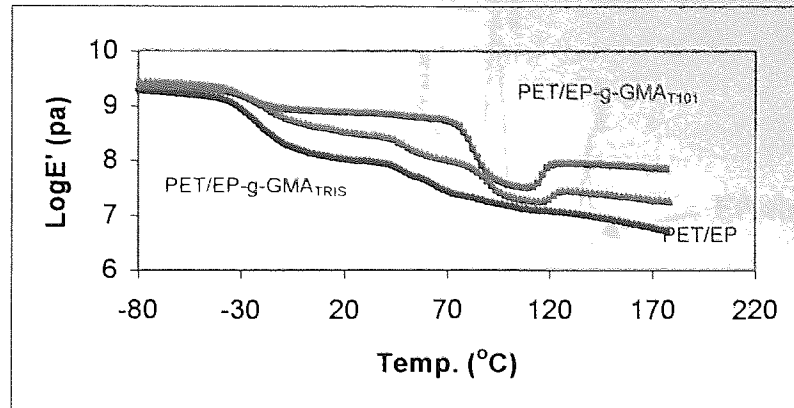
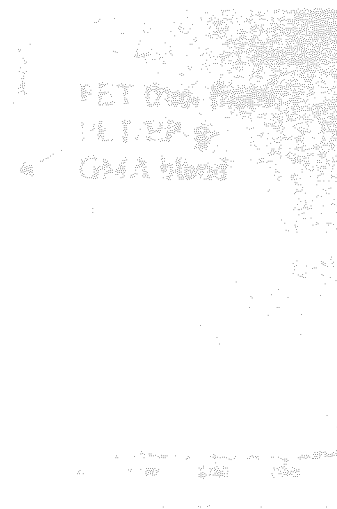
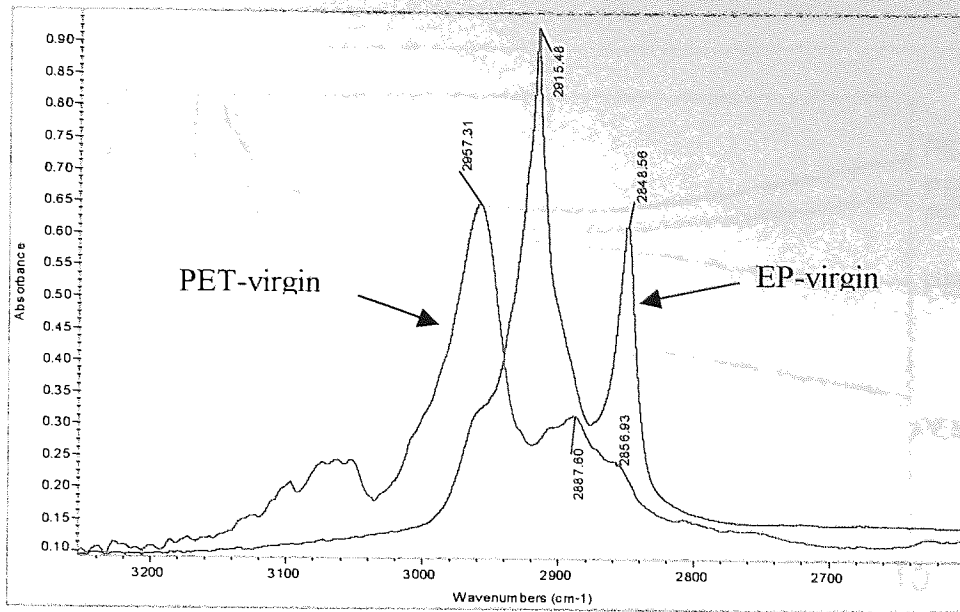
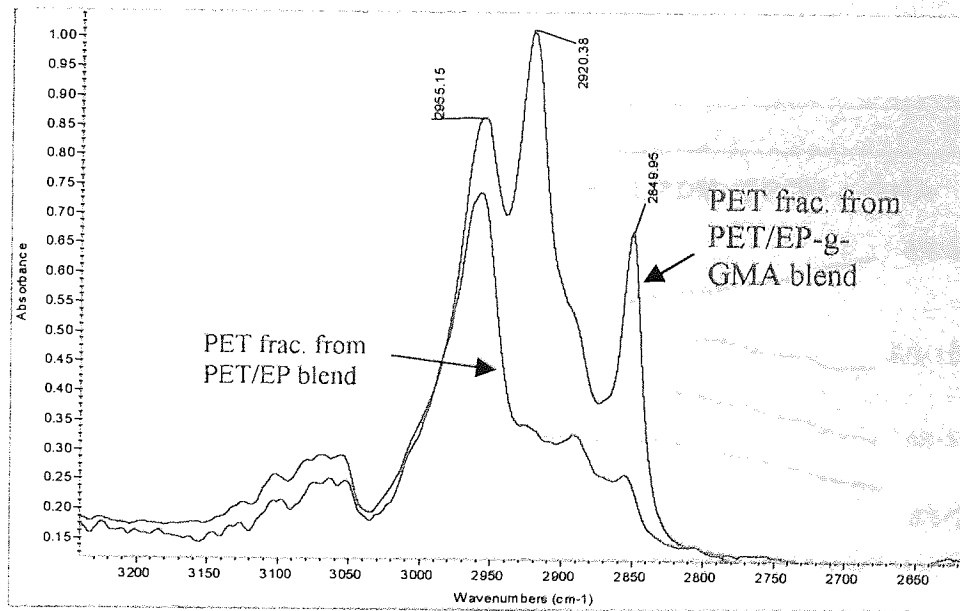


Figure 5-18 DMTA curves for PET/EP (EP-g-GMA) 50/50 blends as a function of E'





(a) Spectra of EP (virgin) and PET (virgin)



(b) Spectrum of PET fraction from PET/EP and PET/EP-g-GMA

Figure 5-19 Comparison of FTIR spectra of virgin polymers (PET and EP) and separated PET fraction from PET/EP blend and PET/EP-g-GMA blend (80/20w/w)

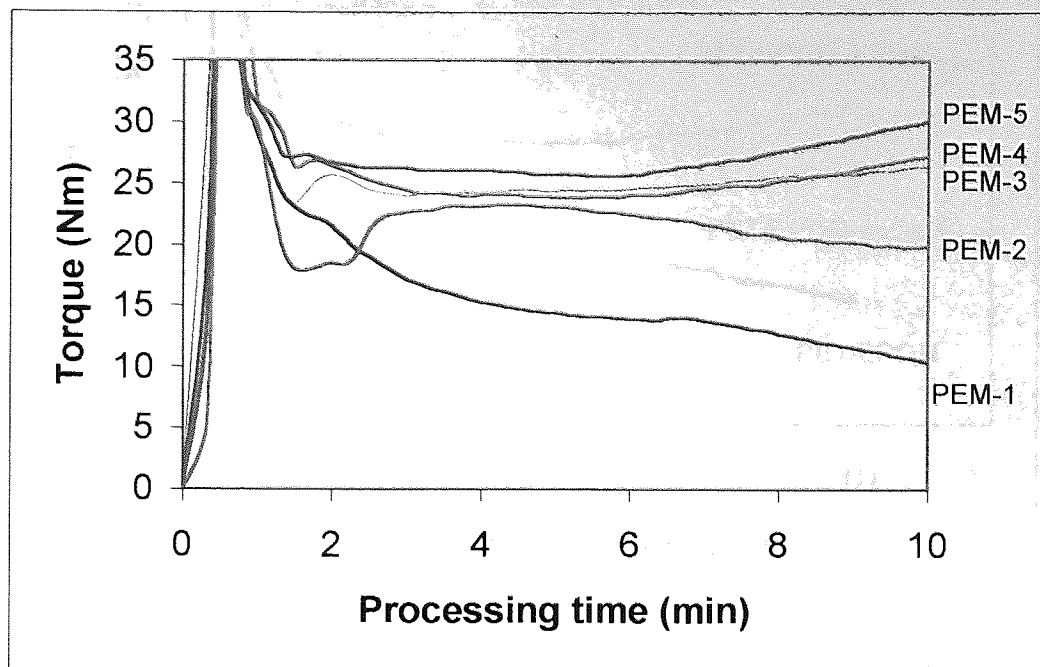


Figure 5-20 Comparison of torque-time curves of blends of PET with different EPDM-g-GMA samples (see Table 5-3 for detailed composition)

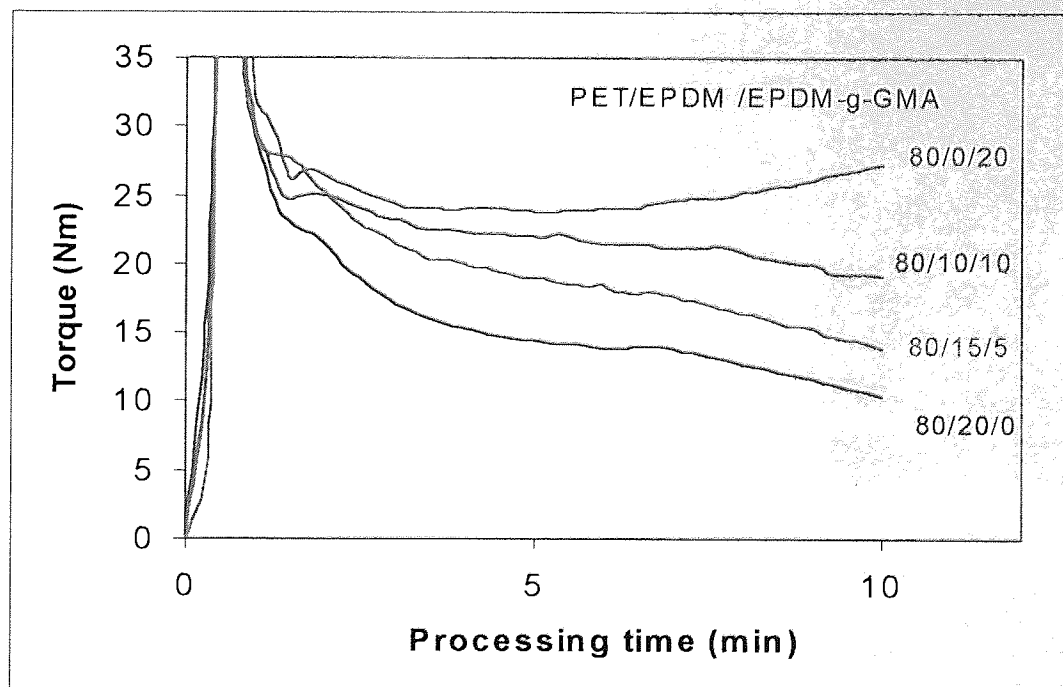


Figure 5-21 Comparison of torque-time curves of ternary blends of PET/EPDM/EPDM-g-GMA with different weight ratios ( EPDM-g-GMA sample: DM-4) (see Table 5-3 for detailed composition of PEM-4, PEM-4-1 and PEM-4-2)

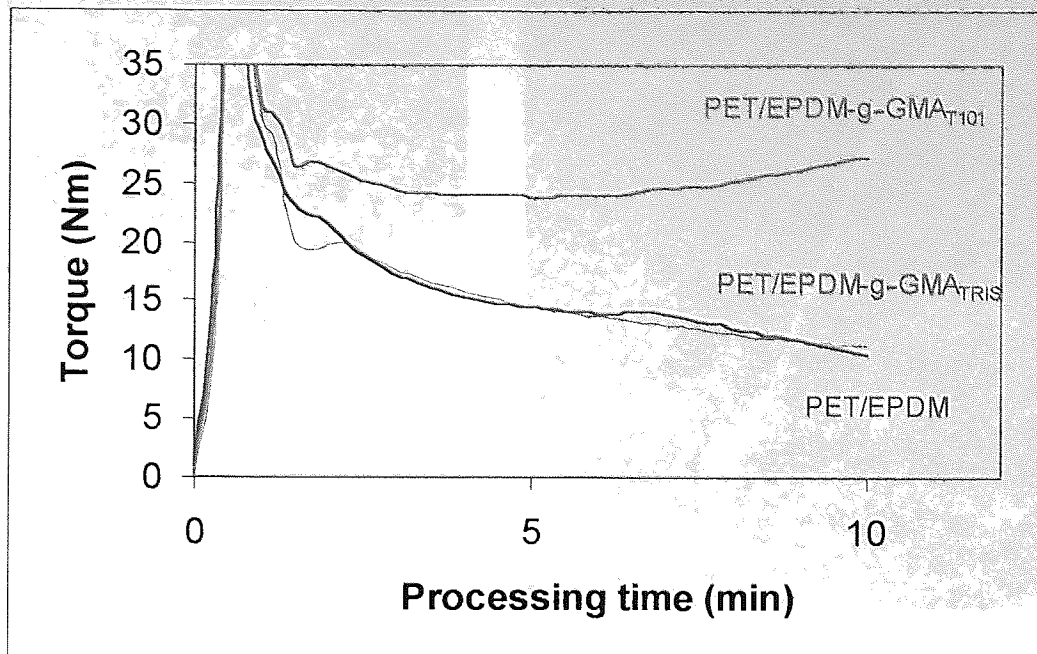
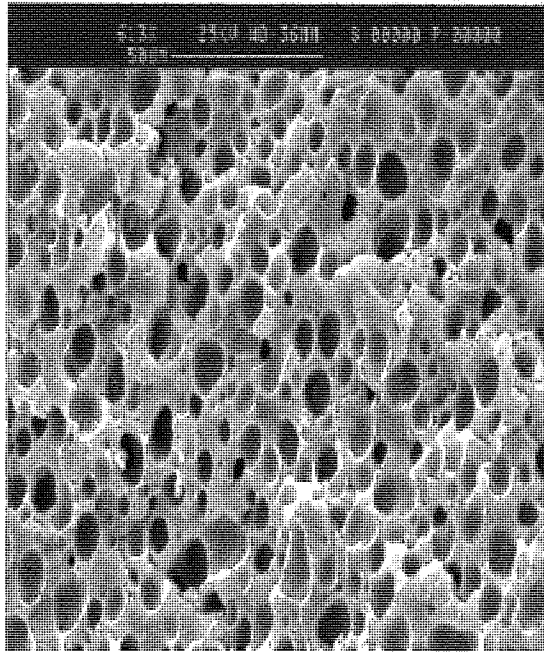
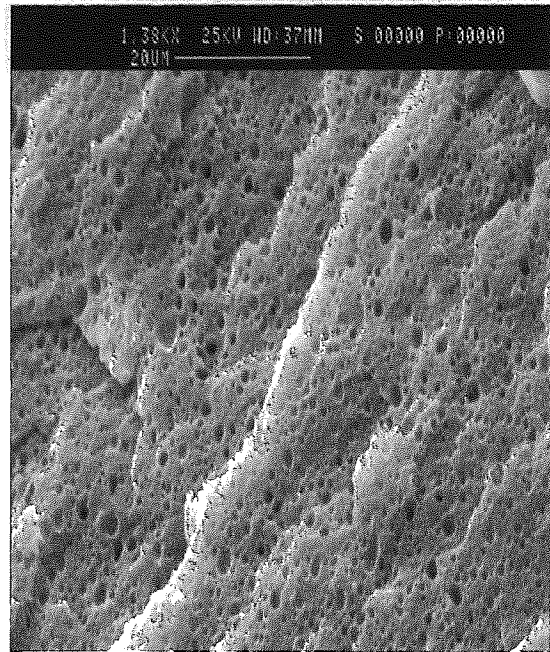


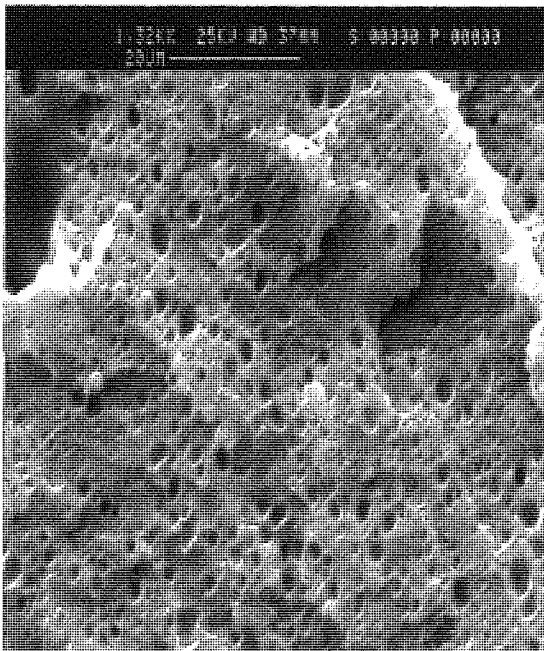
Figure 5-22 Comparison of torque-time curves of blends of PET with different types of EPDM-g-GMA (EPDM-g-GMA<sub>T101</sub>; sample DM-4 and EPDM-g-GMA<sub>TRIS</sub>; sample DM-10) or EPDM (see Table 5-3 for detailed composition)



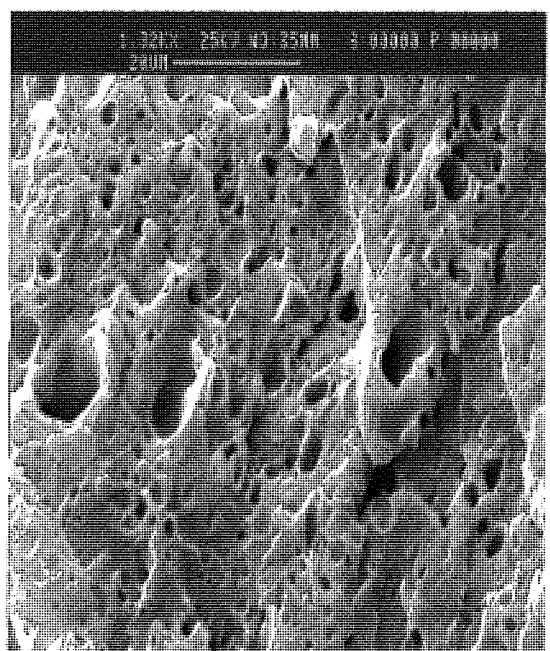
(a) PET/EPDM



(b) PET/EPDM-g-GMA  
(DM-2) (g-GMA=0.35%)

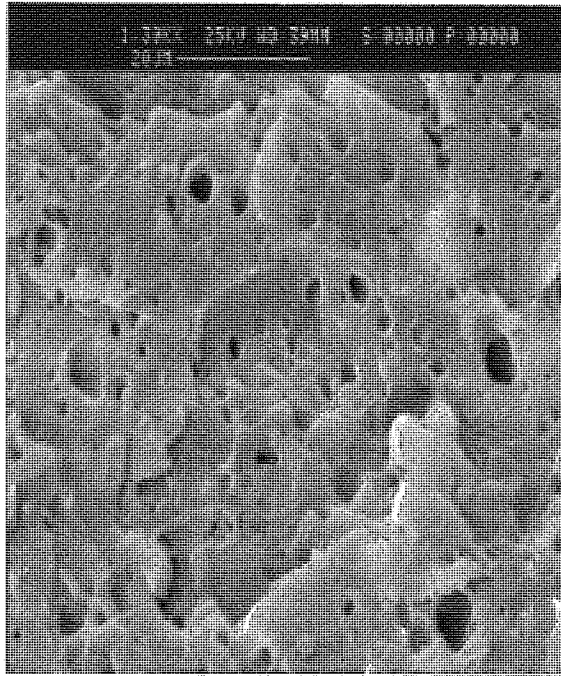


(c) PET/EPDM-g-GMA  
(DM-3) (g-GMA=0.63%)

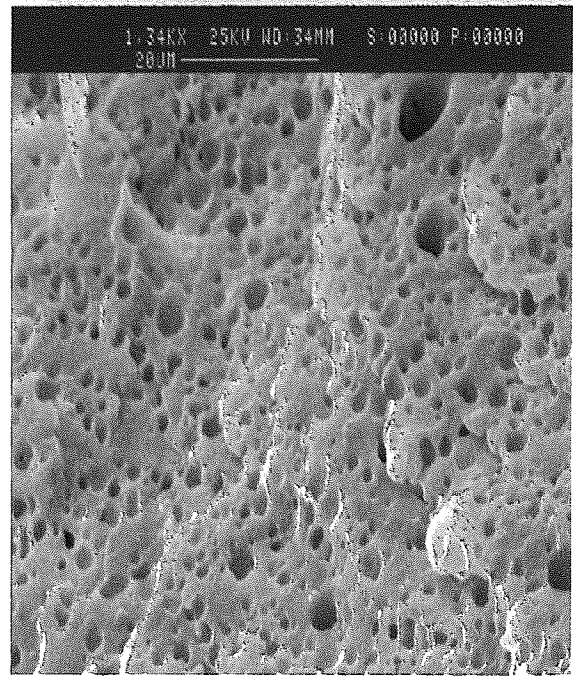


(d) PET/EPDM-g-GMA  
(DM-4) (g-GMA=1.21%)



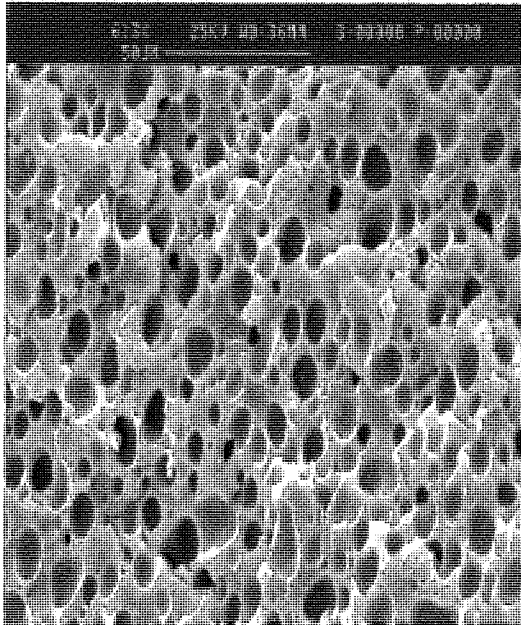


(e) PET/EPDM-g-GMA  
(DM-5) (g-GMA=1.69%)

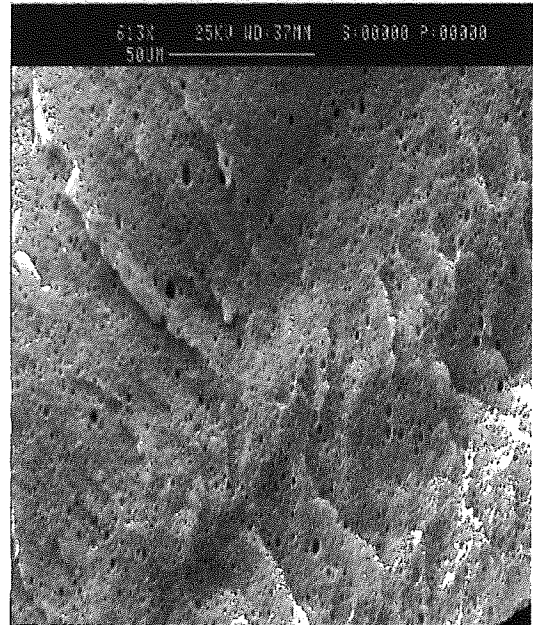


(f) PET/EPDM-g-GMA (DM-  
10) (g-GMA=2.46%)

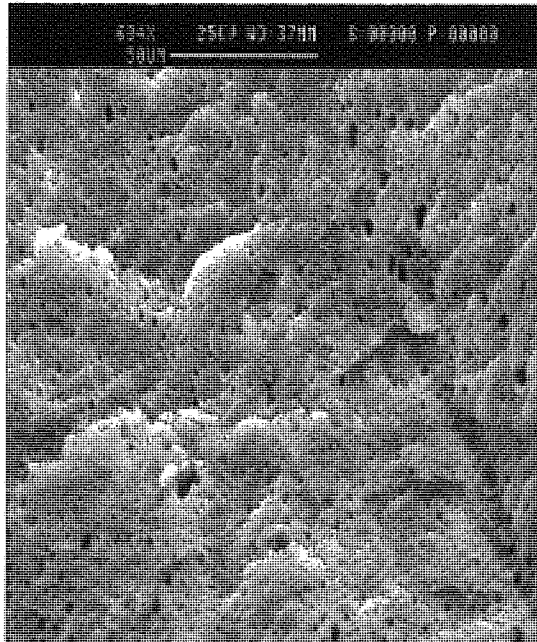
Figure 5-23 SEM of physical blend of PET/EPDM 80/20 and compatibilised blends PET/EPDM-g-GMA (Note the magnification of PET/EPDM is small than others)



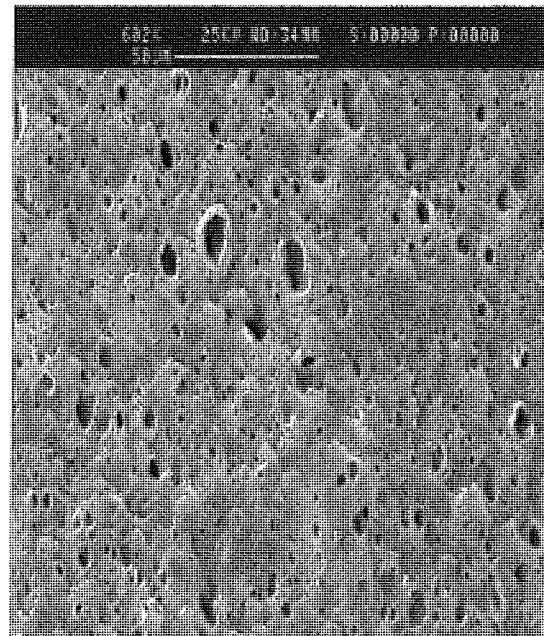
(a) PET/EPDM



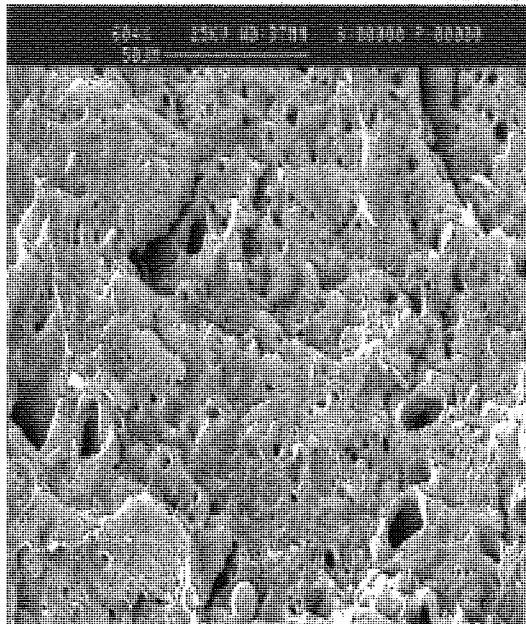
(b) PET/EPDM-g-GMA  
(G-1) (g-GMA=0.35%)



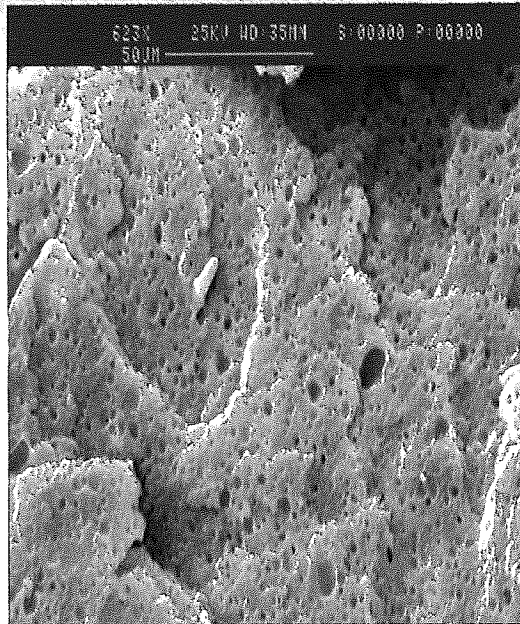
(c) PET/EPDM-g-GMA  
(G-2) (g-GMA=0.63%)



(d) PET/EPDM-g-GMA  
(G-3) (g-GMA=1.21%)



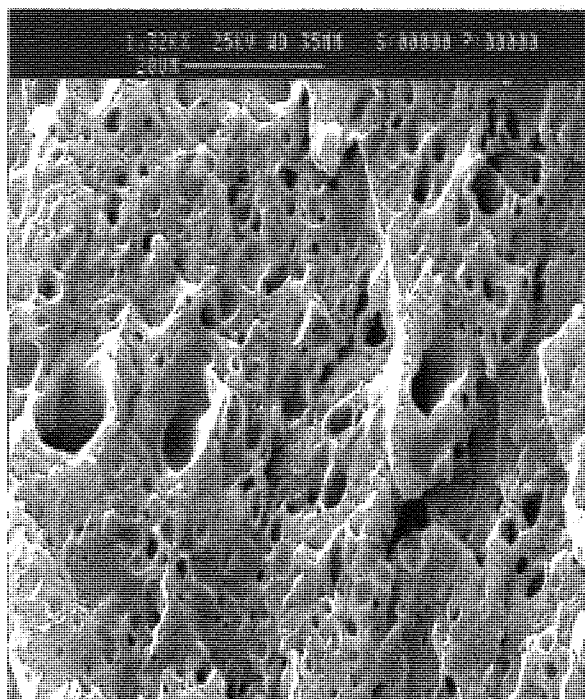
(e) PET/EPDM-g-GMA  
(G-4) (g-GMA=1.69%)



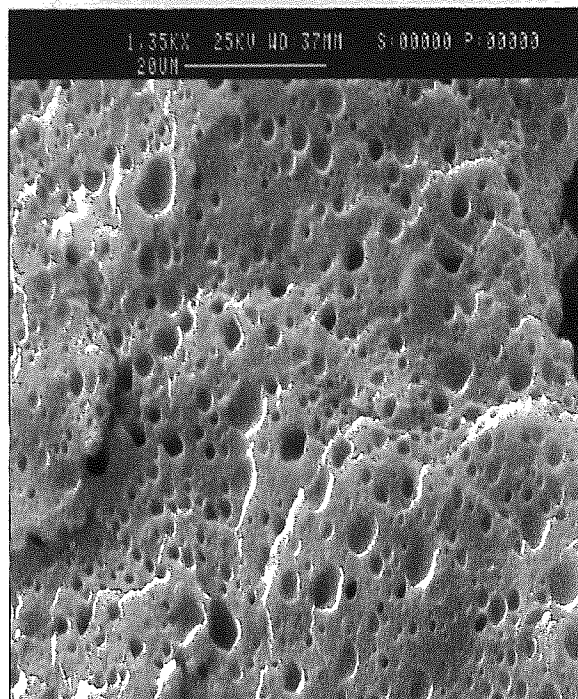
(f) PET/EPDM-g-GMA  
(TR-1) (g-GMA=2.46%)

Figure 5-23a SEM of physical blend of PET/EPDM 80/20 and compatibilised blends PET/EPDM-g-GMA (SEM of the same samples in Figure 5-23, but the magnification of the picture is smaller for better comparison)

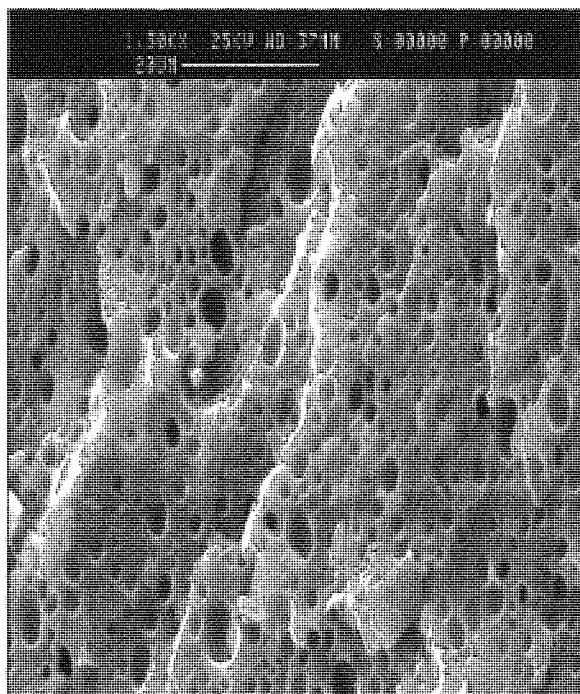




(a) PET/EPDM-g-GMA(G-3)  
80/20 w/w

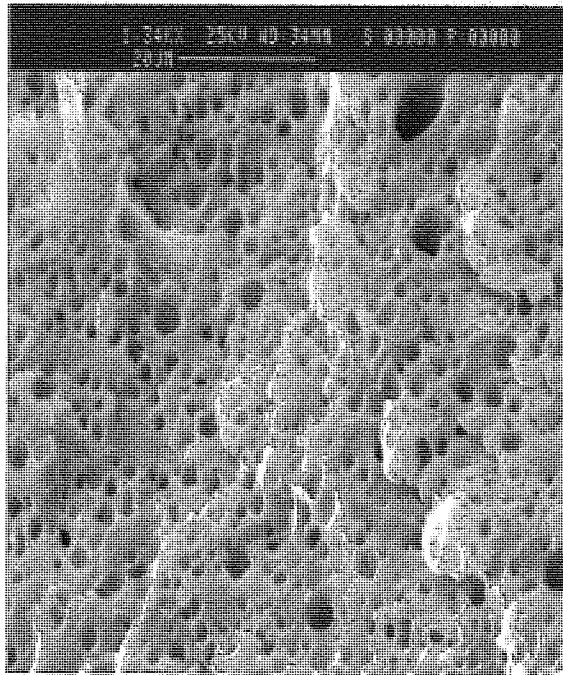


(b) PET/EPDM/EPDM-g-GMA  
80/10/10 w/w

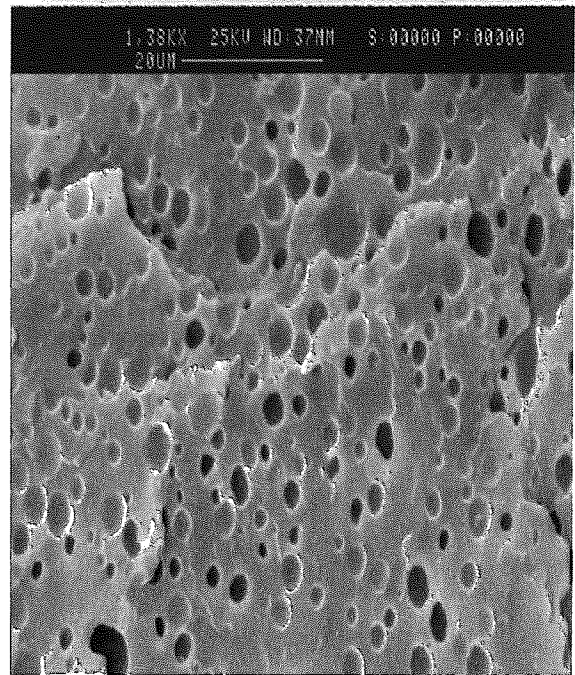


(c) PET/EPDM/EPDM-g-GMA  
80/15/5 w/w

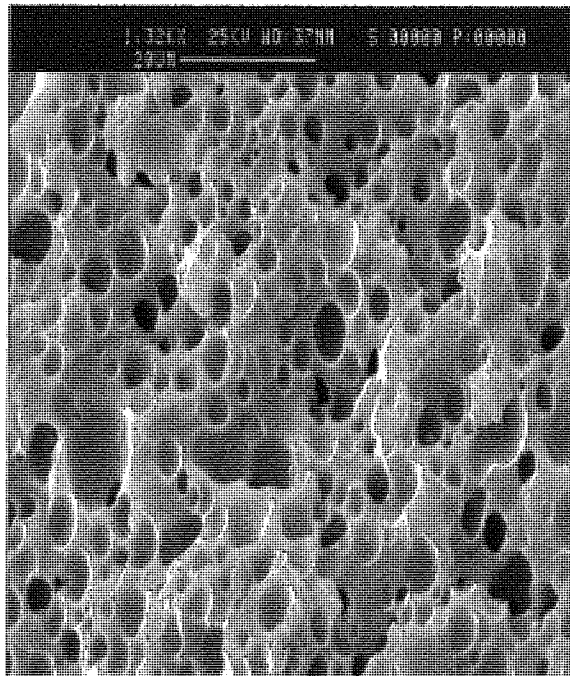
Figure 5-24 SEM of binary blend of PET/EPDM-g-GMA (80/20) and ternary blends of PET/EPDM/EPDM-g-GMA with different ratios (EPDM-g-GMA : sample DM-4)



(a) PET/EPDM-g-GMA<sub>TRIS</sub> (DM-10)  
80/20 w/w

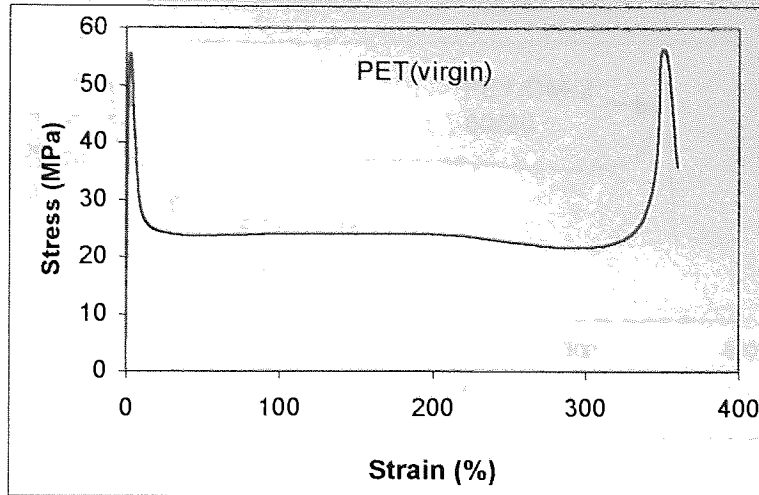


(b) PET/EPDM/EPDM-g-GMA<sub>TRIS</sub>  
80/10/10 w/w

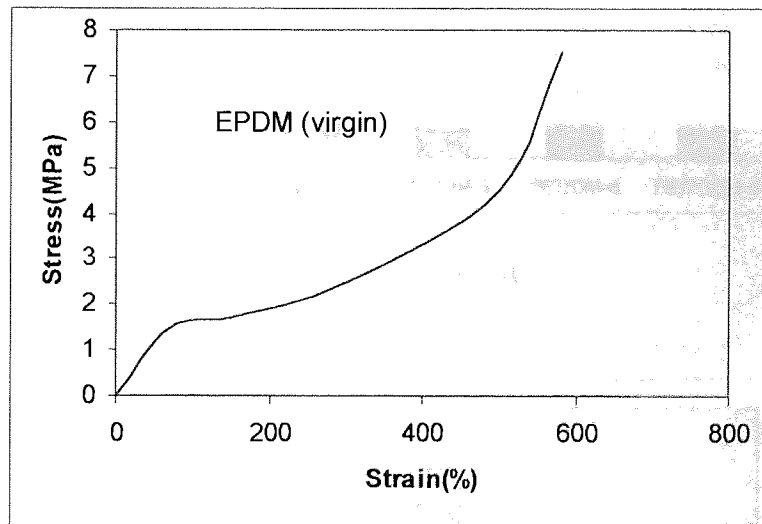


(c) PET/EPDM/EPDM-g-GMA<sub>TRIS</sub>  
80/15/5 w/w

Figure 5-25 SEM of binary blend of PET/EPDM-g-GMA<sub>TRIS</sub> (80/20) and ternary blends of PET/EPDM/EPDM-g-GMA<sub>TRIS</sub> with different ratios (EPDM-g-GMA : sample DM-10)



(a) Stress-strain curve of tensile test of virgin PET



(b) Stress-strain curve of tensile test of virgin EPDM

Figure 5-26 Tensile properties of virgin PET and EPDM

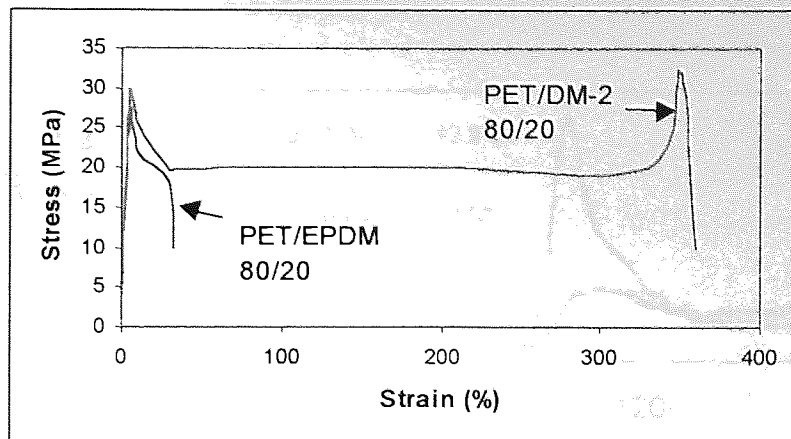
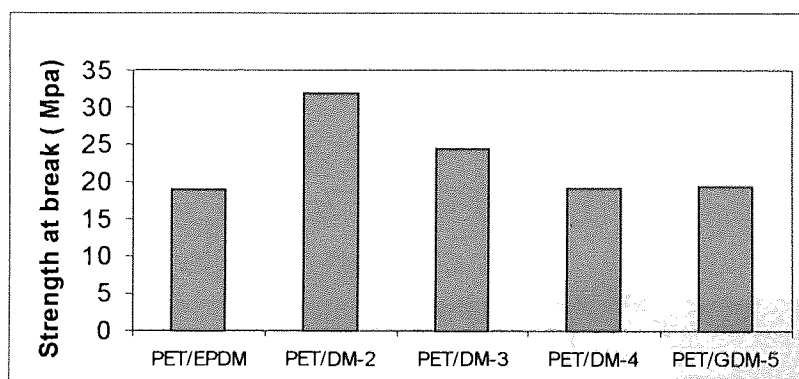
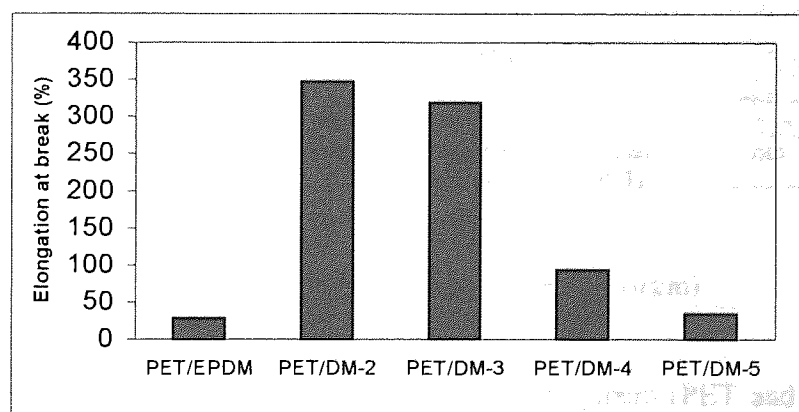


Figure 5-27 Stress-strain curves of tensile test of PET/EPDM (80/20) physical blend and PET/EPDM-g-GMA (80/20) (EPDM-g-GMA used: DM-2, see Table 5-3)



(a) Strength at break



(b)Elongation at break

Figure 5-28 Tensile properties of PET/EPDM or PET/EPDM-g-GMA with different rubber samples (EPDM-g-GMA samples: DM-2--DM-5)

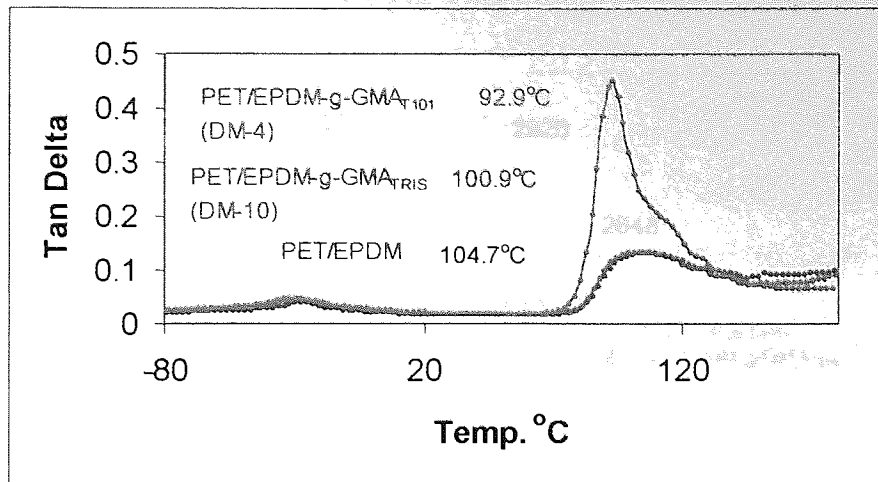
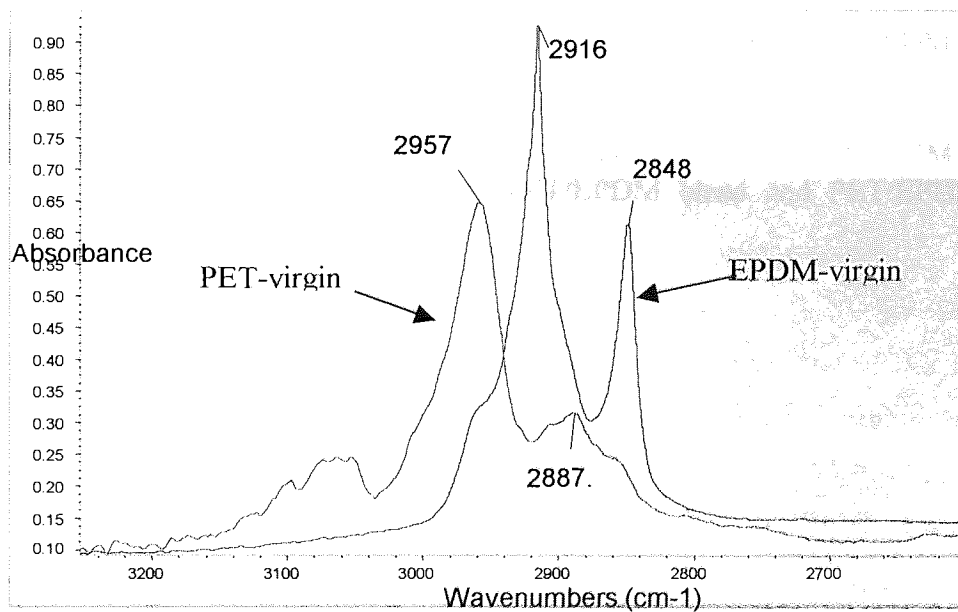


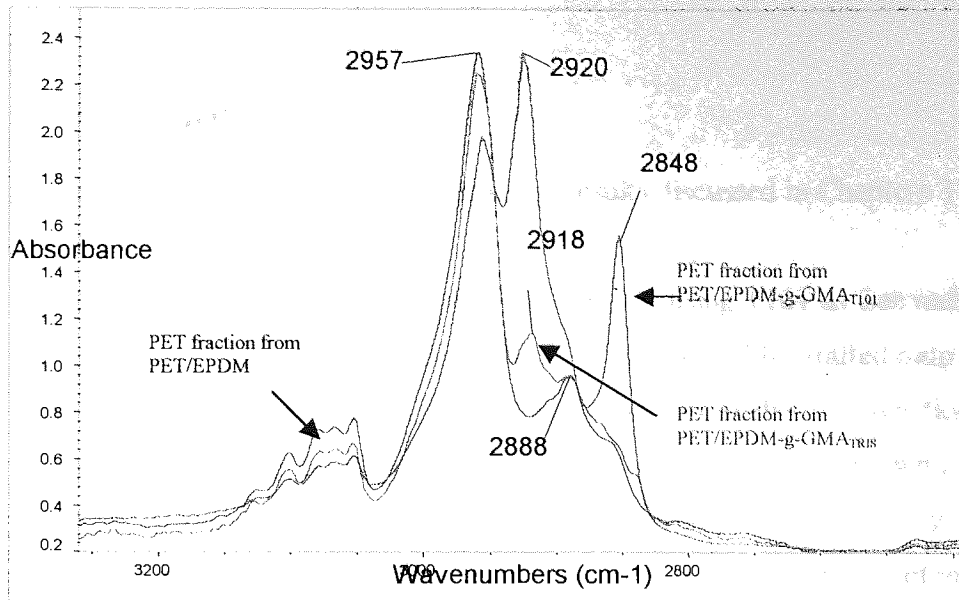
Figure 5-29 DMTA curves for PET/EPDM (80/20) blend and PET/EPDM-g-GMA (80/20) blends as a function of  $Tan\delta$



(a) Spectra of EPDM (virgin) and PET (virgin)

Figure 5-30 Comparison of FTIR spectra of virgin polymers (PET and EPDM) and separated PET fractions from PET/EPDM blend and PET/EPDM-g-GMA blends (80/20w/w)





(b) Spectra of PET fractions separated from PET/EPDM and PET/EPDM-g-GMA<sub>T101</sub> and PET/EPDM-g-GMA<sub>TRIS</sub> blends

Figure 5-30 Comparison of FTIR spectra of virgin polymers (PET and EPDM) and separated PET fractions from PET/EPDM blend and PET/EPDM-g-GMA blends (80/20w/w)

## CHAPTER 6 CONCLUSIONS AND RECOMMENDATIONS FOR FUTURE WORKS

### 6.1 CONCLUSIONS

The following conclusions can be drawn from the results discussed in Chapters 3 to 5:

- 6.1.1 In the free radical melt grafting of GMA onto EP using T101 as free radical initiator (EP+GMA+T101 system), it was found that GMA could be grafted onto EP, though only to a low extent due to strong competition from the side reactions, e.g. the homopolymerisation of GMA and crosslinking/branching of EP, with the desired grafting reaction. The GMA-grafted polymer was characterised by FTIR after purification which removes all ungrafted materials. The infrared results demonstrated that GMA has successfully grafted onto the EP as illustrated by the appearance of new absorption peak at  $1730\text{ cm}^{-1}$  ascribed to the formation of a saturated ester and absorptions at  $908\text{ cm}^{-1}$  and  $844\text{ cm}^{-1}$  ascribed to the presence of the epoxide ring. The formation of the homopolymer of GMA, polyGMA, during the melt grafting was determined by employing a set of purification procedures to separate the various reaction products and characterising them using FTIR (see Section 3.2.3, p100). This confirmed that the presence of polyGMA was indeed present among the GMA grafted EP products (see Figure 3-6, p152). PolyGMA is very likely to be formed during the grafting, especially when high concentrations of the peroxide (T101) are used (see Figure 3-13, p156).
- 6.1.2 When GMA alone was reacted with EP in the presence of T101, the grafting degree increased with the increasing concentration of T101, but the overall grafting yield was low (see Figure 3-10, p155). For example, when 12 phr GMA and 0.5 phr T101 was added to EP, the grafting degree was 0.4%, i.e. only 3.3 % of the total GMA was grafted. When T101 was increased to 1.0 phr, the grafting degree reached to 1.4% (11.6% of total GMA added) and the grafting degree levelled off with further increase of T101 up to 1.5 phr. The increase of GMA concentration also led to higher GMA grafting degree. Meanwhile, increasing the concentrations of peroxide and GMA led to an increase in the formation of polyGMA during the melt grafting. With a constant concentration of 1 phr T101, the formation of polyGMA was

proportional to the increase of GMA initially added but the grafting of GMA initially increased and then levelled off when GMA concentration was over 12 phr. The amount of polyGMA was shown to be much higher than the amount of grafted GMA when 18 phr GMA was added (see Figure 3-14, p156). It is clear that increasing GMA concentration leads to a great increase in the chance of homopolymerisation of GMA.

6.1.3 The EP used in this study is not very liable to form crosslinking and insoluble gel during the melt grafting unless very high concentration of T101 was used, but the observed branching resulted in a significant alteration of the melt rheological properties of the polymer. The extent of alteration was dependent on the concentration of peroxide used. An increase in peroxide concentration reduces significantly the MFI value of the GMA grafted EP (Figure 3-11, p155). Grafting of GMA was therefore accompanied by an increase in the melt viscosity of the polymer.

6.1.4 The addition of TRIS as a reactive comonomer in the melt grafting of GMA on EP (EP+GMA+TRIS+T101 system) could greatly enhance the desired grafting reaction and reduce the side reaction. The results showed clearly that the use of this comonomer led to a significant improvement in the grafting efficiency of GMA on EP and that higher levels of grafting was achieved at much lower peroxide concentration resulting in a negligible degree of degradation of the polymer matrix (see Figure 3-21, p160) with very small amount of polyGMA formation. The need for only a very small concentration of a peroxide to achieve high level of grafting in TRIS-containing system is very significant. For example, when GMA and TRIS concentrations were fixed at 10 phr and 2.5 phr, only 0.005 mole ratio of T101 to GMA+TRIS (T101= 0.123 phr) was enough to achieve a 2% grafting degree. Furthermore, it was shown that the higher the TRIS concentration used, the less the peroxide concentration needed. Ultimately, the optimal grafting in the presence of TRIS, in terms of high grafting of GMA and minimum branching /crosslinking of EP, was only achievable with a delicate balance between the molar ratios of the reagents (monomer, comonomer, initiator) and the process variables (e.g. temperature, processing time).



- 6.1.5 Examination of the kinetics of the grafting reaction in the presence of the comonomer demonstrated that samples processed in the presence of the comonomer did not contain measurable amounts of either the free TRIS-co-GMA copolymer or the poly-TRIS. It was shown clearly that the rate of GMA-grafting is higher in the presence of TRIS when compared to the rate of grafting in its absence and increased further with increasing the comonomer concentration (see Figure 3-24, p162). Moreover, it was observed that the presence of TRIS led to complete grafting reactions in shorter times. The presence of the comonomer in the grafting system, therefore, leads not only to higher GMA grafting yield but also to less competition from side reactions. It was clear that the rate of formation of poly-GMA in the comonomer system was very slow and its final yield was very low, especially when compared to the amount of poly-GMA formed in the absence of TRIS (at the same initial GMA concentration), see Fig. 3-24 a, b, p162.
- 6.1.6 It was shown that the effect of the trifunctional TRIS, as a comonomer, on enhancing the grafting efficiency of the GMA in EP copolymer arose from the fact that TRIS has much higher reactivity towards both GMA and EP copolymer than GMA towards EP. The high reactivity of TRIS towards EP-macroradicals was clearly illustrated from the distinct torque behaviour during the reactive processing (see Figs. 3-18, p158, and 3-19, p159) and the high reactivity of TRIS towards GMA was demonstrated from the formation of GMA-co-TRIS if GMA, TRIS and T101 were added together during the melt grafting. As a result, the comonomer is both effective in trapping the radicals formed on the polymer backbone and such that the propagating radical formed is highly reactive towards the desired monomer.
- 6.1.7 GMA could be successfully grafted onto EPDM via melt free radical grafting reaction using an organic peroxide (T101) as a free radical initiator. The results demonstrated that the desired grafting reaction was accompanied by obvious crosslinking of EPDM (see Figures 3-29, p165, 3-30, p165, and 3-31, p166). High concentrations of the peroxide resulted in high GMA grafting degree but also led to high gel formation. On the other hand, no measurable polyGMA was detected in the GMA grafted EPDM system. This clearly illustrates that different polymer

substrates can lead to completely different grafting features and even different grafting mechanisms.

- 6.1.8 In the absence of TRIS during the melt grafting of GMA on to EPDM, increasing peroxide concentration led to a proportional increase in the grafting yield, while the gel content also increased significantly (see Figure 3-29, p165). However, the overall grafting was low. Even at a high concentration of 1phr T101, the GMA grafting degree did not exceed 1.7% - that is less than 20% of original GMA grafted, but the gel content reached to 36%. It was demonstrated that for the grade of EPDM used in this work, crosslinking was the main side reaction and the reactivity of GMA was low towards EPDM chains as indicated by the high percentage of gelformed and low GMA grafting degree. The high degree of crosslinking of EPDM which was indicated by high torque values during the processing and high amount of gel formation and no measurable homopolymerised GMA (polyGMA) may be attributed to the presence of unsaturation (diene) in EPDM.
- 6.1.9 The addition of TRIS to the system (EPDM+GMA+TRIS+T101) resulted in higher grafting and lower gel. With 2.5 phr TRIS, a very low concentration of peroxide was required to achieve high grafting and low gel. When 0.0025 mole ratio of T101 (actual T101: 0.057 phr in the formulation) was added to the system, about 2.5% GMA grafting degree was measured with only 6% gel (see Figure 3-39, p170). However, higher concentrations of TRIS and T101, also led to both high grafting and high gel. In the presence of TRIS, therefore a proper balance of compositions of TRIS to GMA and peroxide to GMA and TRIS was the key to achieving optimal grafting with minimum crosslinking of EPDM.
- 6.1.10 Differential solvent fractionation analysis of GMA grafted EPDM prepared in the absence and presence of TRIS revealed the significant differences between these two types of GMA modified EPDM system. The fractionation results showed that the sample which was prepared in the absence of TRIS (EPDM-g-GMA<sub>T101</sub>, sample DM-3) had a higher low temperature soluble fraction (hexane soluble fraction), whereas the sample which was prepared in the presence of TRIS (EPDM-g-GMA<sub>TRIS</sub>, sample DM-9) had much less low temperature soluble fraction (hexane

soluble fraction) but higher high temperature soluble fraction (that is toluene and xylene soluble fractions) (see Figure 3-32, p166). This clearly shows that EPDM-g-GMA<sub>TRIS</sub>, has a high fraction of branched EPDM. TRIS has multi-functional groups and is highly reactive towards EPDM chains. This certainly leads to high extent of branching in EPDM.

6.1.11 When a small amount of PP was added to EPDM (EPDM/PP=75/25) during the melt grafting of GMA onto EPDM, the results demonstrated that the amount of gel could be significantly reduced compared to the grafting of GMA onto EPDM alone (see Figs. 3-37, p169, 3-38, p169, and 3-39, p170). In the absence of TRIS, with a fixed concentration of GMA at 10 phr, increasing the concentration of peroxide, T101, from 0 to 0.6 phr led to an increase in the grafting degree while no gel was measured. When the concentration of peroxide, T101, was further raised to 1 phr, the GMA grafting degree levelled off, but more than 10% gel was determined (see Figure 3-37, p169). This clearly shows that the presence of PP does indeed decrease the extent of the crosslinking reaction of EPDM during the melt grafting.

6.1.12 In the reactive processing of NR with MA, it was found that the grafting reaction could be initiated both thermally and by peroxides. In the absence of any peroxide, MA could be grafted onto NR above a certain temperature. When raw NR was used without any purification, a minimum temperature of above 140°C was required to initiate the reaction, but only a very small amount of MA was grafted onto the rubber. With increasing the processing temperature, the grafting efficiency increased linearly. Though high temperature have promoted the reaction, oxidation became unacceptable at a temperature above 220°C hence the processing preferable temperature was 200°C. At a fixed temperature of 200°C, the grafting degree increased with increasing the amount of MA initial added (see Figure 4-12, p207).

6.1.13 In the absence of peroxide, the significant difference was found when purified NR (subjected to Soxhlet extraction with acetone) was used. A certain amount of MA could be grafted onto the rubber even at low temperature, but the reaction products became crumble, indicating crosslinking during the reactive processing. When the temperature was raised to over 150°C, much higher grafting efficiency was

measured. At a fixed temperature of 200°C, the grafting degree increased with increasing the amount of MA initial added (see Figure 4-12, p207). The higher grafting efficiency may be attributed to the removal of some natural substances from the NR which can inhibit the grafting reaction.

- 6.1.14 In the case of peroxide initiation, it was found that T101 was a suitable peroxide to initiate the grafting reaction of MA onto NR. Under optimal conditions the grafting degree initially increased with increasing MA concentration and reached a maximum at about 6-10 phr initial MA concentration and then decreased with a further increase in MA concentration (see Figure 4-16, p209). Furthermore, the reaction rate was slower than that initiated thermally at a temperature of 200°C.
- 6.1.15 The initial analysis results showed that the reaction products obtained by peroxide initiation and thermal initiation via melt processing were different. When the reaction was carried out at a high temperature without peroxide, about one third of the reaction products was soluble in toluene and its FTIR spectrum showed a strong anhydride absorption bands at 1780, 1850  $\text{cm}^{-1}$  and acid band at 1710  $\text{cm}^{-1}$  (Figure 4-21, p212). This confirms the suggestion that partial hydrolysis must be accompanying the maleation reaction. The reaction product obtained at a temperature of 150 °C in the presence of T101 had also about 30% soluble fraction in toluene, but its FTIR spectrum (from the soluble fraction) was shown to have only a weak anhydride absorption band at 1780  $\text{cm}^{-1}$  (Figure 4-20, p211). This indicates that the MA grafting level in the soluble fraction of the peroxide-initiated product is much less than that in the soluble fraction of the thermally maleated rubber.
- 6.1.16 When PET was blended with EP copolymer, as observed from the morphology of PET/EP blends, it was found that EP was not compatible with PET due to the high interphase tension and significant difference in physical and chemical properties between these two polymer. EP phase was dispersed as spherical domains and the interfacial boundaries were very clear and sharp (see Figure 5-6 (a), p251) in PET/EP 80/20 blend and the coarse and unsteady morphology was observed in PET/EP 60/40 blend (see Figure 5-9 (a), p255). When GMA grafted EP was blended with PET, significant improvement in the dispersion of the rubber phase

was observed due to the formation of a copolymer of PET-co-EP through the interfacial reactions of grafted GMA groups in the rubber phase with the carboxylic and hydroxyl end groups of PET. The formation of the copolymer acts to reduce the interfacial tension leading to fine dispersion of the rubber phase in the PET phase, thus improving the interfacial adhesion because the copolymer would locate at the interfaces acting as a linker between the two polymer phases.

6.1.17 It was found that the properties and structure of GMA grafted EP samples play a very important role on the efficiency of the compatibilisation of the PET/rubber blends. The presence of polyGMA in the EP-g-GMA samples which was formed during the melt grafting in EP+GMA+T101 system had a significantly adverse effect on the compatibilisation of the PET/EP-g-GMA blends. During the melt blending with PET, the presence of polyGMA in the EP-g-GMA<sub>T101</sub> samples resulted in crosslinking of the PET phase and reduced the efficiency of the compatibilisation effect, i.e. larger domain size of EP-GMA phase was dispersed in the PET phase (see Figure 5-8, p254). It was demonstrated that in addition to the reaction of epoxy group of the grafted GMA with the end groups of PET the epoxy groups of the polyGMA also reacted with the carboxylic acid groups of PET. In contrast, the EP-g-GMA<sub>TRIS</sub> samples gave rise to better compatibilisation with PET in terms of finer dispersion of the rubber phase and better interfacial adhesion as observed from the SEM micrographs (see Figures 5-6, p252, and 5-9, p255) due to the higher GMA grafting and the absence of the polyGMA in these samples.

6.1.18 It is very important to note that the microstructure of the grafts also affects the efficiency of the compatibilisation. In the blending of PET with EP-g-GMA<sub>T29B90</sub>, it was found that there was less extent of interfacial reactions reflected by low torque values during blending and sharp and smooth interfaces observed in SEM of PET/EP-g-GMA<sub>T29B90</sub> 60/40 blend (see Figure 5-9, p255).

6.1.19 The results also showed that the EPDM-g-GMA<sub>T101</sub> prepared in the GMA+T101 system gave much more efficient compatibilising effect with PET when compared to the EPDM-g-GMA<sub>TRIS</sub> prepared in the GMA+TRIS+T101 system in terms of the very fine dispersion of the rubber phase (see Figure 5-23, p265) and the excellent tensile properties (see Figure 5-28, p271). Though the presence of TRIS enhanced

the grafting reaction, resulting in a higher grafting degree, the microstructure of the grafted GMA may be responsible for the inefficient interfacial reaction. The analysis of EPDM-g-GMA<sub>TRIS</sub> sample and EPDM-g-GMA<sub>T101</sub> showed the significant difference on the fraction distribution during the solvent differential extraction (see Figure 3-32, p166).

6.1.20 EPDM-g-GMA<sub>T101</sub> could also lead to very efficient interfacial reactions during the reactive blending with PET. It was found that only about 0.3% GMA grafting degree was high enough to result in the finer dispersion observed and the excellent mechanical properties seen in the PET/EPDM-g-GMA 80/20 blends (see Figures 5-23, p265, and 5-28, p271). When the GMA grafting degree exceeds this level, the strong interfacial reaction has an adverse effect on the compatibilisation, i.e. a significant increase in the melt viscosity of the PET blends and the uneven domain size distribution of the rubber phase.

6.1.21 In the compatibilisation of PET and GMA grafted EP or EPDM, the evidence indicates clearly that reactions do take place between the PET phase and the rubber phase. The torque-time curves clearly reflect the interfacial reactions by the increase of torque value when PET was blended with either EP-g-GMA or EPDM-g-GMA (see Figure 5-4 for PET/EP-g-GMA blends, p250, and Figure 5-20 for PET/EPDM-g-GMA blends, p262). The higher grafting degree of GMA achieved in the EPDM-g-GMA<sub>T101</sub> phase, the higher were the torque values. Thus, EPDM-g-GMA has a stronger effect on the increase of torque values during the melt blending with PET. The solubility test and FTIR analysis of the blends also gave additional evidence for the occurrence of an interfacial reaction leading to the formation of a copolymer.

## 6.2 RECOMMENDATIONS FOR FURTHER WORK

6.2.1 it was interesting to find that the low temperature (at 115°C) grafting of GMA onto EP, when the peroxide T29B90 was used as a free radical initiator, depended on the concentration of the initial GMA added. Under these low temperature (115°C) grafting condition, nearly no GMA was grafted onto the EP when 6 phr GMA was

used, whereas the grafting degree increased sharply upto 6% when 15 phr GMA was added (see Figure 3-17, p158 ). It seems that a critical value of the initial GMA concentration is needed for this grafting reaction. The amount of polyGMA also increased with increasing GMA concentration, though its overall concentration was relatively low. At such low temperatures, the EP is just softening and the polymer viscosity is very high during the processing. Though high grafting of GMA was measured at high GMA concentration, the grafting mechanism and the structure of the grafted GMA must be different from that obtained at higher temperatures as the polymer viscosity could be much higher at low processing temperatures. GMA might graft onto the EP in long grafts since the efficiency of the interfacial reaction is low and the interfacial adhesion is poor even though high GMA grafting samples was used during the reactive blending (see Figure 5-9 (d), p255). A study of the microstructure of the grafted GMA in the presence of T29B90 under low temperature would be very useful and would help to explain the grafting chemistry and the nature of the interfacial reactions during the reactive blending of the grafted EP-g-GMA with PET. This study would require the utilisation of high sensitive analytical technique, such as FT-NMR to identify the length of the grafts and their microstructure.

6.2.2 Results from this work have shown that the addition of a tri-functional comonomer, TRIS, during the melt free radical grafting of GMA on to EP and EPDM could significantly enhance the desired grafting reaction and reduce the side reactions. Though the effect of the processing conditions and compositions on the grafting yield and melt viscosity (MFI) has been investigated in some detail in this work and the characterisation of the GMA modified polymers has been conducted by using FTIR and differential solvent extraction, more work on the grafting mechanisms, microstructure of the grafts and the alteration of polymers need to be done to have a better understanding of the melt free radical grafting chemistry involved. These include grafting dynamic study, structural analysis of GMA modified polymers in terms of grafting sequence of GMA and TRIS, grafting structure, and mechanistic studies using model compounds in the absence and presence of the comonomer.

6.2.3 It was demonstrated that GMA modified EP and EPDM were very effective in subsequent compatibilisation studies with PET via reactive blending. Strong

evidence showed that grafted GMA in the rubber phase was very reactive towards the end groups of PET (-OH, -COOH). However, it was found that there was a significant difference in the nature of the interfacial reaction of PET during the reactive blending with the different GMA modified polymers studied (i.e. EP-g-GMA<sub>T101</sub> in EP+GMA+T101 system, EP-g-GMA<sub>TRIS</sub> in EP+GMA+TRIS+T101 system, EPDM-g-GMA<sub>T101</sub> in EPDM+GMA+T101 system and EPDM-g-GMA<sub>TRIS</sub> in EPDM+GMA+TRIS+T101 system). Among these samples, EPDM-g-GMA<sub>T101</sub> with low grafting level resulted in the best compatibilisation effect. A further study on the relationship between the grafting structure of GMA modified rubbers and the compatibilisation effect with PET will be very useful to screen the most suitable GMA modified polymer for reactive blending and to get a better understanding of the nature of the interfacial reaction that occurs during the reactive blending step.

6.2.4 In this work the functionalisation of EP and EPDM with GMA was carried out in a batch internal mixer. Due to its particular structure, the mixing chamber is not perfectly sealed. This may bring about complications when adding volatile liquid monomers such as GMA into the mixing chamber. The loss of GMA during the reactive processing may be a reason for the overall low grafting efficiency. It is suggested that the melt grafting of GMA onto polymers is carried out in a twin-screw extruder, which would be ideally suited for continuous production of reactively processed material and has a better handling of liquid reactant with special designed barrel segment configuration.

6.2.5 A further difficulty experienced where using the internal mixer for the compatibilisation of PET with GMA-grafted-EP or -EPDM was due to the high processing temperature (temperature setting is 275°C) needed for PET blending. The limitations of handling and the design of the internal mixer meant that the oxidation of the blends can not be avoided which was occur at such a high temperature. As a result, it is hard to prepare high quality samples for performance evaluation. Based on the current highly encouraging results, further work on reactive blending of PET with GMA functionalised polymers using a twin screw extruder is highly recommended since this could provide a much better processing control.



## References

1. P.S.Hope and M.J.Folkes, *Chapter 1 Introduction*, in 'Polymer Blends and Alloys' Eds. By M.J.Folkes and P.S.Hope, Blackie Academic and Professional, London (1993).
2. M.Xanthos, *Interfacial Agents for Multiphase Polymer System: Recent Advances*, Polym.Eng.Sci., **28**, (1988) 1392.
3. European Plastics News, 23, 14 (1996 September).
4. V.Tanruttanakul, A.Hiltner, E.Baer, W.G.Perkins, F.L.Massey and A.Moet, *Toughening PET by Blending with a Functionalised SEBS Block Copolymer*, Polymer, **38**, (1997) 2191.
5. V.Tanruttanakul, A.Hiltner, E.Baer, W.G.Perkins, F.L.Massey and A.Moet, *Effect of Elastomer Functionality on Toughened PET*, Polymer, **38**, (1997) 4117.
6. M.Heino, J.Kirjava, P.Hietaoja and J.Seppala, *Compatibilisation of Polyethylene Terephthalate/Polypropylene Blends with Styrene-Ethylene/Butylene-Styrene (SEBS) Block Copolymers*, J. Appl. Polym. Sci., **65**, (1997) 241.
7. N.K.Kalfoglou, D.S.Skafidas, J.K.Kallitsis, J.C.Lambert and L.Vanderstappen, *Comparison of Compatibiliser Effectiveness for PET/HDPE Blends*, Polymer, **36** (1995) 4453.
8. A.Jha and A.K.Bhowmick, *Thermoplastic Elastomeric Blends of Poly(ethylene terephthalate) and Acrylate Rubber: 1. Influence of Interaction on Thermal, Dynamic Mechanical and Tensile Properties*, Polymer, **38** (1997) 4337.
9. R.Fayt, R.Jerome, and P.Teyssie, *Molecular Design of Multicomponent Polymer System XIV: Control of Mechanical Properties of PE-PS Blends by Block Copolymers*, J. Polym. Sci. Part B Polym. Phys., **27** (1989) 775.
10. S. Krause, *Chapter 2 Polymer-Polymer Compatibility*, in Polymer Blends, Vol.1, Eds. By D.R.Paul and S. Newman, Academic Press, London (1978).
11. J.G.Bonner and P.S.Hope, *Chapter 3 Compatibilisation and Reactive Blending*, in 'Polymer Blends and Alloys' Eds. By M.J.Folkes and P.S.Hope, Blackie Academic and Professional, London (1993).
12. A. Kumar and R.K.Gupta, *Chapter 9 Thermodynamics of Polymer Mixtures*, in Fundamentals of Polymer, McGraw-Hill, (1998).

13. O.Olabisi, L.M.Robeson and M.T.Shaw, *Chapter 2 Thermodynamics of Polymer-Polymer Miscibility*, in *Polymer-Polymer Miscibility*, Academic Press, New York (1979).
14. G.I.Taylor, Proc. R. Soc. London, A146 (1934)501.
15. J.A.Manson and L.H.Sperling, *Polymer Blends and Composites*, Plenum Press, New York (1976).
16. M.Xanthos and S.S.Dagli, *Compatibilisation of Polymer Blends by Reactive Blending*, Polym.Eng.Sci.,**31**, (1991) 929.
17. D.R.Paul, *Chapter 12 Interfacial Agent ("Compatibilisers")for Polymer Blends*, in *Polymer Blends*, Vol.2 Eds. By D.R.Paul and S. Newman, Academic Press, London (1978).
18. L.A.Utracki, Part 2 Polymer/polymer Miscibility, in *Polymer Alloys and Blends: Thermodynamic and Rheology*, Hanser Publisher, New York, (1989).
19. S.Cimmino, L.D'orazio, R.Greco, G.Maglio, M.Malinconico, C.Mancarella, E.Martuscelli, R.Palumbo, and G.Ragosta, *Morphology-Properties Relationships in Binary Polyamide 6/Rubber Blends: Influence of the Addition of a Functionalised Rubber*, Polym.Eng.Sci., **24**, (1984) 48.
20. M.V.Duin and R.J.M.Borggreve, *Chapter 3 Blends of Polyamides and Maleic-Anhydride-Containing Polymers: Interfacial Chemistry and Properties*, in 'Reactive Modifiers for Polymers', Ed. S. Al-Malaika, Blackie Academic and Professional, London, (1997).
21. M.W.Fowler and W.E.Baker, *Rubber Toughening of Polystyrene Through Reactive Blending*, Polym.Eng.Sci., **28**, (1988) 1427.
22. S.Wu, *Formation of Dispersed Phase in Incompatible Polymer Blends: Interfacial and Rheological Effects*, Polym. Eng. & Sci. **27**, (1987) 335.
23. A.J.Moffett and M.E.J.Dekkers, *Compatibilised and Dynamically Vulcanised Thermoplastic Elastomer Blends of Poly(Butylene Terephthalate) and Ethylene Propylene Diene Rubber*, Polym.Eng. Sci., **32**, (1992) 1.
24. P.Vongpanish, A.K.Bhowmick and T.Inoue, *Structure-property Relationship during Reactive Processing of Blend of Poly(butylene terephthalate)and Functionalised Ethylene-propylene Rubber*, *Plastics, Rubber & Composites Process. & Appl.*, **21**, (1994) 109.

25. M.Okamoto, K.Shiomi and T.Inone, *Structure and Mechanical Properties of Poly(butylenes terephthalate)/Rubber Blends Prepared by Dynamic Vulcanisation*, *Polymer* , **35**, (1994) 4618.
26. K.H.Yoon, H.W.Lee and O.O.Park, *Properties of Poly(ethyleneterephthalate) and Maleic Anhydride-Grafted Polypropylen Blends by Reactive Processing*, *J.Appl.Polym.Sci.*,**70**, (1998) 389.
27. L.Chen, B.Wong, and W.E.Baker, *Melt Grafting of Glycidyl methacrylate Onto Propylene and Reactive Compatibilisation of Rubber Toughened Polypropylene*, *Polym. Eng. Sci.* ,**36**, (1996) 1594.
28. N.C.Liu, H.Q. Xie and W.E.Baker, *Comparison of the Effectivness of Different Basic Functional Groups for the Reactive Compatibilisation of Polymer Blends*, *Polymer*, **34**, (1993) 4680.
29. T.Vainio, G.Hu, M.Lambla, and J.Seppala, *Functionalised Polypropylene Prepared by Melt Free Radical Grafting of Low Volatile Oxazoline and Its Potential in Compatibilisation of PP/PBT Blends*, *J.Appl.Polym.Sci.*, **61**, (1996) 843.
30. G.Hu, Y.Sun, and M.Lambla, *Effects of Processing Parameters on the In Situ Compatibilisation of Polypropylene and Poly(butylene terephthalate) Blends By One-step Reactive Extrusion*, *J. Appl. Polym. Sci.*, **61**, (1996) 1039.
31. G.Hu, Y.Sun and M.Lambla, *Functionalisation of Polypropylene with Oxazoline and Reactive Blending of PP with PBT in a Corotating Twin-Screw Extruder*, *Polym.Eng. & Sci.*, **36**, (1996) 676.
32. M.K.Akkapeddi, B.V.Buskirk, C.D.Mason, S.S.Chung, and X.Swamikannu, *Performance Blends Based on Recycled Polymers*, *Polym. Eng. Sci.* ,**35**, (1995) 72.
33. J.K.Kim, S.Kim and C.E.Park, *Compatibilisation Mechanism of Polymer Blends with an in-situ Compatibiliser*, *Polymer*, **38**, (1997) 2155.
34. H.K Jeon and J.K.Kim, *Morphological Development with Time for Immiscible Polymer Blends with an In-situ Compatibiliser under Controlled Shear Conditions*, *Polymer*, **39**, (1998) 6227.
35. H.K Jeon and J.K.Kim, *The Effect of the Amount of in Situ Formed Copolymers on the Final Morphology of Reactive Polymer Blends with an In Situ Compatibiliser*, *Macromolecules*, **31** (1998) 9273.

36. Y.Pietrasanta, J.Robin, N.Torres and B.Boutevin, *Reactive Compatibilisation of HDPE/PET blends by Glycidyl Methacrylate Functionalised Polyolefins*, *Macromol.Chem.Phys.*, **200**, (1999)142.
37. W.Hale, H.Keskkula and D.R.Paul, *Effect of Crosslinking Reactions and Order of Mixing on Properties of Compatibilised PBT/ABS Blends*, *Polymer*, **40**, (1999) 3665.
38. W.Hale, H.Keskkula and D.R.Paul, *Compatibilisation of PBT/ABS blends by Methyl Methacrylate-glycidyl Methacrylate-Ethyl Acrylate Terpolymers*, *Polymer*, **40**, (1999) 365.
39. W.Hale, J.Lee, H.Keskkula, D.R.Paul, *Effect of PBT Melt Viscosity on the Morphology and Mechanical Properties of Compatibilised and Uncompatibilised Blends with ABS*, *Polymer*, **40**, (1999) 3621.
40. R.M.Holsti-Miettinen, M.T.Heino, and J.V.Seppala, *Use of Epoxy Reactivity for Compatibilisation of PP/PBT and PP/LCP Blends*, *J. Appl. Polym. Sci.*, **57**, (1995)573.
41. C.Tsai and F.Chang , *Polymer Blends of PBT and PP Compatibilised by Ethylene-co-glycidyl Methacrylate Copolymer*, *J. Appl. Polym. Sci.*, **61**, (1996)321.
42. X.Zhang and J.Yin, *The Characterisation of the Interfacial Reaction in Polyamide1010/poly(propylene)-graft-(glycidyl methacrylate) Blends*, *Macromol. Chem. Phys.*, **199**, (1998) 2631.
43. S.C.Wong and Y.W.Mai, *Effect of Rubber Functionality on Microstructures and Fracture Toughness of Impact-modified Nylon 6,6/Polypropylene Blends: I. Structure-Property Relationships*, *Polymer*, **40**, (1999) 1553.
44. S.Thomas and G.Groeninckx, *Reactive compatibilisation of Heterogeneous Ethylene Propylene Rubber (EPM)/nylon 6 by the Addition of Compatibiliser Precursor EPM-g-MA*, *Polymer*, **40**, (1999) 5799.
45. J.Lepers, B.D.Favis, C.Lacroix, *The Influence of Partial Emulsification on Coalescence Suppression and Interfacial Tension Reduction in PP/PET Blends*, *J. Polym. Sci. Part B: Polym.Phys.*, **37**, (1999) 939.
46. H.Cartier and G-H.Hu, *Compatibilisation of Polypropylene and Poly(butylene terephthalate) Blends by Reactive Extrusion: Effects of the Molecular Structure of a Reactive Compatibiliser*, *J.Mat. Sci.*, **35**, (2000) 1985.

47. K.L.BØRVE, H.K.Kotlar, and C.-G.Gustafson, *Polypropylene-Phenol Formaldehyde-Based Compatibiliser. II. Application in PP/PA6 75/25 (wt/wt) Blends*, J. Appl. Polym. Sci., **75**, (2000)355.
48. K.L.BØRVE, H.K.Kotlar, and C.-G.Gustafson, *Polypropylene-Phenol Formaldehyde-Based Compatibiliser. II. Application in PP/PBT and PP/PPE Blends*, J. Appl. Polym. Sci., **75**, (2000) 361.
49. S.H.Park, K.Y.ark and K.D.Suh, *Compatibilising Effect of Isocyanate Functional Groupon Polypropylene Terephthalate/Low Density Polyethylene Blends*, J. Polym. Sci. Part B: Polym.Phys., **36**, (1998) 447.
50. J-S.Lee, K-Y.Park, D.Yoo and K.-D.Suh, *In Situ Compatibilisation of PET/PS Blends Through Carbamate-Functionalised Reactive Copolymers*, J. Polym. Sci. Part B: Polym.Phys., **38**, (2000) 1396.
51. S.A.Jabarin, *Poly(ethylene terephthalate) (Chemistry & Preparation)*, in Polymeric Materials Encyclopedia, CRC Press, **Vol. 8**, 6078 (1996).
52. S.A.Jabarin, *Poly(ethylene terephthalate) (Heat Setting & Thermal Stabilisation)*, in Polymeric Materials Encyclopedia, CRC Press, **Vol. 8**, 6091(1996).
53. *Plyester*, in Encyclopidia of Polymer Sci. Eng. , Eds. Mark, Bilales, Overberger and Menges, 2<sup>nd</sup> Edition, **Vol. 12**, 19 (1989).
54. J.W.Barlow and D.R.Paul, *Mechanical Compatibilisation of Immiscible Blends*, Polym. Eng. Sci. , **24**, (1984) 525.
55. T.L.Carte and A.Moet, *Morphological Origin of Super Toughness in Poly(ethylene Terephthalate)/Polyethylene Blends*, J. Appl. Polym. Sci., **48**, (1993) 611.
56. L.-M.Chen and C.-M.Shiah, *Toughening of PET/HDPE Polyblends from Recycled Beverage Bottles*, ANTEC'89, (1989) 1803.
57. P.Bataille, S.Boisse, and H.P.Schreiber, *Mechanical Properties and Polypropylene and Poly(ethylene terephthalate) Mixtures*, Polym. Eng. Sci. , **27**, (1987) 623.
58. M.Xanthos, M.W.Young, and J.A.Biesenberger, *Polypropylene/Polyethylene Terephthalate Blends Compatibilised Through Functionalisation*, Polym. Eng. Sci. , **30**, (1990) 355.
59. J.Lepers, B.D.Favis, and R.J.Tabar, *The Relative Role of Coalescence and Interfacial Tension in Controlling Dispersed Phase Size Reduction during the*



- Compatibilisation of Polyethylene Terephthalate/Polypropylene Blends*, J. Polym. Sci. Part B: Polym.Phys., **35**, (1997) 2271.
60. Y.X.Pang, D.M.Jia, H.J.Hu, D.J.Hourston, and M.Song, *Effects of a Compatibilising Agent on the Morphology, Interfacial and Mechanical Behaviour of Polypropylene/Poly(ethylene terephthalate) Blends*, *Polymer*, **41**, (2000) 357.
61. G.Hu, Y.Sun, and M.Lambla, *Devolatilization: A Critical Sequential Operation for in situ Compatibilization of Immiscible Polymer Blends by One-step reactive extrusion*, *Polym. Eng. Sci*, **36**, (1996) 676.
62. T.Vainio, G.Hu, M.Lambla, and J.Seppala, *Functionalisation of Polypropylene with Oxazoline and Reactive Blending of PP with PBT in a Corotating Twin-Screw Extruder*, *J.Appl.Polym.Sci.*, **63**, (1997) 883.
63. A.Cecere, R.Greco, G.Ragosta, and G.Scarinzi, *Rubber Toughened Polybutylene Terephthalate: Influence of Processing on Morphology and Impact Properties*, *Polymer*, **31**, (1990) 1239 .
64. F.C.Chang, in *Handbooks of Thermoplastics*, Eds. O.Olabisi, Marcel Dekker, New York, (1997).
65. L.A.Utracki, *History of Commercial Polymer Alloys and Blends (From a Perspective of the Patent Literature)*, *Polym. Eng. Sci*, **35**, (1995)2.
66. E.Hage,W.Hale, H.Keskkula, and D.R.Paul, *Impact Modification of Poly(butylenes terephthalate) by ABS Materials*, *Polymer* ,**38**, (1997) 3237.
67. V.Bordereau, Z.H.Shi, L.A.Utracki, P.Sammut, and M.Carrega, *Development of Polymer Blend Morphology During Compounding in a Twin-Screw Extruder. Part III: Experimental Procedure and Preliminary Results*, *Polym. Eng. Sci*, **32**, (1992) 1846.
68. X.Zhang, G.Li, D.Wang, Z.Yin and J.Yin, *Morphological Studies of Polyamide 1010/Polypropylene Blends*, *Polymer* ,**39**, (1998) 15.
69. B.Ohlsson, H.Hassander and B.Tornell, *Effect of the Mixing Procedures on the Morphology and Properties of Compatibilised Polypropylene/Polyamide*, *Polymer* , **39**, (1998) 4715.
70. A.Y.Coran Chapter7 in *Thermoplastic Elastomer, A comprehensive Review*, eds. N.B.Legge, G.Holden and H.E.Schroeder, Hanser Publishers, Munich (1987).
71. D.C.Sherrington, *Reactions of Polymers*, in *Encyclopidia of Polymer Sci. Eng.* , Eds. by H.F.Mark, N.M.Bikales, C.G.Overberger and G.Menges, J.I.Kroschwitz, 2<sup>nd</sup> Edition, **Vol.14**, 101 (1988).

72. M. Lambla, *Chapter 21: Reactive Processing of Thermoplastic Polymers*, in *Comprehensive Polymer Science* 1<sup>st</sup> supplement, Eds. By G.Allen and J.C.Bevington, Pergamon, New York, 1993.
73. G.Hu, J.Flat and M.Lambla, *Chapter 1 Free-radical Grafting of Monomers onto Polymers by Reactive Extrusion: Principles and Applications*, in 'Reactive Modifiers for Polymers', Ed. S. Al-Malaika, Blackie Academic and Professional, London, (1997).
74. S.B.Brown, *Reactive Extrusion*, in *Encyclopedia of Polymer Sci. Eng.*, Eds. by H.F.Mark, N.M.Bikales, C.G.Overberger and G.Menges, J.I.Kroschwitz, 2<sup>nd</sup> Edition, Vol.14, 169 (1988).
75. G.Moad, *The Synthesis of Polyolefin Graft Copolymers by Reactive Extrusion*, *Prog. Polym. Sci.*, **24**, (1998) 81.
76. D.J.Burlett and J.T.Lindt, *Reactive processing of Rubbers*, *Rubber Chem.Technol.*, **66**, (1987) 411.
77. M.Xanthos, *Reactive Extrusion*, Hanser Publisher 1992 Chpt.4.
78. B.C.Trivedi and B.M.Culbertson, *Maleic Anhydride*, (Chapter 11, p466), Plenum Press 1982.
79. S.F.Thames, A.Rahman, and P.W.Poole, *The Maleinisation of Low Molecular Weight Guayule Rubber*, *J. Applied Polym. Sci.*, **49**, (1993) 1963.
80. R.G.R.Bacon and E.H.Farmer, *The Interaction of Maleic Anhydride with Rubber*, *Rubber Chem. & Technol.*, **12**, (1939) 200.
81. C. Azuma, N. Hashizume, K. Sanui, and N. Ogata, *J. Applied Polym. Sci.*, **28**, (1983) 543.
82. J.L.Bras and P.Compagnon, *The Chemistry of Rubber—The interaction of Ethylenic Compounds and Rubber*, *Rubber Chem. & Technol.*, **20**, (1947) 938.
83. J.L.Bras, *A New Material : Anhydride Rubber ( I )*, *Rubber Chem. & Technol.*, **19**, (1946) 313.
84. P.Compagnon and O. Bonnet, *Anhydride Rubber. ( II ) Production and Vulcanisation*, *Rubber Chem. & Technol.*, **19**, (1946) 319.
85. E.Carone.Jr, U.Kopcak, M.C.Goncalves and S.P.Nunes, *In Situ Compatibilisation of Polyamide 6/Natural Rubber Blends With Maleic Anhydride*, *Polymer*, **41**, (2000) 5929.
86. C.Pinazzi, J.C.Danjard, and R.Pautrat, *Addition of Unsaturated Monomers to Rubber and Similar Polymers*, *Rubber Chem. & Technol.*, **35**, (1962) 282.

87. 'Chemical Reactions of Polymers', Ed. E.M.Fettes, Interscience Publishers(1964) p194.
88. A.Hogt, *Modification of Polypropylene with Maleic Anhydride*, ANTEC'88, 1478 (1988).
89. B.D.Roover, M.Sclavons, V.Carlier, J.Devaux, R.Legras, and A.Momtaz, *Molecular Characterisation of Maleic Anhydride-Functionalised Polypropylene*, J. Polym. Sci. Part A: Polym. Chem., **33**, (1995) 829.
90. S.H.P.Bettini and J.A.M.Agnelli, *Grafting of Maleic Anhydride onto Polypropylene by Reactive Processing. I. Effect of Maleic Anhydride and Peroxide Concentration on the Reaction*, J.Appl.Polym.Sci., **74**, (1999) 247.
91. S.N.Sathe, G.S.Srinivasa, and S.Devi, *Grafting of Maleic Anhydride onto Polypropylene: Synthesis and Characterisation*, J.Appl.Polym.Sci., **53**, (1994) 239.
92. C.Rosales, R.Perera, M.Ichazo, J.Gonzalez, H.Rojas, A.Sanchez, and A.D.Barrios, *Grafting of Polyethylenes by Reactive Extrusion. I. Influence on the Molecular Structure*, J.Appl.Polym.Sci., **70** (1998) 161.
93. K.Kelar, and B.Jurkowi, *Preparation of Functionalised Low-density Polyethylene by Reactive Extrusion and its Blend with Polyamide 6*, Polymer, **41**, (2000) 1055
94. N.C.Liu, W.E.Baker, and K.E.Russell, *Functionalisation of Polyethylenes and Their Use in Reactive Blending*, J.Appl.Polym.Sci., **41**, (1990) 2285.
95. B.G.Soares, R.S.C.Colombaretti, *Melt Functionalisation of EVA Copolymers with Maleic Anhydride*, J.Appl.Polym.Sci., **72**, (1999) 1799.
96. G.Chen, J.Yang, and J.Liu, *Preparation of the HIPS/MA Graft Copolymer and Its Compatibilisation in HIPS/PA 1010 Blends*, J.Appl.Polym.Sci., **71**, (1999) 2071.
97. C.-M.Shiah and C.-M.Chen, *Grafting of Maleic Anhydride onto Thermoplastic Elastomers by Melt Blending*, ANTEC'89, 1398 (1989).
98. E.Passagia, S.Ghetti, F.Picchioni, and G.Ruggeri, *Grafting of Diethyl Maleate and Maleic Anhydride onto Styrene-b-(ethylene-co-1-butene)-b-styrene Triblock Copolymer (SEBS)*, Polymer, **41**, (2000) 4389.
99. C.Rosales, R.Perera, J.Gonzalez, M.Ichazo, H.Rojas, and A.Sanchez, *Grafting of Polyethylenes by Reactive Extrusion. II. Influence on Rheological and Thermal Properties*, J.Appl.Polym.Sci., **73**, (1999) 2549.



100. L.Marquez, I.Rivero, and A.J.Müller, *Application of the SSA Calorimetric Technique to Characterise LLDPE Grafted with Diethyl Maleate*, *Macromol Chem. Phys.*, **200**, (1999) 330.
101. R.Greco, G.Maglioi, P.Musto, and G.Scarinzi, *Bulk Functionalisation of Ethylene-Propylene Copolymers. II. Influence of the Initiator Concentration and Chain Microstructure on the Reaction Kinetics*, *J.Appl.Polym.Sci.*, **37**, (1989) 777.
102. A.J.Oostenbrink and R.J.Gaymans, *Maleic Anhydride Grafting on EPDM Rubber in the Melt*, *Polymer*,**33**, (1992) 3086.
103. C.H.Wu and A.C.Su, *Functionalisation of Ethylene-Propylene Rubber via Melt Mixing*, *Polym.Eng.Sci.*, **31**, (1991) 1629.
104. R.Greco, G.Maglioi, P.Musto, and G.Scarinzi, *Bulk Functionalisation of Ethylene-Propylene Copolymers. III. Structural and Superreticular Order Investigations*, *J.Appl.Polym.Sci.*, **37**, (1989) 789.
105. N.G.Gaylord, M.Meththa, and R.Mehta, *Degradation and Cross-linking of Ethylene-Propylene Copolymer Rubber on Reaction with Maleic Anhydride and/ or Peroxides*, *J.Appl.Polym.Sci.*, **33**, (1987) 2549.
106. F.M.B.Coutinho and M.I.P.Ferreira, *Optimisation of Reaction Conditions of Bulk Functionalisation of EPDM Rubbers with Maleic Anhydride*, *Eur. Polym. J.*, **30(8)**, (1994) 911.
107. N.G.Gaylord and S.Maiti, *Participation of Exited Species in Radical Catalyst Homopolymerisation*, *J.Polym.Sci., Polym. Lett. Ed.*, **11**, (1973) 253.
108. N.G.Gaylord, R.Mehta, V.Kumar and M.Tazi, *High-density Polyethylene-g-Maleic Anhydride Preparation in Presence of Electron-donors*, *J. Appl. Polym. Sci.*, **38**, (1989) 359.
109. N.G.Gaylord and J.Y.Koo, *Participation of Cationic Intermedlates in Radical-induced Homopolymerisation of Maleic Anhydride*, *J.Polym.Sci., Polym. Lett. Ed.*, **19**, (1981) 107.
110. N.G.Gaylord and R.Mehta, *Radical-catalysed Homopolymerisation of Maleic Anhydride in the Presence of Polar Organic Compounds*, *J.Polym.Sci., Part A*, **26**, (1988) 1903.

111. N.G.Gaylord and M.K.Mishra, *Nondegradative Reaction of Maleic Anhydride and Molten Polypropylene in the Presence of Peroxides*, J.Polym.Sci. Polym. Lett. Ed., **21**, (1983) 23.
112. N.G.Gaylord and M.Mehta, *Role of Homopolymerisation in the Peroxide-catalyzed Reaction of Maleic Anhydride and Polyethylene in the Absence of Solvent*, J.Polym.Sci., **B20**, (1982) 481.
113. R.Gallucci and R.C.Going, *Preparation and Reaction of Epoxy-Modified Polyethylene*, J. Appl. Polym. Sci., **27**, (1982) 425.
114. X.Zhang, Z.Yin,L.Li, and J.Yin, *Grafting of Glycidyl Methacrylate onto Ethylene-Propylene Copolymer: Preparation and Characterisation*, J. Appl.Polym.Sci., **61**, (1996) 2253.
115. European patent application EP 0274744 A2 (1987).
116. European patent application EP 0275141 A2 (1987).
117. U.S. Patent 4,956,501 (1990).
118. G.Hu and H.Cartier, *Styrene-assisted Melt free Radical Grafting of Glycidyl Methacrylate onto an Ethylene and Propylene Rubber*, J. Appl. Polym. Sci., **71**, (1999) 125.
119. H.Cartier and G.H.Hu, *Styrene-Assisted Melt Free Radical Grafting of Glycidyl Methacrylate onto Polypropylene*, J.Polym.Sci., Part A Polym.Chem. **36**, (1998) 1053.
120. Y.Sun, G.Hu, and M.Lambla, *Free-Radical Grafting of Glycidyl Methacrylate onto Polypropylene*, Angew. Makromol. Chew.,**229**, (1995) 1.
121. Y.Sun, G.Hu, and M.Lambla, *Free-Radical Grafting of Glycidyl Methacrylate onto Polypropylene in a Co-Rotating Twin Screw Extruder*, J.Appl.Polym.Sci., **57**, (1995) 1043.
122. H. Huang and N.C. Liu, *Nondegradative Melt Functionalisation of Polypropylene with Glycidyl Methacrylate*, J. Appl. Polym. Sci., **67**, (1998) 1957.
123. L.Chen, B.Wong and W.E.Baker, *Melt Grafting of Glycidyl methacrylate Onto Propylene and Reactive Compatibilisation of Rubber Toughened Polypropylene*, Polym.Eng. Sci., **36**, (1996) 1594.
124. B. Wong and W.E.Baker, *Melt Rheology of Graft Modified Polypropylene*, Polymer, **38**, (1997) 2781.

125. N.C.Liu, H.Q. Xie and W.E.Baker, *Comparison of the Effectiveness of Different Basic Functional Groups for the Reactive Compatibilisation of Polymer Blends*, *Polymer*, **34**, (1993) 4680.
126. H.Cartier and G.Hu, *Styrene-assisted free Radical Grafting of Glycidyl Methacrylate onto Polyethylene in the Melt*, *J. Polym. Sci: Part A: Polym. Chem.*, **36**, (1998) 2763.
127. U.Anttila, C.Vocke and J.Seppala, *Functionalisation of Polyolefins and Elastomers with an Oxazoline Compound*, *J. Appl. Polym. Sci.*, **72**, (1999) 887.
128. N.C.Liu, W.E.Baker, *Basic Functionalisation of Polypropylene and the Role of Interfacial Chemical Bonding in its Toughening*, *Polymer*, **35**, (1994) 988.
129. W.E.Baker and M.Saleem, *Coupling of Reactive Polystyrene and Polyethylene in Melts*, *Polymer*, **28**, (1987) 2057.
130. W.E.Baker and M.Saleem, *Polystyrene-Polyethylene Melt Blends Obtained Through Reactive Mixing Process*, *Polym.Eng.Sci.*, **27**, (1987) 1634.
131. N.C.Liu, W.E.Baker,., *The Separate Roles of Phase Structure in Toughening a Brittle Polymer*, *Polym.Eng. Sci.*, **32**, (1992) 1695.
132. R.Scaffaro, G.Carianni, F.P.L.Mantia, A.Zeroukhi, N.Mignard, and R.Granger, *On the Modification of the Nitrile Groups of Acrylonitrile/Butadiene/Styrene into Oxazoline in the Melt*, *J. Polym. Sci: Part A: Polym. Chem.*, **38**, (2000) 1795.
133. J.Piglowski, I.Gancarz, and M.Wlajak, *Oxazoline-functionalised Hydrogenated Nitrile Rubber as Impact Modifier for Polyamide-6*, *Polymer*, **41**, (2000) 3671.
134. F.Severini, M.Pegoraro, and L.D.Landro, *Grafting Reaction of Methylmethacrylate onto EPR and EPDM Rubbers—Toughening Effects of Graft Copolymers on Polycarbonate and Poly(methylmethacrylate)*, *Angew Makromol.Chemie*, **190**, (1991) 177.
135. Z.Song and W.E.Baker, *Melt Grafting of Tert-Butylaminoethyl Methacrylate onto Polyethylene*, *Polymer*, **33**, (1992) 3266.
136. Z.Song and W.E.Baker, *Basic Functionalisation of Molten Linear Low-density Polyethylene with 2-(Dimethylamino)ethyl Methacrylate in an Intermeshing Corotating Twin-screw Extruder*, *J.Appl.Polym.Sci.*, **41**, (1990) 1299.

137. G.Samay, T.Nagy, and J.White, *Grafting Maleic Anhydride and Comonomers onto Polyethylene*, J.Appl.Polym.Sci., **56**, 1423(1995).
138. S.Al-Malaika and N.Suharty, *Reactive Processing of Polymers: Mechanisms of Grafting Reactions of Functional Antioxidants on Polyolefins in the Presence of a Coagent*, Polym. Degr. & Stab. **49**, (1995) 77.
139. S.Al-Malaika and G.Scott, Inter. Pat. Appli. No: PCT/W090/01506 (1990) and US Patent 5,382,633 (1995).
140. S.Al-Malaika, H.H.Sheena and G.Scott, GB Patent Appli. No 9511785.9,9.6. (1995).
141. S.Buniran, Ph.D Thesis, Aston University (1998).
142. S. Costa and M.Felisberti, *Blends of Polyamide 6 and Epichlorohydrin Elastomers. II. Thermal, Dynamic Mechanical, and Mechanical Properties*, J. Appl. Polym. Sci. **72**(1999)1835.
143. G.G.Bandyopadhyay, S.S.Bhagawan, K.N.Ninan and S.Thomas, *Dynamic Properties of NR/EVA Polymer Blends: Model Calculations and Blend Morphology*, J. Appl. Polym. Sci. **72**(1999)165.
144. S.George, N.R.Neelakantan, K.T.Varughese and S.Thomas, *Dynamic Mechanical Properties of Isotactic Polypropylene/Nitrile Rubber Blends: Effects of Blend Ratio, Reactive Compatibilisation, and Dynamic Vulcanisation*, J. Polym. Sci. Part B: Polym.Phys. **35**(1997)2309.
145. D.Singh, V.P.Malhotra and J.L.Vats, *The Dynamic Mechanical Analysis, Impact, and Morphological Studies of EPDM-PVC and MMA-g-EPDM-PVC Blends*, J. Appl. Polym. Sci. **71**(1999)1959.
146. S.Thomas and A.George, *Eur. Polym. J.* **28**(1992)145.
147. N.Papke and J.Karger-Kocsis, *Thermoplastic Elastomers Based on Compatibilised Poly(ethylene terephthalate) Blends: Effect of Rubber Type and Dynamic Curing*, Research Project Report, University of Kaiserslautern, Germany, 1999
148. S. Al-Malaika and W.Kong, *Reactive Processing of Polymers: Melt Grafting of Glycidyl Methacrylate on Ethylene Propylene Copolymer in the Presence of a Coagent*, J. Appl. Polym. Sci. (to appear ).
149. M. Lemattre and R. Werth, Europ. Pat. 81700974.2 (1985).
150. R.J.Mborggreve and R.J.Gaymans, *Impact Behaviour of Nylon-rubber Blends: 4. Effect of the Coupling Agent, Maleic Anhydride*, Polymer, **30**, (1989), 63.

151. AKZO Technical sheet.
152. D.Barnard, Lecture "AN OVERVIEW OF THE CHEMICAL MODIFICATION OF NATURAL RUBBER".
153. P.Guegan, C.W.Macosko, T.Ishizone, A.Hirao, S.Nakahama, *Kinetics of Chain Coupling at Melt Interfaces*, *Macromolecules*, 27, (1994) 4993.
154. N.C.Beck Tan, S.-K.Tai, R.M.Briber, *Morphology control and interfacial reinforcement in reactive polystyrene/amorphous polyamide blends*, *Polymer*, 37, (1996) 3509.